

PREDICTING THE VULNERABILITY OF TYPICAL
RESIDENTIAL BUILDINGS TO HURRICANE DAMAGE

By

ANNE D. COPE

A DISSERTATION PRESENTED TO THE GRADUATE SCHOOL
OF THE UNIVERSITY OF FLORIDA IN PARTIAL FULFILLMENT
OF THE REQUIREMENTS FOR THE DEGREE OF
DOCTOR OF PHILOSOPHY

UNIVERSITY OF FLORIDA

2004

Copyright 2004

by

Anne D. Cope

This work is dedicated to those who have given their lives in the defense of our freedom.

ACKNOWLEDGMENTS

I would like to extend sincere thanks to the many people who made this accomplishment possible. First, I would like to thank my advisor, Dr. Kurt Gurley for his encouragement, support, and guidance, especially when recent world political events became very personal. I would also like to thank Dr. Jean-Paul Pinelli for his leadership of the engineering team for the Public Loss Hurricane Projection Model. For sincere critique and professional advice, I would like to thank Dr. Emil Simiu, Dr. Tim Reinhold, and Dr. Peter Vickery. Many thanks also go to the members of my committee and to fellow researchers (especially Liang Zhang, Luis Aponte, and Josh Murphree). I thank the providers of the University of Florida Alumni Scholarship for financial support of my education, and the Florida Department of Insurance for funding this research. For their unwavering support and loving advice, I thank my husband, my parents, and my extended family. Lastly, I would like to thank Adrienne Pickett for her support and warm hospitality during the completion of this project.

TABLE OF CONTENTS

	<u>Page</u>
ACKNOWLEDGMENTS	iv
LIST OF TABLES	ix
LIST OF FIGURES	xi
ABSTRACT	xix
CHAPTER	
1 INTRODUCTION	1
Research Hypothesis.....	4
Goals and Objectives	5
Summary of Dissertation	5
2 SUMMARY OF PREVIOUS RESEARCH	7
Background Information on Structural Wind Loads	7
Efforts to Quantify Extreme Wind Loads.....	12
Defining the Behavior of Near-Surface Hurricane Winds	12
Characterizing Surface Pressures on Structures	14
Characterizing and Codifying Structural Loads.....	17
Summary of Efforts to Quantify Extreme Wind Loads.....	17
Post-Damage Investigations	18
Damage Prediction Models.....	20
Fundamental Concepts in Damage Prediction	20
Damage Prediction Models in the Public Domain	24
Proprietary Damage Prediction Models	26
Public Loss Hurricane Projection Model	28
3 RESIDENTIAL STRUCTURES IN FLORIDA	30
Sources of Information	31
Florida Hurricane Catastrophe Fund Exposure Database	31
County Property Appraiser Databases.....	32
Manufactured Home Builder Literature	33
Post-Damage Investigations	34
Results of the Building Population Investigation	34

	Characterization of Site-Built Homes	34
	Characterization of Manufactured Homes.....	40
	Building Component Selection.....	41
4	STRUCTURAL WIND LOADS FOR TYPICAL	44
	Use and Modification of the ASCE 7-98 Code Provisions to Represent Load	
	Conditions during Extreme Wind Events	45
	Modifications to Surface Pressure Equations.....	46
	Use and Modifications to External Pressure Coefficients.....	48
	Main Wind Force Resisting System external pressure coefficients.....	49
	Component and Cladding external pressure coefficients.....	50
	Use and Modifications to Internal Pressure Coefficients.....	54
	Application of the Modified ASCE 7-98 Code Provisions to Produce Extreme	
	Wind Event Load Conditions on Selected Building Components.....	54
	Roof Cover and Roof Sheathing Loads.....	55
	Roof-to-Wall Connection Loads	56
	Wall Loads.....	57
	Load Conditions for Openings	59
	Load Conditions for Tie-Down Anchors.....	65
	Summary of Wind Load Conditions Used in the Simulation Engine.....	65
5	PROBABILISTIC WIND RESISTANCE CAPACITIES FOR RESIDENTIAL DWELLING COMPONENTS	67
	Fundamental Concepts Applied During the Selection of Load Resistance	
	Values	68
	Site-Built Home Resistance Values.....	71
	Wind Resistance Capacity of Roof Cover on Site-Built Homes.....	71
	Wind Resistance Capacity of Roof Sheathing on Site-Built Homes.....	75
	Wind Resistance Capacity of Roof-to-Wall Connections on Site-Built Homes	76
	Wind Resistance Capacity of Site-Built Home Walls.....	79
	Wood shear wall capacity	80
	Wood frame out-of-plane load capacity.....	81
	Wood frame uplift capacity.....	83
	Wood frame sheathing capacity	83
	Masonry shear wall capacity.....	84
	Masonry out-of-plane load capacity.....	85
	Masonry uplift capacity.....	86
	Wind Resistance Capacity of Site-Built Home Openings.....	86
	Wind resistance capacity of doors for site-built homes	87
	Wind resistance capacity of garage doors for site-built homes.....	87
	Wind resistance capacity of windows for site-built homes.....	88
	Manufactured Home Resistance Values.....	89
	Wind Resistance Capacity of Roof Sheathing and Cover on Manufactured Homes	90

	Wind Resistance Capacity of Roof-to-Wall Connections for Manufactured Homes	91
	Wall Capacity for Manufactured Homes.....	92
	Wind Resistance Capacity of Manufactured Home Openings.....	93
	Wind Resistance Capacity of Tie-Down Anchors.....	93
	Summary of Resistance Values Used in Structural Damage Simulation	94
6	SIMULATION ENGINE.....	97
	Selection of Structural Type and Definition of Geometry.....	97
	Variables for Site-Built Homes	98
	Variables for Manufactured Homes	100
	Loop for Angle of Incidence.....	101
	Loop for Wind Speed.....	102
	Loop for the Simulated Homes.....	102
	Randomization of Wind Speed and Pressure Coefficients.....	103
	Initial Load Calculations	105
	Sampling of Resistances.....	105
	Roof cover and roof sheathing resistance sampling.....	106
	Roof-to-wall connection resistance sampling	107
	Wall resistance sampling.....	109
	Opening resistance sampling.....	111
	Tie-down anchor resistance sampling	112
	Initial Failure Check.....	112
	Initial failure check for roof sheathing.....	112
	Initial failure check for walls	113
	Initial failure check for openings	115
	Internal Pressure Evaluation and Recalculation of Loads.....	116
	Final Failure Check and Damage Tally.....	117
	Structural Damage Output Files	122
	Summary.....	123
7	STRUCTURAL DAMAGE VALIDATION AND RESULTS.....	124
	Structural Damage Validation	126
	NAHB Report on Hurricane Andrew	127
	Application of the NAHB Report Data as a Validation Tool.....	128
	Validation of Individual Components	130
	Validation of window damage	132
	Validation of masonry wall damage.....	135
	Validation of wood frame wall damage	137
	Validation of roof-to-wall connection damage	138
	Validation of roof sheathing damage	140
	Validation of roof cover damage.....	142
	Investigation of Selected Topics.....	144
	Investigation of the Batch Selection Method for Roof Sheathing.....	144
	Investigation of the Batch Selection Method for Roof-to-Wall Connections ...	146

	Investigation of the Difference between Hip and Gable Roofs.....	148
	Structural Damage Results	150
	Results for Site-Built Homes in the South Florida and Florida Keys Region...	151
	Results for Manufactured Homes.....	153
	Summary.....	156
8	APPLICATION OF RESULTS AND CONCLUSION	157
	Relating Structural Damage to Monetary Loss	158
	Cost Estimate Model	159
	Insured Loss Model	162
	Research Contributions.....	164
	Future Uses of the Structural Damage Model	165
APPENDIX		
A	SOUTH / KEYS REGION CONCRETE BLOCK GABLE ROOF (CBG) HOMES	167
B	SOUTH / KEYS REGION CONCRETE BLOCK HIP ROOF (CBH) HOMES.....	175
C	SOUTH / KEYS REGION WOOD FRAME GABLE ROOF (WG) HOMES.....	183
D	SOUTH / KEYS REGION WOOD FRAME HIP ROOF (WH) HOMES.....	191
E	FLORIDA MANUFACTURED SINGLEWIDE HOMES	199
F	FLORIDA MANUFACTURED DOUBLEWIDE HOMES	205
G	FLORIDA PRE-HUD CODE MANUFACTURED HOMES	211
	LIST OF REFERENCES.....	217
	BIOGRAPHICAL SKETCH	222

LIST OF TABLES

<u>Table</u>	<u>page</u>
3-1. Four most common structural types	36
3-2. Population of most common structural types in defined geographic regions	36
3-3. Additional structural types	37
3-4. Population of additional structural types in defined geographic regions	37
3-5. Structural type models for each geographic region.....	38
4-1. Zones 1-6 MWFRS pressure coefficients	49
4-2. Zones 1E-6E MWFRS pressure coefficients	49
4-3. Roof zone C&C pressure coefficient values for selected roof pitches.....	53
4-4. Wall C&C pressure coefficient values	54
4-5. Summary of load conditions applied to simulate extreme wind events.....	66
5-1. Manufacturer's uplift capacity for typical roof-to-wall connections	78
5-2. Mean failure pressures for typical unprotected windows.....	89
5-3. Site-built home summary of wind resistance capacities	95
5-4. Manufactured home summary of wind resistance capacities.....	96
6-1. Site-built home dimensions.....	100
6-2. Manufactured home dimensions	101
7-1. Modeled structural types	125
7-2. Structural types with damage based on combinations of modeled buildings	125
7-3. Hurricane Andrew damages surveyed in the 1993 NAHB report.....	127
7-4. Wood frame home damages surveyed in the 1993 NAHB report.....	128

7-5. Window damage from Hurricane Andrew vs. simulated data	132
7-6. Masonry wall damage from Hurricane Andrew vs. simulated data	135
7-7. Wood frame wall damage from Hurricane Andrew vs. simulated data	137
7-8. Roof-to-wall connection damage from Hurricane Andrew vs. simulated data	139
7-9. Roof sheathing damage from Hurricane Andrew vs. simulated data	141
7-10. Roof cover damage from Hurricane Andrew vs. simulated data	143
8-1. Structural repair cost ratios for Central Florida masonry homes	160
8-2. Non-structural repair cost ratios for Central Florida masonry homes	160

LIST OF FIGURES

<u>Figure</u>	<u>page</u>
2-1. Wind speed vs. height profiles.....	8
2-2. Pressure locations for the differential pressure calculation in Equation 2-8	10
2-3. Pressure tap locations and wind angles.....	15
2-4. Ratio of aggregate pressure to maximum uplift capacity.	16
2-5. Example probability distribution function of damage at a given wind speed.....	21
2-6. Vulnerability curve generation	21
2-7. Fragility curve generation for 60% overall structural damage	22
2-8. Fragility curve for the damage state of 60% overall structural damage	23
2-9. Family of fragility curves for a particular structural type.....	23
3-1. Regional boundaries for building classification.	35
3-2. Distribution of conventional (site-built) home roof pitch values according to the National Association of Home Builders Research Center.....	39
3-3. Distribution of manufactured home roof pitch values according to the National Association of Home Builders Research Center.....	41
3-4. Structural components selected for modeling in the hurricane damage-prediction simulation engine.....	42
4-1. MWFRS pressure zones.....	50
4-2. C&C roof pressure zones.....	51
4-3. C&C wall pressure zones.....	51
4-4. Roof pressure zones for winds perpendicular to the ridgeline.....	52
4-5. Roof pressure zones for winds parallel to the ridgeline.....	52

4-6.	Roof pressure zones for cornering winds.....	52
4-7.	Method of determining shear wall loads from MWFRS pressures.....	57
4-8.	Tributary area for C&C pressures transferred into lateral connections on wood frame walls.....	58
4-9.	Tributary area after significant roof-to-wall connection damage for C&C pressures transferred into lateral connections on wood frame walls.	58
4-10.	Values of the parameter <i>A</i> used in the determination of missile impact.....	61
4-11.	Values of the parameter <i>B</i> used in the determination of missile impact.....	62
4-12.	Values of the parameter <i>D</i> used in the determination of missile impact	64
4-13.	Probability of missile strike causing breakage of a medium (3.5 x 5 ft) window on a 44 ft long windward wall.	65
5-1.	Gaussian distributions with a mean of 100 units and varying coefficients of variation.	69
5-2.	Lognormal vs. Gaussian for a mean of 100 units and coefficient of variation of 0.2	70
5-3.	Truncated Gaussian distribution with a mean of 100 units and a <i>COV</i> of 0.4.....	71
5-4.	Typical arrangement of tie-down anchors for manufactured homes.	94
6-1.	Structural damage simulation engine flowchart	98
6-2.	Angles of wind incidence used for each wind speed	102
6-3.	Flowchart for realizations of a structural type	103
6-4.	Modeled structural components.....	106
6-5.	Batch sampling method for roof-to-wall connections	109
6-5.	Location of forces for the overturning failure check on manufactured homes....	121
7-1.	Histograms of window damage on South/Keys CBG homes.	133
7-2.	Window damage vulnerability of South/Keys CBG homes.	134
7-3.	Fragility curves for 1, 3, 5, 7, and 10 damaged windows for South/Keys CBG homes.....	134
7-4.	Wall damage vulnerability of South/Keys CBG homes.	136

7-5.	Fragility curves for 1, 2, 3, and 4 damaged walls for South/Keys CBG homes.....	136
7-6.	Wall damage vulnerability of South/Keys WG homes.....	138
7-7.	Fragility curves for 1, 2, 3, and 4 damaged walls for South/Keys WG homes....	138
7-8.	Roof-to-wall connection damage vulnerability of South/Keys CBG homes.....	140
7-9.	Fragility curves for 2%, 5%, 10%, 25%, and 50% roof-to-wall connection damage for South/Keys CBG homes.....	140
7-10.	Roof sheathing vulnerability of South/Keys CBG homes.....	141
7-11.	Fragility curves for 2%, 5%, 10%, 25%, and 50% roof sheathing damage for South/Keys CBG homes.....	142
7-12.	Roof cover vulnerability of South/Keys CBG homes.....	143
7-13.	Fragility curves for 2%, 5%, 10%, 25%, and 50% roof cover damage for South/Keys CBG homes.....	144
7-14.	Histograms of roof sheathing damage on South/Keys CBG homes.....	145
7-15.	Histograms of roof-to-wall connection damage on South/Keys CBG homes.....	147
7-16.	Fragility curves for 2%, 5%, 10%, 25%, and 50% roof-to-wall connection damage on South/Keys CBG homes.....	147
7-17.	Histograms of roof-to-wall connection damage on South/Keys concrete block homes.....	149
7-18.	Histograms of roof sheathing damage on South/Keys concrete block homes.....	149
7-19.	South/Keys CBG homes mean damages for roof cover, roof sheathing, roof-to-wall connections, and walls.....	151
7-20.	South/Keys CBH homes mean damages for roof cover, roof sheathing, roof-to-wall connections, and walls.....	152
7-21.	South/Keys WG homes mean damages for roof cover, roof sheathing, roof-to-wall connections, and walls.....	152
7-22.	South/Keys WH homes mean damages for roof cover, roof sheathing, roof-to-wall connections, and walls.....	153
7-23.	Singlewide manufactured homes mean damages for roof cover, roof sheathing, roof-to-wall connections, and walls.....	154

7-24.	Doublewide manufactured homes mean damages for roof cover, roof sheathing, roof-to-wall connections, and walls.....	155
7-25.	Pre-HUD Code singlewide manufactured homes mean damages for roof cover, roof sheathing, roof-to-wall connections, and walls.....	155
8-1.	Preliminary results of the relation of structural damage to insurable content loss compared with insurance claims data from Hurricane Andrew.	161
A-1.	Concrete block gable roof South/Keys Region home comparative levels of roof cover, roof sheathing, connections, wall, and gable end sheathing damage.....	168
A-2.	Vulnerability to roof cover damage for South/Keys CBG homes.....	168
A-3.	Fragility curves for 2%, 5%, 10%, 25%, and 50% damage to roof cover for South/Keys CBG homes.	169
A-4.	Vulnerability to roof sheathing damage for South/Keys CBG homes.....	169
A-5.	Fragility curves for 2%, 5%, 10%, 25%, and 50% damage to roof sheathing for South/Keys CBG homes.....	170
A-6.	Vulnerability to roof-to-wall connection damage for South/Keys CBG homes.....	170
A-7.	Fragility curves for 2%, 5%, 10%, 25%, and 50% damage to roof-to-wall connections for South/Keys Region CBG homes.....	171
A-8.	Vulnerability to wall damage for South/Keys Region CBG homes.....	171
A-9.	Fragility curves for 1, 2, 3 and 4 damaged walls for South/Keys Region CBG homes.....	172
A-10.	Vulnerability to window damage for South/Keys Region CBG homes.....	172
A-11.	Fragility curves for 1, 3, 5, 7, and 10 damaged windows for South/Keys Region CBG homes.....	173
A-12.	Vulnerability to exterior door damage for South/Keys Region CBG homes.....	173
A-13.	Fragility curves for 1 and 2 damaged exterior doors for South/Keys Region CBG homes.....	174
A-14.	Vulnerability to garage door damage for South/Keys Region CBG homes.....	174
B-1.	Concrete block hip roof South/Keys Region home comparative levels of roof cover, roof sheathing, connections, wall, and gable end sheathing damage.....	176

B-2.	Vulnerability to roof cover damage for South/Keys CBH homes.....	176
B-3.	Fragility curves for 2%, 5%, 10%, 25%, and 50% damage to roof cover for South/Keys CBH homes.....	177
B-4.	Vulnerability to roof sheathing damage for South/Keys CBH homes.....	177
B-5.	Fragility curves for 2%, 5%, 10%, 25%, and 50% damage to roof sheathing for South/Keys CBH homes.....	178
B-6.	Vulnerability to roof-to-wall connection damage for South/Keys CBH homes.....	178
B-7.	Fragility curves for 2%, 5%, 10%, 25%, and 50% damage to roof-to-wall connections for South/Keys Region CBH homes.....	179
B-8.	Vulnerability to wall damage for South/Keys Region CBH homes.....	179
B-9.	Fragility curves for 1, 2, 3 and 4 damaged walls for South/Keys Region CBH homes.....	180
B-10.	Vulnerability to window damage for South/Keys Region CBH homes.....	180
B-11.	Fragility curves for 1, 3, 5, 7, and 10 damaged windows for South/Keys Region CBH homes.....	181
B-12.	Vulnerability to exterior door damage for South/Keys Region CBH homes.....	181
B-13.	Fragility curves for 1 and 2 damaged exterior doors for South/Keys Region CBH homes.....	182
B-14.	Vulnerability to garage door damage for South/Keys Region CBH homes.....	182
C-1.	Wood frame gable roof South/Keys Region home comparative levels of roof cover, roof sheathing, connections, wall, and gable end sheathing damage.....	184
C-2.	Vulnerability to roof cover damage for South/Keys WG homes.....	184
C-3.	Fragility curves for 2%, 5%, 10%, 25%, and 50% damage to roof cover for South/Keys WG homes.....	185
C-4.	Vulnerability to roof sheathing damage for South/Keys WG homes.....	185
C-5.	Fragility curves for 2%, 5%, 10%, 25%, and 50% damage to roof sheathing for South/Keys WG homes.....	186
C-6.	Vulnerability to roof-to-wall connection damage for South/Keys WG homes.....	186

C-7.	Fragility curves for 2%, 5%, 10%, 25%, and 50% damage to roof-to-wall connections for South/Keys Region WG homes.	187
C-8.	Vulnerability to wall damage for South/Keys Region WG homes.....	187
C-9.	Fragility curves for 1, 2, 3 and 4 damaged walls for South/Keys Region WG homes.....	188
C-10.	Vulnerability to window damage for South/Keys Region WG homes.....	188
C-11.	Fragility curves for 1, 3, 5, 7, and 10 damaged windows for South/Keys Region WG homes.....	189
C-12.	Vulnerability to exterior door damage for South/Keys Region WG homes.....	189
C-13.	Vulnerability to exterior door damage for South/Keys Region WG homes.....	190
C-14.	Vulnerability to garage door damage for South/Keys Region WG homes.....	190
D-1.	Wood frame hip roof South/Keys Region home comparative levels of roof cover, roof sheathing, connections, wall, and gable end sheathing damage.....	192
D-2.	Vulnerability to roof cover damage for South/Keys WH homes.....	192
D-3.	Fragility curves for 2%, 5%, 10%, 25%, and 50% damage to roof cover for South/Keys WH homes.....	193
D-4.	Vulnerability to roof sheathing damage for South/Keys WH homes.	193
D-5.	Fragility curves for 2%, 5%, 10%, 25%, and 50% damage to roof sheathing for South/Keys WH homes.	194
D-6.	Vulnerability to roof-to-wall connection damage for South/Keys WH homes.....	194
D-7.	Fragility curves for 2%, 5%, 10%, 25%, and 50% damage to roof-to-wall connections for South/Keys Region WH homes.	195
D-8.	Vulnerability to wall damage for South/Keys Region WH homes.....	195
D-9.	Fragility curves for 1, 2, 3 and 4 damaged walls for South/Keys Region WH homes.....	196
D-10.	Vulnerability to window damage for South/Keys Region WH homes.....	196
D-11.	Fragility curves for 1, 3, 5, 7, and 10 damaged windows for South/Keys Region WH homes.....	197
D-12.	Vulnerability to exterior door damage for South/Keys Region WH homes.....	197

D-13.	Vulnerability to exterior door damage for South/Keys Region WH homes.....	198
D-14.	Vulnerability to garage door damage for South/Keys Region WH homes.....	198
E-1.	Singlewide manufactured home comparative levels of roof cover, roof sheathing, connections, wall, and gable end sheathing damage.....	200
E-2.	Vulnerability to roof cover damage for singlewide manufactured homes.....	200
E-3.	Fragility curves for 2%, 5%, 10%, 25%, and 50% damage to roof cover for singlewide manufactured homes.....	201
E-4.	Vulnerability to roof sheathing damage for singlewide manufactured homes. ...	201
E-5.	Fragility curves for 2%, 5%, 10%, 25%, and 50% damage to roof sheathing for singlewide manufactured homes.....	202
E-6.	Vulnerability to roof-to-wall connection damage for singlewide manufactured homes.....	202
E-7.	Fragility curves for 2%, 5%, 10%, 25%, and 50% damage to roof-to-wall connections for singlewide manufactured homes.....	203
E-8.	Vulnerability to wall sheathing damage for singlewide manufactured homes. ...	203
E-9.	Fragility curves for 2%, 5%, 10%, 25%, and 50% damage to wall sheathing for singlewide manufactured homes.....	204
F-1.	Doublewide manufactured home comparative levels of roof cover, roof sheathing, connections, wall, and gable end sheathing damage.....	206
F-2.	Vulnerability to roof cover damage for doublewide manufactured homes.....	206
F-3.	Fragility curves for 2%, 5%, 10%, 25%, and 50% damage to roof cover for doublewide manufactured homes.....	207
F-4.	Vulnerability to roof sheathing damage for doublewide manufactured homes.....	207
F-5.	Fragility curves for 2%, 5%, 10%, 25%, and 50% damage to roof sheathing for doublewide manufactured homes.....	208
F-6.	Vulnerability to roof-to-wall connection damage for doublewide manufactured homes.....	208
F-7.	Fragility curves for 2%, 5%, 10%, 25%, and 50% damage to roof-to-wall connections for doublewide manufactured homes.....	209

F-8.	Vulnerability to wall sheathing damage for doublewide manufactured homes.	209
F-9.	Fragility curves for 2%, 5%, 10%, 25%, and 50% damage to wall sheathing for doublewide manufactured homes.	210
G-1.	Pre-HUD Code manufactured home comparative levels of roof cover, roof sheathing, connections, wall, and gable end sheathing damage.	212
G-2.	Vulnerability to roof cover damage for pre-HUD Code manufactured homes.	212
G-3.	Fragility curves for 2%, 5%, 10%, 25%, and 50% damage to roof cover for pre-HUD Code manufactured homes.	213
G-4.	Vulnerability to roof sheathing damage for pre-HUD Code manufactured homes.	213
G-5.	Fragility curves for 2%, 5%, 10%, 25%, and 50% damage to roof sheathing for pre-HUD Code manufactured homes.	214
G-6.	Vulnerability to roof-to-wall connection damage for pre-HUD Code manufactured homes.	214
G-7.	Fragility curves for 2%, 5%, 10%, 25%, and 50% damage to roof-to-wall connections for pre-HUD Code manufactured homes.	215
G-8.	Vulnerability to wall sheathing damage for pre-HUD Code manufactured homes.	215
G-9.	Fragility curves for 2%, 5%, 10%, 25%, and 50% damage to wall sheathing for pre-HUD Code manufactured homes.	216

Abstract of Dissertation Presented to the Graduate School
of the University of Florida in Partial Fulfillment of the
Requirements for the Degree of Doctor of Philosophy

PREDICTING THE VULNERABILITY OF TYPICAL RESIDENTIAL
BUILDINGS TO HURRICANE DAMAGE

By

Anne D. Cope

August 2004

Chair: Kurtis Gurley
Cochair: Gary Consolazio
Major Department: Civil and Coastal Engineering

Hurricanes have caused billions of dollars in losses in the United States and could devastate up to \$1.5 trillion worth of existing structures in Florida alone. The population density on Florida's 1200-mile coastline continues to grow, and potential losses will continue to mount. The insurance industry and the Florida insurance regulatory agency both require a means of estimating these expected losses. Only a handful of studies exist in the public domain to predict aggregate hurricane damage. Most published studies use regression techniques with post-disaster investigations or claims data to develop vulnerability curves. This approach is highly dependent on the type of construction common to the areas represented in the data, thus limiting the predictive capabilities to regions of similar construction. A promising approach used by one commercial model estimates vulnerability by explicitly accounting for the resistance capacity of building components and load produced by wind. This so-called component approach applies

claims data from previous storms as a validation (rather than calibration) tool, and can be readily adapted to different regions with varying predominant construction.

The Florida Department of Insurance (FDOI) sponsored the development of a public hurricane risk model. The goal of this ongoing project is to predict hurricane wind-induced insurance losses by zip code for the State of Florida, on an annualized basis and for predefined scenarios. The engineering team is responsible for relating specific wind speeds to predicted losses for typical residential buildings in the state of Florida. Our study developed a probabilistic model predicting structural damage from hurricane winds in Florida. The core of this model is a Monte Carlo Simulation engine that generates damage information for typical Florida homes, using a component approach. The simulation compares deterministic wind loads, and the probabilistic capacity of vulnerable building components to resist these loads, to determine the probability of damage. In this manner, probabilistic structural damage is identified over a range of assigned wind speeds. Monetary loss associated with structural damage and the likelihood of occurrence for discrete wind speeds will be determined by models under development by other groups in the project.

CHAPTER 1 INTRODUCTION

Windstorms produce billions of dollars in property and other economic losses annually in the United States. Before Hurricane Andrew struck Florida and Louisiana in 1992, many insurance-industry experts thought the worst possible windstorm would cause no more than \$8 billion in insured property damage (Insurance Information Institute May 2001 Update). Hurricane Andrew resulted in \$15.5 billion in insured property losses, \$26.5 billion in total losses, and 61 fatalities [1]. Before Hurricane Hugo's landfall in 1989, no hurricane had resulted in claims in excess of \$1 billion (Insurance Information Institute May 2001 Update). Hugo resulted in \$7 billion in total losses, and 86 fatalities. In 1999, Hurricane Floyd resulted in \$6 billion in total losses, and 56 fatalities [1]. According to the National Oceanographic and Atmospheric Administration, wind-related disasters far outpace other natural disasters in total loss in the United States. In light of these facts, efforts to estimate expected losses and mitigate damage to residential structures from high-wind events are necessary to maintain the viability of the increasing coastal population and infrastructure along the coastal United States.

The effort to predict and mitigate hurricane damage is of particular importance in the state of Florida (which lies in an area vulnerable to these high-wind events, and has a large and increasing coastal population). Both the insurance industry and the Florida insurance regulatory agency require a means of predicting future losses. In the public domain, only a handful of studies predict aggregate hurricane damage. Most published

studies use regression techniques to develop vulnerability curves from post-disaster investigations or available insurance claims data. Several of these studies are detailed in Chapter 2. This approach of using data from previous storms is highly dependent on the type of construction common to the areas represented in the data. Thus, the vulnerability curves developed in the studies are limited to predicting damage for regions of similar construction. For example, the observed-damage studies and claims data from Hurricane Andrew can be used to develop a relationship between wind speed and probable damage to homes of typical South Florida construction (mostly masonry). These relations would not be suitable for predicting damage from hurricane winds to homes in North Florida, where timber construction is more common. Thus, regression techniques must be enhanced with methodologies that do not require large observed-damage data sets.

A promising approach used by one commercial model estimates vulnerability by explicitly accounting for the resistance capacity of individual building components and load produced by wind, within a probabilistic framework. This so-called component approach applies claims data from previous storms as a validation (rather than calibration) tool, and can be readily adapted to different regions with varying predominant construction. While the overall framework of the Federal Emergency Management Agency sponsored HAZUS® model has been discussed in public literature [2-4], the complex wind-structure interaction choices and assumptions involved in this commercial model are not presented in full detail. Because this particular model and other commercial models sponsored by the insurance industry are largely proprietary, many of the details and assumptions used in their analysis are not available for public use or critique.

In response to the need for a public model to predict hurricane wind-induced insurance losses, the Florida Department of Financial Services sponsored a multi-university project coordinated by the International Hurricane Research Center, and involving meteorological, engineering, actuarial, and computer-resource components. The product of this effort is the prediction of hurricane wind-induced insurance losses for residential structures by zip code in Florida, on both an annualized basis and for predefined scenarios (specific hurricanes).

The engineering team is responsible for relating specific wind speeds to predicted losses, for typical residential buildings in the state of Florida. The University of Florida's contribution to the project, presented in this dissertation, is the development of the model that defines the complex relationships between hurricane wind speed and the resultant structural damage, in a probabilistic framework. The core of this model is a Monte Carlo simulation engine that uses a component approach to generate damage information for typical Florida homes. The Monte Carlo simulation compares deterministic wind loads and the probabilistic load-resistance capacity of building components to determine the probability of damage. In this manner, probabilistic structural damage is identified over a range of assigned wind speeds. This component approach may be developed based on laboratory studies of the capacity of individual components, and proper accounting of load paths and load sharing among components. This allows great flexibility with regard to the types of structures that can be modeled. The development of damage relations is not dependent on the existence of observed hurricane wind damage, but such information can be used to validate and refine the model. The component approach also allows the incorporation of future knowledge (such as additional capacity information on various

components) and the effects of mitigation measures (such as gable end bracing). All of the data, decisions, and assumptions used in the model development are available for public critique.

Research Hypothesis

The complex wind-structure interaction that leads to damage of typical residential buildings during hurricane events can be broken down into three main components: local wind field acting on the building, structural loads caused by the wind field, and resistance capacity of the building components. If the relationship between the local wind field and the structural loads is defined, then the problem of quantifying the risk of wind damage can be addressed by applying a probabilistic framework to the structural loads and resistance capacities of the building components.

The level and likelihood of structural damage will depend on parameters describing the probabilistic representation of loads and resistance. Significant information on probabilistic wind loading is available through wind tunnel and full-scale data sets, provided the assumption that hurricane wind fields can be modeled by the log-law or power-law holds true. These two modeling laws are described in Chapter 2. Laboratory testing and post-storm damage reports provide valuable information on structural resistance. Using this information to simulate the occurrence of hurricane events on typical residential buildings will provide a measure of the ability of current typically constructed residential buildings to withstand hurricane-force winds. Incorporating new construction practices and retrofits (which alter component resistances) into the same probabilistic framework will provide a means of calculating the benefit to homeowners of adding hurricane-damage mitigation features to their homes.

Goals and Objectives

The focus of the research is the development of a simulation engine that provides the probability of structural damage for typical Florida residential structures as a function of peak gust wind speeds. Structural-damage information provided by this simulation engine will serve as the backbone for the engineering component of the first publicly available hurricane-wind damage-prediction models for residential structures. This focus can be represented by four research objectives:

- Select residential models representative of the current building stock in the state of Florida, and identify components of those structures for damage-prediction modeling.
- Quantify the wind-induced loads on the identified components, and select appropriate load paths.
- Identify the probabilistic capacities of individual components to resist wind loads.
- Create a probability-based system-response model that will simulate the performance and interaction of the components of typical Florida homes, and evaluate their vulnerability during interaction with hurricane winds.

Summary of Dissertation

The research objectives described above are detailed in Chapters 3 through 8, following a brief summary in Chapter 2 of previous work in the field of hurricane damage mitigation. Specifically, Chapter 3 presents the results of a survey of current building stock to select typical residential building types and structural components necessary to predict wind damage. Chapters 4 and 5 provide background information and final decisions for the structural wind loads and building component capacities, respectively. Chapter 6 describes the Monte Carlo simulation engine which uses the determined loads and capacities to predict the vulnerability of typical Florida homes to hurricane damage. Results obtained from the simulation process are presented in Chapter

7 and will be used to further develop the public hurricane risk model sponsored by the Florida Department of Financial Services and coordinated by the International Hurricane Research Center. Conclusions about the model, modeling process, and potential for future use are discussed in Chapter 8.

CHAPTER 2 SUMMARY OF PREVIOUS RESEARCH

Previous research in the area of hurricane damage mitigation can be divided into three main groups: efforts to quantify extreme wind loads, post-damage investigations, and damage-prediction models. While numerous articles provide accounts of damage from individual storms, few articles exist on the accurate prediction of hurricane damage before a storm occurs. Most of the damage-prediction models that currently exist are proprietary and unavailable to the public. Information available from post-damage investigations and current methods of predicting future hurricane damage are detailed in the following paragraphs, after an introductory section describing structural wind loads.

Background Information on Structural Wind Loads

At any given instant, a snapshot of wind speed vs. height at a location near a building might resemble the curve in Figure 2-1 A. Removing the turbulent component to consider the mean wind speed over some averaging time at each height increment provides a smooth curve that might resemble the one in Figure 2-1 B. This curve is typically modeled using one of two methods: the log law or the power law. Each method results in a curve similar to the one in Figure 2-1 B, which has a mean wind speed of zero at the ground surface and a constant mean wind speed at a distance above the ground referred to as gradient height. Typically at elevations of 200 meters, the gradient (or reference) height is the level at which the wind speed is no longer affected by the surface roughness.

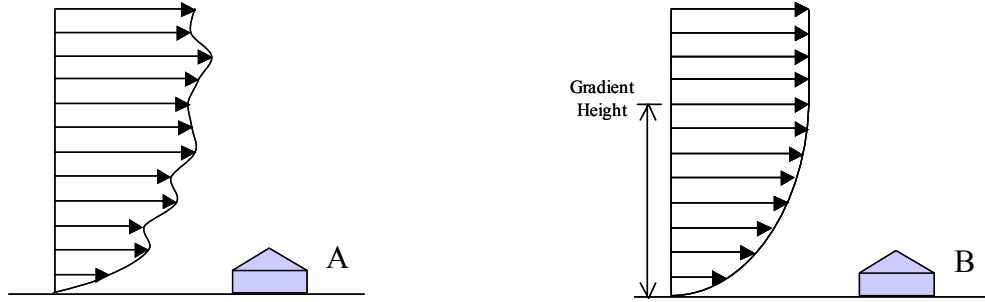


Figure 2-1. Wind speed vs. height profiles. A) Typical profile at any given time. B) Mean wind speed profile.

The log-law and power-law equations used to model the mean wind-speed profile are given in Equations 2-1 through 2-3 [5]. Equations 2-1 and 2-2 define the log law, while Equation 2-3 defines the power law.

$$U(z) = u_* \frac{1}{\kappa} \ln \left(\frac{z}{z_0} \right) \quad (2-1)$$

$$u_* = \sqrt{\frac{\tau_0}{\rho}} \quad (2-2)$$

$$U(z) = U(z_{ref}) \left(\frac{z}{z_{ref}} \right)^\alpha \quad (2-3)$$

In Equations 2-1 and 2-2, $U(z)$ is the mean wind speed at height z , κ is the Von Karman constant (approximately 0.4), z_0 is the roughness length of the terrain over which the wind acts, and u_* is the friction velocity (defined by a ratio of the shear stress at the ground surface, τ_0 , and the density of air, ρ). The roughness length represents the size of a characteristic vortex created as the wind moves over the terrain. The parameters u_* and z_0 are modified for each type of terrain [5]. In the power-law equation, $U(z)$ is the mean wind speed at height z , α is a parameter modified for the type of terrain, and $U(z_{ref})$ is the mean wind speed at reference (or gradient) height, z_{ref} . The two methods provide nearly

identical results for the mean wind speed at heights above ground where low-rise structures exist.

The turbulent component of the wind is most often represented as a Gaussian random variable, with a zero mean and a standard deviation that varies with height. Experimentation reveals that the standard deviation remains constant over the height at which most structures and all low-rise structures exist [5]. The standard deviation of the turbulence component in the direction of wind flow, σ_u ; and the turbulence intensity as a function of height, $I_u(z)$, can be calculated using Equations 2-4 and 2-5 (where A is a constant that varies with the roughness length, z_0 , and has a value of approximately 2.5 for open-country terrain) [5].

$$\sigma_u = Au_* \quad (2-4)$$

$$I_u(z) = \frac{\sigma_u}{U(z)} \quad (2-5)$$

Assuming that mean wind-speed profiles fit the models described above, one can find a relationship between the mean wind speed and the pressure acting on areas of the structure. Generally, the effect of the pressure on the structure is assumed to have two parts: one from the mean wind speed, and one from the gusty or turbulent component. The maximum pressure, p_{\max} , that a component will experience as a result of both of these portions can be expressed as the mean response, p_{avg} , multiplied by a gust factor, G , as shown in Equation 2-6 [6].

$$p_{\max} = Gp_{\text{avg}} \quad (2-6)$$

The most common approach in determining design pressures is to place a model building in a wind tunnel, and conduct pressure coefficient studies. This approach was

used to develop the wind loading provisions for the American Society of Civil Engineer's *Minimum Design Loads for Buildings and Other Structures* (ASCE 7-98) [7]. Roughness elements are placed in the section of the wind tunnel preceding the model building such that the mean wind speed vs. height matches that predicted by either the log law or power law, and the turbulence intensity matches that predicted by the equation for $I_u(z)$.

Pressure at a given location along a streamline can be found using Bernoulli's equation for steady, inviscid, incompressible flow (Equation 2-7), where p is pressure, ρ is the density of the fluid (air in this case), V is the upstream velocity, γ is the specific weight of the fluid, and z is the depth or height with respect to a known reference [8].

$$p + \frac{1}{2} \rho V^2 + \gamma z = \text{constant along a streamline} \quad (2-7)$$

For the case of differential pressure between a point on the surface of the model building and a point just in front of the building at mean roof height (Figure 2-2), Equation 2-8 provides relative change in pressure.

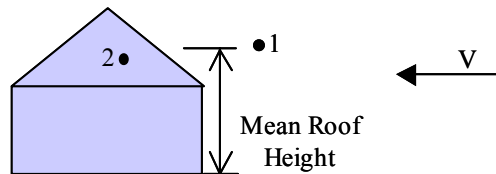


Figure 2-2. Pressure locations for the differential pressure calculation in Equation 2-8

$$p_2 - p_1 = \frac{1}{2} \rho V^2 \quad (2-8)$$

In the wind tunnel, differential pressure is measured at locations of interest on the building with respect to a reference pressure (usually located at gradient height). The raw values of differential pressure are converted to pressure coefficients with respect to the mean roof height of the building by multiplying by a correction factor taken from the simplified version of Bernoulli's equation in Equation 2-8. This process is shown in

Equation 2-9, where C_p is the pressure coefficient at an individual location on the building referenced to mean roof height, P is the measured differential pressure between Locations 2 and 1 as shown in Equation 2-10, $V_{mn_roof_height}$ is the mean velocity at mean roof height, and $V_{gradient_height}$ is the mean velocity at gradient height.

$$C_p = \frac{P}{\frac{1}{2} \rho V_{gradient_height}^2} \left(\frac{V_{gradient_height}^2}{V_{mn_roof_height}^2} \right) \quad (2-9)$$

$$P = p_2 - p_1 \quad (2-10)$$

Fluctuating time histories of C_p at the same location on the building for various angles of wind provide a probabilistic description of the pressure coefficient at that location. This information leads to the selection of pressure coefficient values for component design. Equations 2-11 and 2-12 from ASCE 7-98 illustrate the calculation of design pressure for components and cladding on low-rise structures [7]. Equation 2-11 shows the calculation of velocity pressure at mean roof height, q_h , which is a function of the density of air. The 0.00256 value in Equation 2-11 is $\frac{1}{2}\rho$ for air in English units, K_h is a terrain exposure coefficient, K_{zt} is a topographic effect factor to account for speed up over hills, K_d is a directionality factor, V is the design wind speed, and I is an importance factor for the building. The velocity pressure can be thought of as the pressure measured at Location 1 in Figure 2-2 for the true geographic location of the structure being designed. Multiplying q_h by a wind tunnel generated pressure coefficient provides the pressure acting on the face of the structure at a particular location. The design pressure, p , for each piece is found by multiplying q_h by the difference between the external and internal pressure coefficients with the gust factors built in, GC_p and GC_{pi} , respectively. This process is shown in Equation 2-12.

$$q_h = 0.00256K_hK_{zt}K_dV^2I \quad (\text{ASCE 7-98 Eq 6-13}) \quad (2-11)$$

$$p = q_h [GC_p - GC_{pi}] \quad (\text{ASCE 7-98 Eq 6-18}) \quad (2-12)$$

The parameters for Equations 2-11 and 2-12 provided in ASCE 7-98 are intended to envelope the realistic worst-case scenarios that might occur for the building, so that it will be designed to withstand winds from any angle using a factor of safety worthy of the importance of the building to the community.

Efforts to Quantify Extreme Wind Loads

The ASCE 7-98 design equations for wind pressure on the surface of a building presented in the previous section are intended to envelope a realistic worst-case scenario. Studies have show that this approach can lead to designs that are still un-conservative, or conversely over conservative [9, 10]. Addressing the complexities of wind loading and structural response in a more case-specific manner can rectify these design problems. The accuracy of predicting structural wind loads is directly related to both the exactness with which the behavior of near-surface winds can be predicted and the precision of modeling the wind-structure interaction. The behavior of near-surface winds is highly variable and sensitive to numerous localized characteristics (such as terrain). Moreover, the wind-structure interaction is a highly complex and nonlinear problem, making detailed characterization of wind loads difficult. Efforts to quantify extreme wind loads on structures have sought to increase our understanding of hurricane wind behavior, structural surface pressure characterization, and structural loading effects.

Defining the Behavior of Near-Surface Hurricane Winds

The ASCE 7-98 design equations provided in the previous section are based on the assumption that the winds encountered by a building will behave in a manner predictable

by either the log law or power law previously described. There is some evidence, though, that this assumption can lead to non-conservative predictions of maximum gusts [11].

That is, gust factors used to account for dynamic fluctuations from the mean wind speed may not be suitable when applied to hurricane winds. In-field hurricane wind data collection is a critical component to characterizing gust structure behavior in hurricanes.

Extensive data collection has been conducted for normal weather prediction, and the operation of aircraft and airports. Unfortunately, this information does not provide adequate data for the characterization of near-surface hurricane winds. Recently, several institutions have begun efforts to collect ground level wind data during hurricane landfall. Some of these include the National Hurricane Center, Texas Tech University, Johns Hopkins University, University of Oklahoma, and Clemson University in conjunction with the University of Florida.

The University of Florida and Clemson University have begun a hurricane data collection project known as the Florida Coastal Monitoring Program (FCMP), sponsored by the Florida Department of Community Affairs. One of the main goals of this project is to help improve the fundamental understanding of the dynamic and turbulent action of high-speed hurricane gusts. This is done through the collection of high-resolution wind velocity, pressure, rainfall, humidity, and temperature data using custom-built instrumentation set in the path of a land-falling hurricane. A set of ten and five meter portable towers, equipped with vane and gill anemometers, barometers, hygrometers, and rain gauges, are used to collect the data at several sites within the radius of influence of the land falling hurricane. The FCMP has also instrumented houses in South Florida and the Florida Panhandle area with removable pressure transducers to collect information on

wind forces in the building envelope. The FCMP has produced data sets from named storms over the past four hurricane seasons. Findings from these datasets are still preliminary, but continued efforts will produce a large dataset from which conclusions can be drawn about the nature of hurricane winds at ground level. Information gained about the turbulence intensity and gust eddy size may show that hurricane wind behavior is unique at low-rise structure levels. Until that time, however, the assumption that hurricane winds behave in a manner similar to non-hurricane winds will be used.

Characterizing Surface Pressures on Structures

The values obtained for GC_p in Equation 2-12 are dependent on the effective wind area for the structural member in question. As the effective wind area decreases, the value of the coefficient increases. This trend results from the gust structure of the wind acting on the structure. The turbulent component of the wind acting on a structure results from the buffeting action of wind gusts. These gusts are made of large and small clusters of swirling fluid referred to as eddies. The physical size of eddies is an important characteristic. Small eddies hit the structure in an uncoordinated manner, while the correlated winds of a large eddies can affect the entire effective wind area of some structural components at the same time. The degree of linear correlation between pressures at different locations on model buildings in a wind tunnel can be used to determine the size of the gusts. More importantly, when the buildings are subjected to wind tunnel tests known to model typical open-country conditions, the degree of linear correlation between pressure tap locations can be used to better characterize the nature of wind pressures on specific building components, such as roof sheathing.

A study conducted by the author to better characterize loads on low rise roof structures explored both the spatial correlation and probability characteristics of pressure coefficients acting on the roof and eaves of typical gable roof homes [12]. Investigations were conducted to determine if regions of roof sheathing would have both highly correlated surface pressures and a strong deviation from Gaussian probability. These conditions represent a departure from the assumptions used in the gust factor approach, and indicate that the roof sheathing is likely more vulnerable to damage than current design methods suggest. Several standard non-Gaussian PDF models were associated with different regions in the building envelope using goodness of fit procedures comparing models to wind tunnel data. Significant combined effects (non-Gaussian loads and high correlation over a surface) were found for cornering winds and winds perpendicular to the gable end of the structure.

A follow-up study was conducted to investigate the results of the combined effects of spatial correlation and non-Gaussian probability content on the aggregate loading of one 4 ft x 8 ft piece of roof sheathing located at the ridgeline on the gable end of a typical structure [13]. A non-Gaussian simulation algorithm was used to produce realizations of pressure coefficient time histories at the 14 pressure taps representing a single piece of roof sheathing (Figure 2-3).

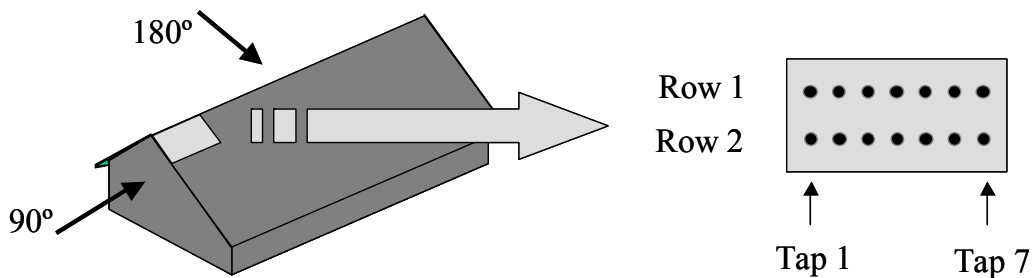


Figure 2-3. Pressure tap locations and wind angles

Using the pressure coefficient time histories, realizations of the aggregate pressure on the sheathing panel were obtained for cases of high, moderate, and low correlation among the pressure taps. The effects of the level of correlation are significant, as demonstrated through comparison of higher-moments of the aggregate pressure coefficient, as a ratio of aggregate pressure with ASCE 7-98 load conditions, and as a ratio of aggregate pressure with an experimentally determined uplift capacity. Figure 2-4 shows the ratios of the aggregate pressure resulting from a 150-mph. 3-second gust wind (ASCE 7-98 wind conditions for South Florida) to the uplift capacity of a typical Douglas fir panel with 6d nails in a 6/12 nail pattern [14]. Results indicate that regions experiencing highly correlated non-Gaussian pressure fields will frequently see loads greater than the capacity of the system (a ratio larger than 1), while the assumption that the pressure field is not correlated, but non-Gaussian results in loads well within the capacity of the system. Complete results can be found in Gioffre, Gurley, and Cope (2002).

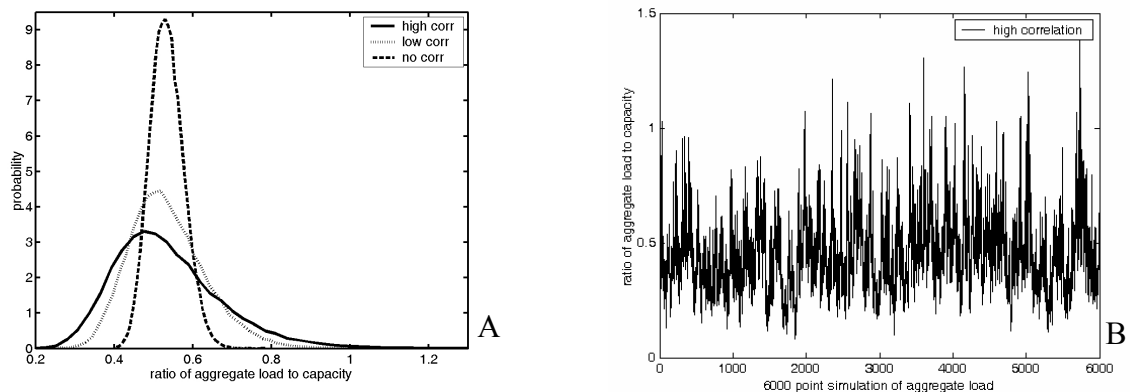


Figure 2-4. Ratio of aggregate pressure to maximum uplift capacity. A) PDF for three levels of correlation among taps. B) Time history for high correlation

Characterizing and Codifying Structural Loads

Some wind engineers seek to incorporate the non-Gaussian qualities of wind pressures discussed in the previous section into better building codes by using database-assisted design methods. Current technology allows design engineers to analyze structural responses with nimble accuracy, yet the wind load provisions remain crudely broad brush. Using wind pressure and climatological databases instead of current wind pressure tables and plots would provide a more risk-consistent design and would allow for the use of the structures own influence lines as opposed to generic, cookie-cutter structural influences built in to current methods [9]. Studies conducted for the development of database-assisted design software reveal the non-Gaussian nature of wind load effects. Specifically, time histories of the bending moments in a steel frame low-rise structure indicate that the Gamma distribution is most appropriate when selecting the maximum peak load [10]. Additional studies reveal that the inclusion of wind directionality effects allows for a more risk-consistent design over the current approach of using a global directionality factor, K_d , of 0.85 (Eq. 2-11). In fact, the current approach for wind directionality effects may lead to an underestimation of the structural wind load in approximately 10–15% of buildings designed using the 1998 standard [9].

Summary of Efforts to Quantify Extreme Wind Loads

Investigations into the nature of hurricane near-surface winds from full-scale data and the nature of wind-structure interaction in the form of pressure coefficient data from wind tunnel testing will continue at the University of Florida and other institutions. Synthesis of the information gained from these efforts will lead to the development of better building codes and design practices. The current body of information concerning wind surface loads on low-rise structures is not robust enough to allow full incorporation

in the Monte Carlo simulation developed for the FDOI hurricane loss projection model. The simulation engine described in subsequent chapters relies on aggregate pressures calculated from pressure coefficient zones. These zones are based on values in ASCE 7-98, but they are modified for directionality using knowledge gained in the previously described research. The details of modification are described in Chapter 4. Inclusion of non-Gaussian behavior and correlation between surface pressures is a promising topic that could be incorporated into the developed model at a later date.

Post-Damage Investigations

Post-damage investigations provide an assessment of how structures perform in extreme wind events and can indicate strengths and weaknesses in design codes and construction practices. Numerous papers discuss damage from Hurricanes Alicia, Andrew, Hugo, Iniki, and Opal [15-23]. In general, the reports contain valuable information on types of failures commonly encountered and recommendations to prevent similar failures in future events, but these observations by experts in the field are not backed by statistically significant numbers of evaluations. For example, the damage to buildings in the Houston-Galveston area during Hurricane Alicia was attributed to the lack of adequate hurricane resistant construction, rather than to the severity of the storm [17, 18]. A similar conclusion was reached on damage to buildings during Hurricane Hugo [23]. A reliability analysis of roof performance during Hurricane Andrew found actual performance to be better than predicted by the governing building code at the time, although the authors stress the need for further research to quantify statistically both construction characteristics and damage due to storms [21]. Phang also offers several observations of the damage on low-rise buildings caused by Andrew. He found that plywood sheathing performed remarkably better than board sheathing, diagonal bracing

was critical at gable ends, and gable roofs showed much more structural damage than hip roofs [22]. Research has also been conducted in Australia by Mahendran who gives an overview of the typical damages encountered by low-rise buildings in the tropics, subjected to either hurricanes or severe storms. In addition, he and the Australian scientific community also stress the fact that full-scale testing is necessary to better predict to behavior of the entire building system when subjected to high-speed winds. While these studies are extremely valuable for the development of safer housing, they do not offer a sufficient basis from which to draw reliable quantitative conclusions [24]. The information obtained from these studies does, however, provide a means of validating the results of a probabilistic approach relating peak wind speeds to structural damage. One would expect the most common types of failures detailed in post-disaster reports to be same as the types of failure obtained from Monte Carlo simulations of hurricane-force winds and structural component resistance.

Post-damage studies also provide a means of estimating the distribution of the building stock in Florida cities. The most comprehensive studies, undertaken by the National Association of Home Builders (NAHB) following Hurricanes Andrew and Opal, include information on the sample size and types of homes investigated [19, 20]. This information, in combination with data from County Property Appraisers and other resources, is useful for predicting typical sizes and types of homes in other Florida areas, as detailed in Chapter 3. Furthermore, the storm damage reports serve as a benchmark by which to set priorities for research efforts since these reports identify the building components that experience the most frequent or most debilitating damage.

Damage Prediction Models

Damage prediction models make use of the current knowledge base to predict damage in future extreme wind events. While several post-damage reports exist in the public domain, there are few damage prediction models available for public review. Those that can be found follow one of two paths. The most common approach is to use post-damage investigation results to create vulnerability or fragility curves for structures (defined in the following section). A second approach is to build a probabilistic model to generate structure fragility curves for damage prediction. This latter approach requires some assumptions about the strength of buildings and type of terrain. Simulations are used to create the curves and data sets to calibrate and validate the results. The advantage to this approach is the ability to generate rational approximations of damage curves for structural types that have not yet experienced a major hurricane. Developing curves based on damage data alone requires the existence of large sets of damage data, while the development of curves based on probabilistic assumptions and simulations can incorporate laboratory data sets and engineering judgment when damage data sets are not available.

Fundamental Concepts in Damage Prediction

Vulnerability and fragility curves are both indicators of the ability of a specified structure to withstand hurricane-force winds. To develop each type of curve, the level of damage or damage state must be defined. For instance, one could identify damage states involving roof failure, wall failure, or some other type of failure. For demonstration purposes, damage can be thought of as a percentage of overall structural damage. Each building will either be undamaged (0% damage), partially damaged by some percentage,

or totally destroyed (100% damage). At a given wind speed, there will be a distribution of percent damage to structures of the same type (Figure 2-5).

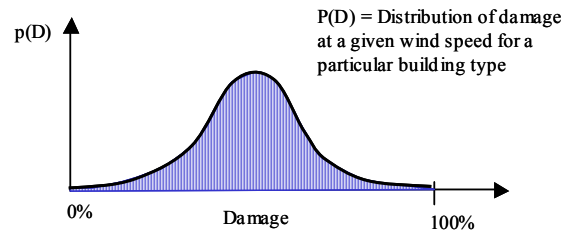


Figure 2-5. Example probability distribution function of damage at a given wind speed

Once the distribution of damage is known over a range of wind speeds, the vulnerability for that type of structure can be determined. The vulnerability curve is a means of measuring the performance of the structure, and is generated from the location of the mean percent damage value from the damage distribution at each wind speed. Figure 2-6 shows the process of vulnerability curve generation from individual PDFs associated with particular wind speeds. The generated vulnerability curve defines the mean damage for a particular structural type as a function of wind speed, where mean is defined as the damage level at which 50% of all structures of that type will be less damaged, and 50% more damaged.

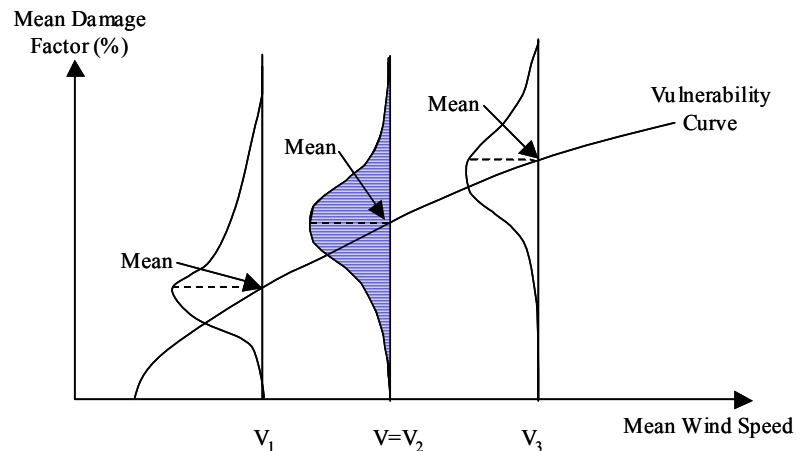


Figure 2-6. Vulnerability curve generation

Fragility curves are another means of describing the performance or reliability of the structure. A fragility curve provides the probability that a certain level of damage will be met or exceeded at a given wind speed, and can be used to determine how many buildings of similar type in an area will experience at least a certain level of damage. This can be thought of as a conditional probability of exceedence. Given the maximum wind speed for a particular wind event, the fragility curve for a type of structure provides the likelihood of damage exceeding a certain threshold. Figure 2-7 and Figure 2-8 show how the fragility curve for a given structural type is determined from available damage distributions at different wind speeds. The example demonstrates how to calculate the fragility curve corresponding to 60% damage by setting a threshold in Figure 2-7 and integrating under each damage distribution from the 60% threshold point to the positive extreme. The integrated values (shaded areas in Figure 2-7) become the data points for the fragility curve at each wind speed (Figure 2-8). The limit on the vertical axis of the fragility curve in Figure 2-8 is 1.0, representing a 100% likelihood of occurrence for the given damage state.

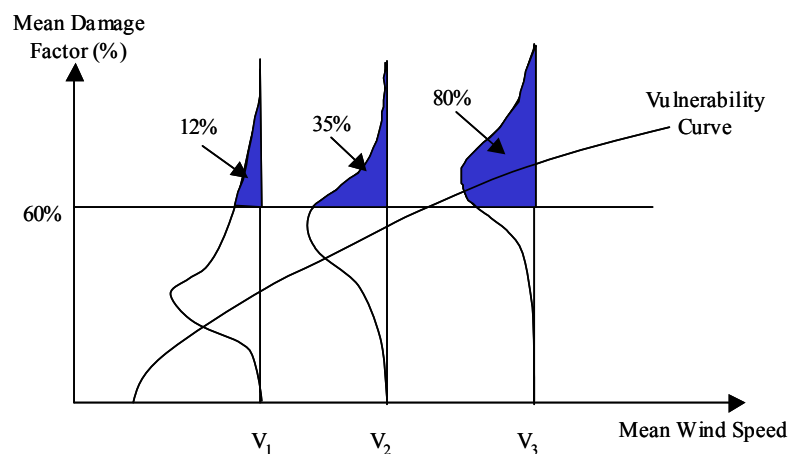


Figure 2-7. Fragility curve generation for 60% overall structural damage

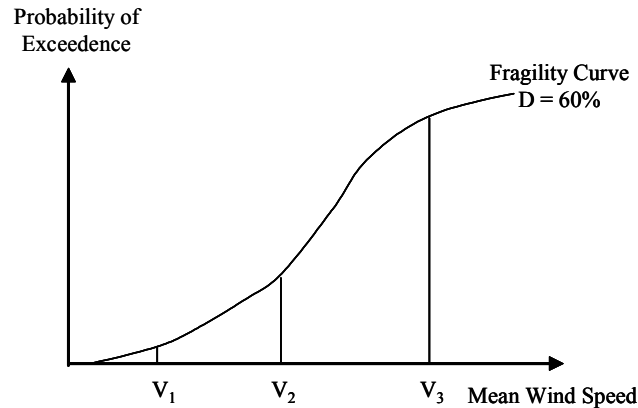


Figure 2-8. Fragility curve for the damage state of 60% overall structural damage

Other damage thresholds can be set to generate a family of fragility curves for this structural type (Figure 2-9). To clarify, the vulnerability curve shows the most likely mean damage that will occur to a given structure as a function of mean wind speed, while the fragility curve shows the probability of exceeding a specific level of damage as a function of wind speed. With vulnerability and fragility curves for structure-type ‘A’, the following types of questions can be answered: 1) for a 90 mph. gust, what is the average expected damage to houses of type ‘A’ (using vulnerability curve) and 2) for a 90 mph. gust, what is the likelihood of seeing 80% damage or greater (using fragility curve)?

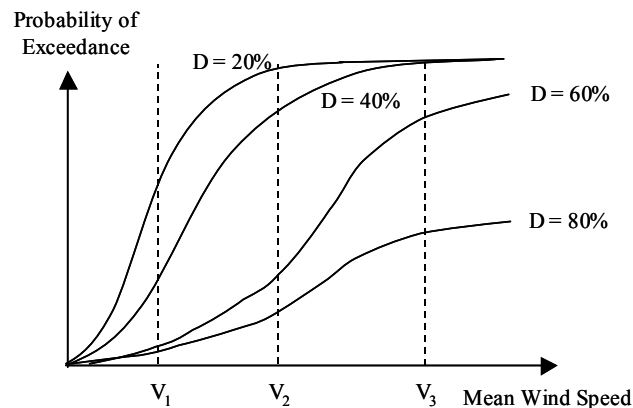


Figure 2-9. Family of fragility curves for a particular structural type

Damage Prediction Models in the Public Domain

Damage prediction models in the public sector using the approach of fitting vulnerability curves from post-damage investigation results include two studies that rely heavily on insurance claim information. The first of these studies determined the relationship between insurance claim figures and wind speed for Typhoons Mireille and Flo [25]. The second performed a similar analysis for Hurricane Andrew [26]. Since the buildings involved in the first study were residential buildings in Japan, the results are not readily applicable to typical residential structures in Florida. The second study used data collected from two large insurance companies in Dade County, Florida to calculate the vulnerability function as a percentage of loss vs. mean wind speed at gradient height. This information is clearly helpful in determining how residential structures typical of those existing in South Florida in 1992 will perform in a hurricane event of similar magnitude. However, this data is a snapshot in time, capturing the damage on structural types that existed when the extreme wind event took place. The data cannot take into consideration improvements in building construction over time, nor can it be readily applied to areas where the terrain and type of construction are notably different.

Others in the public sector have predicted damage using probability-based simulation models to generate the likelihood of damage vs. wind speed. One such study presents the vulnerability curve for a fully engineered building using the assumption that the resistance capacity of the building is lognormally distributed [27]. Since the model was developed for engineered structures, the approach is not likely to yield the best results for predicting damage to typical residential buildings in the state of Florida. Another study presents a method of predicting the percentage of damage within an area as a function of the gradient wind speed, gust factor, average value of the buildings, and

two parameters which govern the rate of damage increase with wind speed [28]. These last two parameters are empirically determined based on experience and knowledge of the area. Since the results of this study were not reproducible, the model is not considered a reasonable approach for the prediction of damage to residential buildings in the state of Florida, given the information currently available.

Insurance data from Hurricane Hugo is used as an example to illustrate the probabilistic approach presented in a recent study for long-term risk analysis [29]. The authors calculated and published statistics for hurricane simulation parameters based on previous storms that made landfall in Florida, North Carolina, and South Carolina. Simulations of hurricane events over 50 year periods and investigation into historical wind speed records were used to predict 50-year mean recurrence interval (MRI) wind speeds at gradient height for selected coastal areas [5]. These 50-year MRI wind speeds at gradient height were converted to ground wind speeds based on the type of terrain present and used in conjunction with fragility curves generated from insurance loss data to predict damage in areas of interest. The authors provided a graphical representation of the generated 50-year MRI wind speeds at gradient height and a fragility curve generated from two sources: insurance claims in Florida after Hurricane Andrew, and claims in South Carolina after Hurricane Hugo. The damage levels predicted by this method are the amount of damage likely to recur once every 50 years, or that have a 2% chance of being exceeded annually in the area of interest, provided the building stock remains relatively unchanged. The difficulty with using this method of damage prediction is the reliance on insurance data from only two events to generate the fragility curve from which losses are predicted for future storms. Unfortunately, information from which to determine accurate

fragility curves for a certain type of structure or family of structures is currently limited. Even if larger data sets were available from other storms, the models would only be valid when used to predict damage to structures of like-construction. This reliance on post-disaster information restricts the ability to project the effects of design modifications, code changes, and retrofit measures on the vulnerability of existing structures. This realization has led to the pursuit of approaches that seek to model damage at the component level rather than for the entire structure. Structural risk assessment is then a matter of combining the vulnerability of the individual parts making up a structure. The so-called component approach allows the flexibility to including new components and retrofit measures, provided lab tests are performed to assess their probabilistic resistance.

Proprietary Damage Prediction Models

Private sector damage prediction models also exist. In the wake of Hurricane Andrew (which generated insurance claims totaling nearly twice the amount thought possible by experts in the field), private sector insurance industry groups contracted damage prediction models from engineering firms to develop a better understanding of the risks associated with a hurricane strikes in heavily populated areas. Access to this information is limited, since the projects are largely proprietary. Currently, some information has been published describing the strategy used to predict damage for these projects. One such study used a re-arranged version of the design pressure equation from ASCE 7-98 (Equation 2-13) to calculate the wind speeds at which individual components will fail [30].

$$V_{failure} = \sqrt{\frac{P_{failure}}{0.00256K_h K_{zt} I [(GC_p) - (GC_{pi})]}}, \quad (2-13)$$

In Equation 2-13, $p_{failure}$ is the statistically sampled failure pressure of the component, K_h is an ASCE-defined terrain exposure coefficient, K_{zt} is an ASCE-defined topographic effect factor to account for speed up over hills, I is an ASCE-defined importance factor, GC_p is a statistically sampled external pressure coefficient, and GC_{pi} is an ASCE-defined internal pressure coefficient. After calculating failure speeds for each component, the researchers determined damage histories for buildings during simulated hurricane events. The result of this analysis was a vulnerability curve for a particular type of building, which can be used with replacement cost information to determine probable insurance losses. The methodology for this study has been published, but the vulnerability results are not available.

The most recent damage prediction model is the HAZUS® Multi-hazard model, which addresses wind, flood, and earthquake hazards. Under the direction of the National Institute of Building Sciences and the Federal Emergency Management Agency, the HAZUS® hurricane model was developed by Applied Research Associates (ARA) over a period of several years. A preview of this model was released to hurricane prone regions of the United States in 2002 that allows users to estimate and evaluate disaster relief resources and policies through scenario analysis [3]. The information supplied by the preview model includes planning for the number of displaced persons, sheltering requirements, and post-storm debris removal. ARA has published a description of the hurricane model's six components: hurricane hazard, terrain, wind pressure, wind borne debris, damage, and losses for buildings. The distinct advantage of the HAZUS® methodology over previous damage prediction methods lies in the fact that it is a component-based model rather than a regression curve fitting model. The HAZUS®

model explicitly accounts for the resistance capacity of individual building components and wind loading, within a probabilistic framework. Using information from British, Australian, and American wind loading codes, as well as boundary layer wind tunnel testing, ARA developed an empirical model for the pressure coefficients on the surface of typical buildings. Techniques for estimating the risk of wind borne debris impact and the effects of sheltering from nearby buildings were also developed. This information was used to create a computer simulation tool that would apply a hurricane wind model (also developed by ARA) to a typical building and evaluate the damage accrued every 15 minutes as a result of wind pressure or wind borne debris impact. Monetary losses resulting from structural damage were obtained by calculating the replacement cost explicitly for the external portion of the building and implicitly for the internal structure and contents. This model has been validated with available insurance records and is considered to be the state of the art in hurricane damage prediction. While the framework for the model has been well defined in public literature, many decisions and assumptions used in the determination of wind loads remain proprietary.

Public Loss Hurricane Projection Model

The Public Loss Hurricane Projection Model is currently under development for the Florida Department of Financial Services, with a scheduled release date of May, 2005. This multi-university project (coordinated by the International Hurricane Research Center) will predict hurricane wind-induced insurance losses for residential structures by zip code for the State of Florida, on both an annualized basis and for predefined scenarios (specific hurricanes). Since the model is sponsored in the public domain, the data, decisions, and assumptions used will be available for public critique. The framework of the model includes a meteorology component to generate probabilistic information about

wind speeds on an annualized basis for each zip code in Florida, an engineering component to relate specific wind speeds to physical damage to residential structures typical of Florida homes, and a financial component to relate physical damage to both content loss and total insurance dollar loss. Subsequent chapters outline the strategies employed in the engineering component of calculating physical damage to typical residential buildings in Florida as function of a series of peak 3-second wind speeds. This model, like the HAZUS® hurricane model, is component-based, explicitly accounting for resistance capacities of structural components and wind loading within a probabilistic framework. The public model is not as complex as the one developed by ARA, foremost in that it does not time step through the entire life cycle of a hurricane. The public model does incorporate, to the extent possible, the current state of the art knowledge in wind pressures, windborne debris and resistance capacities for typical residential buildings in the state of Florida.

CHAPTER 3 RESIDENTIAL STRUCTURES IN FLORIDA

Defining appropriate residential structural models for the state of Florida is a critical step in the development of a simulation engine to predict structural damage in the state as a function of peak gust wind speeds. Wind loading characteristics are heavily dependent on the shape and component make-up of the individual structure under consideration. Thus, the accuracy and reliability of the damage-prediction simulation engine is dependent on proper characterization of the building population in the state. Additionally, the efficiency of the simulation model relies on correctly identifying building components that are susceptible to wind damage. Finally, the resulting damage predictions will be useful only for statistically significant building types. Therefore, knowledge of the types of structures, the components of those structures most susceptible to wind damage, and the distribution of structural types throughout the state is critical to the success of each step in the prediction of hurricane damage.

Research partners in this joint project conducted an in-depth study of building classifications. This chapter summarizes three contributions: statistical analysis of the residential building population of Florida conducted by Liang Zhang of the Florida Institute of Technology, with assistance from the author [31, 32]; manufactured housing research conducted by Luis Aponte of the University of Florida; and a building component investigation conducted by the author. Sources of information for characterizing residential structures in the state of Florida include the Florida Hurricane Catastrophe Fund (FHCF) exposure database, databases of individual county property

appraiser's offices, manufactured home builder literature, and post-damage investigations.

Sources of Information

Florida Hurricane Catastrophe Fund Exposure Database

The FHCF exposure database consists of insurance portfolio data for buildings in the state of Florida. At this time, data available to the team of researchers working on the damage-prediction simulation engine consists of a statistical analysis of the FHCF database for single family residences (SFR) only. Information concerning the population of manufactured homes by ISO classification is not available.

Unfortunately for wind researchers, the ISO classifications used in insurance portfolios focus largely on fire hazards. This information alone does not provide an adequate structural characterization of Florida residences, with respect to wind loading. It can be used (in combination with other sources of information) to identify regional boundaries within the state. For example, the population of masonry homes vs. wood frame homes was found to be consistent among groups of counties in the same geographic area. The ISO construction classifications (described in greater detail in a master's thesis written by a research partner [32]) are

- Frame
- Joisted Masonry
- Non-Combustible
- Masonry Non-Combustible
- Modified Fire Resistive
- Fire Resistive
- Heavy Timber Joisted Masonry
- Superior Non-Combustible
- Superior Masonry Non-Combustible
- Masonry Veneer
- Unknown

County Property Appraiser Databases

The most comprehensive sources of detailed structural information currently available are the individual county property appraiser databases. Each county gathers residential and commercial property data for tax purposes. Database architecture and contents (beyond those required by the Florida Department of Revenue) vary, but each database can be separated into four general categories: commercial property, SFRs, condominiums, and manufactured homes. Commercial property and condominiums are outside the scope of the current work, so the two categories of interest are SFR and manufactured homes. Nearly all of the SFRs in each county are listed in the county property appraiser's database. A large number of manufactured homes are taxed through the Department of Motor Vehicles; however, and are not listed in the property database.

Processing database information from each of the 67 counties in Florida is not feasible for the current project; therefore a selection of counties spread throughout the state is used to obtain information about the characteristics of typical Florida homes. The team was able to gather databases from several counties, but approximately half were unusable because files did not match the database layout provided by the property appraiser's office. The nine counties that supplied databases from which useful structural information was gained are

- Brevard County
- Broward County
- Escambia County
- Hillsborough County
- Leon County
- Monroe County
- Palm Beach County
- Pinellas County
- Walton County

From the databases of the nine listed counties, the type of roof, type of roof cover, exterior wall material, stories, square footage, and year built are investigated for SFRs. This information is useful in identifying the most common residential structural types, but is incomplete as a characterization of homes, with respect to wind loads. Because the information is used for taxation, database categories often describe qualitative information (rather than structural details). For instance, exterior walls may be listed as ‘average’, without indicating the building material. Some database fields lump structurally significant details into a single category. Many counties, for example, use a single designation of ‘hip or gable roof’ instead of separating the two. This difference is structurally significant, as post-damage investigations have noted during past wind events [19]. Additionally, some structurally significant information is not listed in the databases, such as the presence of a garage. In spite of these limitations, the databases supplied by the nine listed counties allowed the research team to develop models representative of typical Florida homes.

Manufactured Home Builder Literature

Information about manufactured homes could not be easily discerned from the individual county property appraiser databases. Since many of these homes are taxed by the Department of Motor Vehicles, construction information from the tax authority is limited. Manufactured home information has been obtained from a report compiled by the National Association of Home Builders (NAHB) Research Center for the Department of Housing and Urban Development comparing site-built and manufactured housing [33] and from contacts with the Partnership for Advancing Technology in Housing (personal correspondence by a research partner, June 2003) and Nobility Homes (personal correspondence by a research partner, June 2003).

Post-Damage Investigations

Literature searches of post-damage reports reveal that observations by experts in the field are useful in supporting the statistical information on building population characteristics gained from other sources of data. However, the post-damage reports themselves usually do not contain enough building evaluations to be considered a statistically significant database from which to characterize Florida's building population. The one exception is the NAHB Research Center report that describes the damage in South Florida after Hurricane Andrew [19]. In this report, the damage to residences is provided within a statistical framework. Unfortunately, this information is available for only one small geographic region following one storm.

Though they are not a source of statistical information about the building population, post-damage reports are vital in determining which building components to model in a hurricane damage simulation engine. The expert opinions in post-damage reports indicate where severe wind damage occurs in typically constructed homes and, therefore, where the most benefit is to be gained from mitigation efforts.

Results of the Building Population Investigation

The information gained in researching the FHCF database, individual county property appraiser databases, manufactured home builder literature, and post-damage reports is detailed in this section. The discussion is divided into two sections: site-built home information is presented first, and manufactured home data follows.

Characterization of Site-Built Homes

The results gained from the nine individual county property appraiser's databases can be generalized to four regions of the state. The choice of regional boundaries is governed in part by the statistics of wood frame houses in each county (an analysis of the

FHCF database conducted by the meteorology team). Additional selection criteria included having at least two representative counties in each defined region and following the population density trends in South Florida. The resulting regions (defined as North, Central, South, and Florida Keys) are outlined on the county map of Florida shown in Figure 3-1. The shaded counties indicate the location of the nine from which property appraiser database information was obtained and successfully processed. A master's thesis written by a research partner details the process of determining the regional borders shown in Figure 3-1 [32].

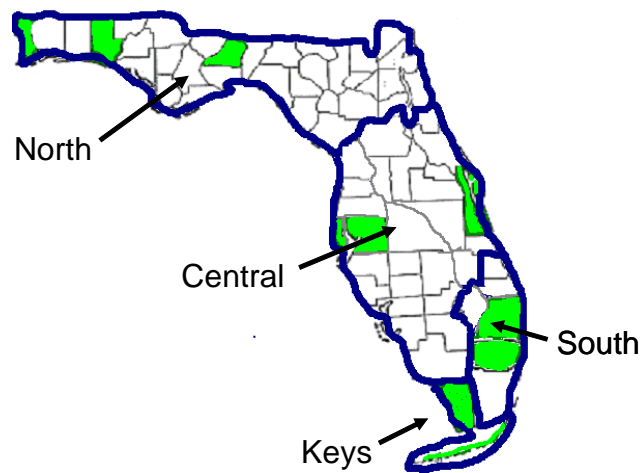


Figure 3-1. Regional boundaries for building classification.

Review of each processed county property appraiser database and the post-Andrew NAHB report [19] indicate that the most common structures in the state can be summarized into four types, provided in Table 3-1. Table 3-2 shows the estimated percentage, \hat{p} , of each type per region and the mean square footage of temperature controlled area, A , for each case. The areas provided for the Keys Region are marked with an asterisk due to their large standard deviation [32]. Because the average home size in the Keys is likely affected by a few grand estates, values from the South Region are used.

Table 3-1. Four most common structural types

Structural Type	Characteristics
CBG	Concrete block gable roof one story home with shingles or tile
CBH	Concrete block hip roof one story home with shingles or tile
WG	Wood frame gable roof one story home with shingles or tile
WH	Wood frame hip roof one story home with shingles or tile

Table 3-2. Population of most common structural types in defined geographic regions

Structural Type	North Region		Central Region		South Region		Florida Keys	
	\bar{p}	A (ft ²)	\bar{p}	A (ft ²)	\bar{p}	A (ft ²)	\bar{p}	A (ft ²)
CBG	12%	1702	42%	2222	46%	2147	23%	3295*
CBH	6%		22%		23%		11%	
WG	39%	1908	12%	1941	4%	2022	12%	2771*
WH	20%		6%		2%		6%	
Sum of most common	77%		82%		75%		52%	
Unknown	14%		13%		11%		23%	
Total coverage	91%		95%		86%		75%	

* Large standard deviation from observed data

The third row from the bottom of Table 3-2 represents the percentage of the SFR population covered by the most common structural types. Those not covered include two story homes, unusually constructed homes, and homes of unknown structural type. Unfortunately, the percentage of homes listed in available data as having an unknown structural type is significant in each region, as shown in the next to last row of Table 3-2. Since these homes cannot be classified, the population represented by this category will be assigned an average value of structural wind damage obtained from an investigation of other structural types in that region. Further details concerning this process are provided in Chapters 7 and 8, in which the structural damage results and conclusions are presented.

The population of SFRs covered by the four most common structural types is adequate in the North, Central, and South Regions, but the Keys Region has a significant number of homes not represented in Table 3-2. Additional structural types are listed in

Table 3-3. The site-built home population represented by these additional groups is provided in Table 3-4, rounded to the nearest whole percent. Using these additional categories, the portions of the building population not counted in Table 3-2 are covered.

Table 3-3. Additional structural types

Structural Type	Characteristics
2CBWG	Concrete block 1 st story, wood frame 2 nd story, gable roof home with shingles or tile
2CBWH	Concrete block 1 st story, wood frame 2 nd story, hip roof home with shingles or tile
2WG	Wood frame two story gable roof home with shingles or tile
2WH	Wood frame two story hip roof home with shingles or tile
2Keys	Two story home of unspecified frame and roof cover
CBGM	Concrete block gable roof one story home with metal roof
CBHM	Concrete hip gable roof one story home with metal roof
WGM	Wood frame gable roof one story home with metal roof
WHM	Wood frame hip roof one story home with metal roof

Table 3-4. Population of additional structural types in defined geographic regions

Structural Type	North Region \hat{p}	Central Region \hat{p}	South Region \hat{p}	Florida Keys \hat{p}
2CBWG	1%	2%	8%	
2CBWH	1%	1%	4%	
2WG	5%	1%	1%	
2WH	2%	1%	1%	
2Keys				3%
CBGM				8%
CBHM				4%
WGM				7%
WHM				3%
Sum of most common types (from Table 3-2)	77%	82%	75%	52%
Unknown	14%	13%	11%	23%
Total	100%	100%	100%	100%

For the Keys Region, a significant portion of the population previously uncounted in Table 3-2 is listed in the categories with an ‘M.’ These match descriptions of the four most common structural types with the exception of the type of roof cover. For the North, Central, and South Regions, two story homes make up the difference. The population of

individual types of two story homes shown in Table 3-4 is small in comparison to the overall population in these three larger regions. Additionally, the entire population of two story homes in the Keys represents only 3% of the population of this smaller region of the state. Given the contribution of two story homes relative to the overall SFR population, separate models are not developed for each two story type listed in Table 3-3. Instead, the performance of two story SFRs is predicted using the one story models in each region. In the North region, the WG and WH models are used as a framework for determining two story damages. Two story homes in the Central and South Regions are based on the CBG and CBH models. A two story model for the Florida Keys uses information from each of the single story models.

Plan dimensions are selected for each type of single story home such that the square footage remains close to the mean area plus an unheated garage of approximately 400 ft², while providing the largest number of whole sheathing panels on the roof surface. Unusually shaped sheathing panel cuts are avoided. The resulting site-built models for single story homes are described in Table 3-5, where the plan dimensions represent the wall lengths. An overhang of two feet on each side adds a total of four feet to both plan dimensions to give the size of the roof surface.

Table 3-5. Structural type models for each geographic region

Structural Type	North Region		Central Region		South Region and Florida Keys Region	
	Plan (ft)	Area (ft ²)	Plan (ft)	Area (ft ²)	Plan (ft)	Area (ft ²)
CBG or CBH	56x38	2128	60x44	2640	60x44	2640
WG or WH	60x38	2280	60x38	2280	56x44	2464

The information presented in Tables 3-1 through 3-5 represents the bulk of information from the available property appraiser databases useful to the structural wind load characterization of SFRs. Unfortunately, additional information critical in the

determination of wind loading conditions is required, but generally not available, from this source. As a result, some structurally descriptive characterizations must be made on a statewide basis, rather than regionally. One of these critical structural characteristics not obtained from the county property appraiser's databases is the slope (or pitch) of the roof, a critical factor in the determination of wind loads on roof surfaces and in the sizing of roof components. A national distribution of typical roof pitch values is presented in Figure 3-2, where the numerator and denominator represent the number of inches of rise and run, respectively. The data for the figure is taken directly from the NAHB Research Center's 1998 report comparing factory built and site-built housing.

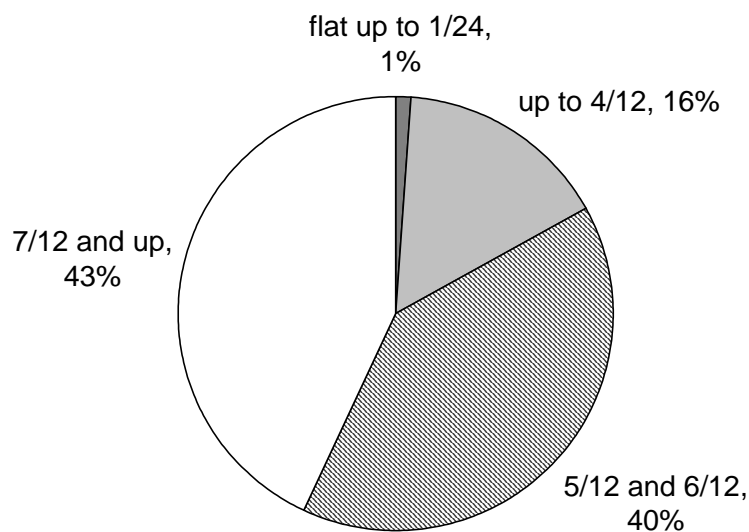


Figure 3-2. Distribution of conventional (site-built) home roof pitch values according to the National Association of Home Builders Research Center.

From the national information presented in Figure 3-2, and discussions with Dr. Leon Wetherington of the University of Florida College of Building Construction (personal correspondence, September, 2002) a pitch of 5 on 12 (5 inches of rise to the linear foot), corresponding to a roof slope, θ , of approximately 23° , is selected as the most representative value for the population of site-built homes in Florida. This choice

becomes an integral part of the wind load criteria for the structure. One section of the wind load provisions of the American Society of Civil Engineers requires interpolation by roof slope, while the other divides structures into three categories: $\theta \leq 10^\circ$, $10^\circ < \theta \leq 30^\circ$, and $30^\circ < \theta$ [7]. Thus, a 5 on 12 pitch falls near the middle of the second category. The wide range of roof slopes covered in this category certainly covers the majority of typical site-built homes. Given the sparseness of data with which to validate separate models, a single representative roof pitch is assigned to the entire population of SFRs in lieu of using the statistics in Figure 3-2 to determine what population of Florida homes should be modeled with separate values of roof pitch.

Characterization of Manufactured Homes

The common structural types presented in Tables 3-1 through 3-5 represent the most prevalent site-built homes in Florida. A similar categorization cannot be made for manufactured homes, given the lack of information about these residences on regional basis. Instead, three types of manufactured home are used for the entire state. The two models representing typical modern manufactured homes are referred to as MH 1 and MH 2 for singlewide and doublewide homes, respectively. Additionally, a separate model, MH-pre, is created to represent older manufactured homes that pre-date the changes in building requirements for these homes enacted in 1975. All three are modeled with gable roofs, in accordance with NAHB Research Center findings that 97% of manufactured home roofs in the United States are gable type [33].

The national distribution of typical roof pitch values for manufactured homes, taken from the NAHB Research Center's 1998 report, is presented in Figure 3-3, where the numerator and denominator represent the number of inches of rise and run,

respectively. Using this national information, a pitch of 4 on 12, corresponding to a roof slope of approximately 18° , is selected to be most representative of the population of manufactured homes in Florida. For the same reasons discussed in the site-built homes section, the roof pitch is selected such that a representative value is applied to population of manufactured homes across the state.

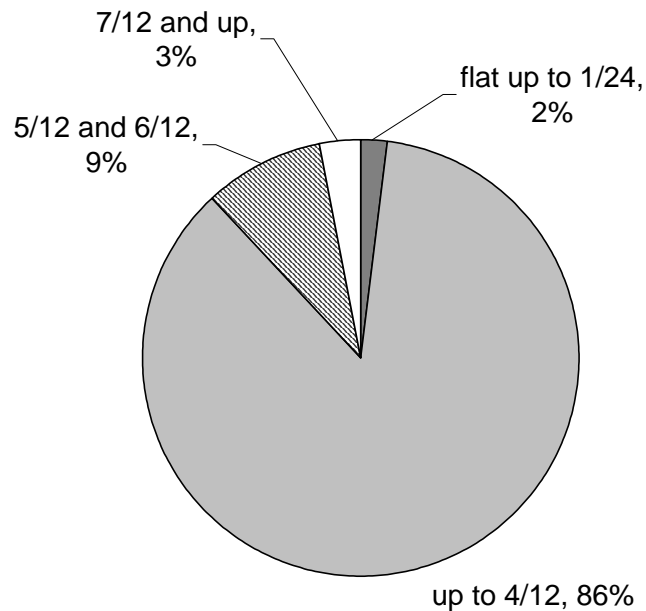


Figure 3-3. Distribution of manufactured home roof pitch values according to the National Association of Home Builders Research Center.

Building Component Selection

It would be impractical and inefficient to model every possible structural component in each of the building types identified in the previous section. Post-damage investigation reports are used to select building components common to all of the structural types that are susceptible to wind damage. In this manner, all of the most commonly observed forms of damage are incorporated into the simulation model, and the results will be comparable across residential classifications.

In a 1993 report detailing Hurricane Andrew damage, the three most critical home characteristics were the protection of openings (windows and doors), type of roof covering, and roof sheathing attachment [19]. Additional post-damage reports and investigations indicate that a reasonable list of wind damage-prone components for typically constructed gable roof residential structures includes the roof covering, roof sheathing, roof-to-wall connections, wall systems, and openings [16-24]. Given this information, the structural building components selected for modeling site-built homes in the simulation engine are (from top to bottom, not by order of importance) roof covering, roof sheathing, roof-to-wall connections, walls, and openings. These broadly defined components are depicted in Figure 3-4. Each of the structural types in Table 3-5 are modeled based on the capacities of these components. Differences among models of the various structural types come from the definitions of capacity, load paths, failure mode, and wind loading. For example, concrete block and wood frame home models both include wall components, though the failure mechanisms and capacities of these systems differ. Also, wind loading differs from hip to gable roofs, though the roof cover capacity is defined as the same.

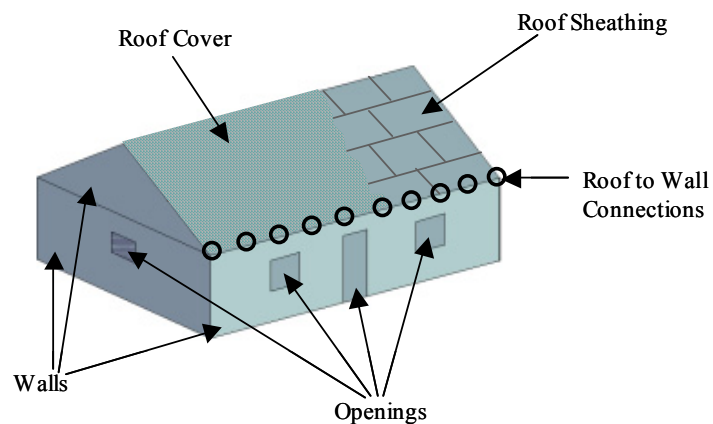


Figure 3-4. Structural components selected for modeling in the hurricane damage-prediction simulation engine.

The five components shown in Figure 3-4 are also used on the manufactured home model, with the addition of tie-down anchors. Further details concerning the building components (specifically the wind loads applied during simulated hurricane events and the resistance capacity of each component) are discussed in Chapters 4 and 5. The method by which the simulation engine uses this information to predict probabilistic damage information for each type of structure is detailed in Chapter 6. Validation of the methods using available data from Hurricane Andrew is presented in Chapter 7.

CHAPTER 4 STRUCTURAL WIND LOADS FOR TYPICAL

This chapter details the loads applied to simulate an extreme wind event on a typical residential structure. The load cases described here are used in the Monte Carlo simulation engine discussed in Chapter 6 to predict the vulnerability of typical Florida homes to structural damage. These loading conditions are not intended to represent design levels. Instead, load values are selected to best represent the pressure or uplift acting on each component of the home during an extreme wind event, such as a hurricane or tropical storm. The preferred method would be to use wind tunnel data to accurately model the spatial and temporal characteristics of the pressure coefficient on the surface of the building as a function of the wind direction. As discussed in Chapter 2, however, the current body of wind tunnel test data does not support the use of laboratory generated surface pressure characteristics on typical Florida residences. This conclusion is not at all surprising. Wind tunnel tests have been conducted successfully over the years to determine the envelope of worst-case loads for appropriate wind load codification. The probabilistic character of surface pressures was not investigated to the level of detail necessary to randomly generate appropriately scaled and correlated surface pressures on all sides of a structure during a hurricane event. Inclusion of non-Gaussian behavior and correlation between surface pressures in design loads is a promising topic that is currently being investigated [9, 10], and it might be possible to incorporate this data into the developed model at a later date. At this time, however, appropriate wind loads for each building component must be determined from the existing body of data, which includes

current wind load design provisions, wind tunnel data, and full scale data sets described in Chapter 2.

Engineering judgment, based on this supporting body of information, must be used to select the most appropriate external and internal pressures to use in the calculation of event-specific wind loads for building components. For this reason, the wind loads selected for each building component are based on a modified version of the 1998 Minimum Design Loads for Buildings and Other Structures (ASCE 7-98) code provisions. Changes made to the code provisions include modifying the equations used to calculate surface pressures, re-mapping the pressure coefficient zones on the roof surface as a function of the wind direction, and recalculating the internal pressure after initial damage has occurred. Details of these modifications to the code provisions for the purpose of representing storm event loads are discussed in the first section of this chapter. Following that is a discussion of the application of the modified code provisions on the structural components of typical Florida homes. Load conditions placed on roof cover, roof sheathing, roof-to-wall connections, walls, openings, and tie-down anchors (on manufactured homes only) for the purpose of simulating extreme wind events are identified. A summary table of the wind load conditions applied during the structural damage simulation engine is provided at the end of the chapter.

Use and Modification of the ASCE 7-98 Code Provisions to Represent Load Conditions during Extreme Wind Events

Wind loads used for the prediction of structural damage in the simulation model must represent surface pressures acting on each component during an extreme wind event. They should not match design pressures that envelope the worst-case scenarios, but should instead be dependent on the direction of the wind, and representative of the

pressure at a given moment in time. With this in mind, the load cases for the structural damage simulation engine are generated by removing the conservatism incorporated in the ASCE 7-98 code provisions and by changing the external pressure coefficient zones such that the map of pressures on the roof surface is dependent on the wind direction.

Modifications to Surface Pressure Equations

Wind pressures on the surface of simulated homes are generated using modified versions of the ASCE 7 design wind pressure equations discussed previously in Chapter 2. Equations 2-11 and 2-12, for calculation of the velocity pressure at mean roof height, q_h , and the design pressure, p , are reprinted here for clarity. The value 0.00256 in Equation 2-11 is a function of the density of air in English units, K_h is a terrain exposure coefficient, K_{zt} is a topographic effect factor to account for speed up over hills, K_d is a directionality factor, V is the design wind speed, and I is the importance factor. Equation 2-12 illustrates the calculation of p from q_h , where C_p and C_{pi} are the external and internal pressure coefficients, respectively, and G is the gust factor.

$$q_h = 0.00256 K_h K_{zt} K_d V^2 I \quad (2-11)$$

$$p = q_h [G C_p - G C_{pi}] \quad (2-12)$$

Three of the four factors in Equation 2-11 are removed in the development of the equation for use in the simulation routine. The importance factor, I , is discarded because it is used to scale loads according to the importance of the structure to the local community. This factor plays a critical role in design, but does not assist in the determination of actual loads during a hurricane event. Additionally, the directionality factor, K_d , is removed. This factor reduces design pressures to account for the fact that every section of the building will not be loaded to the design level at a given time. Since

the directionality of the wind will be explicitly accounted for in the re-mapping of the external pressure coefficient discussed in the following section, the reduction factor K_d is removed. Lastly, few places in the state of Florida would warrant an escarpment factor greater than 1.0, therefore K_{zt} is unnecessary in the current endeavor. The remaining factor, K_h , has a prescribed value of 0.85 for low-rise structures ($h \leq 15$ ft) in open-country terrain (Exposure C). Substituting the value of K_h into Equation 2-11 and removing the three factors I , K_d , and K_{zt} ; the resulting equation used to calculate the velocity pressure in the simulation routine is provided in Equation 4-1, where V is the maximum 3-second gust wind associated with a particular storm or recurrence interval.

$$q_h = 0.00256(0.85)V^2 \quad (4-1)$$

The time scale of 3 seconds is selected to match the design wind speeds of ASCE 7-98. Use of a different time scale would necessitate additional modifications to the external pressure coefficients used in the simulated wind load equations. It can be assumed that the maximum 3-second gust wind speed will occur several times over the period of the storm, since hurricanes generally last several hours. Therefore, damage can be assessed using this discrete value without undue concern for the length or cyclic nature of the load application.

The safety factor embedded in the ASCE Component and Cladding (C&C) pressure coefficients on roof surfaces was determined by experimentation to be 1.25. This number was obtained from an unpublished study conducted by the author to compare uplift values on a roof shape for which wind tunnel data was available, and through extensive discussions with Dr. Emil Simiu, an expert in the field, about the codification of wind tunnel pressures and the available damage statistics from Hurricane Andrew (personal

communication, November 2001). Assuming that the same level of risk is maintained in the design provisions for all building components, a factor of 0.8 is added to the calculation of surfaces pressures represented in Equation 2-12. In this manner, the reduction factor of 0.8 is used to remove the ‘safety factor’ embedded in the code provisions for load calculations. A similar procedure described in Chapter 5 is used to factor resistance values. Factors to increase expected loads and decrease expected resistances are necessary in the design process to account for the uncertainty of each and reduce the risk of failure. Removal of these factors is necessary such that ‘true’ loads during generated wind events can be compared to probabilistically ‘true’ capacities in the process of predicting of structural damage vulnerability.

The application of the 0.8 factor to remove the built in safety value in the code provisions yields Equation 4-2. Together, Equations 4-1 and 4-2 are the basis for all wind load calculations used for structural damage prediction in the Florida Department of Financial Services sponsored Public Loss Hurricane Projection Model.

$$p = q_h (0.8) [GC_p - GC_{pi}] \quad (4-2)$$

Use and Modifications to External Pressure Coefficients

External pressure coefficients in the ASCE 7-98 provisions include both Main Wind Force Resistance System (MWFRS) coefficients and Component and Cladding (C&C) coefficients. For brevity’s sake, a full description of the design process is not provided in this document. Simply put, the MWFRS loads are applied to the structure as a unit (to provide checks for items such as diaphragm shear walls), while the C&C loads are applied to individual members (for single unit capacity checks). It is important to note, however, that both provisions (MWFRS and C&C) must be satisfied in the design.

The structural damage-prediction model uses a combination of these two provisions to best represent the load cases on modeled components during hurricane winds. Table 4-5, at the end of the chapter, provides a summary table of the load conditions (MWFRS or C&C) applied to each modeled component during the simulation routine. This section details the MWFRS and C&C external pressure coefficients taken from the ASCE 7-98 provisions and the modifications made for use in the damage-prediction model.

Main Wind Force Resisting System external pressure coefficients

The ASCE 7-98 MWFRS provisions are wind-direction dependent, and require no modification for use in Equation 4-2. Values for the external pressure coefficient, C_p , used in Equation 4-2 for MWFRS conditions are provided in Tables 4-1 and 4-2. To each value, a gust factor, G , of 0.85 is applied to obtain GC_p in Equation 4-2. The location of each pressure zone is provided in Figure 4-1, taken directly from ASCE 7-98. Values for Case A are interpolated for two roof pitches (5 on 12 for site-built homes and 4 on 12 for manufactures homes) from the values provided in ASCE 7-98. The characteristic dimension, a , is the lesser of 10% of the smallest horizontal dimension and 40% of the mean roof height, but not less than 4% of the smallest horizontal dimension or 3 feet [7].

Table 4-1. Zones 1-6 MWFRS pressure coefficients

	MWFRS Pressure Zones (shown in Figure 4-1)					
	1	2	3	4	5	6
Case A for 5 on 12	0.538	-0.456	-0.467	-0.414	NA	NA
Case A for 4 on 12	0.516	-0.690	-0.469	-0.415	NA	NA
Case B (all roof pitches)	-0.450	-0.690	-0.370	-0.450	0.400	-0.290

Table 4-2. Zones 1E-6E MWFRS pressure coefficients

	MWFRS Pressure Zones (shown in Figure 4-1)					
	1E	2E	3E	4E	5E	6E
Case A for 5 on 12	0.771	-0.722	-0.648	-0.598	NA	NA
Case A for 4 on 12	0.780	-1.070	-0.673	-0.609	NA	NA
Case B (all roof pitches)	-0.480	-1.070	-0.530	-0.480	0.610	-0.430

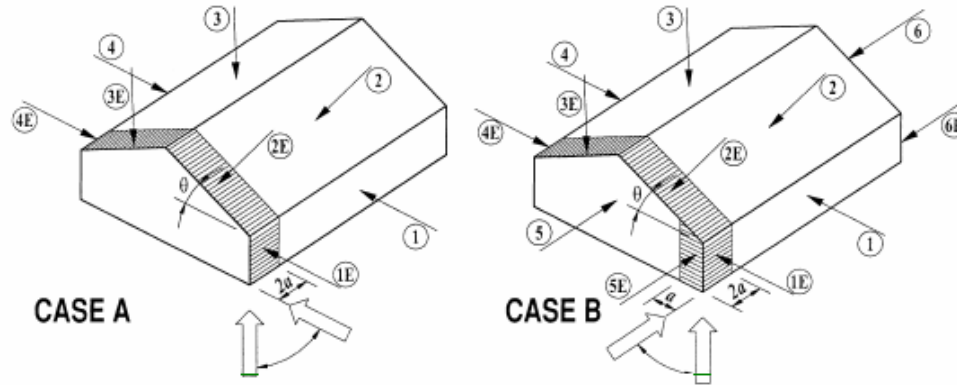


Figure 4-1. MWFRS zones. A) Winds perpendicular to the ridgeline through cornering winds. B) Cornering winds through winds parallel to the ridgeline. (ASCE 7-98 Standard, Minimum Design Loads for Buildings and Other Structures, American Society of Civil Engineers, New York, NY. Fig 6-4, p. 43)

Component and Cladding external pressure coefficients

Modifying the C&C pressure coefficients on the roof surface and walls to account for the directional nature of wind pressures is accomplished by manipulating the mapped zones to represent observed damage patterns and wind tunnel pressure investigation results. The ASCE 7-98 pressure zones for the design of roof cladding on gable and hip roofs are shown in Figure 4-2. Zone 3 (the highest magnitude of suction) is applied at each corner, and Zone 2 is applied to locations of discontinuity on the roof surface. Zone 1 (the lowest magnitude of suction) is applied to all areas not covered by Zones 2 and 3. Figure 4-3 indicates the pressure zones for the wall surfaces. Zone 5 (the highest in magnitude) is applied to each corner and Zone 4 is applied to all other surfaces.

The ASCE pressure zones provided in Figures 4-2 and 4-3 envelope the worst-case scenarios for the life of the structure. Using these provisions, the designer is not required to determine which way the building will face relative to the most likely wind direction. Components in all corners are designed to the same wind pressures. Structures will not experience pressures in this manner during actual loading conditions, however.

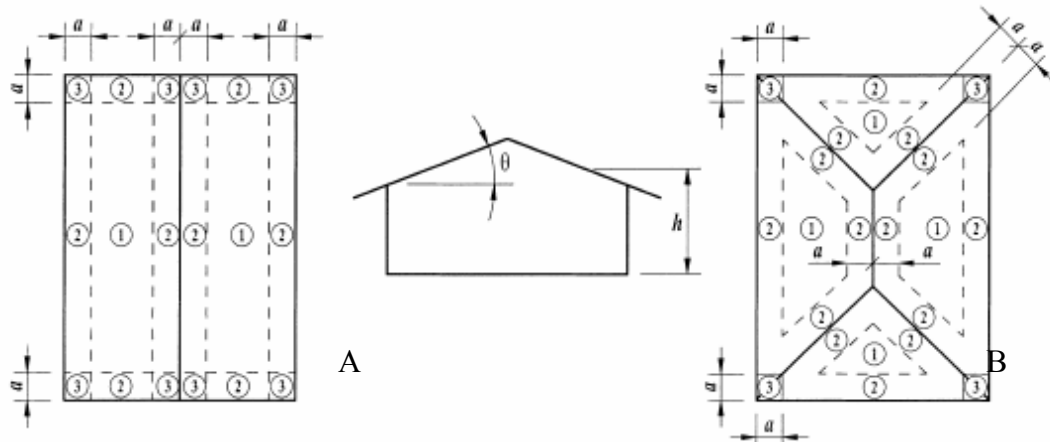


Figure 4-2. C&C roof pressure zones. A) Gable roof zones. B) Roof slope diagram. C) Hip roof zones. (ASCE 7-98 Standard, Minimum Design Loads for Buildings and Other Structures, American Society of Civil Engineers, New York, NY. Fig 6-5B, p. 46)

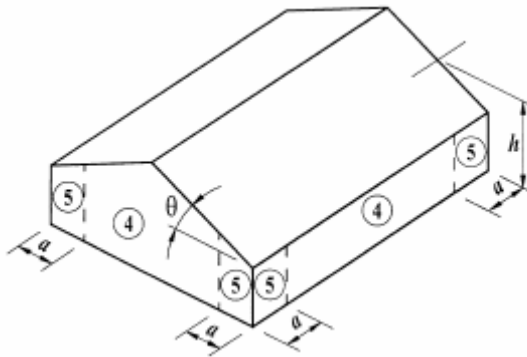


Figure 4-3. C&C wall pressure zones. (ASCE 7-98 Standard, Minimum Design Loads for Buildings and Other Structures, American Society of Civil Engineers, New York, NY. Fig 6-5A, p. 44)

Engineering judgment is required to manipulate the map of design pressures into a layout that is dependent on the wind direction. Modifications to the ASCE 7-98 Component and Cladding roof pressure zones for varying angles of wind are shown in Figures 4-4 through 4-6. The characteristic dimensions for zone width, a , remains as described in ASCE 7-98, with the exception of the cornering wind case. The width of Zone 3 and the width of Zone 2 over much of the windward side are increased to $2a$ for

cornering winds on gable roof structures. Figures 4-4 through 4-6 are not drawn to scale. Modifications to the wall pressure zone layout (no figure) include removing the edge zone on the windward and leeward walls to apply a single uniform pressure across the face of the wall. The leading edge zone on the side walls is maintained, and the trailing edge zone is removed.

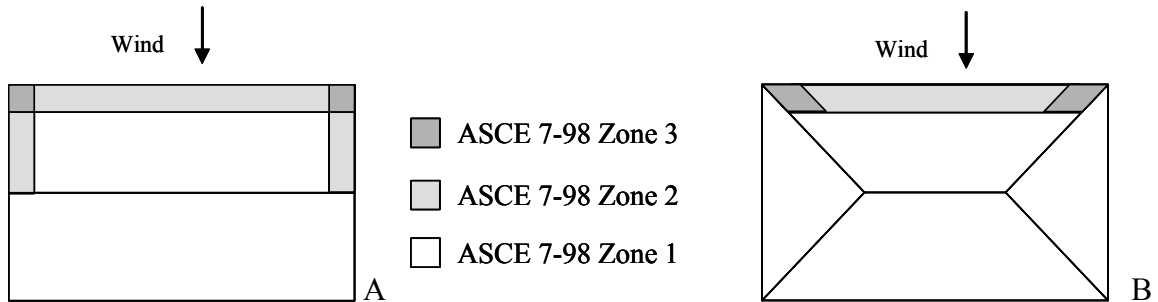


Figure 4-4. Roof pressure zones for winds perpendicular to the ridgeline. A) Gable roof zones. B) Hip roof zones.

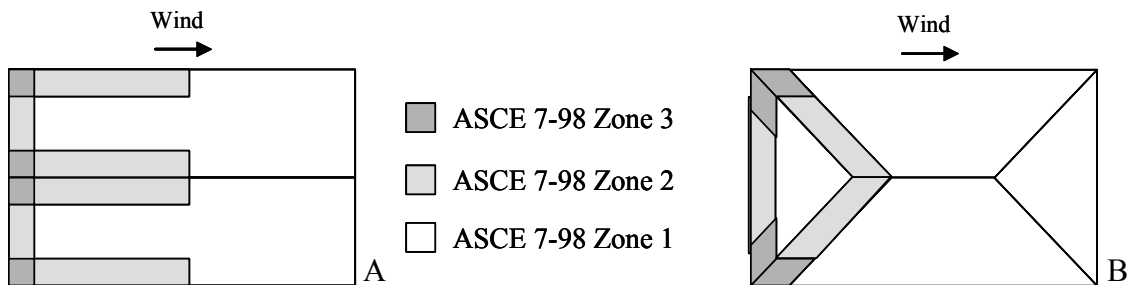


Figure 4-5. Roof pressure zones for winds parallel to the ridgeline. A) Gable roofs zones. B) Hip roof zones.

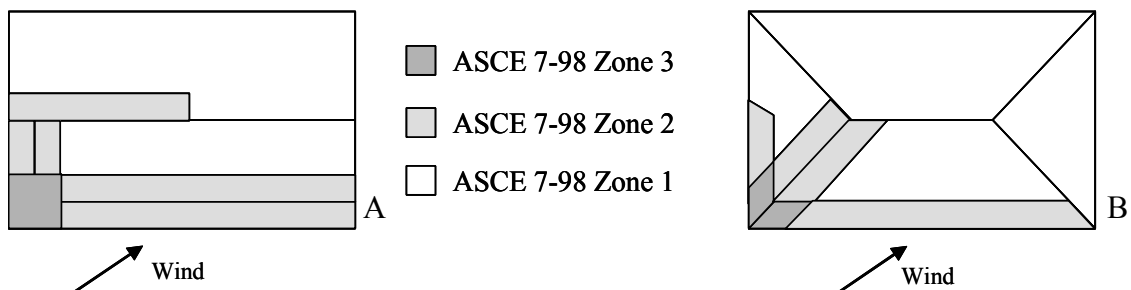


Figure 4-6. Roof pressure zones for cornering winds. A) Gable roofs zones. B) Hip roof zones.

In the ASCE design provisions, the gust factor and external pressure coefficient for C&C loads are combined into one term, GC_p , which is dependent on the effective wind area of the component being designed and, in the case of roof components, on the roof pitch as well. The effective wind area for components is defined by ASCE as the maximum of two possible values: the tributary area for the component in question, and the span length times an effective width of one-third of the span length. The effective wind area for fasteners is the worst-case tributary area for an individual fastener [7]. As the effective wind area decreases, the magnitude of the external pressure coefficient increases, providing smaller areas with larger magnitude load cases and larger areas with smaller magnitude pressures. Since the entire region of a large tributary area is not likely to be loaded to maximum capacity at the same time, a uniform design load of smaller capacity is applied to the surface of large areas. In the structural damage simulation program, efforts have already been taken to eliminate the conservatism or ‘safety factor’ built into the design code, and to map the pressure coefficients such that the layout is dependent on the wind direction. Given this approach, and the reliance of most of the modeled components on fasteners (e.g. sheathing), the values taken from the ASCE 7-98 provisions for C&C external pressure coefficients are those with an effective wind area of 10 ft² or less. Values for roof zone pressure coefficients are provided in Table 4-3, and values for wall surfaces are provided in Table 4-4. The modified location of roof pressure zones is given in Figures 4-4 through 4-6.

Table 4-3. Roof zone C&C pressure coefficient values for selected roof pitches

	GC_p
Zone 1	-0.9
Zone 2	-2.1
Zone 3	-2.1

Table 4-4. Wall C&C pressure coefficient values

	GC_p
Windward Wall	1.0
Side Wall Leading Edge (distance of a from the corner)	-1.4
Side Wall	-1.1
Leeward wall	-0.8

Use and Modifications to Internal Pressure Coefficients

Since extremely low barometric pressures mark hurricane events, the internal pressure in modeled homes is assumed to be greater than the outside pressure before any damage occurs to the structure. With this rationale, the default value of internal pressure assigned to all homes in the structural damage simulation model is obtained by setting the internal pressure coefficient in Equation 4-2 equal to +0.18, the value provided in ASCE 7-98 for enclosed structures. As described in Chapter 6 of this document, initial failure checks are conducted to determine whether individual windows, doors, pieces of roof sheathing, or shear walls fail. A subsequent internal pressure, dependent on the level of initial damage to the home, is calculated as the weighted average of the pressure at the location of broken doors and windows, to include the garage door. This value is used in the final round of failure checks, described in greater detail in Chapter 6.

Application of the Modified ASCE 7-98 Code Provisions to Produce Extreme Wind Event Load Conditions on Selected Building Components

The modified external and internal pressure coefficients discussed in the previous section are used with Equations 4-1 and 4-2 to generate the load conditions which simulate the occurrence of an extreme wind event on both site-built and manufactured Florida homes. In this section, the selection of modified external pressure coefficients for load conditions placed on roof cover, roof sheathing, roof-to-wall connections, walls, openings, and tie-down anchors (on manufactured homes only) are specifically identified.

Resistances to these wind loads are discussed in Chapter 5, and the order of application and failure checking conducted by the simulation engine are detailed in Chapter 6.

Roof Cover and Roof Sheathing Loads

Roof covering materials and roof sheathing panels are treated as cladding during the structural damage simulation. The most likely sheathing panel arrangement for each of the models described in Table 3-3 and for both of the manufactured home models is obtained by starting with a full sheathing panel on one of the lowest corners, and placing additional panels in an offset pattern. Given the amount of uncertainty in roof cover loading and wind resistance, any efforts to define the area of an individual roof cover unit would not add to the accuracy of the damage prediction results. In light of this information, a section of roof cover is assigned to each sheathing panel on the drawn roof sheathing arrangement. The individual sections of roof cover thus have the same square footage as the underlying sheathing panels. The resulting model-specific roof layouts are used to obtain aggregate external pressure coefficients for each individual piece of sheathing and roof cover at each wind angle using the pressure coefficient maps of Figures 4-4 through 4-6. Reasons for using the aggregate pressure over point pressures are discussed in the section of Chapter 5 devoted to the resistance capacity of roof cover and sheathing.

Wind loads for each piece of roof sheathing are obtained by using the aggregate external pressure from the model-specific layout with the appropriate internal pressure coefficient for the state of the building in Equation 4-2. Since the roof cover is attached to the outside surface of the roof sheathing, it is not subject to the same internal pressure fluctuations. In order to best represent the load case that would occur during an actual storm event, the wind loads for roof cover areas are obtained by using the aggregate

external pressure from the model-specific roof layout and an internal pressure coefficient of zero in Equation 4-2.

Roof-to-Wall Connection Loads

Roof-to-wall connections are modeled in tension, using the dead load and wind-induced uplift from the roofing system. As described further in Chapter 6, these connections are one of the last building components checked for failure. The loads applied result from the remaining roof sheathing. In this manner, overloaded roof sheathing panels are assumed to fail before passing the overloaded condition to the trusses. An assumed dead load of 10 psf (which includes the weight of typical roof cover, roof sheathing, suspended ceiling, insulation, and ductwork) is applied to each sheathing panel that remains on the roof surface after the initial failure check. Wind uplift is obtained from the loads previously described for the sheathing panels, and individual connection loads are calculated using a tributary area approach, assuming that trusses are spaced at 2 feet on center in most homes. Gable end trusses are assumed to have a total of eight gable end type connectors. Loads on the two end trusses for gable roof structures are equally distributed to these connections.

Roof-to-wall connections are the only building component in the developed Public Loss Hurricane Projection Model where the redistribution of load is applied. Redistribution is not appropriate for other components, but is used here to capture the failure mechanism by which the entire roof separates from the walls [19]. Once a roof-to-wall connection fails, the load is redistributed to the surrounding connections until the system reaches a point of equilibrium. Additional details of this method are provided in Chapter 6.

Wall Loads

Walls on site-built homes are modeled in shear, uplift, and bending. The total shear for each wall is computed using the MWFRS pressure coefficients from ASCE 7-98 provided in Tables 4-1 and 4-2 and the standard practice of modeling the roof diaphragm as a simply supported beam. In this manner, the surface pressures on opposite sides of the house can be multiplied by half of the building height to produce a distributed load on the length of the roof diaphragm beam. Shear loads in each supporting wall are the reactions to this distributed load. This method is shown in Figure 4-7. During cornering winds, both cases are applied independently.

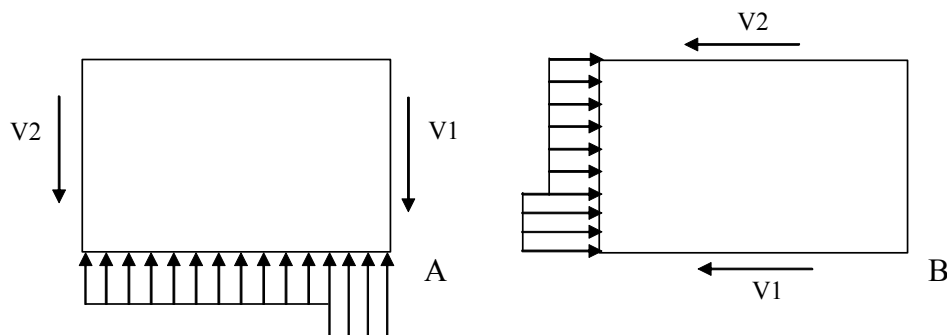


Figure 4-7. Method of determining shear wall loads from MWFRS pressures. A) Winds perpendicular to the ridgeline through cornering winds. B) Cornering winds through winds parallel to the ridgeline.

The uplift forces on each wall are obtained per foot of wall by averaging the total uplift from the attached roof-to-wall connections over the length of the wall. Lateral pressures for wall surfaces are obtained using Equation 4-2 with C&C coefficients given in Table 4-4 and the appropriate internal pressure coefficient for the building. From these lateral pressures, the bending moments per foot of wall for concrete block walls are obtained with the assumption of simple supports at the roof and floor. This assumption is maintained unless more than half of the roof-to-wall connections fail, at which point the

bending moment is amplified by a factor of 2.8. This factor (70% of the multiplier between simply supported and cantilevered moments) is selected for use over the pure cantilever condition since the wall would retain some support from the side and interior walls, even if the roof-to-wall connections have failed.

Wood framed walls exhibit different behavior when confronted with out of plane load conditions; therefore the bending moment is not calculated for these types of walls. Instead, the lateral force at the wall connection that results from C&C surface pressures on the wall is used. In this procedure, the presence of at least one interior wall on each of the four perimeter walls is assumed. Under this premise, the tributary area of pressure transferred directly into the lateral wall connections for each of the four perimeter walls is represented by the two trapezoids shown in Figure 4-8. The tributary area represented in Figure 4-8 relies on the assumption that the rest of the building is undamaged. This assumption is maintained unless more than half of the roof-to-wall connections on the depicted wall fail. After significant roof-to-wall connection damage, the tributary area is adjusted to the two triangles shown in Figure 4-9.

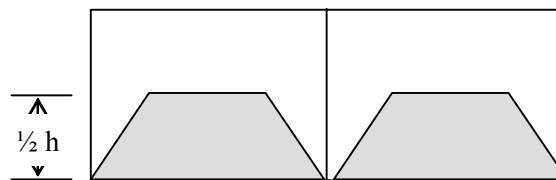


Figure 4-8. Tributary area for C&C pressures transferred into lateral connections on wood frame walls.

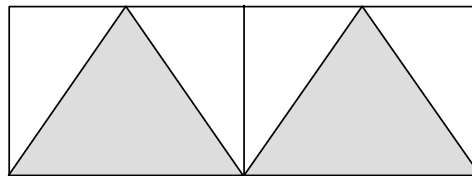


Figure 4-9. Tributary area after significant roof-to-wall connection damage for C&C pressures transferred into lateral connections on wood frame walls.

Surface pressures are calculated using Equation 4-2 with the C&C coefficients for walls given in Table 4-4 and the appropriate internal pressure coefficient for state of the building. The total load calculated by applying these surface pressures to the tributary area shown in Figure 4-8 or Figure 4-9 for each of the four perimeter walls is distributed evenly to all of the lateral connections at the base of each wall.

An additional wall load check for wood framed walls and the primary check for manufactured home walls is the potential loss of wall sheathing. Aggregate panel loads for individual pieces of wall sheathing are obtained in much the same way as roof sheathing loads. A length-specific layout is obtained for each wall. For wood frame walls, the layout is obtained by starting at one end with a full-size upright (4 ft wide by 8 ft tall) sheathing panel, and adding upright sheathing panels along the length of the wall, side by side. For manufactured homes, the layout is obtained by stacking typically sized pieces of vinyl siding along the wall length. The surface pressures are calculated using Equation 4-2 with appropriate Component and Cladding external pressure coefficients, and the internal pressure coefficient for the particular building.

Load Conditions for Openings

This category covers a wide variety of building components. Incorporated into the simulation program are doors, garage doors, and windows. Each modeled house is assumed to have one front and one back door. The load applied to each is the surface pressure calculated using Equation 4-2 with the appropriate C&C pressure coefficient from Table 4-4, and the internal pressure coefficient for the current state of the building. Additionally, houses with garages are assumed to have the garage door on the front wall. The surface pressure applied to the garage door is the same as the pressure applied to the front door.

Unprotected windows are loaded in two distinct ways: pressure loads and impact loads. The pressure load scenario is similar to that described for the doors. Surface pressures at the window locations are obtained by using Equation 4-2 with the appropriate external C&C pressure coefficient from Table 4-4, and the internal pressure coefficient for the building.

Impact loads to windows are caused by windborne debris from neighboring homes. To model this behavior, an equation based on the cumulative exponential distribution (which describes the likelihood of rare and unrelated discrete events) is used to predict missile strikes. In Equation 4-3 below, $p_D(V)$ is the probability of impact causing a broken opening, given the 3-second maximum gust, V . A represents the fraction of potential missile objects (e.g., shingles) in the air. N_A is the total number of available missile objects (e.g., number of shingles on the nearest house). B is the fraction of airborne missiles that hit the house, C is the fraction of the impact wall that is glass, and D is the probability that the impacting missiles have momentum above damage threshold.

$$p_D(V) = 1 - \exp[-A * N_A * B * C * D] \quad (4-3)$$

Equation 4-3 can be used to predict the likelihood of impact for several scenarios. This equation can eventually be used to predict the likelihood of impact by several different sources of debris (e.g., shingles, wood studs, and grapefruit). These varied results could be superimposed to determine the final tally of total impacts. With the information currently available, Equation 4-3 is used to determine the likelihood of windborne debris impact on the windows from any potential missile. Specific choices for each parameter and the methods by which these parameters could be honed in future work are discussed in the following paragraphs.

Parameters that define objects in the air include N_A and A . The total number of available missile objects, N_A , is related to the type and density of the building population around the modeled house. The current selection for this number is an empirical choice of 100. This number is expected to change regionally in future iterations of the Public Loss Hurricane Projection Model, as the results from the initial model guide improvements in future work. A is related to the capacities of the upwind building components that will become windborne debris, and is thus a function of peak wind speed. This parameter is modeled as a Gaussian cumulative density function (CDF). That is, at low peak gust wind speeds, relatively few of the available missiles are torn off upwind buildings to become windborne debris. As wind speed increases, more available debris is torn off upwind structures at a faster rate, until the function levels off at 1.0 (at which point 100% of potential missiles are in the air). In the current version of the structural damage-prediction model, the Gaussian CDF defining A has a mean value at a peak 3-second gust of 135 mph, and a standard deviation of 15 mph. This function is shown in Figure 4-10.

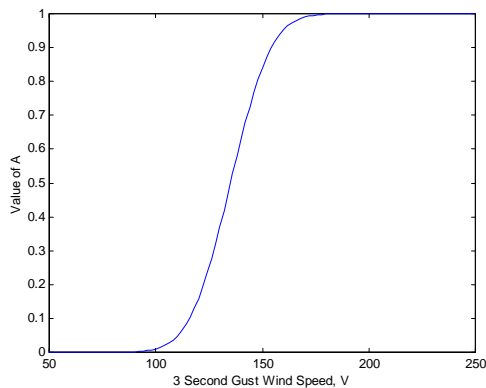


Figure 4-10. Values of the parameter A used in the determination of missile impact

Parameter B in Equation 4-3 determines how many of the missiles in the air actually strike the modeled home. This parameter is dependent on several factors,

including proximity of the missile starting point and the ability of the missile to stay airborne (which is a function of wind speed and missile type). Engineering judgment indicates that missiles will fly further and stay in the air longer with increasing wind speeds. For lack of better information, a linear function describing the parameter B is selected to have a value of zero (no airborne missiles striking the building) at 50 mph 3-second gusts and a value of 0.40 at 250 mph 3-second peak gusts. Values of B are provided in Figure 4-11.

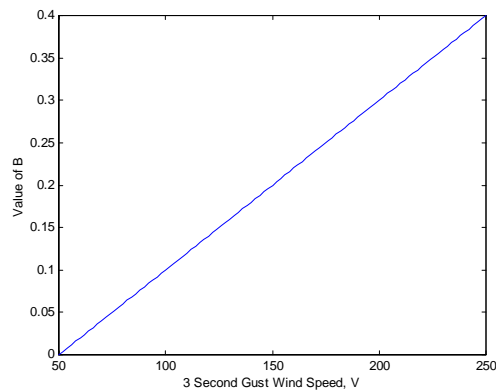


Figure 4-11. Values of the parameter B used in the determination of missile impact

Of the missiles striking the house, a fraction will hit windows (rather than other surfaces). This value is described by the parameter C , which defines the fraction of the windward wall space that is occupied by unprotected glass windows. In the current structural damage-prediction model, the windward wall space is the area of one of the perimeter walls except for the case of cornering winds, when two of the walls are vulnerable to missile strike. As described later in Chapter 5, windows on the modeled houses are categorized in four sizes. For accounting purposes inside the structural damage model, the four sizes of windows are treated independently at this point in the development of the missile impact equation. A value of C for each size of window is calculated as the area of that type of window divided by the wall space vulnerable to

impact. The probability of impact, $p_D(V)$, generated from using these values of C in Equation 4-3 is the likelihood that a window of a certain size will be impacted and broken by a windborne debris missile, given the peak 3-second gust wind speed, V .

The parameter that determines whether the striking missile will cause the window to break is D . This value is dependent on the momentum of the impacting missile and the resistance capacity of the window. Shingles, a numerous and readily available windborne missile type, are used to generate a function for the parameter D . The momentum of a windborne object, p_m , is defined by Equation 4-4, where m is the mass of the object, V is the wind speed, and R is a reduction factor. The value of $V(R)$ is then the wind speed at which the missile object is traveling. (Note that the subscript m for momentum is added by the author to the commonly used variable p to distinguish between momentum and pressure.)

$$p_m = mV(R) \quad (4-4)$$

Conservatively assuming that a typical shingle weighs 0.06 lbs (a mass of 0.03 kg), and that the maximum value of R for single shaped missiles 0.64 [34], one can determine the momentum of a shingle moving in a wind gust of 110 mph. (49 m/s) to be 0.944 kg-m/s. Given the impact resistance capacity of typical glass windows to be 0.025 kg-m/s [3], the momentum of a windborne shingle in a 110 mph 3-second gust wind event would exceed the capacity of typical unprotected window by a factor of approximately 37. It should be noted that additional reduction factors might apply, since the shingle might strike at an angle or not reach terminal velocity before hitting the window. However, these additional reduction factors will not overcome the significant difference between the missile's momentum and the resistance capacity of a typical window. Because

Equation 4-3 encompasses all types of missiles, the shingle example is used to determine likely thresholds for the parameter D , and not specifically used to generate D as a function of wind speed. The values for D used in the current structural damage simulation program are taken from a Gaussian CDF generated using a mean value of 70 mph and a standard deviation of 10 mph. Using this function, the likelihood of breakage, given the fact that a missile has impacted the window, is provided in Figure 4-12.

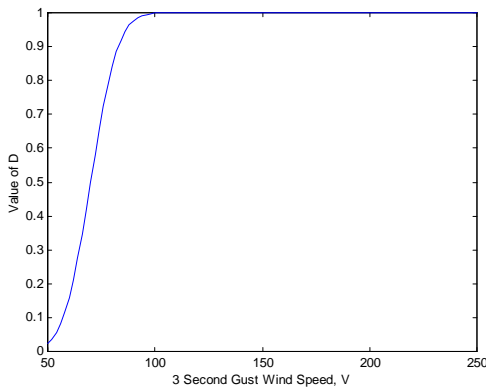


Figure 4-12. Values of the parameter D used in the determination of missile impact

Using the parameters described, the likelihood of an impact causing breakage during a specific wind event represented by a 3-second maximum gust is determined with Equation 4-3. Values are dependent on the size of window and the size of the windward wall. The eight possible angles of wind exposure create three possible windward wall scenarios: short wall facing the wind, long wall facing the wind, and cornering winds, in which one short and one long wall are both vulnerable to missile impact. The function $p_D(V)$ must be generated for each of the four window sizes during each windward wall scenario, for a total of 12 functions per modeled building. As an example, $p_D(V)$ for a medium sized window on the short side of the concrete block, gable roof house in the Central Region of Florida is provided in Figure 4-13.

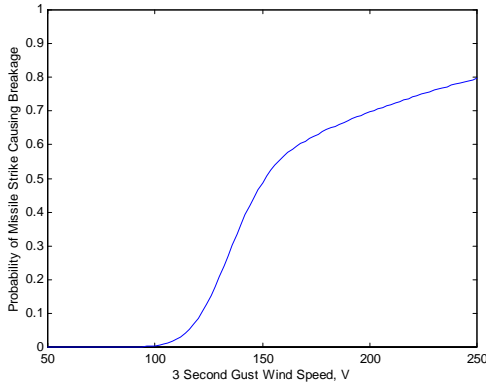


Figure 4-13. Probability of missile strike causing breakage of a medium (3.5 x 5 ft) window on a 44 ft long windward wall.

Load Conditions for Tie-Down Anchors

The load cases described in previous sections apply to both site-built and manufactured residences. Because of the differences in foundations, however, two load cases are unique to manufactured housing. These are sliding and overturning loads. Both cases are calculated using MWFRS pressure coefficients provided in Tables 4-1 and 4-2, and located in Figure 4-1. The overall lateral sliding force for a particular manufactured home is calculated as the vector sum of the resultant wall surface loads. This force will be resisted by the anchors as well as the friction between the house and foundation piles. The overturning moment is calculated about the leeward wall support pier and is resisted by the assumed weight of the house as well as the anchor system. Discussion of the resistance to both of these load conditions is described in Chapter 5. Additional details on the overturning and sliding failure checks are provided in Chapter 6.

Summary of Wind Load Conditions Used in the Simulation Engine

A summary of the wind load conditions applied to individual components during simulation is provided in Table 4-5. Sources described as MWFRS and C&C refer to the modified versions of the ASCE 7-98 provisions for Main Wind Force Resistance System

and Component and Cladding, respectively. Resistance values for each condition are described in Chapter 5 and the process by which the simulation engine applies and checks these conditions is detailed in Chapter 6.

Table 4-5. Summary of load conditions applied to simulate extreme wind events

Building Component		Limit State	Source of Loads	Additional Notes
Roof Cover		Separation or pull off	C&C	Pressure coefficients aggregated over the area of the underlying sheathing panel; no internal pressure applied
Roof Sheathing		Separation or pull off	C&C	Pressure coefficients aggregated over the area of the individual panel
Roof-to-Wall Connections		Tension	Roof sheathing	Dead plus wind; load redistribution applied
Walls	Concrete Block	Shear wall	MWFRS	
		Combined uplift and bending	C&C	Uplift – Roof-to-Wall Connections Bending – C&C
	Wood Frame	Shear wall	MWFRS	
		Uplift	Roof-to-Wall Connections	
		Lateral loading	C&C	
		Sheathing pull off	C&C	Pressure coefficients aggregated over the area of the individual panel
Manufactured Homes	Sheathing pull off	C&C	Pressure coefficients aggregated over the area of the individual panel	
Openings	Doors and Garage Doors	Over-pressure	C&C	
	Windows	Over-pressure	C&C	
		Impact damage	$p_D(V)$	
Tie-Down Anchors		Overturn	MWFRS	Manufactured housing
		Sliding	MWFRS	Manufactured housing

CHAPTER 5 PROBABILISTIC WIND RESISTANCE CAPACITIES FOR RESIDENTIAL DWELLING COMPONENTS

This chapter describes the resistance capacities selected for use in the structural damage simulation model. Capacities typical of the building components in Florida homes are selected from available literature and manufacturer data for each load case described in Chapter 4. Using this information, truncated Gaussian distributions are created to represent populations of typical building material resistances to the load cases identified in Table 4-5. These resistance distributions will be used in conjunction with the load values discussed in Chapter 4 to determine whether individual structural members fail when subjected to extreme wind loading. The operational flow of the simulation routine determining structural damage to typical Florida homes is provided in Chapter 6. Results and validation of the process are discussed in Chapter 7.

In this chapter, the details and selection process for the distribution of resistance values for each building component load case are provided. The first section of the chapter describes choices and arguments common to the selection of all building component resistance values. Following this introductory discussion are sections detailing the selected capacities for roof cover, roof sheathing, roof-to-wall connections, walls, openings, and tie-down anchors. The chapter is divided into a section detailing the resistance capacities of typical site-built homes and a latter section providing information for manufactured homes. At the end of the chapter, Tables 5-3 and 5-4 provide a summary of all resistance values incorporated in the structural damage simulation model.

Fundamental Concepts Applied During the Selection of Load Resistance Values

Resistance values described in this chapter represent the un-factored ability of each structural component to withstand loads induced by extreme wind events. As described in Chapter 4, the conservative factor built into the wind loading provisions of ASCE 7 was removed to determine a ‘true’ wind loading condition. In this chapter, the safety factors from manufacturer’s recommendations are removed to determine ‘true’ resistances. In this manner, the simulation program seeks to accurately assess the vulnerability of typically constructed homes to structural wind damage. If the safety factors were not removed, the program would provide the level of risk inherent in the current codification process, not the level of potential structural damage.

Available literature and manufacturer’s data are used to determine appropriate probability density functions for component resistances. Typically, the mean failure value for each component is obtained from available information and the coefficient of variation (*COV*) is determined through engineering judgment. A measure of the spread of the distribution, the *COV* is the standard deviation divided by the mean. The effect of varying the *COV* is shown in Figure 5-1. Each plot in the figure shows a Gaussian (normal) distribution with a mean of 100 units. The x-axis represents differing values of units, while the y-axis represents the likelihood of occurrence. The area under each curve is unity, though the peak value of the distribution with a *COV* of 0.2 is nearly twice that of the distribution with a mean of 0.4. The distribution with a *COV* of 0.2 is more closely centered on the mean value. Thus, there is a higher probability of selecting a value away from the mean (between 0 and 50, for example) using the distribution with a *COV* of 0.4, though both of the plotted distributions have the same mean value of 100 units.

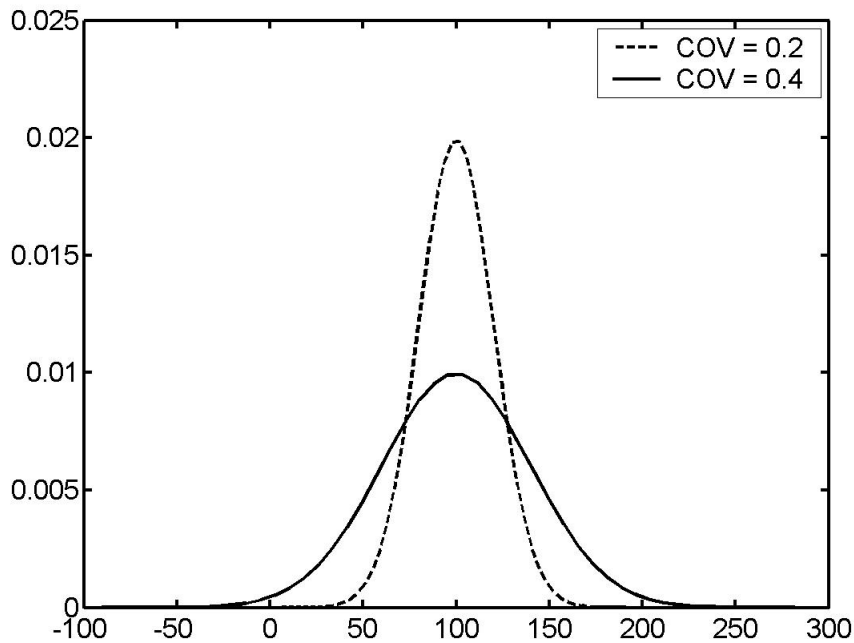


Figure 5-1. Gaussian distributions with a mean of 100 units and varying coefficients of variation.

Gaussian distributions similar to the ones depicted in Figure 5-1 are used to model populations of component capacities. Due to manufacturing quality control processes, individual components are likely to have resistance capacities which follow a lognormal distribution similar to the one shown in Figure 5-2. As compared to a Gaussian distribution with the same mean and *COV*, the lognormal distribution provides a reduced likelihood of occurrence in the low resistance tail region and a slightly greater likelihood of occurrence in the high resistance tail region. These characteristics are representative of manufacturing processes where the minimum allowable capacity is a quality control measure. Gaussian distributions are selected over lognormal and other alternate distribution choices, however, to incorporate additional variables. The variation in type, quality, size, and installation for building components on homes of differing plan dimensions increases the variety of the population under consideration. As the number of

variables increases, the central limit theorem leads to the conclusion that the distribution which would best characterize each capacity is Gaussian.

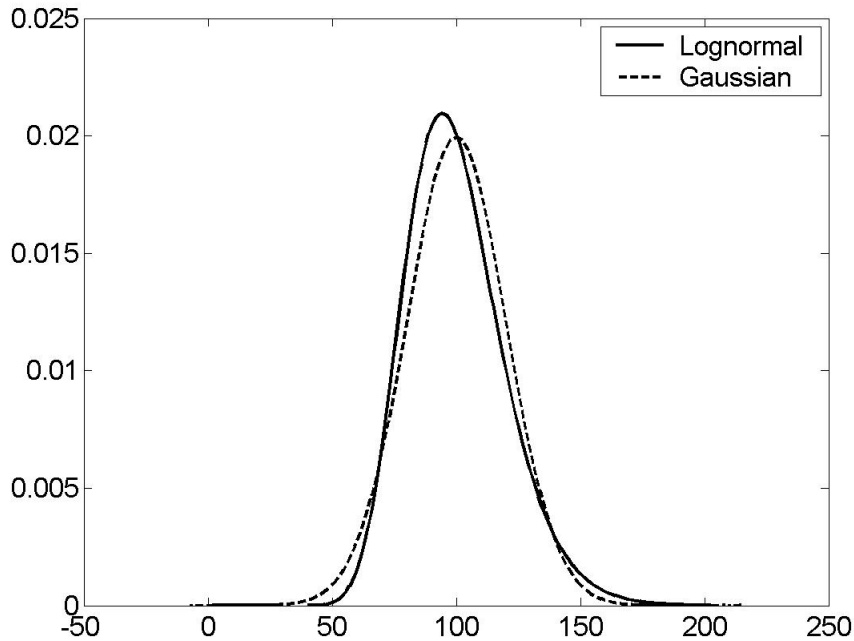


Figure 5-2. Lognormal vs. Gaussian for a mean of 100 units and coefficient of variation of 0.2

Chapter 6 describes the process by which the Gaussian values are sampled and used to simulate individual homes, while the characteristics of each distribution are described in the following sections of this chapter. As demonstrated by the distribution in Figure 5-1 with a *COV* of 0.4, this can lead to the possibility of selecting a value less than zero. To avoid the occurrence of physically impossible or impractical resistance values, truncation is applied to each of the capacity distributions described in the following sections. Sampled resistance values are bound within two standard deviations of the mean. The application of these upper and lower limits results in a distribution similar to the example shown in Figure 5-3 for a mean of 100 units and a *COV* of 0.4.

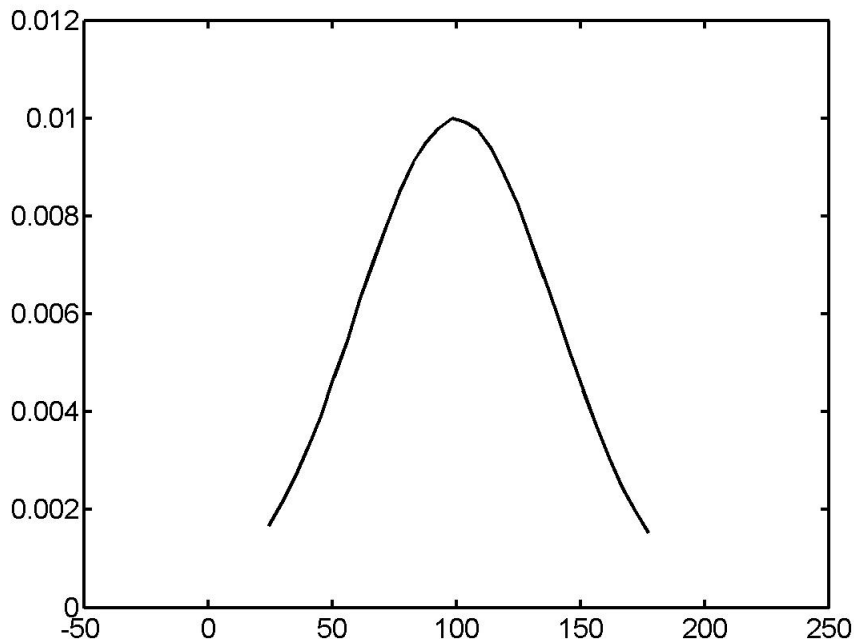


Figure 5-3. Truncated Gaussian distribution with a mean of 100 units and a *COV* of 0.4.

Site-Built Home Resistance Values

Building components modeled for typical site-built homes consist of roof covering, roof sheathing, roof-to-wall connections, walls, and openings. These are depicted in Figure 3-2. The following paragraphs detail the resistance values obtained from available literature, manufacturer's data, and engineering judgment for each load condition described in Table 4-5 for site-built homes. The values provided in this section are used to characterize capacity distributions similar to the example provided in Figure 5-2. The sampling process by which the distributions are used to create representative Florida homes is discussed in Chapter 6.

Wind Resistance Capacity of Roof Cover on Site-Built Homes

The resistance capacity of the roof covering is the ability of the shingles or tiles to stay attached to the roof sheathing, preventing rain water from entering and damaging the

contents. In general, there is limited information available about the uplift capacity of shingles and tiles, in spite of the fact that loss of roof covering contributes significantly to insurance losses. One experimental study provides an approach for estimating the wind action on shingles, but does not predict failure loads, citing the unknown capacity of the adhesive [35].

Factory Mutual (FM), Underwriters Laboratories (UL), and the American Society for Testing and Materials (ASTM) have developed test methods for commercial and residential roof coverings. Unfortunately, the tests do not provide information about the ultimate failure capacity of these building materials, nor do they adequately represent the conditions these components would face in hurricane events. Many use constant pressure systems instead of using a turbulent wind condition. During the standard FM test, a constant pressure is applied to the underside of a test specimen to simulate uplift [36]. Products that withstand the pressure for one minute without separating or delaminating are given a rating. FM Class 1-60 indicates a 60 psf test, while FM Class 1-180 indicates a 180 psf test. UL 580, “Standard for Tests for Uplift Resistance of Roof Assemblies,” and UL 1897, “Standard for Uplift Tests for Roof Covering Systems,” also use constant pressure systems to determine ratings [37]. These FM and UL static tests do not accurately simulate the wind action on the roof covering that will lead to shingle peeling and nail pull through.

The ASTM standard testing protocol D3161, “Standard Test Method for Wind-Resistance of Asphalt Shingles,” and the UL 997, “Standard for Wind Resistance of Prepared Roof Covering Materials,” specify a horizontal wind created by a fan, but the required wind speed is only 60 mph, far below the design wind speeds for Florida [37]. A

recent provision has been created in Dade County, Florida which is similar to D3161 and UL 997, but uses a 110 mph fan instead of a 60 mph fan for asphalt shingle testing. Tiles and other roofing materials, however, are still tested for Dade County approval using static uplift tests [37].

While the Dade County provision for shingles does include a wind test using speeds in Category II of the Saffir-Simpson scale, the test is considered a ‘pass or fail’ event. That is, a product either qualifies for use in Dade County by passing the test, or does not qualify by failing the test. The provisions do not require determination of the actual failure capacity. Experimental data predicting the adhesive failure or nail pullout of typical roof coverings (shingles or tiles) of average age is not currently available, and could be the focus of a future research effort.

In the absence of experimental data, the capacity of typical residential roof coverings is estimated from the average of two calculations. The basis of the first logical argument is to infer that the majority of roof coverings were originally manufactured to the 1970’s era Southern Building Code Congress International (SBCCI) requirement that cladding materials withstand an external positive or negative pressure of 25 psf. An additional necessity for this argument is to assume that, while improvements have been made, the fundamental manufacturing process for shingles and tiles has not changed radically in the last few decades. Given these two assumptions, one can predict that 90% of the roof coverings currently on the market in Florida would meet or exceed the requirement of withstanding a 25 psf load under typical quality of workmanship in installation. Using a Gaussian distribution to represent the failure strength of all roof covering products used in the state of Florida, the standard distribution tables can be used

to determine the mean failure strength. Equation 5-1 provides the method of converting a value to the standard Gaussian distribution. In this equation, x is any value in the Gaussian distribution, μ is the mean of that distribution, COV is the coefficient of variation, and z is the value in a standard Gaussian distribution with the same likelihood of occurrence as the value x .

$$z = \frac{x - \mu}{COV\mu} \quad (5-1)$$

The assumptions listed above are represented by setting x equal to 25 psf and obtaining a z value of -1.28 from the standard tables in Ang and Tang [38]. This z value represents a location at which 90% of the products would meet or exceed the capacity. A COV of 0.4 is selected to represent the wide variety of products and quality of workmanship. With these values, Equation 5-1 can be rearranged to solve for a mean failure capacity. Using the argument presented above, 51 psf would be the most reasonable mean failure capacity for typical roof coverings.

A second argument begins with the recent Dade County uplift test for shingles, which uses a 110 mph fan. If the fan speed is used as the design wind speed, V , in the ASCE design pressure equations (Equations 2-11 and 2-12) with the assumptions that the building is enclosed and in open terrain, a corresponding surface design pressure can be calculated. Interestingly enough, the value obtained is 51 psf, the mean failure capacity of typical roof coverings from the previous exercise. Products are required to pass this test to be certified for use in South Florida, which means that the mean failure capacity of roof coverings is likely to be higher than the calculated value. Assuming that 90% of products pass the test, and again selecting a COV of 0.4 to represent the wide variety of products and quality of workmanship, the same procedure described in the first argument

can be used to determine a possible Gaussian mean for South Florida shingles. A value of approximately 104 psf is obtained using this argument.

Engineering judgment and knowledge of the degree of damage following Hurricane Andrew and other past storms [15-23] indicate that the mean value from the second argument is too high, and the mean value from the first argument is too low, for use as a representative mean for all typical roof coverings in the state of Florida. A value that would best represent the entire population of roof coverings (to include both shingles and tile products, as well as old and new construction) lies between the two values. Using this conclusion, a value of 70 psf with a *COV* of 0.4 is selected for the mean failure capacity of typical roof coverings.

Wind Resistance Capacity of Roof Sheathing on Site-Built Homes

A critical component in the overall vulnerability of a residence to hurricane damage is the ability of the sheathing to remain fastened to the trusses or rafters. A considerable body of research has been conducted in this area in the wake of the Hurricane Andrew damage. One such study conducted at Clemson University indicates that the capacity of sheathing panels is best represented by treating the panel as a whole, rather than evaluating the capacity of individual fasteners. Sheathing panel failure usually begins with the pullout or pull-through of a single critical interior fastener, but if any fastener is improperly installed, the failure mechanism is most likely to begin at that location, whether it is interior or not [39]. Given the difficulty in predicting the most probable failure location, the best means of comparing resistance to load is to use the aggregate load on the entire sheathing panel, and compare it with average failure loads from tests of whole panels, not just single fasteners.

Results from the study discussed in the preceding paragraph and from additional studies provide mean failure pressures and coefficients of variation for panels of different wood species with different fastener sizes and schedules [39-41]. Unfortunately, the means differ significantly, and considerable uncertainty exists concerning the species of wood and the most typical fastener type and size used in each area of Florida. A simple arithmetic mean of the failure capacities would not necessarily best represent the building population of the state.

As an alternative to using laboratory data, in situ data exists for a limited number of homes in South Carolina. These homes were flood damaged during Hurricane Floyd in 1999 and were subsequently purchased for the purpose of testing and evaluation of retrofit measures. The homes varied in age and construction. Approximately half of the homes had planked roofs, one had oriented strand board (OSB), and the rest were plywood. After removing one outlier (a planked roof with a high failure capacity of 450 psf) the sheathing failure test results average to value of approximately 150 psf, with the highest value at 196 psf and the lowest at 105 psf [42]. Though the houses tested were in South Carolina, they are fairly representative of the types and ages of construction present in Florida. Since only a limited number of homes were tested, the *COV* obtained from the eight test values is not used as the *COV* for a distribution representative of typical Florida roof sheathing. Instead, a value of 0.4 is selected to account for differences in workmanship and materials throughout the state.

Wind Resistance Capacity of Roof-to-Wall Connections on Site-Built Homes

The link between the roof system and the external walls occurs at the roof-to-wall connections. Uplift capacities of several types of roof-to-wall connections for light frame wood construction are available [43, 44]. The study conducted by Reed [44] further

investigated the potential for load sharing between rafter connections and found that load sharing existed in nailed connections, but not in hurricane strap connections. No studies have been located that investigate the possible differences in uplift capacity for roof to masonry wall connections, though masonry structures make up a considerable portion of the building stock, as described in Chapter 3. In the absence of test data, the uplift capacity for typical roof-to-wall connections on masonry homes can be estimated from manufacturer information. In order to maintain consistency between types of houses, manufacturer's data is used for both masonry and wood frame homes.

Personal correspondence between the author and Randy Shackelford, a Simpson Strongtie representative, provided information about the connections most frequently used in the state of Florida and the typical factor of safety placed on the capacity specified by the manufacturer (personal correspondence, May 2002). Roof-to-wall connections manufactured by this company vary in uplift strength. Additionally, the same connector has a different strength rating depending on the type of wood used in construction. Generally, roof-to-wall connectors for both wood and masonry construction can be assigned to one of three strength categories: high strength (which includes most hurricane strap connections), medium, and low strength. Table 5-1 provides the values obtained by averaging the manufacturer's rated uplift capacity of the products available in each generalized category. Only two categories were obtained for the case of gable end connectors on masonry walls, and the values for wood construction are obtained assuming Spruce Pine Fir (SPF) construction. In Table 5-1, the term 'side' is used to describe typical roof-to-wall connections at the end of a truss. These connections occur on all four perimeter walls of a hip roof home, but only on the side walls of a gable roof

home. Gable end connections are those that connect the last truss on each end to the wall, and occur only on gable roof homes in the simulation model.

Table 5-1. Manufacturer's uplift capacity for typical roof-to-wall connections

Construction	Connector	Connector Strength Category		
		High (lb)	Medium (lb)	Low (lb)
Wood Frame	Side	1240	690	460
	Gable	1260	650	380
Masonry	Side	1400	1065	700
	Gable	640	225	

Discussions with a Bob Carter, a Brevard County architect, (personal correspondence, June 2003) in addition to the correspondence with the Simpson Strongtie representative indicate that nearly all of the homes constructed in Florida over the last 15-20 years would fall in the category of high-strength roof-to-wall connections. Based on this information, the high-strength values in Table 5-1 are used as the manufacturer's rated capacity for each type of home construction. Specific values for other types of connections (such as toe-nailed connections) are not incorporated in the model at this time, due to a lack of information concerning the distribution of connection types throughout the state.

According the testing conducted by Simpson Strongtie, a factor of safety of 3 is applied to obtain a mean value of each connector population. Using this value, a mean of 3720 lbs and 4200 lbs in uplift capacity per connector are obtained for the side connectors of wood and masonry homes, respectively. The mean values for gable end connectors are calculated to be 3780 lbs and 1920 lbs in uplift capacity, for wood and masonry homes, respectively. A *COV* of 0.2 is selected for all roof-to-wall fastener distributions, and bounds are placed such that acceptable values lie within two standard deviations of the mean. These distributions result in capacities higher than those obtained

through in situ and laboratory testing [42-44], but the damages predicted using the manufacturer's values correspond well with post-damage information surveyed after Hurricane Andrew. These results are provided in Chapter 7.

To capture an observed failure mechanism where the entire roof detaches from the walls [19], the roof-to-wall connection strength for each simulated house is batch selected. A representative value is generated for the entire house from the Gaussian distribution representing the population of roof-to-wall connections for that type of structure (wood or masonry). This value becomes the mean of a Gaussian distribution having a *COV* of 0.05 from which individual connection capacities are randomly generated. This process represents obtaining the connectors from the same manufacturer or batch, and using the same quality of installation for the home. Additional details on the batch selection process are provided in Chapter 6. Roof-to-wall connections are the only structural components to be selected in this manner, specifically to incorporate the observed damage state of having the entire roof detach from the walls. The method of batch selection is not used for other structural components because it results in predicted damages that are not observed in post-damage reports [19].

Wind Resistance Capacity of Site-Built Home Walls

Wall failures are much less commonly cited in post-damage reports than roofing system failures. In many cases, wall failures could be attributed to improper installation of connections or to the loss of structural integrity of the roof system [19]. Capacities to resist shear, out-of-plane loading, and uplift are considered for wood frame walls and masonry walls in the following paragraphs.

Resistance capacities for wood walls are obtained from the 1997 National Design Specification for Wood Construction (NDS) [45], as well as from laboratory tests. Wood

capacities are distinctly difficult to generalize over a large population of homes because the load carrying capability of wood connections varies significantly with different types of lumber. To best represent the types of wood typically found in Florida, southern species of wood, such as Spruce Pine Fir (SPF) and Southern Yellow Pine (SYP), are used in resistance calculations.

Damage to masonry walls was less prevalent than damage to wood frame walls, and masonry walls were less dependent on the integrity of the roof system [19]. However, damage surveys [46] have shown that un-reinforced masonry might be a weak link in the structural system. After the failure of an opening, increased internal pressure can lead to the collapse of masonry walls, which trigger the collapse of the whole structure. One study was obtained predicting the failure pressure for simply reinforced and pre-stressed wall sections [47]; however, this study alone is not enough information to adequately predict failure conditions for typical residential structure walls. In the absence of a significant population of laboratory test data, design provisions are used, with adjustments to allow for the best representation of true failure loads.

Wood shear wall capacity

Shear wall loads are transferred through the wall sheathing in wood frame walls. As a result, the capacity of the wall to resist shear wall loads is dependent on the nailing pattern and thickness of the attached plywood. Using 3/8 inch plywood sheathing with 8d nails spaced at 6 inches on center along sheathing edges, the shear flow capacity of a typical wall is 310 lbs per linear foot, according to the NDS. A factor of safety of 3.5 is applied to this capacity, to account for both the safety built into the design code, as well as the uncertainty in the contribution of other building materials. Wood homes are generally covered with some other form of cladding, which contributes to the ability of

the wall to resist shear loading. The extent of the load resisting contribution of different materials (e.g. stucco) is difficult to predict. Additionally, the shear walls are tied into other pieces of the structure, such as interior walls. These load sharing contributions are not considered in the design process, so they must be accounted for when using design loads to predict the true failure capacity. The resulting Gaussian distribution representing the failure capacity of wood frame shear walls has a mean of 1085 lbs per linear foot, with a *COV* of 0.2. Values are truncated at a distance of two standard deviations away from the mean.

Wood frame out-of-plane load capacity

Out-of-plane loading applied to wood frame walls is transferred from the wall cladding into the studs, and then into the stud wall connections. The weak link in the load path occurs at the connections, and not in the stud itself, under most circumstances [19]. Using the minimum nailing requirements from the Florida Building Code presented in Table 2306.1, this weak link occurs at the bottom end of the stud, which is toe-nailed to the sill plate with four 8d nails [48]. Though usually not taken into account for design capacity calculations, the connection shares this lateral load with the sheathing nails that penetrate the sill plate. To best represent the true failure capacity, both the toe nail connection and the contribution of some sheathing nails are taken into account.

From the NDS, the equation for determining the lateral resistance (Z) of the nailed connection is presented in Equation 5-2, where C_D is the load duration factor, C_M is the wet service factor, C_t is a factor for temperature, C_d is a penetration factor, C_{eg} is a factor for end grain nailing, C_m is a factor for toe nailing, N is the number of nails per connection, and z is the lateral capacity of an individual nail in a particular species of wood.

$$Z = C_D C_M C_t C_d C_{eg} C_m N \cdot z \quad (5-2)$$

To best represent Florida construction, the value of z is taken to be 78 lbs, which is the average of the values for SYP, Southern Douglas Fir (South DFIR), SPF, and Southern SPF. C_D for wind loads is 1.6, and C_M is set at 0.85, assuming that rain water has potentially leaked into the walls. The factors C_t , C_d , and C_{eg} are each assigned a value of 1 because temperatures are not expected to be over 100°F, and the conditions of limited nail penetration or end grain nailing do not apply. Since the connection is toe-nailed, C_m is assigned a value of 0.83. Using these figures with an N of four, a design value of 352.2 lbs per connection is obtained. To this value, a factor of 3.5 is applied to account for the safety factor built into the NDS code.

The Florida Building Code dictates that the minimum nailing pattern for wall sheathing consists of 6d nails at 6 inches on center along edges and 12 inches on center at intermediate supports. For a typical 4 x 8 ft sheathing panel installed vertically, this arrangement results in 9 nails along the bottom edge, or 2.25 nails per linear foot of wall. Assuming a specific gravity of 0.45 for typical southern woods, 6d nails have a withdraw capacity of 21 lbs per inch of penetration [45]. Using a C_D for wind loads of 1.6 and a penetration of 1.5 inches, the design contribution for the end of the sheathing panel is found to be 113.4 lbs per linear foot. To this value, a factor of 3.5 is applied to account for the safety factor built into the wood design code.

The total lateral resistance capacity of a typical wood frame wall is obtained by summing the toe nail and sheathing panel nail contributions. The first value is found using a Gaussian distribution with a mean value of 1232 lbs, a COV of 0.25, and truncation at a distance of two standard deviations away from the mean. The distribution

representing the sheathing nail contribution is found using a typical stud spacing of 24 inches on center. This distribution is also Gaussian, with a mean of 794 lbs per connection location and a *COV* of 0.25. Each value is independently obtained from its respective distribution, and then the two are summed to represent the total lateral capacity at a point along a typical wood frame wall.

Wood frame uplift capacity

The capacity of a wood wall to resist uplift is modeled at the location of the wall to sill plate connection, the same connection which is the weak link for typical wood wall lateral capacity. The toe-nailed configuration of this connection results in an uplift strength that is identical to the lateral (out-of-plane) capacity. Since the nails are toed in at a 45 degree angle, both uplift and out-of-plane loads result in a lateral load in the nailed connection. The additional strength provided by the cladding and other attached building materials might vary slightly between the uplift and out-of-plane load conditions, but the difference is neglected for modeling purposes. The capacity of the wood wall connections in out-of-plane and uplift are taken as identical values, though the load conditions are checked individually. Additional detail on the failure check procedures is provided in Chapter 6.

Wood frame sheathing capacity

Plywood sheathing attached to wood frame walls behaves similarly to sheathing attached to the roof. The ability of plywood sheathing to remain attached to the framing during wind load conditions is directly related to the type of wood, the type of fastener, and the fastening pattern. Unfortunately, statistics defining the most popular sheathing and fastening characteristics are not available. Additional variables that cannot be adequately considered include architectural building materials that cover the sheathing

and form the exterior wall covering. These materials contribute to the sheathing's ability to remain fastened to the wall frame, but to an unknown extent.

Engineering judgment dictates that wall sheathing is typically thinner and/or fastened with smaller nails than roof sheathing. Comparing the baseline withdraw capacity of two typical fasteners from NDS provides a reasonable assumption about the difference in resistance of typical roof and wall sheathing. Using wood with a specific gravity of 0.45, the un-factored withdraw capacities for 8d and 6d nails are 25 lb and 21 lb per inch of penetration, respectively [45]. The 6d capacity is approximately 84% of the value of the 8d capacity. Neglecting the small difference in penetration length that would result from thinner wall sheathing, but incorporating the difference in fastener size, one can assume that the typical wall sheathing panel would have a pressure resistance capacity of roughly 84% of a typical roof sheathing panel. This factor is used to reduce the mean capacity of 150 psf, found for typical roof sheathing during in situ testing [42], to a mean value for typical wall sheathing of 126 psf. A *COV* of 0.4 is applied to account for a wide variety of wall coverings over the sheathing, and to account for the differences in workmanship and quality of construction.

Masonry shear wall capacity

The ability of typical masonry walls to resist shear wall loads is obtained from the masonry design code. The maximum allowable shear stress, F_v , is defined by Equation 5-3, where f'_m is the capacity of the mortar [49].

$$F_v = \frac{4}{3} \cdot \min\{1.5\sqrt{f'_m}, 37 \text{ psi}\} \quad (5-3)$$

Equation 5-3 is not dimensionally correct, because f'_m is entered under the square root symbol in psi, and the result is obtained in psi. Using a typical value of 1500 psi (for

mortar in residential construction), F_v is calculated from Equation 5-3 to be 49 psi. A factor of safety of 4 (slightly higher than the value of 3.5 used for wood) is assumed to be built into the code values for masonry, therefore the calculated F_v is multiplied by 4 to obtain a mean shear failure stress of 196 psi. A *COV* of 0.2 is assumed for the Gaussian distribution of shear stress capacity. Details of the comparison made between this capacity (psi) and the total shear load (lbs) are provided in Chapter 6.

Masonry out-of-plane load capacity

The behavior of masonry walls in out-of-plane load conditions can be predicted by yield line theory and analysis of crack patterns [3]. This combined method requires knowledge of the aspect ratio and end support conditions of each section of wall. Given the uncertainty in predicting detailed aspect ratios, the computing resources necessary to employ a yield line theory method, and the uncertainty involved in predicting insurance losses based on wall damages; a simpler method is selected. The out-of-plane capacity of a typical masonry wall is modeled on capacities obtained from ACI 530 for a one-foot mid-span section.

The bending strength of a typical masonry section is calculated as the section modulus, S , times the allowable tensile stress, F_t [49]. S is obtained from the geometry of typical masonry units, which are nominally 8 x 8 x 16 inches. Actual measurements are slightly lower than these values, and typical widths for webs and flanges are 1 and 1 ¼ inches, respectively. Using these dimensions, S for a one foot section of a typical concrete block wall without reinforcement is calculated to be 87 in³. The allowable tensile stress is provided by ACI 530 as 33.3 psi, thus a typical one-foot section of a concrete block wall has the code based strength to resist a moment of 2897 in lb (241 ft

lb). A factor of safety of 4 is assumed to be built into the masonry code; therefore the mean capacity of a typical wall in bending is taken as 11,588 in lb. A *COV* of 0.2 is assumed to create a Gaussian distribution of bending strength. Details are provided in Chapter 6 for the combined failure check of masonry walls in bending and uplift, which incorporates this capacity of masonry walls in out-of-plane load conditions.

Masonry uplift capacity

The uplift capacity of typical masonry construction is obtained similarly to the out-of-plane loading capacity. A one-foot mid-span section of concrete block wall is used to determine the strength of a typical wall in uplift, based on values from the ACI code. The value of F_t , the maximum tensile stress allowed by the ACI code, is 33.3 psi. Multiplying this value by a nominal area of 30 in², a value of approximately 1000 lbs is obtained for the typical uplift design capacity. This value is multiplied by 4 (the factor of safety assumed to be built into the masonry code) to obtain a mean uplift capacity of 4000 lbs. A *COV* of 0.2 is assumed to create a Gaussian distribution of resistance to uplift loads. Details are provided in Chapter 6 for the combined failure check of masonry walls in bending and uplift.

Wind Resistance Capacity of Site-Built Home Openings

Openings included in the damage prediction simulation consist of doors, garage doors, and windows. Each of these is subjected to a component and cladding pressure, as described in Chapter 4. Site-built residences modeled in the structural damage simulation engine are assumed to have a wood or metal front door, a glass or mostly glass back door, and a total of 15 windows. The number of windows is obtained from a comparison study between site-built and manufactured homes, where 15 was found to be the average number of windows for site-built construction [33]. Additionally, homes with garages are

assumed to have a two-car sized garage door. The capacity of each to resist pressure loads is described in the following paragraphs.

Wind resistance capacity of doors for site-built homes

Several types of doors with numerous locking mechanisms can be found in the building population of Florida. A statistical analysis of the failure capacity of the different types of doors with many different fastening and locking mechanisms would require resources beyond the scope of this project. In lieu of this information, mean failure capacities of 100 psf and 50 psf are selected for typical front and back doors, respectively. The choice for back doors is distinctly lower than front doors to incorporate the likelihood of the back door being larger and consisting of unprotected glass. (French doors and sliding glass doors are popular in Florida.) The mean failure capacities are used in a Gaussian distribution with a *COV* of 0.2 to predict individual door strengths during simulation.

Wind resistance capacity of garage doors for site-built homes

The ability of typical garage doors to resist wind pressure loads is obtained from a manufacturer's trade group. The Door & Access Systems Manufacturers Association (DASMA) provides testing provisions for commercial and residential garage doors based on the 1997 Uniform Building Code. Individual tests for positive and negative design pressures include 1-minute duration design load application and 10-second duration of 1.5 times the design pressure [50]. For one story double size (two-car) garage doors, 29.6 psf and -30.8 psf are the assigned design pressures. Doors pass if they remain operable and recover at least 75% of their maximum deflection after the tests [50].

Assuming that 95% garage doors on the market pass the DASMA test described above, a mean failure capacity for garage doors can be calculated using Equation 5-1. For

the case of garage doors, x is given the value of 30 psf, and a z value of -1.645 is obtained from the standard tables in Ang and Tang [38]. This z value represents a location at which 95% of the products would meet or exceed the capacity. A COV of 0.2 is selected to represent the variety of products and quality of workmanship in the building population. With these values, Equation 5-1 is rearranged to solve for a mean 1-minute load capacity of 44.7 psf, and a 10-second load capacity of 67 psf. A corresponding strength to withstand 3-second gust winds would be slightly higher than the 10-second value of 67 psf. This theoretical value would reflect the test criteria of operability and recovery of 75% of the maximum deflection, which does not necessarily indicate whether the door would be replaced as an insured loss. Additionally, a deflected door might allow enough wind into the garage to increase the internal pressure of the house and contribute to the roof sheathing damage. Based on this information, a lower value of 52 psf is selected as the mean pressure at which a garage door would allow wind to penetrate the opening and at which the door would deflect such that it would be replaced under a typical insurance policy. A COV of 0.2 is applied to create a Gaussian distribution of strength.

Wind resistance capacity of windows for site-built homes

The ability of unprotected windows to resist pressure loads is dependent on the size and thickness of the glass panes. Assuming that most typical windows are $\frac{1}{4}$ inch thick, the strength chart for annealed glass provided in ASTM E1300, "Standard Practice for Determining Load Resistance of Glass in Buildings," is used to determine the strength of typically sized windows. The factor of safety built into the design values provided in the chart is known to be 2.5 (personal correspondence with Dr. Jim McDonald, July 22, 2002), thus failure capacities are obtained by multiplying the chart value by 2.5. Mean

failure capacities calculated for each of four selected window sizes are provided in Table 5-2. A Gaussian distribution is used for each case, with a *COV* of 0.2.

Table 5-2. Mean failure pressures for typical unprotected windows

Description	Size (ft x ft)	Mean Failure Capacity (psf)
Small	3.5 x 3.5	104.4
Medium	3.5 x 5.0	69.6
Tall	3.5 x 6.5	52.2
Picture	6.5 x 6.5	37.2

As described in Chapter 4, load cases for windows include both pressure loads and impact loads. Determination of the likelihood of a piece of windborne debris striking a window with enough momentum to cause the window to break is discussed in Chapter 4. The capacity of the window to resist impact is already factored into the debris model and is not repeated here.

Manufactured Home Resistance Values

The building components modeled for typical manufactured homes include the five components of site-built homes as well as tie-down anchors. Unfortunately, the term ‘manufactured home’ describes a great variety of dwellings; a growing population that is not well defined in the state of Florida. Determining resistance values suitable for all types of manufactured homes relies on engineering judgment.

According to a 1998 study conducted by the National Association of Home Builders (NAHB) Research Center, the demand for manufactured homes more than doubled between 1991 and 1996, and includes homes that are increasingly similar to their site-built counterparts [33]. The study goes on to indicate that the median age of manufactured homes in 1995 was 15 years, compared to 30 years for site-built homes. At the time of the study, approximately 35% of the manufactured homes nationwide predate the 1975 Manufactured Home Construction and Safety Standards (also called the "HUD-

Code," in reference to the Department of Housing and Urban Development). These factors indicate that the nationwide population of manufactured homes is becoming increasingly more sophisticated than the stereotype of typical trailer parks might allow, though an older population of homes does still exist.

As a summary, the NAHB report indicates that manufactures homes are typically made in similar fashion, but with slightly lesser quality or thinner members than site-built homes. With these findings in mind, the selected capacities for typical manufactured home components are described in the following sections. A distinction is made between the capacity of typical manufactured home components and the components of manufactured homes that predate the 1975 HUD-Code. Values described in the following sections are used to characterize distributions of capacity similar to the example provided in Figure 5-2. The method by which the distributions are used to create representative homes is discussed in Chapter 6.

Wind Resistance Capacity of Roof Sheathing and Cover on Manufactured Homes

According to the NAHB report comparing manufactured and site-built housing, a surprising 93% of manufactured homes were constructed with oriented strand board (OSB) roof sheathing [33]. This wood product will behave in a similar fashion to the plywood typical of sheathing on site-built houses. Additionally, roofs sheathed with OSB typically have a roof covering of asphalt shingles. This construction type is identical to that of site-built homes, with slightly different mean capacity values. To represent the selection of less expensive or thinner materials, a 0.9 reduction factor is applied to the mean capacities of 70 psf and 150 psf for site-built home roof cover and sheathing, respectively. An additional reduction factor of 0.9 is used to represent the difference between current manufactured housing and that predating the 1975 HUD-Code. The

resulting mean capacities for current and pre-HUD-Code manufactured home roof cover are 63 and 57 psf, respectively. Roof sheathing mean capacity values are 135 and 122 psf. *COV* values of 0.4 are selected for these distributions to represent the wide variety of available products and workmanship.

Wind Resistance Capacity of Roof-to-Wall Connections for Manufactured Homes

Capacity values for typical hardware used in the roof-to-wall connections of manufactured homes are obtained from a leading manufacturer's website [51]. According to this information, the average manufactured home code-approved value for typical single strap rafter ties is approximately 613 lbs per connector. The average strength of a weaker type of connection (the MMH8) is typically 365 lbs per connector. A stronger connection is achieved when a double strap configuration is used, resulting in a typical average value of 900 lbs per connection. Using the same factor of safety of 3 discussed previously for site-built home data, these mean capacities are multiplied to generate typical mean uplift failure loads.

Under the assumption that pre-HUD Code homes use the weaker MMH8 type of connection, all manufactured homes built prior to 1975 are assigned roof-to-wall connection capacities based on the MMH8 value. With the safety factor of 3, the average failure load is 1095 lbs per connection. A wide variety of connectors are assumed for typical modern singlewide homes, therefore the roof-to-wall connection capacity for these homes is calculated as the average of typical single strap rafter ties and typical MMH8 connections. The un-factored value used is 490 lbs per connection, which is multiplied by the manufacturer's safety factor of 3 to obtain the mean failure pressure of 1470 lbs per connection. Modern doublewide homes experience larger roof loads, therefore the capacity of the roof-to-wall connections for these homes are assigned based

on average double strap connection values. With the safety factor applied, the mean capacity for typical doublewide homes is 2700 lbs per connection.

Roof-to-wall connection capacities for all types of manufactured homes are batch sampled, just like their site-built counter parts. For each home, a value is selected from a Gaussian distribution with a *COV* of 0.2. The mean of this distribution varies by type of manufactured home, as discussed in the previous paragraph. The sampled value becomes the mean capacity for an individually simulated home. The distribution of capacities for individual fasteners on the home is based on the sampled mean, with a *COV* of 0.05. Additional details concerning this process are provided in Chapter 6.

Wall Capacity for Manufactured Homes

Under the assumption that roof damage, overturning, or sliding failures resulting in significant insurance losses will occur before whole wall failures, the wall damage modeled for manufactured homes consists of siding failure only. The wind pressure capacity of typical vinyl siding is obtained from manufacturer's websites [52-54]. From the obtained manufacturer's information a value of 44 psf is selected as the typical pressure resistance capacity of vinyl siding in the medium-priced category. To this value, a factor of safety of 1.5 is applied to obtain a mean failure pressure of 66 psf. The applied safety factor is lower than others used in capacity modeling due to the nature of the product. Vinyl siding is regarded as a non-structural element, in spite of the fact that a siding failure allows wind and water to penetrate the building envelope. For this reason, it is assumed that the manufacturing process would include a lower factor of safety than structural components. No safety factors were obtained directly from manufacturers.

Distributions for vinyl siding capacities are obtained for manufactured homes using a *COV* of 0.2. The mean capacity for modern homes is the value of 66 psf described

above. For pre-HUD-Code homes, this mean value is reduced by a factor of 0.9 to account for aging and for the difference in products available a few decades ago.

Wind Resistance Capacity of Manufactured Home Openings

Openings modeled for typical manufactured homes include doors and windows. Just like their site-built counterparts, manufactured homes contain a wide variety of doors with differing locking mechanisms and windows of different sizes. A statistical analysis of the population of these openings is not feasible, so engineering judgment is applied to determine the most likely arrangement and capacity. Capacities for typical front and back doors are selected with the NAHB findings in mind. Specifically, manufactured homes are far less likely to have glass doors, and the capacity of typical non-glass doors is likely to be lower than those used in site-built homes [33]. Given these two factors, the front and back doors on each manufactured home model are assigned a capacity based on a Gaussian distribution with a mean value of 80 psf and a *COV* of 0.2.

One notable exception to the typical differences between site-built and manufactured homes is the capacity of windows. A pane thickness of ¼ inch is selected for both site-built and manufactured homes. Thus, the capacity to resist pressure loading is the same for both types of construction. Mean capacities for typically sized windows are presented in Table 5-2. Like site-built homes, manufactured homes are also subject to windborne debris. The likelihood of a piece of debris impacting and breaking a typical window is discussed in Chapter 4. This argument applies to both site-built and manufactured homes, and is not repeated in this section.

Wind Resistance Capacity of Tie-Down Anchors

Tie-down anchors are used to resist both sliding and overturning of manufactured homes. The systems generally consist of an earth screw attached to the underside of the

home and anchored in the soil. Unfortunately, the resources necessary to conduct a thorough study of the population of manufactured homes in the State of Florida which would reveal the various types of anchors, installation methods, and the variation in soil capacities are beyond the scope of the current effort. A general arrangement of anchors is assumed for all of the manufactured homes in Florida, based on work conducted by Marshall and Yokel [55, 56]. Two lines of anchors are assumed, 7 feet apart, as shown in Figure 5-3 (a sketched side view of a typical manufactured home). Each line consists of five anchors installed at a 45 degree angle, for a total of ten anchors per home.

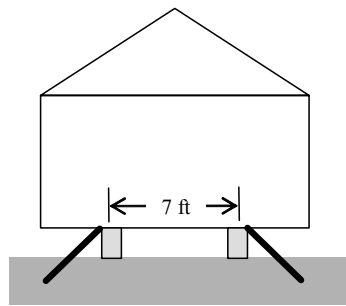


Figure 5-4. Typical arrangement of tie-down anchors for manufactured homes.

Tie-down anchors are characterized by a Gaussian distribution of pull-out capacity with a mean value of 1550 lbs and a *COV* of 0.4. The mean value is obtained from work conducted by Yokel, but a value of 0.4 is substituted for the reported *COV* of 0.3 [56]. The increase of *COV* reflects an additional uncertainty from installation techniques and soil quality not observed during the test. The mean value of pull-out capacity is confirmed for use in typical Florida soils by comparison with a limited test conducted by Hayes for 8-inch helix screws in sand [57].

Summary of Resistance Values Used in Structural Damage Simulation

Capacity values described in the preceding sections for site-built and manufactured homes are summarized in Tables 5-3 and 5-4. Table 5-3 provides a description of the

limit state, and capacity distribution characteristics for selected building components of site-built homes, while Table 5-4 provides similar information for manufactured homes. Values provided in these tables are used to simulate individual homes representative of typical Florida structures. The resistance of these simulated structures is compared to wind loads described in Table 4-5 to determine if structural failures occur during high-wind events. Details of the simulation process are provided in Chapter 6.

Table 5-3. Site-built home summary of wind resistance capacities

Building Component		Limit State	Mean Capacity	COV	Additional Notes
Roof Cover		Separation or pull off	70 psf	0.4	
Roof Sheathing		Separation or pull off	150 psf	0.4	
Roof-to-Wall Connections	Concrete Block	Tensile failure	4200 lbs (side) 1920 lbs (gable)	0.2	Batch selected
	Wood	Tensile failure	3720 lbs (side) 3780 lbs (gable)	0.2	Batch selected
Walls	Concrete Block	Shear wall failure	196 psi	0.2	
		Combined uplift and bending failure	4,000 lbs (uplift) 11,588 in lb (bending)	0.2	Capacities separate, failure check is combined.
	Wood	Shear wall failure	1085 lb/ft	0.2	
		Lateral failure	1232 lb (connection)	0.25	Contributions summed for total capacity
			794 lb (additional)	0.25	
		Uplift Failure	616 lb/ft (connections)	0.25	Same as lateral
			397 lb/ft (additional)	0.25	
Sheathing failure	126 psf	0.4			
Openings	Doors	Pressure failure	100 psf	0.2	
	Garage Doors	Pressure failure	52 psf	0.2	
	Windows	Pressure Failure	Small	104.4 psf	0.2
			Medium	69.6 psf	0.2
			Tall	52.2 psf	0.2
Picture			37.2 psf	0.2	

Table 5-4. Manufactured home summary of wind resistance capacities

Building Component		Limit State	Mean Capacity (<i>pre HUD-Code</i>)	COV	Additional Notes
Roof Cover		Separation or pull off	63 psf (57 psf)	0.4	
Roof Sheathing		Separation or pull off	135 psf (122 psf)	0.4	
Roof-to-Wall Connections		Tensile failure	2700 lbs (double) 1470 lbs (single) (1095 lbs)	0.2	Batch selected
Walls		Siding failure	66 psf (59 psf)	0.2	
Openings	Doors	Pressure failure	80 psf	0.2	
	Windows	Pressure Failure	Small	104.4 psf	0.2
			Medium	69.6 psf	0.2
			Tall	52.2 psf	0.2
Picture			37.2 psf	0.2	
Tie Down Anchors		Pull out	1550 lbs	0.3	

CHAPTER 6 SIMULATION ENGINE

This chapter details the probability-based system-response model developed for the Florida Department of Financial Services sponsored Public Loss Hurricane Projection Model described in Chapter 2. The developed structural damage model is a *MatLAB* based Monte Carlo Simulation (MCS) engine that uses the structural wind loads discussed in Chapter 4 and the building component resistance values described in Chapter 5 to simulate the performance and interaction of structural components of typical Florida homes during hurricane winds. The model is based on a series of three nested loops: an outer loop for angles of incidence, an intermediate loop for maximum 3-second gust wind speeds, and an inner loop to simulate individual buildings of a structural type. A flowchart of the developed model is shown in Figure 6-1, where shading identifies tasks within the nested loops. Each of the flowchart tasks listed in Figure 6-1 is detailed in this chapter. Structural damage results are obtained for buildings representative of typical Florida homes using the procedures defined by the flowchart. These building types are defined in Chapter 3, and the structural damage validation and results are presented in Chapter 7.

Selection of Structural Type and Definition of Geometry

The MCS engine begins by initializing variables common to all structural types as well as variables unique to the particular type under consideration (e.g. concrete block gable roof home in the Central Region). Current selections for variables of both site-built and manufactured homes are described in the following sections. Values are selected to

best represent the most common structural types of Florida homes, as described in Chapter 3. While the current values are hard wired into the MCS engine, future uses of the program architecture such as an online learning laboratory could incorporate user input to change building parameters.

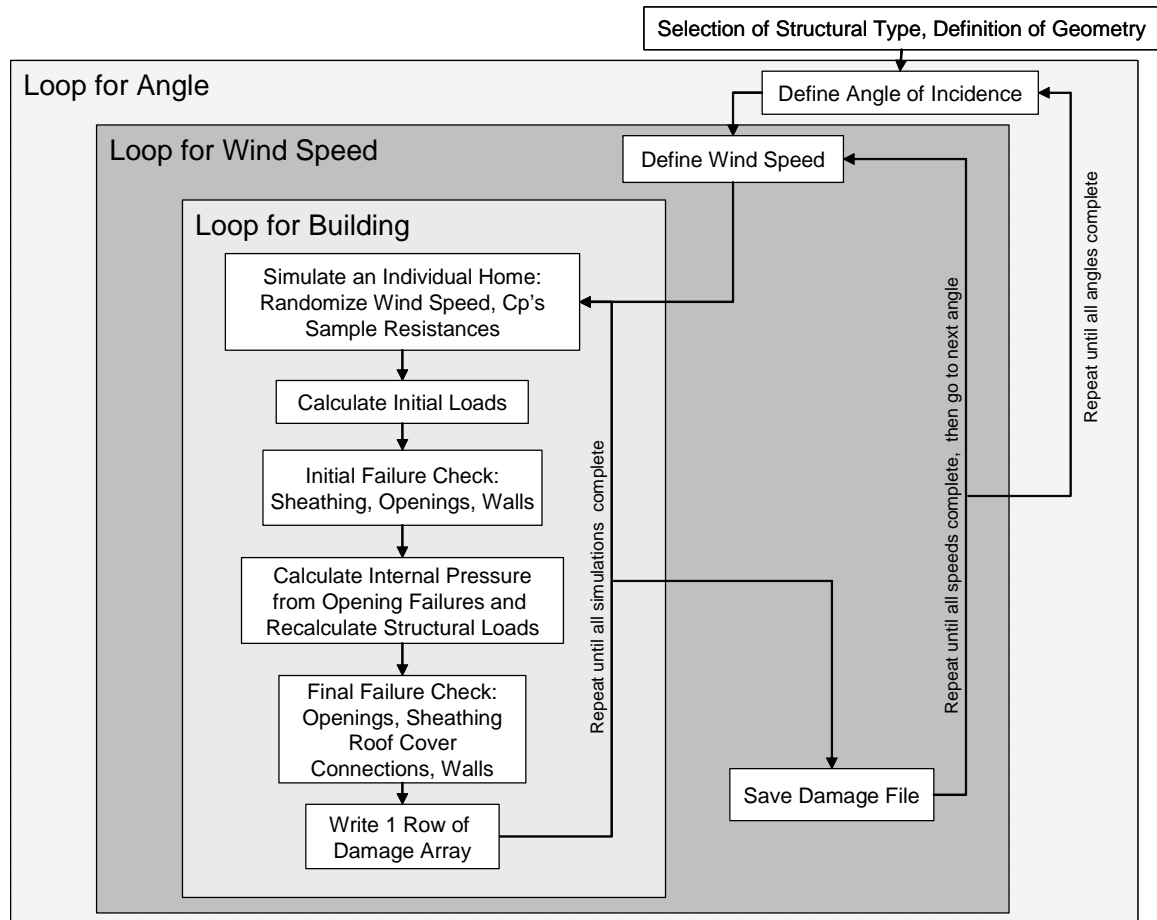


Figure 6-1. Structural damage simulation engine flowchart

Variables for Site-Built Homes

Variables common to all simulated site-built homes include a wall height of 10 ft, an eave overhang of 2 ft, a truss spacing of 2 ft on center, and a roof pitch of 5 on 12. The openings on site-built homes are distributed such that three medium-sized windows, a door, and a two-car garage door occupy the front wall. The front windows are assumed to

be on the interior section of the wall, not in the higher-pressure edge zone that occurs when a neighboring wall is the windward wall. A glass door and four medium-sized windows occupy the back wall. Of the four windows on the back wall, two are situated such that they lie in the edge zone. The two side walls are identical, with four small windows each. Two of these four windows on each side wall lie in the edge zone.

Dimensions for each of the single story site-built structural types described in Chapter 3 are provided in Table 6-1, to include the pressure zone width, a . Sheathing patterns on the roof surface, numbers of roof-to-wall connections, and wood wall sheathing patterns are determined from these dimensions. The designations CB and W refer to concrete block and wood, respectively. G and H are used to denote gable or hip roof types. The dimensions provided for the North and Central Region wood frame homes are the same, since the average values obtained from county property databases were found to be nearly identical. This is also true for the concrete block homes in the Central Region and the combined South and Keys Region. The regional designations for each of these homes are maintained throughout this document for clarity, in spite of the fact that simulations using the data currently available will produce identical results. (As knowledge is gained concerning the regional characteristics of home construction, the resistance values of specific building materials, or the interaction between hurricane winds and low-rise structure, these regionally defined models are likely to change.) Additional details about the variables and matrices used in the MCS engine are provided in the sections describing resistance capacity sampling. Typical window sizes are provided in Table 5-2.

Values are not provided in Table 6-1 for two story homes. As discussed in Chapter 3, these homes make up a small percentage of the population. Structural damages for two story homes will be based on the results of the single story homes. Two story homes in the North region are based on the performance of North WG and WH models due to the prevalence of wood construction in that region. In the Central and South Regions, the CBG and CBH models are used as a framework for determining two story damages. Lastly, two story homes in the Florida Keys are based on all four single story types in that region. These homes are not described in detail in this chapter. Methods used to predict structural damage for two story homes are presented in Chapter 7.

Table 6-1. Site-built home dimensions

Structural Types	Length (ft)	Width (ft)	a (ft)
North Region CBG or CBH	56	38	3.8
North Region WG or WH	60	38	3.8
Central Region CBG or CBH	60	44	4.4
Central Region WG or WH	60	38	3.8
South and Keys Region CBG or CBH	60	44	4.4
South and Keys Region WG or WH	56	44	4.4

Variables for Manufactured Homes

Variables common to all simulated manufactured homes include a length of 56 ft, a wall height of 8 ft, a crawl space under the building of 3 ft, an overhang of 1 ft, a truss spacing of 2 ft on center, and a roof pitch of 4 on 12. The front and back walls of each simulated manufactured home have a door and three windows. On the front wall, two of the windows are medium-sized and one is large. The back wall has all medium-sized windows. Side walls have small windows; one each for singlewide homes and two each for doublewide homes. Dimensions of the manufactured home models are provided in Table 6-2, where MH 1 and MH 2 refer to single and doublewide homes, respectively. MH-pre is the model which has the same shape as the MH 1 model, but different

component strengths, representative of the manufactured homes that pre-date the manufactured home building code changes enacted in 1975. The dimensions shown in Table 6-2 are used to determine the roof sheathing pattern, wall siding pattern, and number of roof-to-wall connections. Window sizes are described in Table 5-2, and additional details about the variables and matrices used in the MCS engine are provided in the section describing resistance capacity sampling.

Table 6-2. Manufactured home dimensions

Structural Type	Length (ft)	Width (ft)	a (ft)
MH 1	56	13	3
MH 2	56	26	3
MH-pre	56	13	3

Loop for Angle of Incidence

After variables have been defined, the simulation engine enters a series of embedded loops for wind direction and speed. Eight angles of incidence (depicted on the plan view of a typical hip roof building in Figure 6-2) are run for each wind speed during the damage simulation routine. In this manner, the orientation of the building relative to the wind direction is uniformly distributed, while the 3-second gust wind loads are directionally based as indicated in Chapter 4. This is an important distinction, since non-directional loading provides a different result than uniformly distributed orientation combined with directional loading. The current approach uses a uniform distribution of wind angles due to a lack of statistical information on orientation with respect to wind direction during hurricane landfall. Future efforts could weight the angles presented in Figure 6-2; accounting for the most likely neighborhood layouts and for the most likely direction of approach for hurricane winds within particular areas of the state by using different weighting values between regions or zip codes.

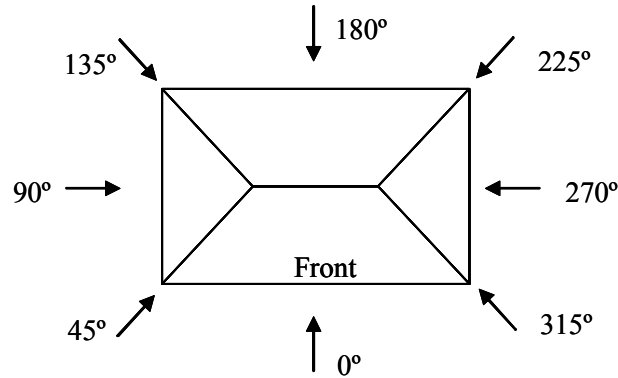


Figure 6-2. Angles of wind incidence used for each wind speed

Loop for Wind Speed

In addition to the eight possible wind approach angles, the MCS engine can be run for any number of wind speeds. The current choice of 3-second gust wind speeds ranging from 50 mph to 250 mph in increments of 5 mph reflect the requirements of the Florida Department of Financial Services and the input of the meteorology team for the Public Loss Hurricane Projection Model. These discrete values define the storm intensity.

Loop for the Simulated Homes

For each combination of angle and wind speed, the MCS engine simulates a user defined number of realizations of the system, which consists of the wind loads and resistances for the particular structural type being investigated. Each realization is created by randomizing the discrete value of the 3-second gust wind speed and pressure coefficients (Cps) defined in Chapter 4, and by sampling from the distributions of component resistances described in Chapter 5. A sequence of failure checks is then used to determine the structural damage for each building simulated at a particular wind speed and angle of incidence. These steps are shown in Figure 6-3, and are described in the following paragraphs as they would occur for a single realization of the structural type (e.g. one of thousands of Central CBG homes). Figure 6-3 represents the building loop

subset of Figure 6-1 (which describes the entire simulation process). Before this loop is initiated, the 3-second gust speed defining storm intensity and the angle of incidence are already selected.

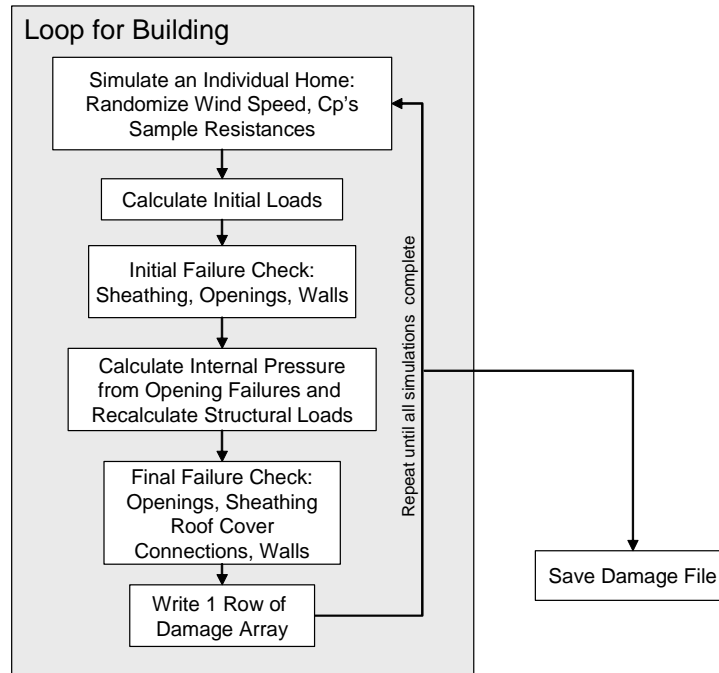


Figure 6-3. Flowchart for realizations of a structural type

Randomization of Wind Speed and Pressure Coefficients

The discrete value of the 3-second wind speed defined in the intermediate loop of Figure 6-1 represents the intensity of the storm to which the simulated buildings are subjected. Selected values are defined between 50 and 250 mph in relatively narrow increments of 5 mph. These choices meet the requirements of the Florida Department of Financial Services commission, and allow for the relation of structural damage results to the meteorology-team-predicted likelihood of maximum 3-second gust wind speeds in different zip codes throughout the state of Florida, on an annualized basis. A single pass within the “Loop for Wind Speed” depicted in Figure 6-1 represents exposure of buildings to a storm with maximum sustained 3-second gusts within a zone of intensity.

For each of these defined storm exposure categories, there exists a degree of uncertainty concerning the exact value of the maximum sustained 3-second gust wind speed observed at the location of the simulated building. Additionally, there is uncertainty concerning the exact value of the pressure coefficients described in Chapter 4. Surrounding obstacles may shelter individual houses, or homes may lie in areas prone to slightly higher than average winds. For these reasons, the discrete value of the wind speed and the discrete values of the pressure coefficients are randomized for each simulated home.

Randomization of the wind speed and pressure coefficient values is achieved in the *MatLAB* based code with the function *randn()*. This command generates a group of numbers randomly sampled from the standard normal distribution, a Gaussian PDF with a mean of zero and a standard deviation of one. The randomly generated numbers are then individually scaled using Equation 6-1, where z is a randomly generated value from the standard normal distribution, μ is the mean value of desired PDF, and COV is the coefficient of variation of the desired PDF. The resulting x is a value in the desired PDF with the same likelihood of occurrence as z .

$$x = (z \cdot COV + 1)\mu \quad (6-1)$$

The COV for wind speed and pressure coefficient variation is selected to be 0.1 (10% of the mean value). Values of μ substituted into Equation 6-1 to generate randomized pressure coefficients are the discrete values presented in Tables 4-1 through 4-4, as well as the internal pressure coefficient of +0.18. In this manner, the MCS engine samples the pressure coefficients using Equation 6-1 to generate a randomly selected value from a PDF with a mean of the discrete pressure coefficient provided by ASCE 7-98 and a COV of 0.1.

Values of μ substituted into Equation 6-1 for the generation of the randomized wind speed are the discrete values of the 3-second maximum gust speed, from 50 to 250 mph in 5 mph increments. The same mean value is used within a single “Loop for Wind Speed,” generating slightly different maximum 3-second gusts for each building simulated within that category of storm intensity. The randomly selected 3-second gust wind speed and the randomized pressure coefficient values are maintained for the life of an individual building simulation (the sequence of steps shown in Figure 6-3). As each new building is simulated, these values are sampled to account for the uncertainty in wind speed and pressure coefficient intensities on the individual building. In this manner, each of the simulated buildings of a structural type represents a home at a slightly different location within a neighborhood exposed to the defined storm intensity.

Initial Load Calculations

Once the wind speed and pressure coefficient values for the individual building simulation are determined using Equation 6-1, the initial wind loads are calculated. During this step, the velocity pressure is obtained using Equation 4-1. The surface pressures described in Chapter 4 are calculated using the randomly generated pressure coefficients and wind speed described in the preceding section in Equation 4-2. From these calculated pressures, the structural loads described in Table 4-5 are obtained.

Sampling of Resistances

The task of sampling resistance values from the distributions described in Chapter 5 is the key that makes the MCS engine a probability-based system-response model. During this step, each individual piece of a typical component is assigned a unique capacity value. In this manner, each of the simulated houses represents one possible realization of the population of typically constructed Florida building types. Details of the

capacity assigning process are described for each component in the following sections. For clarity, Figure 3-4 (illustrating the components of typical site-built homes) is reprinted here as Figure 6-4. Manufactured homes are modeled with the five components illustrated in Figure 6-4 and a sixth component, tie-down anchors.

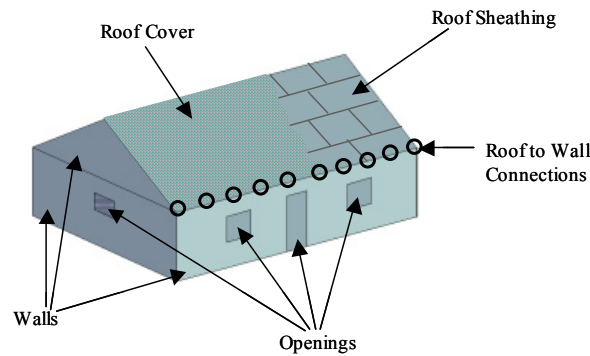


Figure 6-4. Modeled structural components.

Roof cover and roof sheathing resistance sampling

Each of the structural types listed in Tables 6-1 and 6-2 has a predetermined roof sheathing panel layout, as detailed in Chapter 4. Variables describing the roof sheathing and cover are represented in the MCS engine as a series of matrices. Separate matrices with similar indexing strategies are created for the size, aggregate pressure coefficient, and capacity of both roof sheathing and cover. Using these similarly indexed matrices, each individual panel of roof sheathing and representative area of roof cover can be investigated. Additionally, the interaction between sheathing and roof cover can be addressed with the matrix indexing strategy.

Wind resistance values for each individual panel or representative area of roof cover are obtained through independent sampling of the PDFs described in Chapter 5. The *MatLAB* function *randn()* is used to generate a group of numbers randomly sampled from the standard normal distribution. The randomly generated numbers are individually

scaled using Equation 6-1, such that they represent a random sampling of the PDF of sheathing or roof cover capacity. The scaling process described by Equation 6-1 is used for all of the sampled resistances in the MCS engine. For the case of roof sheathing and roof cover, two unique matrices of z values are created using the *randn()* command. The size of the matrix is linked to the predetermined number of individual sheathing panels on the roof surface. One of the matrices is scaled to represent the capacity of roof sheathing, and the other similar, but unique, matrix is scaled to represent the capacity of roof cover for the individual house under simulation.

After the capacity matrices are created using the scaling process represented by Equation 6-1, the values are checked to ensure that they lie within two standard deviations of the mean capacity provided in Table 5-3. This process prevents unrealistic capacities (such as negative values) from being used in the simulation process. If a value lies outside the imposed bounds, it is rejected, and a new value is generated using the sampling and scaling process. This process continues iteratively until all values lie within two standard deviations of the mean capacity.

Roof-to-wall connection resistance sampling

The number of roof-to-wall connections that must be assigned unique capacity values on each wall of a simulated home is determined by the truss spacing. For gable roof homes, the truss spacing is used to determine the number of intermediate trusses attached to the side walls. Each of these trusses has two connections, while the gable end trusses are assumed to be connected to the end wall in eight places. For hip roof homes, each outer wall has a number of connections equal to the length of the wall divided by the truss spacing.

The capacity of roof-to-wall connections is obtained through a batch sampling process discussed briefly in Chapter 5. This process is used in the MCS engine only for roof-to-wall connections, specifically to account for the observed damage state of the entire roof system separating from the remaining structure. Using the batch sampling process, a house-specific starting value is obtained using the *randn()* command. For hip roof homes, this single generated value is the starting point for all roof-to-wall connection capacities on the individual structure. For gable roof homes, separate starting values are generated for the side connectors and gable end connectors.

The starting value(s) for each house are scaled to represent values selected from the PDF of connection capacities using the process defined in Equation 6-1. After scaling, the value(s) are checked to ensure that they lie within two standard deviations of the mean provided in Table 5-3. If a value lies outside of these bounds, it is rejected, and a new value is sampled and scaled. This process continues iteratively as needed. The scaled value(s) generated in this process represent the mean resistance for the population of roof-to-wall connections on the house. Individual connector capacities are obtained using a group of numbers generated by the *randn()* command and scaled using Equation 6-1, with the generated mean for the population of connectors on the house and a *COV* of 0.05. The results of this substitution are shown in Equation 6-2, where y is the resistance capacity of one connector, z is a randomly generated value from the standard normal distribution, and $\hat{\mu}$ is the generated mean resistance for the connectors on the house.

$$y = (z \cdot 0.05 + 1)\hat{\mu} \quad (6-2)$$

The process of sampling represented in Equation 6-2 is shown in Figure 6-5. The distribution on the left represents the PDF of a type of connector, as described in Chapter

5. Selected values from this distribution become mean values for individual homes, as shown on the right hand side.

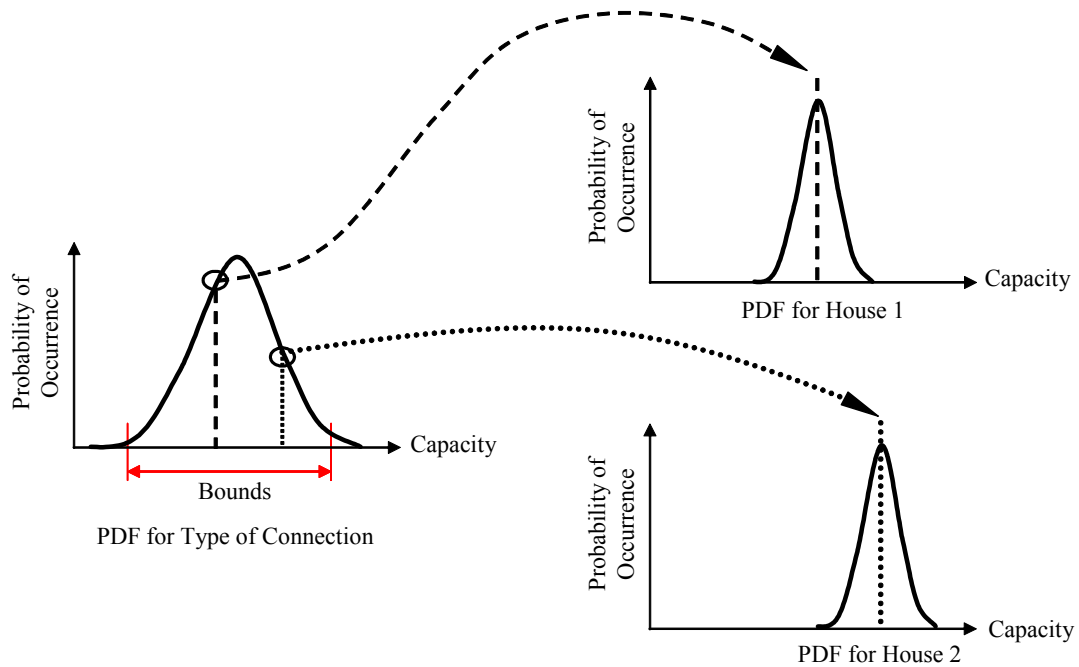


Figure 6-5. Batch sampling method for roof-to-wall connections

The process of batch sampling results in a narrow distribution of connector capacities on an individual building, as depicted by the more tightly centered PDFs on the right hand side of Figure 6-5. Using this method of sampling, and employing a load redistribution scheme for failed roof-to-wall connections allows for the possibility of the entire roof structure pulling off of the structure, a damage state that has been observed in post-damage reports [19].

Wall resistance sampling

Wall resistance capacities are dependent on the structural type. As shown in Table 4-5, concrete block homes, wood frame homes, and manufactured homes have different limit states for walls. Structural damage checks common to site-built homes include shear wall failure, uplift failure, and out-of-plane loading failure. Each of the four perimeter

walls on an individual site-built home is assigned a shear wall, uplift, and out-of-plane capacity using the sampling method common to most components. The *randn()* command is used to generate three sets of four starting values. The four values represent the four perimeter walls. Each set of four values is scaled using the appropriate values from Table 5-3 in Equation 6-1: one set for shear wall resistance, one for uplift, and the third for out-of-plane loading capacity. For concrete block walls, the out-of-plane capacity is the allowable bending moment, while wood walls have an out-of-plane capacity associated with the lateral strength of framing connections. Each of the twelve generated resistance values is compared to the appropriate mean from Table 5-3. Individual values that do not lie within two standard deviations of the mean are rejected, and new values sampled until the truncation criteria are met.

A structural damage check common to most structural types, but conducted on different areas of each, is the wall sheathing failure test. Due to the typical location of plywood or vinyl sheathing, this check is used on the entire wall surface of wood frame and manufactured homes, but only for the triangular gable ends of concrete block homes. Predetermined sheathing panel layouts for each of the structural types listed in Tables 6-1 and 6-2 are used similarly to the roof sheathing panel layouts. A matrix of values is used to represent the capacity of each individual sheathing panel. The number of panels is determined by placing typical 4 x 8 ft pieces of plywood on site-built homes, and 3 x 12 ft pieces of vinyl siding on manufactured homes. The *randn()* command is used to generate a starting value for each panel, which is scaled using the appropriate values from Table 5-3 in Equation 6-1. Individual values that do not lie within two standard deviations of the mean are rejected, and new values sampled until the limits are met.

Opening resistance sampling

Wind pressure resistance values for individual openings are obtained using the number generation and scaling process previously defined. Unique values are generated using the *randn()* command for the front and back entrance doors and for the garage door on site-built homes. Individual windows are also assigned unique z values using the *randn()* command. These are stored in matrices designed to maintain both size and location information for each window. All of the generated z values for openings are scaled using Equation 6-1 with the appropriate mean and *COV* from Table 5.3. For openings, the truncation limits are set at 2.5 times the standard deviation rather than the bounds of two standard deviations used for other components.

Discrete resistance values are not required for the case of windborne debris impact. As discussed in Chapter 4, windows that are not impact-resistant cannot usually withstand a direct hit from a piece of typical debris. Instead, parameters are used to determine the likelihood that a window will be struck and broken, given the wind speed, building geometry, and some assumptions about the surrounding terrain and availability of missiles. Using this approach, both the loading conditions and resistance capability are built into a single distribution, $p_D(V)$. As detailed in Chapter 4, the number of window sizes and windward wall scenarios results in twelve $p_D(V)$ functions per modeled building. A wind speed dependent value for each of the twelve functions is generated during the variable definition step. These values are used in the initial failure check to determine the number of windows broken by windborne debris.

Tie-down anchor resistance sampling

The pull-out capacity of each tie-down anchor on a simulated manufactured home is generated using the random number generation and scaling process defined for roof sheathing and roof cover. A unique value is generated per tie-down anchor using the *randn()* command. These are scaled using Equation 6-1 with the mean and *COV* provided in Table 5.3. Values are screened such that they lie within two standard deviations of the mean.

Initial Failure Check

After the deterministic 3-second gust wind loads and probabilistic component resistance values have been determined, the MCS engine begins a sequence of failure checks to determine the level of structural damage on the individually simulated building. Failure checks are ordered to represent the most likely sequence of events and load paths. Within the initial check, loads and resistance capacities are compared independently for roof sheathing, walls, and openings. Once the damage is calculated from the initial loads, the internal pressure is adjusted. This process is discussed after the initial failure checks are described.

Initial failure check for roof sheathing

The pressure resistance capacities of roof sheathing panels are compared to aggregate wind pressure loads using a panel-by-panel comparison between the load and resistance matrices. Individual sheathing panels with aggregate wind pressure equal to or greater than the sampled resistance capacity are marked as failed by changing the capacity value from a generated number to a value of zero. The similar indexing strategy for the roof cover matrix allows the MCS engine to fail roof covering locations at failed sheathing panels. In this manner, the roof cover over a piece of sheathing that has pulled

off is also assumed to be pulled away, and is assigned a capacity of zero for use in the next round of failure checks.

Initial failure check for walls

During the initial failure check, walls on site-built homes are evaluated in uplift, out-of-plane loading, and shear wall loading. Given the level of uncertainty involved in the loading conditions and strength of typical residential walls, as well as the lack of information with which to compare modeled results, the current MCS engine does not discriminate between degrees of damage to walls that fail in uplift, out-of-plane loading, or shear wall loading. A more sophisticated description of wall failure could be a targeted area of future research for additional iterations of the structural damage model. The current model uses the procedures detailed in this section to mark perimeter walls as ‘failed’ or ‘un-failed’ for these loading conditions.

As described in Chapter 5, concrete block walls and wood frame walls behave differently under similar loading conditions. For concrete block walls, a combined case of uplift and bending is used to determine potential failure. The unity check performed for this condition is described in Equation 6-3, where U is the unity check value, P is the applied uplift per foot of wall from roof-to-wall connection loads, P_{allow} is the sampled value of allowable uplift per foot of wall, M is the applied bending moment at the center of the wall, and M_{allow} is the sampled value of allowable bending moment.

$$U = \frac{P}{P_{allow}} + \frac{M}{M_{allow}} \quad (6-3)$$

The applied bending moment, M , in Equation 6-3 is obtained using the MWFRS pressures described in Chapter 4 along a 1-foot strip of wall with the assumption of simple supports at the top and bottom of the wall. This is an oversimplification of the true

conditions at every point along the wall. Given the current body of information, however; the unity check of Equation 6-3 is an adequate analysis of conditions at the centermost point on each wall, where the effects of interaction with other framing elements are minimal. If the value of U obtained for a wall is greater than or equal to one, then that wall is noted as having a structural failure that requires repair.

Unlike concrete block walls, wood frame walls are checked independently in uplift and out-of-plane loading. The uplift per foot of wall applied by the roof-to-wall connections to wood frame walls is compared to the sampled value of allowable uplift per foot of wall. Additionally, a lateral load failure check is conducted using the trapezoidal tributary area shown in Figure 4-8. The lateral force per foot of wall created by this wind pressure zone is compared to the sampled value of lateral resistance per foot of wall. If the applied load in uplift or lateral wind pressure is greater than or equal to the corresponding sampled resistance, then the wall is marked as having a structural failure.

The shear wall load case described in Chapter 4 is common to both concrete block and wood frame homes. For this loading condition, the shears V_1 and V_2 pictured in Figure 4-7 are divided by the length of the wall to which they are applied to obtain a distribution of load per foot of wall. Case A is applied for winds perpendicular to the ridgeline, and Case B is used for winds parallel to the ridgeline. For cornering winds, Cases A and B are applied independently. The calculated value of shear per foot on each of the perimeter walls subject to this loading condition is compared to its sampled resistance value. If the applied load is greater than or equal to the sampled resistance, then the wall is marked as having a structural failure.

Initial failure checks for walls on manufactured homes are conducted for sheathing pull off. The framework of this check is similar to that of roof sheathing panels. For each panel of vinyl siding, a comparison is made between the wind pressure on the wall at that location and the sampled resistance of the individual panel. Individual panels with wind pressures equal to or greater than the sampled resistance capacity are marked as failed by changing the capacity from a generated number to a value of zero.

Initial failure check for openings

Opening failures consist of door, garage door (site-built homes only), and window pressure failures, as well as window impact failures. For each door (including the garage), the wind pressure on the wall at the location of the door is compared to the sampled resistance capacity. Doors with an applied pressure greater than or equal to the resistance capacity are marked as failed. A similar process is used for windows, after the windborne debris impact check has been conducted.

Windows along the windward wall, or both windward walls in the case of cornering winds, are checked for windborne debris impact failure. For each window on this windward area, a value is sampled from a uniform distribution with a range of 0–100. This value represents a randomly chosen percentage between 0% and 100% for each of the windows subject to potential windborne debris impact. The randomly selected values for each windward window are then compared to the appropriate predetermined value of $p_D(V)$, the windborne debris function described in Chapter 4. Values of $p_D(V)$ represent the likelihood of breakage for specific combinations of wind angle, wind speed, window size, and building geometry. Thus, a $p_D(V)$ value of 60% indicates that a window of particular size, on a given area of windward wall, and subject to defined wind

loading conditions will be broken by debris six out of ten times. If the value sampled from the uniform distribution between 0–100 for this individual window falls below 60 (which has a six in ten chance of occurring), then the window is designated as failed by impact loading. If the sampled value is equal to or greater than 60, then the window is not broken by impact.

Windows failed by impact loading are marked in the simulation routine by setting their pressure resistance capacities to a value of zero. Once this step is complete for the windward windows, the MCS engine conducts the pressure failure check for all windows using a point-to-point method to compare individual window pressure loads to the unique sampled resistance values. Individual failures are tallied when the applied pressure is equal to or greater than the resistance capacity.

Internal Pressure Evaluation and Recalculation of Loads

Following the initial failure check for roof sheathing, walls, and openings, the condition of openings is evaluated to determine the effect of damage on the internal pressure. If no openings have failed, then the internal pressure is left unchanged. If one or more openings are damaged, then a new internal pressure for the structure is calculated as the weighted average of pressures at locations of failed openings.

Given the amount of uncertainty in the modeling of opening size, location, strength, and loading, the weighting factors are not precise ratios of square footage. Instead, windows and typical front and back doors are given an equal weight, while garage doors are factored in at a rate of four times the contribution of other openings. This process is represented in Equation 6-4, where p_{in} is the new internal pressure, p_g is the aggregate pressure on the garage door, p_i is the pressure on an individual failed window or door, and n is the total number of failed windows and doors, other than the garage door. gar is

a variable that takes on a value of one when the garage door has failed, and a value of zero if the garage door has not failed.

$$p_{in} = \frac{4(gar)p_g + \sum_{i=1}^n p_i}{n + 4(gar)} \quad (6-4)$$

Once the new internal pressure has been determined, it is checked against the initial value of internal pressure. This initial value is obtained by setting the values of GC_p and GC_{pi} in Equation 4-2 to zero and 0.18, respectively. If the internal pressure remains the same (no openings have failed, or the average internal pressure happens to agree with the initial value), then the existing component loads are carried forward to the final damage check. If the new internal pressure varies from the original value, then the pressures applied to the simulated home are recalculated using Equation 6-5, which is a modified version of Equation 4-2.

$$p = q_h(0.8)GC_p - p_{in} \quad (6-5)$$

Final Failure Check and Damage Tally

Final damage checks are conducted using the structural wind loads, after the internal pressure adjustment. This series of checks is structured to take advantage of the load path and dependence of some building components. Openings are re-checked for overpressure failure using the new pressure loads. Previously failed openings remained listed as damaged, and a point-by-point comparison is used to determine if any additional windows or doors fail as a result of the change in internal pressure. Once the re-check is complete, the total number of failed windows and doors are recorded for the simulated home.

Roof sheathing panels are also re-checked; maintaining previously failed panels and investigating other panels to determine if additional failures result from the change in internal pressure. The total number of failed sheathing panels is converted into a percentage by summing the square footage of failed panels over the total roof area.

Once the roof sheathing check is complete, the roof cover check is conducted for the first time. This component is not examined during the initial failure investigation because the roof cover loads described in Chapter 4 are independent of the internal pressure. Roof cover failure is dependent on sheathing failure, however. Locations of roof cover over sheathing panels that have been damaged are automatically assigned a capacity of zero, such that the panel-by-panel comparison of loads to resistances for the roof cover areas will result in the failure of these locations. For this reason, the roof cover check is conducted only after the sheathing panels have been investigated. In the same fashion as roof sheathing, the failed locations of roof cover are converted into a percentage by summing the square footage of damaged roof covering over the total area of the roof.

Roof-to-wall connection loads are computed using the wind pressures on the roof sheathing with the adjustment to internal pressure. A tributary area method is used to distribute loads from individual roof sheathing panels into the connections. The first failure check is conducted using these initial connection loads. For each connector, the applied load is compared to the sampled value of resistance. If the applied uplift is greater than or equal to the probabilistically assigned capacity, the individual connection is listed as failed, and its load is redistributed to intact connections. The redistribution subroutine searches for the closest two intact connections on either side of a middle roof-to-wall

connection, sharing the load of the failed connection with four neighboring connectors when possible. Specifically, one-third of the load is shed to each of the two closest connectors, and one-sixth of the load is distributed to the next closest intact connection on either side. When only one intact connection is available to the left or right of the failed connection, it receives half of the load from the failed connection. This failure check and load redistribution process occurs until no new connection failures are discovered, or until an entire side of the roof is unzipped from the supporting wall.

The last components checked on site-built homes are the walls. Each wall is re-checked for failure in uplift, out-of-plane loading, and shear wall loading. For the final damage check, wall support is dependent on roof-to-wall connection failure. Walls with half or less of the roof-to-wall connections intact are no longer assumed to be simply supported. As described in Chapter 4, the bending moment for concrete block walls with more than half of the roof-to-wall connections failed is scaled up by a factor of 2.8, and the tributary area for lateral loads on wood frame walls is increased. Using the new loads, walls are investigated for additional failures with the methods described during the initial failure check.

A final wall check common to every structural type except hip roof concrete block homes, is the investigation of wall sheathing. For manufactured homes, this primary check is re-evaluated here using the adjusted wind loads. Panels previously failed are maintained on the list of damaged members, while the MCS engine looks for additional panel failures. For site-built homes, the wall sheathing check is secondary, conducted only after the other components have been reviewed. The gable end panels of concrete block gable roof homes and the entire wall surface of wood frame homes are checked for

sheathing failure in much the same way that roof sheathing failures are investigated. A panel-by-panel comparison of wall pressure and probabilistically assigned wall sheathing capacity is conducted. Panels with applied loads greater than or equal to the assigned panel capacity are listed as failed. These damages are converted to a percentage by dividing the square footage of damaged panels by the total area of wall sheathing.

The final structural checks for manufactured homes relate to tie-down anchors. Limit states for sliding and overturning are investigated using the probabilistically assigned pull-out capacity of the anchors and the calculated sliding and overturning loads discussed in Chapter 4. The sliding force on the manufactured home is resisted by the combined capacity of the anchors on the home. If the applied load is greater than or equal to the resultant capacity, then the home experiences a sliding failure. This initial sliding may break tie-down anchors, but not move the home off of its foundation. To check whether the home has been removed from the foundation, an additional check is conducted. In this case, the static friction of the home on the pile foundation is added to the sliding resistance. For this calculation, the weight of the home is probabilistically assigned by sampling from a distribution with a *COV* of 0.25 and mean of 30 psf times the square footage of the home. Weights outside the truncation limits of two standard deviations are re-sampled. The coefficient of friction is assumed to be 0.2, a value typical of wood on metals under wet conditions [58]. During this check, if the resultant sliding force is greater than or equal to 1.2 times the newly calculated resistance value, then the home is assumed to have major sliding damage.

An independent anchor check is conducted for overturning. In this case, the capacity to resist overturning is calculated by summing the resistive moment from the tie-

down anchors and the structural weight about at the location of the support pier for the leeward wall. As shown in Figure 6-6, the entire weight of the home is assumed to act at the centerline. A resultant wind force acting at mid wall height is calculated from the Main Wind Force Resisting System (MWFRS) wall loads, and the tie-down anchor forces on the windward wall side contribute at a 45 degree angle. Moments are summed about the foundation pier on the leeward side of the home, represented by a small black circle shown on the right hand side of Figure 6-6. The anchors on the leeward side of the home do not contribute to the overturning resistance capacity, since they act through the location of the summation of moments.

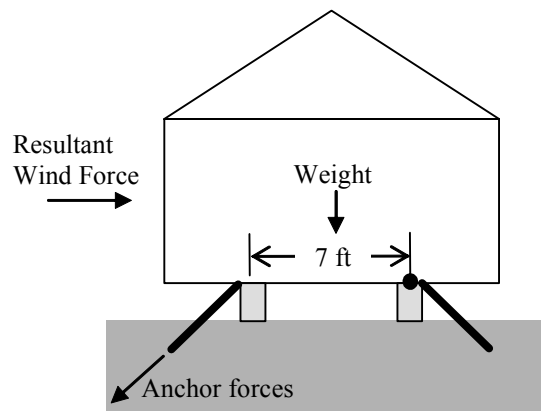


Figure 6-5. Location of forces for the overturning failure check on manufactured homes

If the applied overturning moment is greater than or equal to the resistive moment of the weight and tie-down anchors, then the home has overturned. Due to the geometry of typical manufactured homes, overturning is not expected to occur prior to sliding when the winds approach parallel to the ridgeline or from the corners. For this reason, overturning is considered only for wind angles perpendicular to the ridgeline.

In case of overturning and/or sliding, no attempt is made to identify the discrete number of failed tie-down anchors. Given the amount of uncertainty in predicting

damage to manufactured homes and in quantifying the monetary loss associated with damage, efforts to identify individual tie-down anchor loss would not add to the accuracy of end results. The state of overturning or sliding applies to the entire home, not to individual tie-down anchors.

Structural Damage Output Files

The results of the structural damage-prediction model will be used to develop insured loss functions for the Public Loss Hurricane Projection Model. These functions will include repair and replacement costs as well as additional costs for loss of contents. For ease in post-processing and to maintain the flexibility of including additional insured loss variables which might be linked to specific damages, the structural damage output from the MCS engine is stored in individual output files for each combination of wind speed, angle, and building type. For example, a typical output file holds the results of several hundred thousand simulations of South Region Concrete Block Hip Roof (CBH) homes at 45° 150 mph 3-second gust winds. For site-built homes, the damage information for each simulated home includes

- Percent (by area) of failed roof sheathing
- Percent (by area) of failed roof cover
- Percent (of total) roof-to-wall connections failed
- Number of damaged walls (4 total)
- Number of damaged windows (15 total)
- Number of damage windows that were broken as a result of debris impact
- Number of failed entry doors (2 total)
- Indicator variable for the garage door (0 = unfailed, 1 = damaged)
- Percent (by area) of damaged gable end panels (0 for hip roof buildings)
- Percent (by area) of damaged wall sheathing panels (for wood homes)
- The calculated internal pressure

Similar information is stored for manufactured homes, with the addition of two variables for sliding and overturning. Damage information for manufactured homes includes

- Percent (by area) of failed roof sheathing
- Percent (by area) of failed roof cover
- Number of roof-to-wall connections failed (58 total)
- Number of damaged windows (8 total for singlewide, 10 total for doublewide)
- Number of damage windows that were broken as a result of debris impact
- Number of failed entry doors (2 total)
- Percent (by area) of damaged vinyl siding panels
- Indicator variable for sliding (0 = no sliding, 1 = minor, 2 = major)
- Indicator variable for overturning (0 = not overturned, 1 = overturned)

Summary

The MCS engine described in this chapter simulates the performance and interaction of components of typical Florida homes during hurricane winds, using the structural loads discussed in Chapter 4 and the building component resistances described in Chapter 5. This model is developed in partial fulfillment of the engineering tasks for the Public Loss Hurricane Projection Model. Results of this effort, presented in Chapter 7, will be used to create insured loss functions for the prediction of annual risk in the State of Florida. Additional uses for the MCS engine outside the scope of the current project include the development of an online learning laboratory, where engineering students and homeowners can learn about extreme wind loads through the use of a graphical user interface to the MCS engine that allows the user to change building construction and storm parameters, and then see a visual representation of the resulting structural damage.

CHAPTER 7 STRUCTURAL DAMAGE VALIDATION AND RESULTS

Results detailed in this chapter represent the structural vulnerability of typically constructed homes to wind damage, using the Monte Carlo Simulation engine described in Chapter 6. Wind loads and building component capacities incorporated in the damage simulation are described in Chapters 4 and 5, respectively. Structural damage results obtained from the simulation engine are used to determine insured losses on an annualized basis or as the result of a specific storm for the Public Loss Hurricane Projection Model (PLHP). A discussion of the methodology and preliminary findings for the relation of physical damage to insured losses is provided in Chapter 8.

A descriptive list of the homes selected to represent the Florida building stock is provided in Tables 7-1 and 7-2. Homes modeled in the simulation process detailed in Chapter 6 are described in Table 7-1, while Table 7-2 provides a list of structures for which the vulnerability is based on the performance of selected types in Table 7-1. The process of selection of structural types and relevant building components is discussed in greater detail in Chapter 3. As described earlier, two sets of homes selected for modeling have the same dimensions and structural description. These are the North and Central wood frame homes and the Central and South/Keys concrete block homes. Results for the pairs will be the same because these homes were similarly described in the county property databases. The regional descriptions are maintained throughout this document, however, for clarity of the methodology used to generate insured losses. Additionally, future iterations of the PLHP model are expected to incorporate changes to these models.

Table 7-1. Modeled structural types

Structural Type	Description	Roof Type	Area (ft ²)
North CBG	1 Story concrete block in North FL	Gable	2128
North CBH	1 Story concrete block in North FL	Hip	2128
North WG	1 Story wood frame in North FL	Gable	2280
North WH	1 Story wood frame in North FL	Hip	2280
Central CBG	1 Story concrete block in Central FL	Gable	2640
Central CBH	1 Story concrete block in Central FL	Hip	2640
Central WG	1 Story wood frame in Central FL	Gable	2280
Central WH	1 Story wood frame in Central FL	Hip	2280
South/Keys CBG	1 Story concrete block in South FL or Keys	Gable	2640
South/Keys CBH	1 Story concrete block in South FL or Keys	Hip	2640
South/Keys WG	1 Story wood frame in South FL or Keys	Gable	2464
South/Keys WH	1 Story wood frame in South FL or Keys	Hip	2464
MH 1	Manufactured home	Gable	728
MH 2	Manufactured home	Gable	1456
MH-pre	Pre-HUD Code Manufactured home	Gable	728

Table 7-2. Structural types with damage based on combinations of modeled buildings

Structural Type	Models Used to Predict Structural Performance
North 2 story	North WG and North WH
Central 2 story	Central CBG and Central CBH
South 2 story	South/Keys CBG and South/Keys CBH
Keys 2 story	South/Keys CBG, South/Keys CBH, South/Keys WG, and South/Keys WH

The first section of this chapter provides a discussion of the validation of the system using the limited data available from Hurricane Andrew. Results for South/Keys CBG homes are typically used to validate methodology used for all homes in the simulation process, since the Hurricane Andrew data consists mainly of homes of this type. Following the validation discussion is an investigation of the batch selection method used for roof-to-wall connections and an investigation of the results for different roof shapes. The last section provides structural damage prediction results for typical Florida homes. Specifically, results obtained from the simulation engine are presented for site built homes in the South/Keys Region and for manufactured homes. The results provided in this chapter are limited, for the sake of brevity. Additional results for these

structural models are provided in Appendices A through G. Results for the North and Central Regions will be available when the PLHP is released in May, 2005.

Structural Damage Validation

The structural wind loads described in Chapter 4 and building component capacities described in Chapter 5 are based on building codes, available literature, manufacturer data, and engineering judgment. As described in Chapter 6, selected values for loads and resistances are applied within a component-based probabilistic framework for the prediction of damages at varying levels of storm intensity. This approach is also used for the HAZUS® model, developed by Applied Research Associates under the direction of the National Institute of Building Sciences for the Federal Emergency Management Agency [3]. While the component-based method is considered state of the art in hurricane damage prediction, the specific values selected for loads and resistances must be validated with available hurricane damage reports.

Unfortunately, data available for comparison is limited. Most damage reports from past storms provide expert opinion on the types of damages observed, and potential building code or construction mitigation efforts, but few reports provide statistically significant numbers of detailed damage results for individual structures. Only one report has been located to date that offers the type of information necessary to validate choices made in the development of the structural damage simulation engine for the PLHP. Using information provided in the National Association of Home Builders Research Center (NAHB) 1993 assessment of Hurricane Andrew damage [19], load and resistance values used to determine structural damage are validated to the extent possible. A description of the data provided by this 1993 report, a discussion of validation techniques, and comparisons of damage results for individual components are presented in this section.

NAHB Report on Hurricane Andrew

The report conducted by the NAHB Research Center for HUD on the damages observed during Hurricanes Andrew and Iniki was the first post-damage assessment to use standardized forms for damage information collection on a significant number of homes [19]. Data was collected in South Florida and Louisiana for Hurricane Andrew and in Hawaii for Hurricane Iniki. A detailed description of the cluster sampling process by which the 515 homes in South Florida were selected is provided on pages 18-20 in the NAHB report [19]. Of the 515 homes assessed, 460 damage reports were included in the published volume. Levels of damages observed on surveyed Florida homes are presented in Table 7-3, with values taken from Table D-2 of the NAHB report. Cases in which the level of damage was not specified in the NAHB report included homes where tarps or other obstructions prevented observers from adequately characterizing the level of damage.

Table 7-3. Hurricane Andrew damages surveyed in the 1993 NAHB report

Level of Damage	Windows	Walls	Roof-to-Wall Connections	Roof Sheathing	Roof Cover
1/3 or less	33%	96%	85%	57%	18%
1/3 – 2/3	26%	1%	6%	12%	23%
2/3 or more	34%		2%	6%	36%
Not specified	6%	3%	6%	25%	23%

The majority of homes discussed in the NAHB report represent a limited number of structural types. Specifically, 99.6% (464 of 466) of the South Florida homes presented in Table 7-3 above are masonry structures, and 81% have gable roofs [19]. A limited re-survey of 34 structures to gain more information concerning wood frame home damages is summarized in Table D-5 of the NAHB report. Of these wood frame homes, an

unspecified number have masonry first floors with wood frame second stories. The results of the re-survey for wood frame damage are presented in Table 7-4.

Table 7-4. Wood frame home damages surveyed in the 1993 NAHB report

Level of Damage	Windows	Walls	Roof-to-Wall Connections	Roof Sheathing	Roof Cover
1/3 or less	65%	82%	85%	56%	41%
1/3 – 2/3	24%	18%	6%	26%	21%
2/3 or more	9%		6%	18%	38%
Not specified	3%		3%		

Damage levels presented in Tables 7-3 and 7-4 are used as a means of validating the simulation engine results. Specific uses and limitations of the data provided by the NAHB report are described in the following section.

Application of the NAHB Report Data as a Validation Tool

The NAHB report provides a unique dataset of structural damages resulting from hurricane landfall, and it is currently the only source of data with which to compare simulated structural damages for the purpose of validation. The information reported must be considered within an appropriate framework; however, for use as a method of validating damage predicted by the simulation engine. Specifically, the wind speeds, angles of approach, and types of homes represented by the data in the NAHB report impose limits on the use of reported damages to validate simulated damages. The implications of the data characteristics and the validation methodology employed are described in this section.

Homes investigated in South Florida for the NAHB report were closely geographically spaced, indicating that the population represents a narrow value of storm intensity. Thus, a comparison of recorded to simulated damage is not possible for the wide range of wind speeds for which the simulation engine has been developed.

Additionally, the winds speeds incurred during the passage of Hurricane Andrew through the neighborhoods surveyed for damage have been a source of controversy in the years following Andrew's landfall [59]. Therefore, direct comparisons between reported damages and simulated damages obtained from the developed structural damage-prediction model can be made only for a narrow range of wind speeds, the value of which is disputed by experts in the field.

In addition to representing a single value of storm intensity, homes described in the NAHB report most likely represent a limited number of wind approach angles. Given that the buildings were typical aligned in neighborhood rows; the initial damage on most of the surveyed homes in each neighborhood was caused by winds approaching from the same angle with respect to the ridgeline of the roof. The results of the damage-prediction model include eight different wind directions, however. Since the damage-prediction model has been developed to encompass neighborhood layouts in all Florida zip codes, the scope of the work is necessarily broad. The observed damage as a result of Hurricane Andrew is by definition, a single scenario, with a limited scope in terms of wind approach angles. As a result, comparisons between the two efforts at the wind speeds represented by the Hurricane Andrew data should be qualitative. A quantitative comparison such as a calculation of the percent error between the simulated data and the Hurricane Andrew data should not be used as a measure of simulation validity.

Further limitations on the use of the Hurricane Andrew data in the 1993 NAHB report are incurred as a result of the building population in the area of landfall. As described in the previous section detailing the NAHB report results, most of the buildings surveyed were masonry homes with gable roofs. Because they were closely

geographically spaced, the homes were most likely built around the same time with similar materials and construction crews. Individual homes probably had different floor plans, however, with differing numbers of windows, outside dimensions, locations of interior walls, etc. As a result, the population of homes described in the NAHB report represents homes of similar age in one local area, while the damage-prediction model encompasses broader regional zones and homes of all ages. The building classification used in the structural damage model that most closely resembles the building population of the homes surveyed for damage after Hurricane Andrew is the South/Keys CBG described in Table 7-1. This building type is modeled to represent typical homes in the entire South Florida and Florida Keys Region, however. The dimensions, numbers of windows, and other unique aspects of individual homes surveyed for the Hurricane Andrew report are not likely to match the characteristics of the simulated model. These uncertainties reinforce the need for qualitative validation rather than exact numerical comparison of results between the NAHB data and the simulated damage results for South/Keys CBG homes.

Validation of Individual Components

In spite of the limitations described in the previous section, the NAHB data collected in the wake of Hurricane Andrew remains the only source of statistically significant information with which to compare the simulated damage results. Qualitative validation is presented in the following sections for individual building components. Specifically, comparisons of trends and ranges of predicted damages are made between the NAHB report data and simulated damages for 3-second gust wind speeds representative of Category 4 storms on the Saffir-Simpson scale. Wind speeds of 160, 175, and 190 mph 3-second gusts are selected for simulated results because these wind

speeds represent low, medium, and high values of Category 4 storm intensity. Given the limitations of comparison, quantitative measures of similarity between reported damages and simulated damages are typically not calculated. Instead, trend and range comparisons between the narrowly defined Hurricane Andrew population of homes and the more broadly defined South/Keys CBG homes are noted as proof of concept for the methodology used in the damage-prediction model.

In addition to the validation of damage results with the NAHB data, a brief description of the vulnerability and fragility curves are provided for each component discussed in the following sections. Concept descriptions of vulnerability and fragility are provided in Chapter 2, and shown in Figure 2-6 through 2-8. The mean damage results presented in the vulnerability curves and the probabilities of exceeding discrete levels of damage presented in the fragility curves provide detailed information for predicted damages over the entire range of wind speeds for which the simulation model has been developed. These curves cannot be validated with damage results because data is not available at each wind speed. Engineering judgment is used to determine whether the shape and location of each curve represents a reasonable expectation of the level of damage for the component in question.

It is worthy to note at this point in the discussion of validation concepts that a detailed validation of structural damage is unlikely to be made for commercially developed risk models. Typically, the developers of commercial models for the insurance industry have proprietary claims data available for validation purposes. Using the claims data, the methodology of the commercial models is validated at the monetary level. This level of validation will be conducted for the PLHP model before it is released in its

entirety in 2005. At the present time, however, the PLHP is incomplete. The results presented in this dissertation represent one piece of a multi-university project encompassing several fields of study. As a result, the structural damage results presented in this chapter for windows, walls, roof-to-wall connections, roof sheathing, and roof cover are investigated to a much greater extent than similar results for proprietary models are likely to be scrutinized.

Validation of window damage

Using the results obtained from 4,000 individual building simulations, the percentage of homes with windows in each damage category specified by the NAHB report is shown in Table 7-5. Values from Table 7-3 for window damage observed on homes surveyed in Florida after Hurricane Andrew for the 1993 NAHB report are reprinted in Table 7-5 for comparison.

Table 7-5. Window damage from Hurricane Andrew vs. simulated data

Window Damage Level	Hurricane Andrew Data from NAHB	Simulated Data		
		160 mph 3-sec Gust	175 mph 3-sec Gust	190 mph 3-sec Gust
1/3 or less	33%	46.6%	20.4%	7.0%
1/3 – 2/3	26%	51.6%	69.4%	60.6%
2/3 or more	34%	1.8%	10.2%	32.4%
Not specified	6%			

Trends in the data presented in Table 7-5 indicate that the values selected for wind loads and resistances on exposed windows adequately characterize the performance of typical Florida residences. From the Hurricane Andrew data, damage to windows can be interpreted as being close to evenly distributed between the three levels. The simulated data does not appear to be as evenly distributed, but it does indicate that the mean value of damage to windows during Category 4 storms lies in the middle third (1/3 – 2/3 damage). Histograms of window breakage provided in Figure 7-1 for Category 4 wind

speeds indicate that the window damage is more evenly spread in the simulated data than Table 7-5 would suggest. Histograms provided in Figure 7-1 are normalized such that the area under each curve is unity. Specific choices of window size and location in the simulated models result in the lack of smoothness in the histograms in Figure 7-1. This is most apparent for the case of 190 mph 3-second gust winds. The variation of the likelihood of occurrence for numbers of broken windows greater than 10 on a given home, however, will not adversely affect the end product of insurable loss. A qualitative comparison of the damage represented by the histograms in Figure 7-1 with the results of the NAHB study presented in Table 7-5 indicates that the methodology used to determine window breakage in the damage-prediction model is an acceptable representation of typical Florida homes.

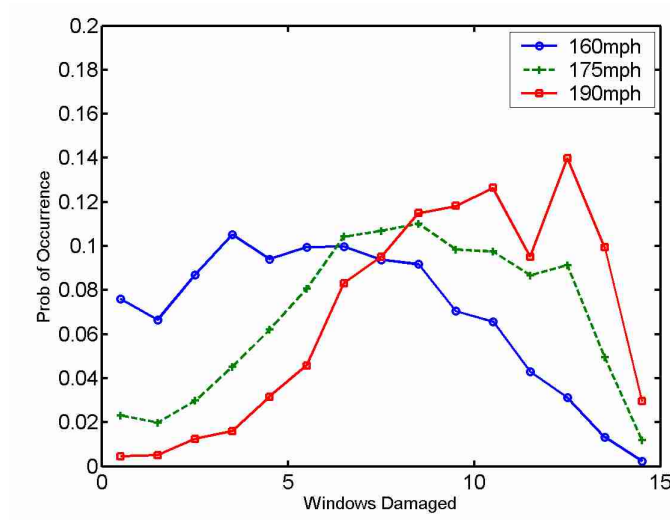


Figure 7-1. Histograms of window damage on South/Keys CBG homes.

Additional conclusions concerning the methodology employed in the modeling of window loads and capacity values can be drawn from the simulated vulnerability and fragility curves. Mean window damage (presented in Figure 7-2) and probabilities of exceeding discrete numbers of broken windows (provided in Figure 7-3) cannot be

validated with existing data. These curves are provided to indicate the predicted levels of damage over the entire range of wind speeds for which the damage simulation model has been developed. The vulnerability curve for window damage and the fragility curves for varying levels of damage indicate that the selected loading mechanisms and resistance values produce simulated window damages that increase with reasonable expectation as the 3-second gust wind speed increases.

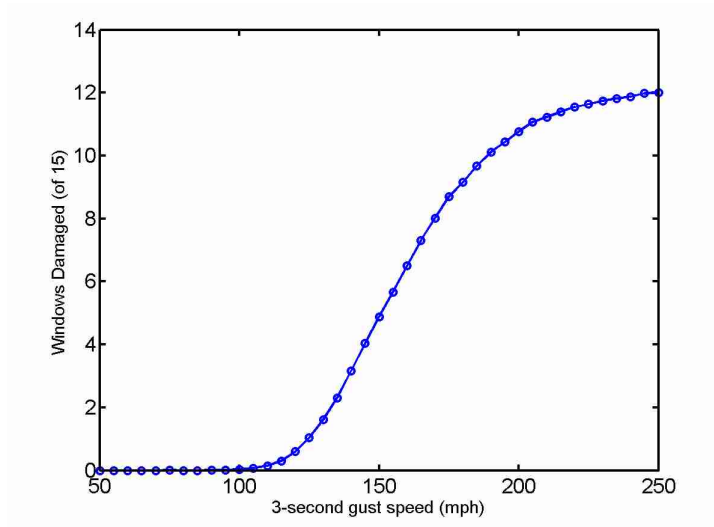


Figure 7-2. Window damage vulnerability of South/Keys CBG homes.

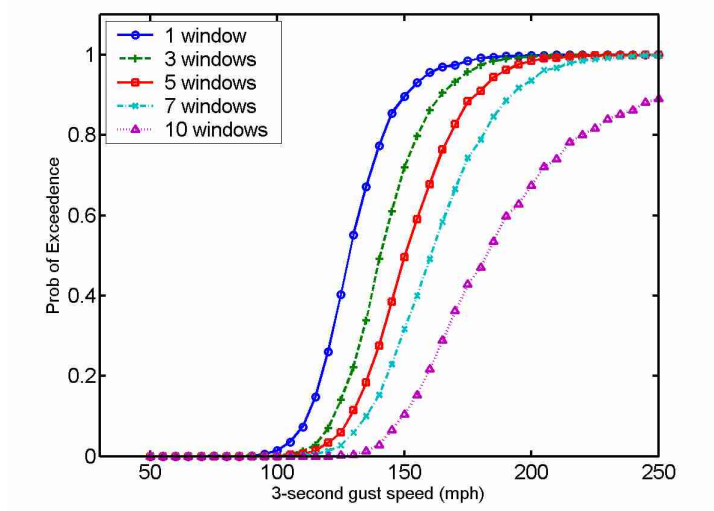


Figure 7-3. Fragility curves for 1, 3, 5, 7, and 10 damaged windows for South/Keys CBG homes.

Validation of masonry wall damage

Using the results of 4,000 individual building simulations, the percentage of South/Keys CBG homes with wall damage in each category specified by the NAHB report is shown in Table 7-6. Values for Hurricane Andrew provided in the 1993 NAHB report and listed in Table 7-3 are reprinted in Table 7-6 for comparison. Masonry wall damage obtained by simulation appears to be higher than the damage observed as a result of Hurricane Andrew. However, possible differences in damage tallying methods exist, which could not be verified. The simulation routine marks a wall as damaged if any masonry wall failure check discussed in Chapter 6 is exceeded. As a result, if a home has two walls with even the smallest of structural cracks at the center, it will be labeled in the middle third (1/3 – 2/3 damage). The NAHB report provides example photographs of homes with varying levels of damage and indicates methods employed for standardizing the results obtained by different observers, but it does not provide a detailed description of the difference between levels of damage specific to walls.

Table 7-6. Masonry wall damage from Hurricane Andrew vs. simulated data

Masonry Wall Damage Level	Hurricane Andrew Data from NAHB	Simulated Data		
		160 mph 3-sec Gust	175 mph 3-sec Gust	190 mph 3-sec Gust
1/3 or less	96%	76.2%	54.0%	26.8%
1/3 – 2/3	1%	23.8%	45.8%	72.4%
2/3 or more		0.0%	0.2%	0.8%
Not specified	3%			

Additional data for masonry wall performance is presented in Figures 7-4 and 7-5. The vulnerability curve shown in Figure 7-4 indicates that the mean damage for Category 4 hurricane winds is, on average, 1.2 walls. Specifically, the values of mean damage at 160, 175, and 190 mph 3-second gust winds are 0.72, 1.26, and 1.69 walls, respectively. Figure 7-5 indicates that damage to three walls is unlikely until wind speeds greater than

approximately 165 mph 3-second gusts are experienced, and damage to four walls is not likely to occur until wind speeds of 200 mph 3-second gusts. For these reasons, the performance of masonry walls using the selected load and resistance values is determined to be adequate for the representation of typical Florida homes. The simulation of masonry wall damage is noted, however, as an area that could be targeted for future research.

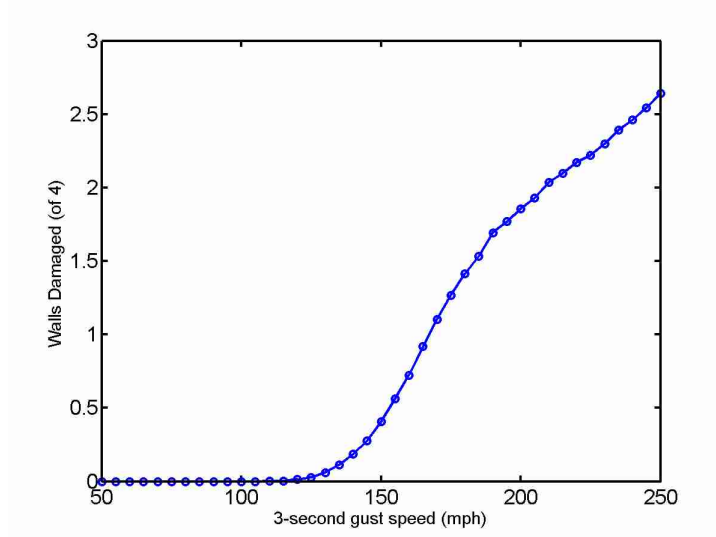


Figure 7-4. Wall damage vulnerability of South/Keys CBG homes.

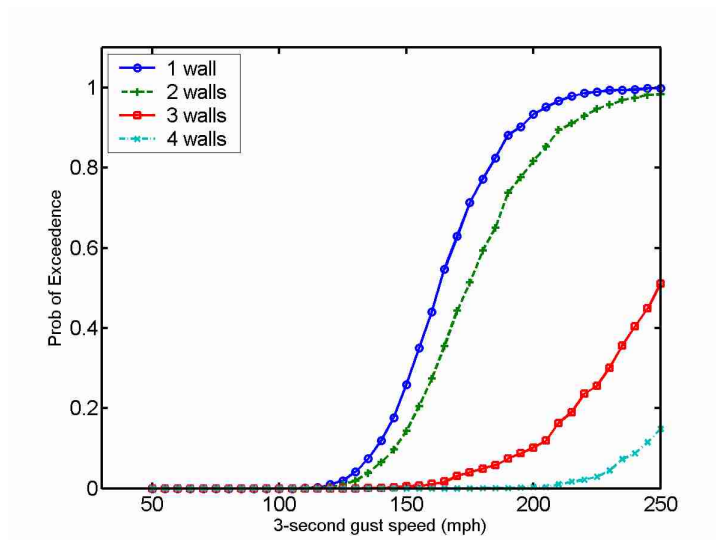


Figure 7-5. Fragility curves for 1, 2, 3, and 4 damaged walls for South/Keys CBG homes.

Validation of wood frame wall damage

Use of the Hurricane Andrew data for the validation of wood wall results is more difficult than for masonry homes. The number of wood frame homes surveyed for damage is small (34 homes), and includes homes with masonry first floors. Since the data presented in the NAHB report is the only benchmark with which to make comparisons, Table 7-7 provides a means of investigating the differences between the NAHB data and the wood wall damage results obtained from a large set of 40,000 individual building simulations of South/Keys WG homes. Wood wall damage obtained by simulation appears to be higher than the damage observed as a result of Hurricane Andrew. However, the limitations in the data and the possible differences in damage tallying methods indicate that strict numerical comparison between the results is not warranted. The methodology used in the simulation of wood wall damage is accepted as an adequate portrayal of the performance of typical wood walls.

Table 7-7. Wood frame wall damage from Hurricane Andrew vs. simulated data

Wood Frame Wall Damage Level	Hurricane Andrew Data from NAHB	Simulated Data		
		160 mph 3-sec Gust	175 mph 3-sec Gust	190 mph 3-sec Gust
1/3 or less	82%	74.4%	52.9%	30.6%
1/3 – 2/3	18%	25.6%	47.1%	69.4%
2/3 or more		0.0%	0.0%	0.0%
Not specified				

Damage to wood walls over the range of wind speeds for which the simulation engine has been developed is presented in Figures 7-6 and 7-7. The vulnerability curve for wall damage to South/Keys WG homes provided in Figure 7-6 and the fragility curves for 1, 2, 3, and 4 walls provided in Figure 7-7 indicate that the simulation routine provides a reasonably expected level of damage over a wide range of wind speeds.

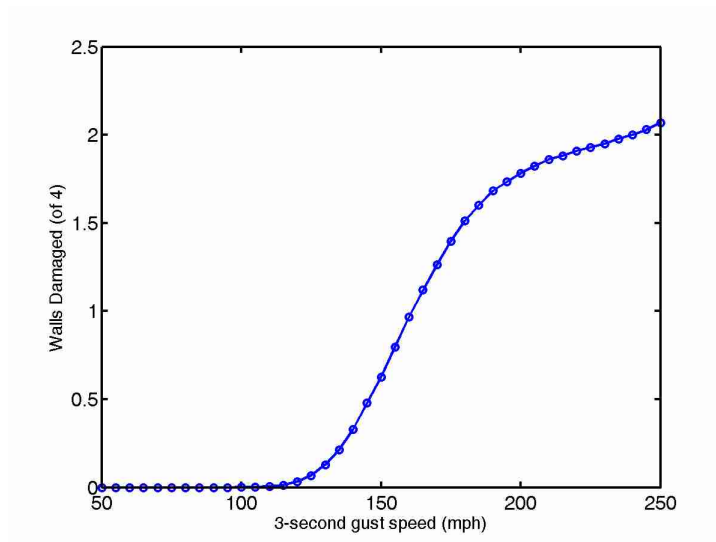


Figure 7-6. Wall damage vulnerability of South/Keys WG homes.

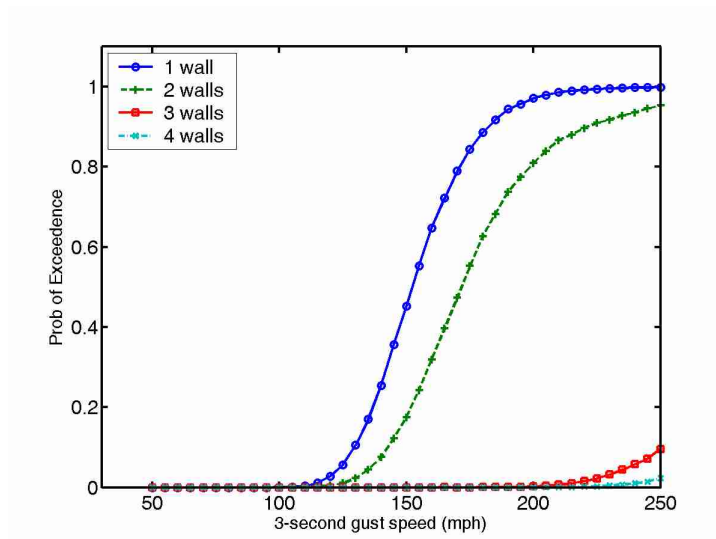


Figure 7-7. Fragility curves for 1, 2, 3, and 4 damaged walls for South/Keys WG homes.

Validation of roof-to-wall connection damage

Observed Hurricane Andrew data indicates a nearly identical performance of roof-to-wall connections for masonry and wood frame homes, in spite of the differences in manufacturer rated capacity. In light of the limited number of wood homes surveyed, the results of the NAHB study are not compared to wood frame roof-to-wall connections. A comparison is made for the masonry homes, to validate the choices selected for loading

and capacity characteristics. Given that the masonry home methods are satisfactory, the same methodology is deemed appropriate for the wood frame homes.

Table 7-8 indicates the percentage of 4,000 individual building simulations of South/Keys CBG homes in each damage state, as compared to the Hurricane Andrew data previously presented in Table 7-3. The Hurricane Andrew data compares closely to the percentage of simulated homes in each category using a 160 mph 3-second gust wind speed. At higher wind speeds within Category 4, the comparison is not as favorable. For 3-second gust wind speeds of 175 and 190 mph, the damage simulation model predicts slightly higher levels of damage than observed after Hurricane Andrew. Given the limitations previously discussed, this qualitative comparison indicates that the methodology selected for the roof-to-wall connections in the damage simulation model adequately represents the performance of typical Florida homes.

Table 7-8. Roof-to-wall connection damage from Hurricane Andrew vs. simulated data

Connection Damage Level	Hurricane Andrew Data from NAHB	Simulated Data		
		160 mph 3-sec Gust	175 mph 3-sec Gust	190 mph 3-sec Gust
1/3 or less	85%	83.2%	67.4%	52.0%
1/3 – 2/3	6%	11.0%	20.2%	28.6%
2/3 or more	2%	5.8%	12.4%	19.4%
Not specified	6%			

Additional roof-to-wall damage information, over the broad range of wind speeds for which the damage simulation model has been developed, is provided in the vulnerability curves and fragility curves of Figure 7-8 and 7-9. These curves represent a reasonable expectation for the level of damage at varying wind speeds. As a result, the wind load and capacity selections in the damage-prediction model for roof-to-wall connections are accepted as an adequate measure of performance for typically constructed homes.

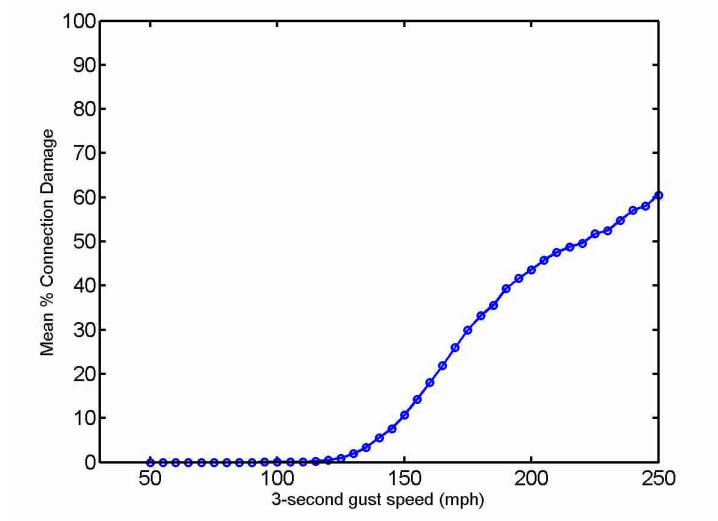


Figure 7-8. Roof-to-wall connection damage vulnerability of South/Keys CBG homes.

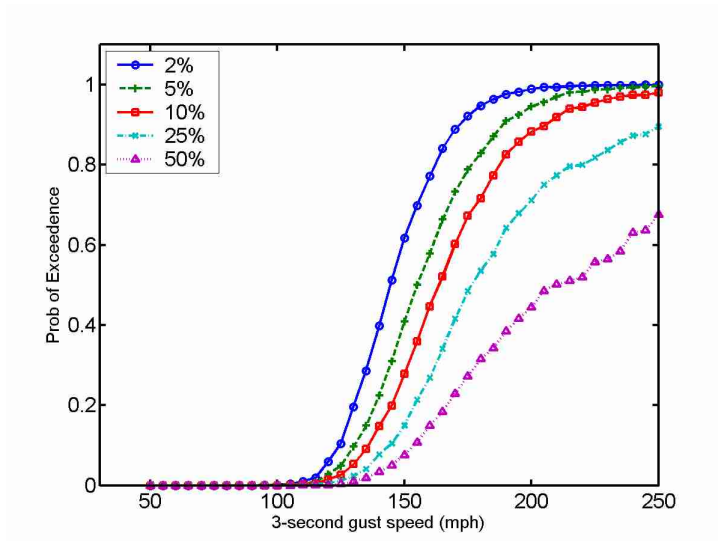


Figure 7-9. Fragility curves for 2%, 5%, 10%, 25%, and 50% roof-to-wall connection damage for South/Keys CBG homes.

Validation of roof sheathing damage

A comparison of roof sheathing damage is made in Table 7-9 for data observed during the simulation of 4,000 individual South/Keys CBG homes vs. reported Hurricane Andrew data previously shown in Tables 7-3 and 7-4. The Hurricane Andrew data compares reasonably well at wind speeds in the vicinity of 175 and 190 mph 3-second gusts, though the simulation engine might predict too little damage at wind speeds close

to 160 mph. It is difficult to make this assertion from the data available from Hurricane Andrew, however, given the limitations previously described and the large number of homes for which roof sheathing damage is unspecified. The qualitative comparison indicates that the damage model predicts sheathing loss consistent with the damages observed during Hurricane Andrew for typical homes.

Table 7-9. Roof sheathing damage from Hurricane Andrew vs. simulated data

Roof Sheathing Damage Level	Hurricane Andrew Data from NAHB		Simulated Data		
	All Homes	Wood Only	160 mph 3-sec Gust	175 mph 3-sec Gust	190 mph 3-sec Gust
1/3 or less	57%	56%	95.0%	76.2%	44.2%
1/3 – 2/3	12%	26%	5.0%	23.2%	50.6%
2/3 or more	6%	18%	0.0%	0.6%	5.2%
Not specified	25%				

The vulnerability of South/Keys CBG homes to sheathing damage presented in Figure 7-10 represents a reasonably expected, increasing curve over the range of wind speeds for which the structural damage model has been developed. Additionally, the fragility curves shown in Figure 7-11 indicate that the rate of increasing damage is reasonable, though the curves are slightly steeper than desired.

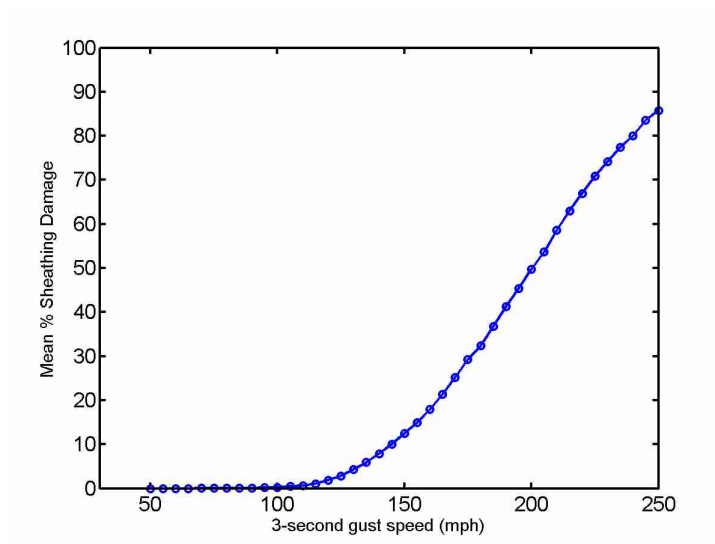


Figure 7-10. Roof sheathing vulnerability of South/Keys CBG homes.

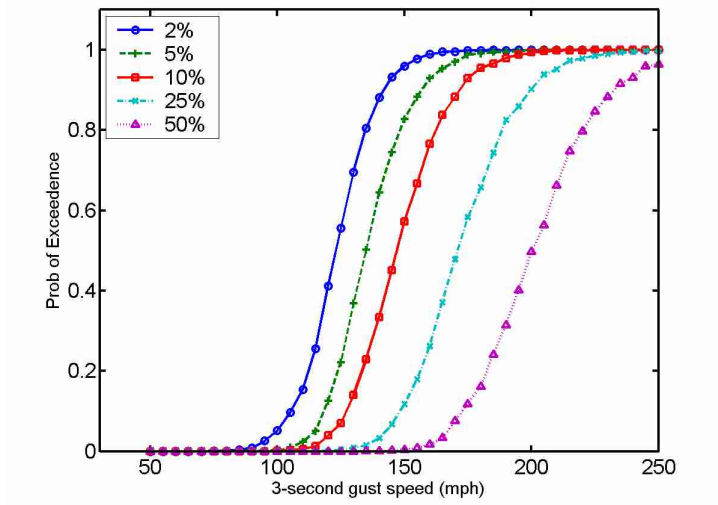


Figure 7-11. Fragility curves for 2%, 5%, 10%, 25%, and 50% roof sheathing damage for South/Keys CBG homes.

Validation of roof cover damage

Using the results obtained from 4,000 simulations, the percentage of South/Keys CBG homes with roof cover damage in each category specified by the NAHB report is shown in Table 7-10. Hurricane Andrew results are reprinted from Tables 7-3 and 7-4. The observations from Hurricane Andrew for all Florida homes are difficult to interpret, due to the large number of homes with unspecified damages. Given the explanation in the NAHB report that homes with unspecified damages were most likely obscured by tarps covering damaged areas, or otherwise blocked from view, it is unlikely that all 23% of homes with unspecified damages in the left hand column would have damages less than or equal to 1/3. Some of these would fall into the middle category of damage, though the exact number is impossible to predict. Additionally, the wood home results in the second column account for a small sample size. As a result, a comparison of simulated damages to those observed after Hurricane Andrew for roof cover is less exact than the comparison for other building components. In spite of these difficulties, data provided in Table 7-10 indicates that the mean value of simulated roof cover loss lies in the middle damage

category for all but the lowest intensity Category 4 storms, a favorable comparison with the data observed during Hurricane Andrew. Additionally, the number of homes with undamaged roof cover is zero or nearly zero for all three wind speeds, as expected from storms of this intensity. Given the current body of information, the methodology employed for roof cover failure checking in the simulation engine is a reasonable approach to predicting the behavior of typical Florida residences during hurricane events.

Table 7-10. Roof cover damage from Hurricane Andrew vs. simulated data

Roof Cover Damage Level	Hurricane Andrew Data from NAHB		Simulated Data		
	All Homes	Wood Only	160 mph 3-sec Gust	175 mph 3-sec Gust	190 mph 3-sec Gust
1/3 or less	18%	41%	45.2%	21.2%	7.4%
1/3 – 2/3	23%	21%	52.6%	66.0%	57.0%
2/3 or more	36%	38%	2.2%	12.8%	35.6%
Not specified	23%				

The roof cover vulnerability of South/Keys CBG homes presented in Figure 7-12 and the fragility curves of Figure 7-13 indicate that the simulation engine provides reasonable results over the broad range of wind speeds for which the model has been developed, though the fragility curves in Figure 7-13 are steeper than desired.

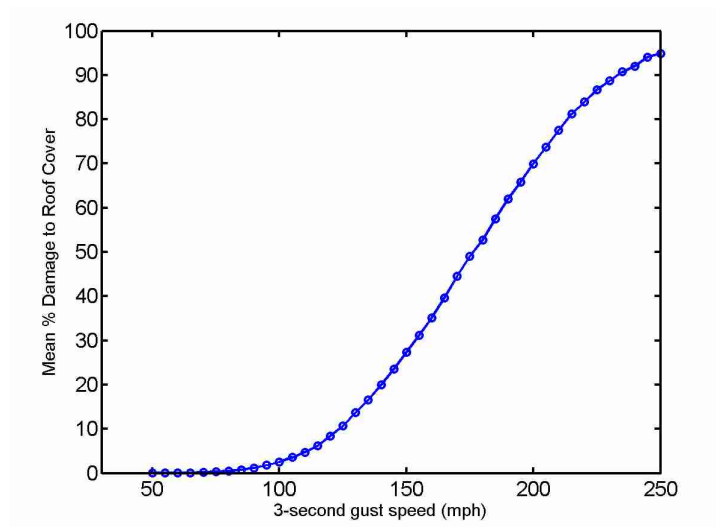


Figure 7-12. Roof cover vulnerability of South/Keys CBG homes.

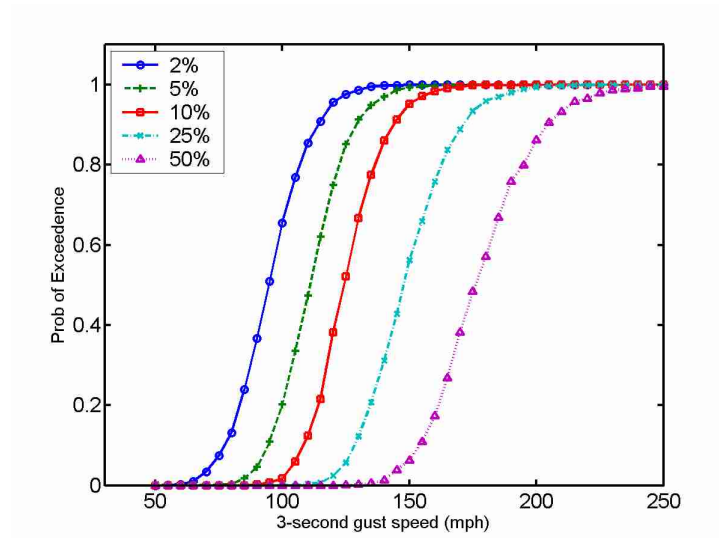


Figure 7-13. Fragility curves for 2%, 5%, 10%, 25%, and 50% roof cover damage for South/Keys CBG homes.

Investigation of Selected Topics

Using the validated load and resistance methodology, additional investigations are conducted for the use of batch selection process and the difference between hip roof and gable roof results. The batch selection process is investigated for roof sheathing and for roof-to-wall connections. Differences in damages to hip and gable roof buildings are also investigated using these two modeled structural components.

Investigation of the Batch Selection Method for Roof Sheathing

The batch selection method of capacity sampling provides a distribution of resistance unique to an individual home. This process represents the logical argument that individual pieces (sheathing panels, for example) come from the same manufacturer and are installed on a home by the same group of workers. The method is employed by using a baseline from the distribution of roof sheathing capacities as a mean capacity for the panels on a single house, and then sampling from a new distribution with a *COV* of 0.05 to determine individual panel capacities. Uncertainties in the building population (such as

the diversity of roof plan layouts) and anomalies which lead to localized damages (such as a row of nails missing a truss on an otherwise well-constructed home) are removed from the damage prediction process using this method, however.

As demonstrated in Figure 7-14 (which provides normalized histograms of roof sheathing damage) the batching method does not adequately model post-storm damage observations for roof sheathing. In fact, the method produces just the opposite result. The majority of homes should have damages in the middle third, according to the Hurricane Andrew report. Figure 7-14A indicates that homes modeled with the batching process applied to roof sheathing would most likely have less than 20% or greater than 80% sheathing damage, with very few homes in the middle. Histograms of sheathing damage at 160, 175, and 190 mph 3-second gusts provided in Figure 7-14B indicate that the roof sheathing damage for homes modeled without batching of the roof sheathing capacities agrees well with the Hurricane Andrew data from Table 7-9. For this reason, batch sampling is not incorporated in the capacity assignments of structural components, with the exception of roof-to-wall connections. The physical argument to support this decision is addressed at the end of the next section describing roof-to-wall connections.

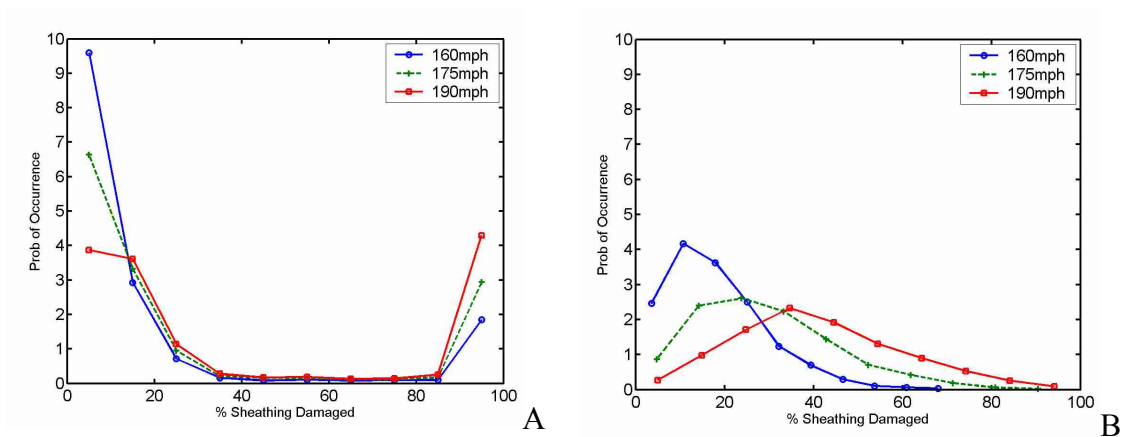


Figure 7-14. Histograms of roof sheathing damage on South/Keys CBG homes. A) Batch selected method. B) Non-batch selected method.

Investigation of the Batch Selection Method for Roof-to-Wall Connections

The batch selection method is demonstrated in the previous section to contradict the observed damage reports for roof sheathing failures. Using this component as an example, the method is not selected for use in capacity definition of structural components, with the exception of roof-to-wall connections. Batch selection of capacity is selected for roof-to-wall connections alone because this component has a unique distribution of observed damage. Specifically, roof-to-wall connection damages should display two distinct and well-separated peaks, representing the observed damage states of little damage or catastrophic damage to the roof. To determine the effectiveness of the batch selection method for the roof-to-wall connections, a comparison is made between batch-selected roof-to-wall connection results and non-batch-selected results. Normalized histograms for connection damage at wind speeds of 160, 175, and 190 mph 3-second gusts are presented in Figure 7-15, and fragility curves are presented in Figure 7-16. In each figure, the left hand side represents data using the batch selection process for roof-to-wall connection capacity. Right hand sides of Figures 7-15 and 7-16 provide data for roof-to-wall connections sampled without the batching process. Data for non-batched connections is taken from a smaller data set of 8000 simulations of individual South/Keys CBG homes.

The difference between batch sampling and non-batch sampling is noted clearly in Figure 7-15, where the likelihood of having only a few damaged roof-to-wall connections using the batch selection method is much higher at each wind speeds than the likelihood of having the same number of damaged wall connections using the non-batch selected method. The distribution of damages in Figure 7-15A indicate the presence of two primary damage states, where the distribution of damages in Figure 7-15B indicate a

single peak value that increases with wind speed. Additionally, the steeper slope of the fragility curves for high levels of roof damage on the right hand side of Figure 7-16 provide a different view of the same issue. The distribution of damages on the left of Figure 7-15 and the fragility curves on the left of Figure 7-16 are more representative of the expected physical damages to typical homes than those appearing on the right hand side of each figure.

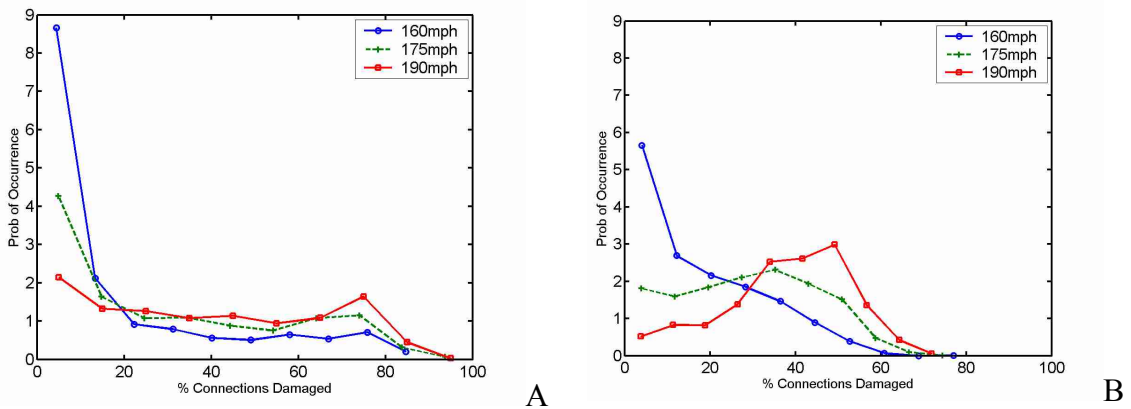


Figure 7-15. Histograms of roof-to-wall connection damage on South/Keys CBG homes. A) Batch selected method. B) Non-batch selected method.

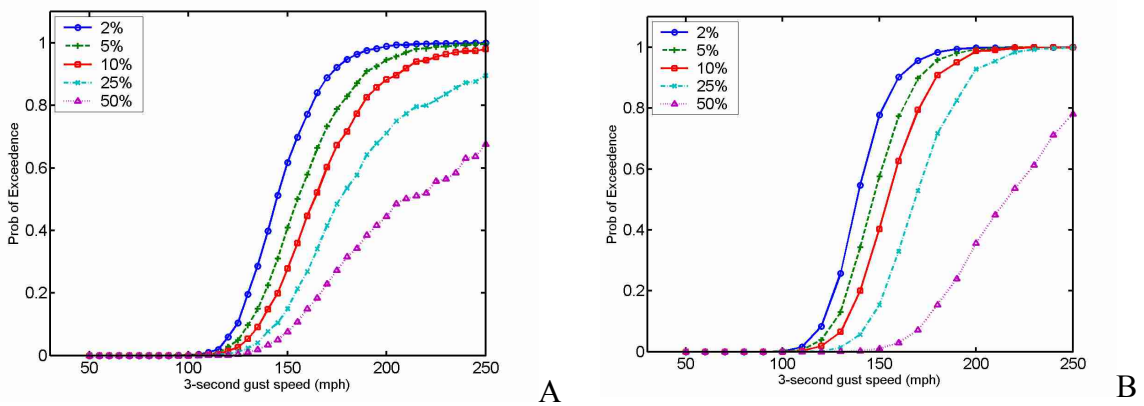


Figure 7-16. Fragility curves for 2%, 5%, 10%, 25%, and 50% roof-to-wall connection damage on South/Keys CBG homes. A) Batch selected method. B) Non-batch selected method.

In addition to the vulnerability and fragility curve data supporting the selection of roof-to-wall connection capacities using a batching process, typical construction practice

supports the use of this methodology as well. Roof-to-wall connection capacity data, unlike data for some other building components, has been well identified through correspondence with a leading manufacturer. Also, the as-built capacities for these pieces of hardware are less susceptible to installation procedure uncertainties than other building components. For these reasons, the batch selection process is maintained for roof-to-wall connections.

Investigation of the Difference between Hip and Gable Roofs

Using the validated methodology, a second comparison is made for the shape of the roof. The data in Table D-2 of the 1993 NAHB report on Hurricane Andrew is largely for gable roof structures; however, a comparison is made for overall roof damage to hip and gable roof homes in the text of the report. Hip roof homes were more likely than gable roof homes to have low roof damage, though the specific numbers for roof-to-wall connections and roof sheathing losses are not available [19].

As a comparison between simulated data for gable roofs and hip roofs, Figure 7-17 provides histograms of roof-to-wall connection damage for South/Keys homes at 160, 175, and 190 mph 3-second gust wind speeds. Figure 7-17A provides data for simulated gable roof homes, while Figure 7-17B provides the distribution of damage on hip roof homes. A clear difference is observed in the results obtained for roof-to-wall connections on gable and hip roof homes at each of the three wind speeds shown. Higher levels of maximum damages are obtained for connections on gable roof homes than those for hip roof homes, as noted by the location on the x-axis of the highest damage level for each wind speed. Additionally, the likelihood of only a few connections being damaged is much higher for hip roof homes at each of the investigated wind speeds than the

likelihood of the same number of connections being damaged on gable roof homes at the same wind speeds.

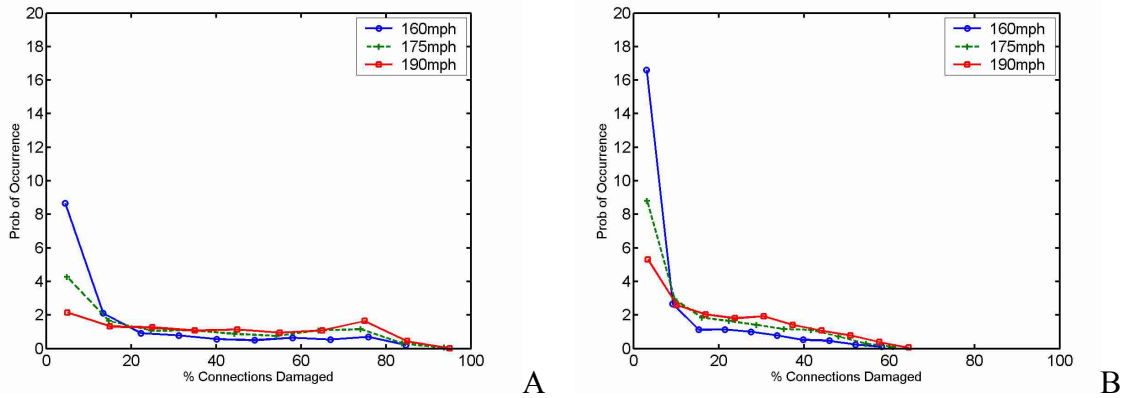


Figure 7-17. Histograms of roof-to-wall connection damage on South/Keys concrete block homes. A) Gable roof homes. B) Hip roof homes.

An additional comparison is made between simulated data for gable roofs and hip roofs in terms of roof sheathing damage. Figure 7-18 provides the histograms for damage to roof sheathing on South/Keys homes at 160, 175, and 190 mph 3-second gust wind speeds. Differences between the curves are slight, indicating that the differences between hip and gable roof performance for roof sheathing are not fully addressed in the damage simulation model.

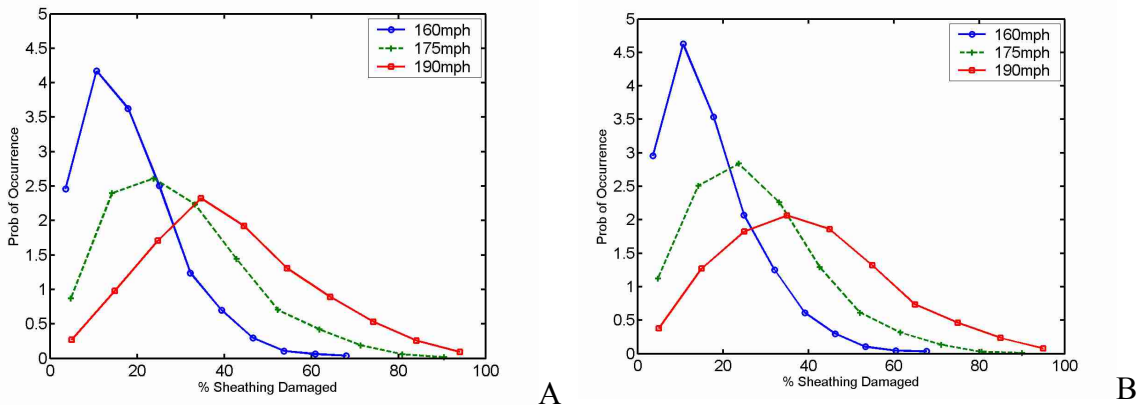


Figure 7-18. Histograms of roof sheathing damage on South/Keys concrete block homes. A) Gable roof homes. B) Hip roof homes.

In spite of the lack of difference obtained between gable and hip roof sheathing loss, the method of loading is selected as an adequate representation of hurricane conditions, given the current body of knowledge. Future study to determine the probabilistic character of roof sheathing loads and other wind load conditions would result in more accurate modeling of the surface wind loads on typical buildings, which would most likely increase the variation in damage results. Given the current information, the methodology used for roof sheathing in the simulation engine is accepted as a reasonable approach for modeling the behavior of typical residential structures. Since the level of roof sheathing damage at which high monetary values of insured loss is incurred is low, the error involved in the lack of difference between gable and hip roof homes in the current model is expected to result in small differences in the end product, prediction of insured loss on an annualized basis.

Structural Damage Results

In this section, limited results are presented for the site-built homes in the South/Keys Region and for manufactured homes. Specifically, a mean damage comparison is provided for each type of residence, illustrating the overall picture of damage at differing wind speeds. For roof cover, roof sheathing, and roof-to-wall connections, the mean damage is presented as a percentage of the total that is damaged. Wall damage is also presented as a percentage, with respect to the total of four walls, and as a percentage of sheathing panels lost on gable ends for those structures with gable roofs. A full body of simulated results is provided for each type of site-built home in the South/Keys Region and for manufactured homes in the appendices. Damages to homes in the North and Central Regions will be available when the PLHP is released in May, 2005.

The structural damages presented in this section are used to determine the insurable loss, as described in Chapter 8.

Results for Site-Built Homes in the South Florida and Florida Keys Region

Mean damages for South Florida and Florida Keys Region concrete block gable roof homes, concrete block hip roof homes, wood frame gable roof homes, and wood frame hip roof homes are presented in Figures 7-19, 7-20, 7-21, and 7-22, respectively. Concrete block homes have lower mean damage percentages for roof-to-wall connections than wood frame homes of the same roof shape. Additionally, gable roof homes are more likely to experience high levels of damage to walls and roof-to-wall connections than their hip roof counterparts, with one exception. For concrete block homes, the damage to walls on hip roof homes surpasses that of gable roof home after 200 mph 3-second gusts are experienced.

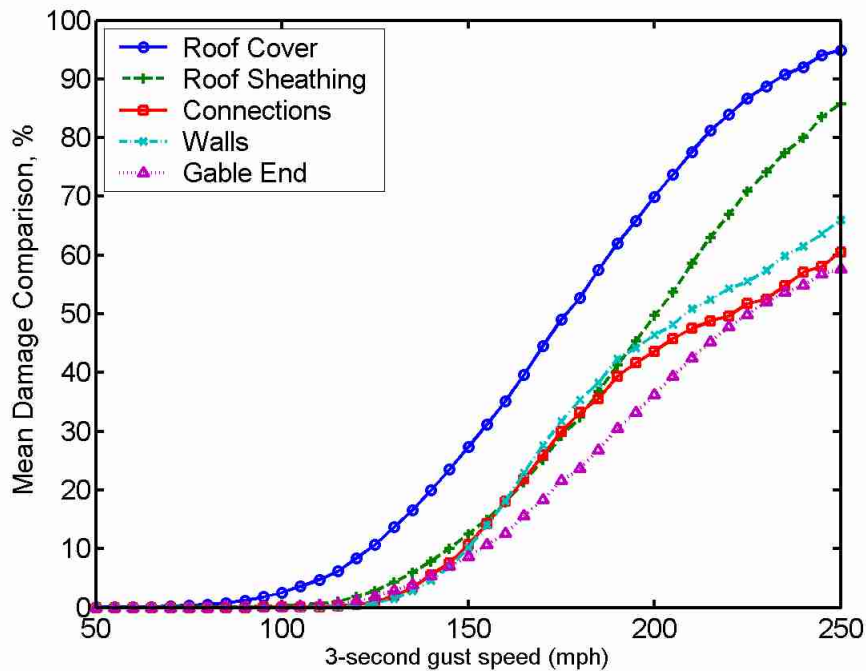


Figure 7-19. South/Keys CBG homes mean damages for roof cover, roof sheathing, roof-to-wall connections, and walls.

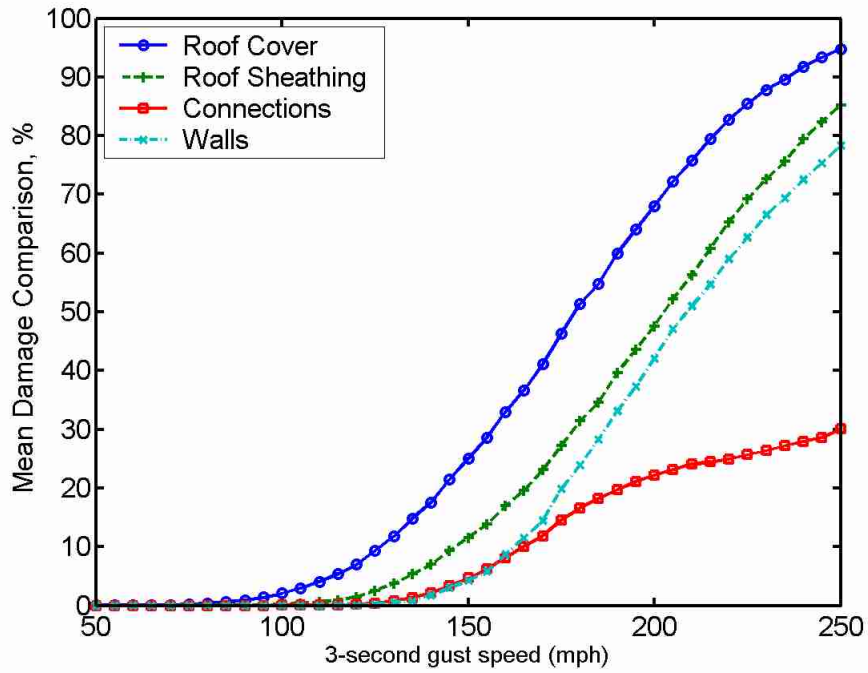


Figure 7-20. South/Keys CBH homes mean damages for roof cover, roof sheathing, roof-to-wall connections, and walls.

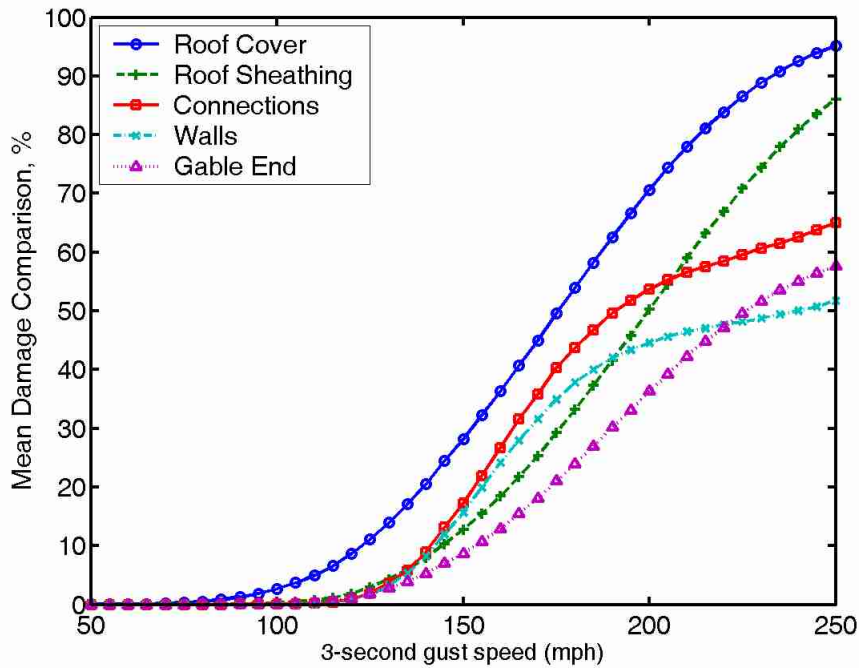


Figure 7-21. South/Keys WG homes mean damages for roof cover, roof sheathing, roof-to-wall connections, and walls.

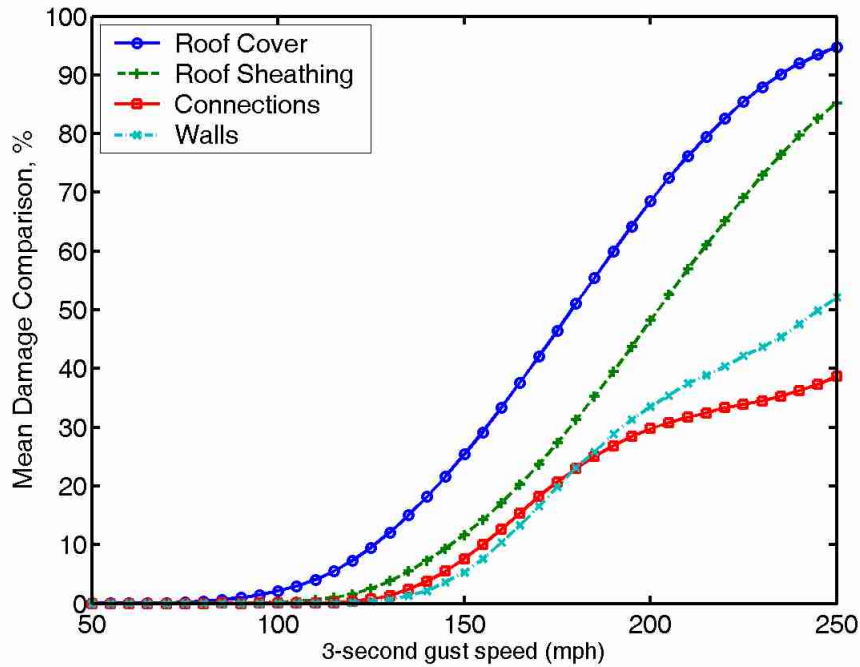


Figure 7-22. South/Keys WH homes mean damages for roof cover, roof sheathing, roof-to-wall connections, and walls.

Results for Manufactured Homes

Mean damage levels for singlewide, doublewide, and pre-HUD Code manufactured homes are presented in Figures 7-34, 7-35, and 7-36, respectively. Damages to each component are presented in terms of percentages. For roof cover, roof sheathing, and roof-to-wall connections the damages are presented in the same format as previously shown for site-built homes. Wall sheathing is similar to roof sheathing, in that the mean percentage of damage to the total is provided. For overturning, a percentage representing the likelihood of the home being overturned is provided. In the simulation model a value of one is recorded for overturned homes and a value of zero represents homes that do not overturn. At each wind speed in Figures 7-34 through 7-36 the mean overturning value is multiplied by 100 to obtain a comparative percent. A similar process is used for sliding, except that there are two possible sliding categories. In the simulated data, a value of one

indicates minor sliding, while a value of two represents major sliding. Zero is used for no sliding damage. For each wind speed, the mean sliding value is multiplied by 100 and divided by 2 to obtain a comparative percent.

Figures 7-34 through 7-36 indicate the most common failure mechanisms for each type of home. Singlewide homes, for example, experience overturning more frequently than doublewide homes, although the larger homes are significantly more susceptible to roof pull off (which occurs when most of the roof-to-wall connections fail). Additionally, Figures 7-34 through 7-36 show that each type of home is more likely to experience a sliding failure than an overturning failure. Damages to all components, with the exception of roof-to-wall connections, are higher on pre-HUD Code homes than on modern manufactured homes.

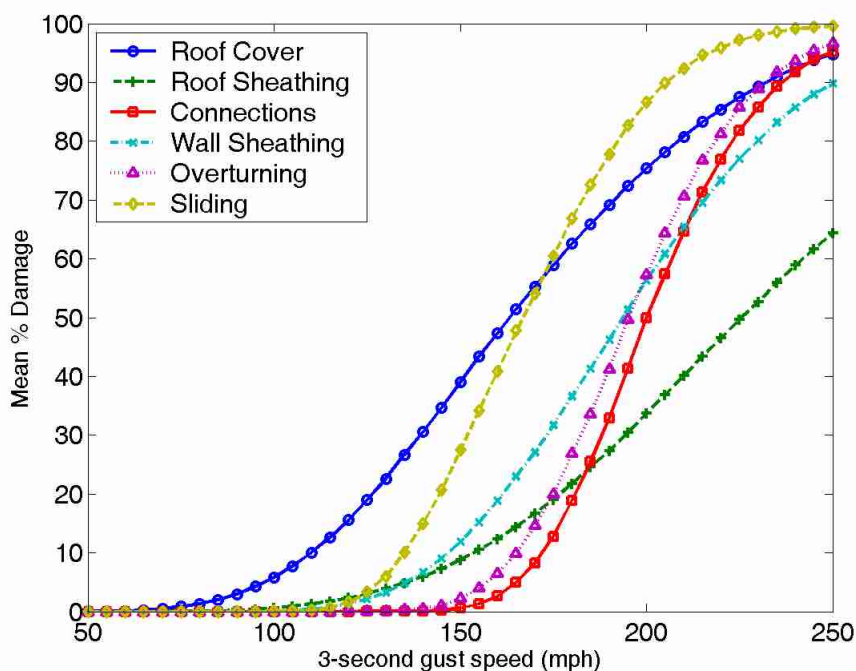


Figure 7-23. Singlewide manufactured homes mean damages for roof cover, roof sheathing, roof-to-wall connections, and walls.

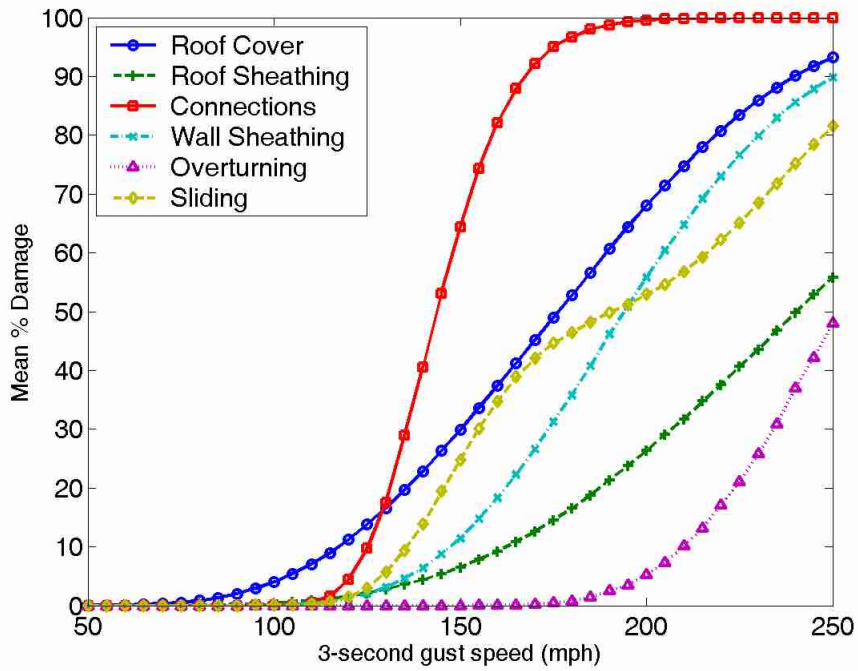


Figure 7-24. Doublewide manufactured homes mean damages for roof cover, roof sheathing, roof-to-wall connections, and walls.

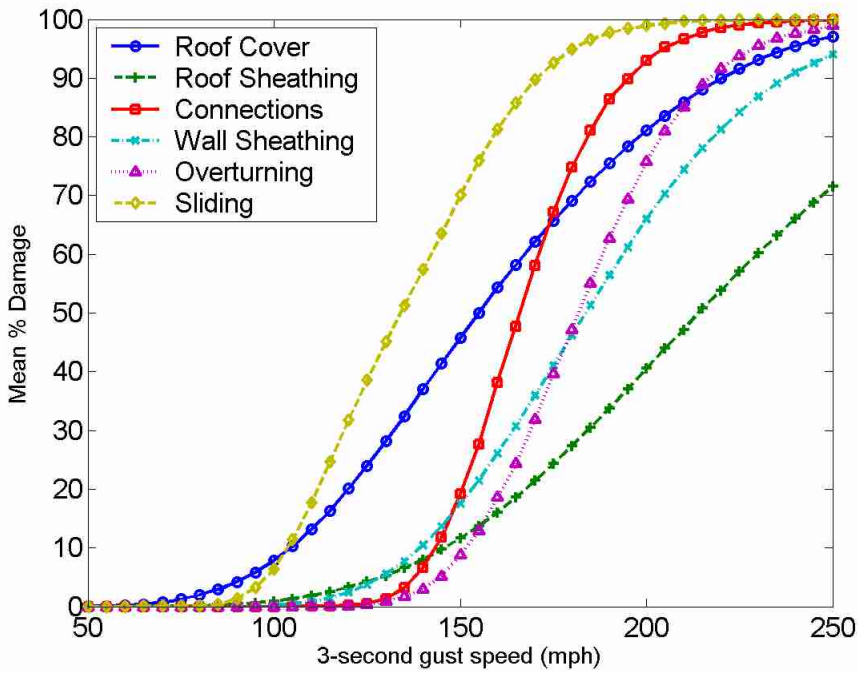


Figure 7-25. Pre-HUD Code singlewide manufactured homes mean damages for roof cover, roof sheathing, roof-to-wall connections, and walls.

Summary

In this chapter, results obtained from the simulation engine are validated with post-damage information from Hurricane Andrew to the extent possible, given the limitations described. Additionally, the vulnerability (mean damage) and fragility (probability of exceeding discrete levels of damage) are investigated for building components as a means of verifying, through the use of engineering judgment, that the damage prediction engine produces reasonable results. The levels of structural damage for each simulated home are not presented, for brevity. Instead, comparative graphs of mean damage results are presented for each site-built home in the South/Keys Region and for manufactured homes. Additional structural damage results for these homes are provided in Appendices A through G. Results for the North and Central Region homes will be available when the PLHP is released in May, 2005. Simulated structural damage results (presented briefly in this chapter and more thoroughly in the appendices) are used to determine the insurable loss associated with each type of building on an annualized basis, and for specific storms. As described in Table 7-2, the performance of two story homes will be a function of the performance of single story homes. Chapter 8 describes how the end product of insurable loss is obtained using the damages calculated during simulation.

CHAPTER 8 APPLICATION OF RESULTS AND CONCLUSION

The previous chapters describe the development of a structural damage prediction engine designed for the Public Loss Hurricane Projection Model (PLHP). Involving meteorological, engineering, actuarial, and computer resource components, the PLHP is a multi-university project scheduled for completion in 2005. The end result of this effort is a prediction of hurricane wind-induced insurance losses for residential structures by zip code in Florida on both an annualized basis and for predefined scenarios (specific hurricanes). In support of this goal, three separate models are being developed: a hurricane model to provide probabilistic wind speed information for each zip code in the state, a structural damage model relating specific wind speeds to predicted losses for typical residential buildings in the state of Florida, and a financial model to relate structural damage to insurable losses. Combined, these three segments will become the final PLHP model.

The University of Florida's contribution to the project is the development of the structural damage prediction engine relating maximum 3-second gust wind speeds into predicted structural damage. The Monte Carlo simulation engine described in previous chapters uses a probabilistic framework based on a component view of typical homes. This approach explicitly accounts for the capacity of individual structural components, load paths, and load sharing, to the extent possible with available knowledge. Using this method, the developed simulation engine compares wind loads with the load-resistance capacity of building components to identify the likelihood of structural damage over a

range of storm intensities. Steps necessary to the development of the component based damage-prediction model include

- Characterization of homes representative of the residential building stock in the state of Florida and identification of components critical to wind damage-prediction modeling, presented in Chapter 3
- Quantification of the wind-induced loads on building components and identification of appropriate load paths and load sharing for modeling purposes, discussed in Chapter 4
- Characterization of the probabilistic capacities of individual components to resist applied wind loads, detailed in Chapter 5
- Creation of a probability-based system-response model that will simulate the performance and interaction of the components of typical Florida homes and evaluate their vulnerability during interaction with hurricane winds, presented in Chapter 6 and validated in Chapter 7.

The results of the structural damage-prediction model (presented in Chapter 7) will be incorporated into the final PLHP model. The other two components (the hurricane model and the financial model) are currently being developed by research partners on the PLHP team, and are not detailed in this dissertation. This chapter briefly describes the process by which the three developed models will interact to predict insurable losses. Also provided in this chapter are a summary of the research contributions made by the author and a description of future uses for the developed simulation engine.

Relating Structural Damage to Monetary Loss

The Monte Carlo simulation engine presented in the previous chapters of this dissertation predicts exterior structural damage on typical Florida homes resulting from extreme wind events. Determining annualized and specific event related insurance losses from the structural damage information provided by this model is a two-step process. First, a cost estimate model is used to determine the monetary value of physical damage as a ratio of the value of the home. Second, an insured loss model combines the cost ratio

data and insurance policy features determined by the actuarial team and the probabilistic wind characteristics provided by the meteorology team to determine insured losses, on annualized basis or for specific storms. These two steps are not included in the research work conducted for the completion of this dissertation, but are presented briefly in the following sections for the sake of completeness in the description of the PLHP model. Further details will be available when the PLHP Model is released in 2005.

Cost Estimate Model

A cost estimate model to relate physical damage to monetary loss is being developed by research partners at Florida Institute of Technology. Preliminary results are available for this model, which define the cost ratio of damage as a percentage of home value. The methodology uses three pieces of information to determine a cost ratio for each damaged home: 1) structural damages from the Monte Carlo simulation engine, 2) non-structural damage, and 3) replacement cost ratios. The first item (structural damage) is taken directly from the results presented in Chapter 7. Non-structural damages include building components such as kitchen cabinets, carpeting, interior walls, interior doors, ceilings, plumbing, mechanical, and electrical assemblies which are not included in the Monte Carlo simulation engine. Damages to these non-structural items must be determined as a function of the level of exterior damage predicted by the structural simulation model. Once the level of total damage is determined, replacement cost ratios for structural and non-structural building components are used to characterize damage to individual homes. Additionally, damages to personal property (contents) in the home are predicted as a percentage of the total value.

Tables 8-1 and 8-2 provide estimated replacement costs, as a percentage of the value of a new home, for subassemblies of a typical masonry house in Central Florida

with a shingle roof and hurricane shutters [60]. Replacement costs for the non-structural elements of the home, shown in Table 8-2, represent a significant portion of insurable losses. Because repairs to existing construction are more expensive than new construction, the sum of the structural replacement cost ratios in Table 8-1 and the non-structural cost ratios in Table 8-2 exceeds 100%.

Table 8-1. Structural repair cost ratios for Central Florida masonry homes

Structural Subassembly	Repair Cost Ratio
Roof Sheathing	5%
Roof Cover	7%
Trusses	9%
Exterior Walls	22%
Windows	4%
Shutters	2%
Exterior Doors	1%
Garage	1%
Total	51%

Table 8-2. Non-structural repair cost ratios for Central Florida masonry homes

Non-Structural Subassembly	Repair Cost Ratio
Plumbing	10%
Mechanical	7%
Electrical	7%
Other non-structural components	35%
Total	59%

Ratios presented in Tables 8-1 and 8-2 are used to determine the total cost ratio of physical damage. If 3 of 15 windows are damaged, for example, a value of 20% is multiplied by the replacement ratio for windows. Additionally, equations currently being developed by research partners at the Florida Institute of Technology (FIT) relate structural and non-structural damages in terms of percentages, which can then be multiplied by the cost ratios. A sum of the physical damage percentage times the cost ratio for each item listed in Tables 8-1 and 8-2 provides a building component

replacement ratio conditional upon the damage state obtained from the structural prediction model as well as the type of home (e.g. wood frame home in North Florida).

In addition to the building damage, the cost of contents is factored into the total cost ratio. Research partners at the FIT are currently developing a framework of equations to relate the structural damages presented in Chapter 7 to insurable contents loss. Preliminary results for the content loss estimation portion of this framework are provided in Figure 8-1, where damages to roof cover, roof sheathing, and openings have been interpreted as a Building Damage Ratio which is used to predict a ratio of loss of insurable contents [61]. Complete details concerning the prediction of damage to non-structural components will be available when the PLHP Model is released in 2005.

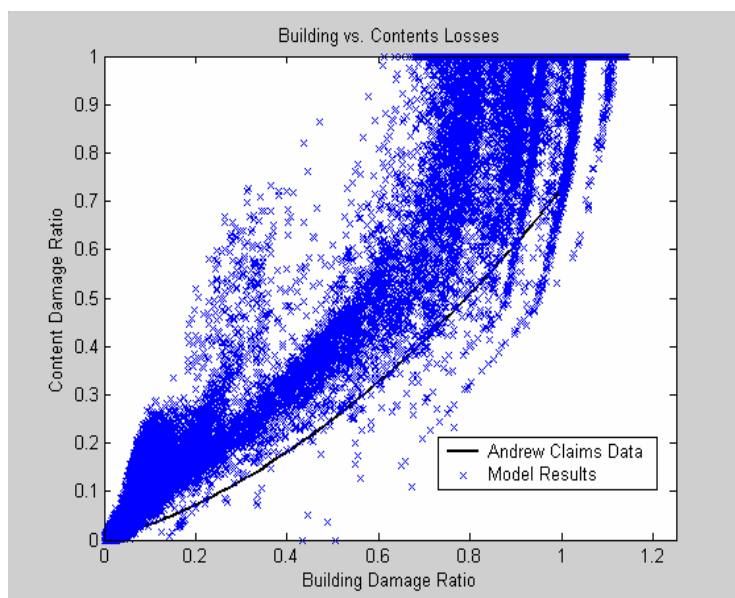


Figure 8-1. Preliminary results of the relation of structural damage to insurable content loss compared with insurance claims data from Hurricane Andrew.

The content loss ratios shown in Figure 8-1 are used in combination with the building component replacement ratios to develop the damage ratio (DR) for each simulated building. From this database, a vulnerability matrix of damage ratios vs. wind

speeds for each type of structure is obtained, where each cell provides the probability of occurrence of a damage ratio conditional upon the wind speed. Using this format, the matrices represent discretized conditional probability distribution functions. By summing the product of the likelihood of occurrence and the DR for all possible DR s, the vulnerability of each type of home is described. This process is shown in Equation 8-1, where $Vulnerability_{(type\ m | v)}$ is obtained in terms of a percentage of value conditional upon the building type, shown as type m , and the wind speed, V ; DR_i is a particular damage ratio; and $P(DR_i | V, type_m)$ is the likelihood of occurrence of DR_i conditional upon V and the type of building. Conditional vulnerability curves produced using Equation 8-1 are the product of the cost estimate model.

$$Vulnerability_{(type\ m | v)} = \sum_i P(DR_i | V, type_m) * DR_i \quad (8-1)$$

Insured Loss Model

Insured losses for typical Florida structures are obtained using the cost estimate model discussed in the preceding section in combination with wind speed data provided by research partners. This information must then be filtered using knowledge of typical insurance practices, such as deductible and limits. The result is the prediction of insurance risk by zip code on an annualized basis.

Within each zip code, the probability density function of the largest yearly wind speed, v , will be defined by the PLHP meteorology team as $P(v)$. It is assumed that the probability of occurrence of particular storms within a specified interval can be defined by Equation 8-2, where V_i is a particular 3-second gust wind speed as discussed in the preceding chapters for the structural damage simulation model and Δv is the increment of 5 mph in terms of 3-second gust wind speeds.

$$P(V_i - \frac{\Delta v}{2} < v < V_i + \frac{\Delta v}{2}) = P(v)\Delta v \quad (8-2)$$

The mean annual damage equation for a particular structure of type m can then be obtained as the sum of the conditional vulnerability defined in Equation 8-1 times the likelihood of wind speed occurrence provided in Equation 8-2, summed over all possible wind speeds. This expression is provided in Equation 8-3.

$$\text{Annual_Mean_Damage}_{\text{type } m} = \sum_i \text{Vulnerability}_{(\text{type } m | v)} P(V_i - \frac{\Delta v}{2} < v < V_i + \frac{\Delta v}{2}) \quad (8-3)$$

Furthermore, the mean annual damage for a geographic area or a portfolio of homes can be obtained by summing the value of $\text{Annual_Mean_Damage}_{\text{type } m}$ times the probability of the home being of type m , over all possible building types in the given area or insurance portfolio. A statistical analysis of the Florida building stock described in Chapter 3 and documented by Pinelli and Zhang [31, 32] provides the regional likelihood of occurrence of each of the building types as $P(\text{type } i)$. Using this information, the expression for the mean annual damage for a geographic area or portfolio is described in Equation 8-4.

$$\text{Annual_Mean_Damage} = \sum_i \text{Annual_Mean_Damage}_{\text{type } i} P(\text{type } i) \quad (8-4)$$

Since the cost estimate model described in the preceding section of this chapter focuses on the cost as a ratio of the value of the home, the result obtained from Equation 8-4 will be in the form of a percentage. This mean annual damage figure is multiplied to the value of each home in a geographic area or insurance portfolio to obtain a monetary value per home. Using this information, the insured loss function is obtained by truncating the distribution of monetary losses according to insurance policy deductibles

and limits. A complete discussion of this process will be available in 2005, with the release of the PLHP Model.

Research Contributions

As a multi-university project encompassing a variety of academic fields, the PLHP represents a synthesis of work conducted by several researchers. The specific research contributions of the author include building classification efforts, building component modeling, and conceptual development of the damage-prediction model, to include structural wind load analysis and limit state definition.

Research partners at FIT conducted the building classification study described in Chapter 3, with assistance from the author. Specifically, the author was directly responsible for the investigation of post-damage reports to determine which building components were susceptible to wind damage, and therefore the most critical to model. Additionally, the author was instrumental in the selection of residential characteristics researched during the classification study.

The author is responsible for the conceptual development of the probabilistic framework for the determination of structural wind damage. The selected network of embedded loops to predict structural damage at various storm intensities for buildings typical of Florida residences is similar to the model developed for the HAZUS® project, in that it is a component-based damage-prediction model. The method varies significantly from the HAZUS® method however, in the application of wind loads and tallying of structural damage. A time stepping routine is used in the HAZUS® damage-prediction model, during which individually simulated hurricane events are passed over a generated home in a series of fifteen-minute intervals. At each interval, the wind field model

defines the wind speed and direction of action for used in wind load calculations. Additionally, the extent of damage already suffered by the house is used in the determination of the internal pressure at each time step [3]. The results of this resource-intensive time stepping model are vulnerability curves for typical residential and commercial structures. In a fast running model, the developed vulnerability curves are used to predict insurable loss [3]. The resources necessary to develop a similar time stepping model for the determination of residential structural vulnerability are beyond the scope of the current work. Instead, the component-based probabilistic framework described in Chapter 6 has been developed by the author to model the performance of typical Florida homes during extreme wind events. Characterization of the applied wind loads described in Chapter 4 and the typical building component resistances described in Chapter 5 as well as decisions concerning load placement, load sharing, applicable limit states, and the inclusion of load paths within the failure check sequence are contributed by the author.

Future Uses of the Structural Damage Model

The main goal of the research presented in this dissertation is the relation of specific wind speeds to predicted damages for typical residential buildings in the state of Florida. The simulation engine detailed in this body of work is specifically intended for the development of the PLHP Model, a multi-university project sponsored by the Florida Department of Financial Services and coordinated by the International Hurricane Research Center. The *MatLAB* based Monte Carlo Simulation (MCS) engine has been created with a capacity for use in future projects, however. Because the model is based on the component approach, it can be refined as the understanding of the complex interaction between hurricane winds and structures increases. With additional detail, the

model can also be used to quantify specific hurricane damage mitigation strategies. Furthermore, the MCS engine created for this project can serve as the spring board for a future online learning laboratory to serve as an academic tool for undergraduate civil engineers, or as a public service to homeowners in Florida and other hurricane prone regions of the United States.

APPENDIX A
SOUTH / KEYS REGION CONCRETE BLOCK GABLE ROOF (CBG) HOMES

This appendix contains simulated structural damage to typical concrete block homes in the South Florida and Florida Keys Region with gable roofs. Figure A-1 provides a measure of comparison between different building components. In this figure, the mean damages to roof cover, roof sheathing, and roof-to-wall connections are presented as a percentage of the total that is damaged. Wall damage is also presented as a percentage, with respect to the total of four walls, and as a percentage of damaged panels on gable ends. Additional figures provide the vulnerability (mean damage) or fragility (probability of exceeding defined damage states) for individual building components.

In a few cases, the fragility curves for simulated damages conflict with engineering judgment. One would expect damages to increase with wind speed, yet the damages to exterior doors (in Figure A-13) decrease after reaching 200 mph 3-second gust wind speeds. This anomaly is a function of the nature of the simulation routine. The damage-prediction engine simulates damages that would occur as a result of the entire storm from one snapshot of wind speed in time. It does not step through the entire duration of the storm, accumulating damages as the wind speed increases. For this reason, and due to internal pressure effects in the model, the damages to exterior doors decrease after 200 mph 3-second gusts. The monetary value of damage at the point at which the drop in damage to these two components occurs is already substantial; thus these unusual results will not adversely affect the end product of insurable loss.

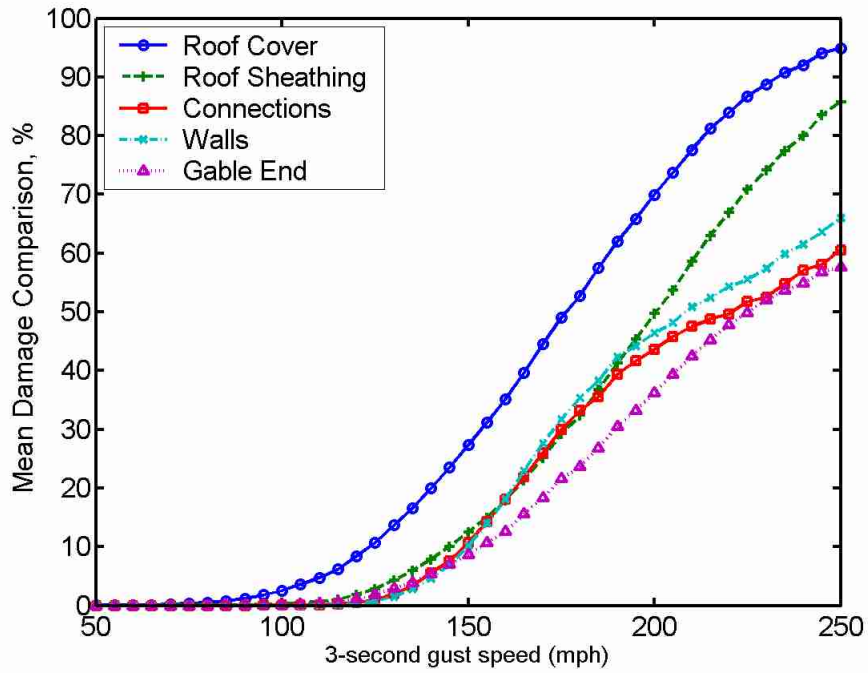


Figure A-1. Concrete block gable roof South/Keys Region home comparative levels of roof cover, roof sheathing, connections, wall, and gable end sheathing damage.

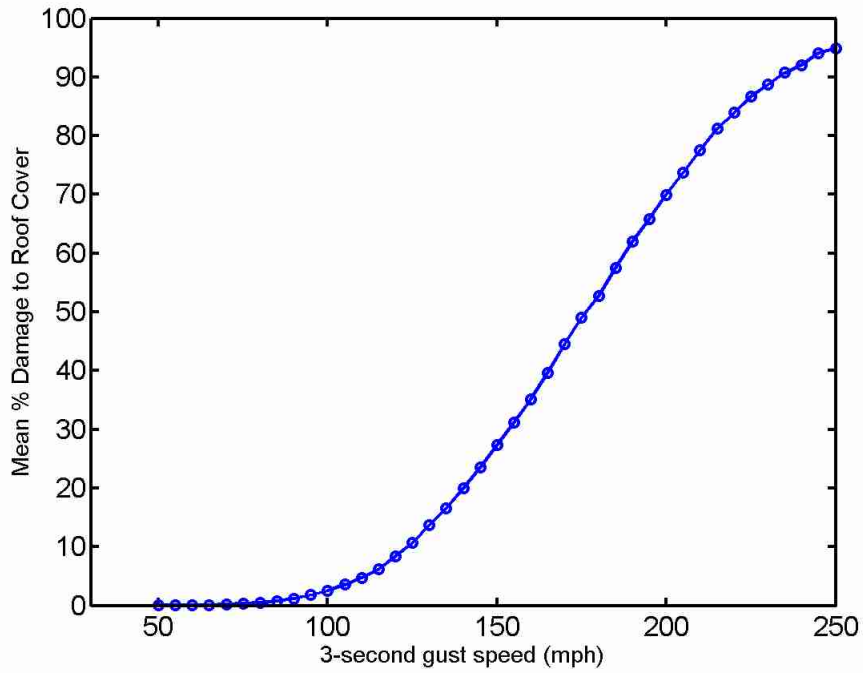


Figure A-2. Vulnerability to roof cover damage for South/Keys CBG homes.

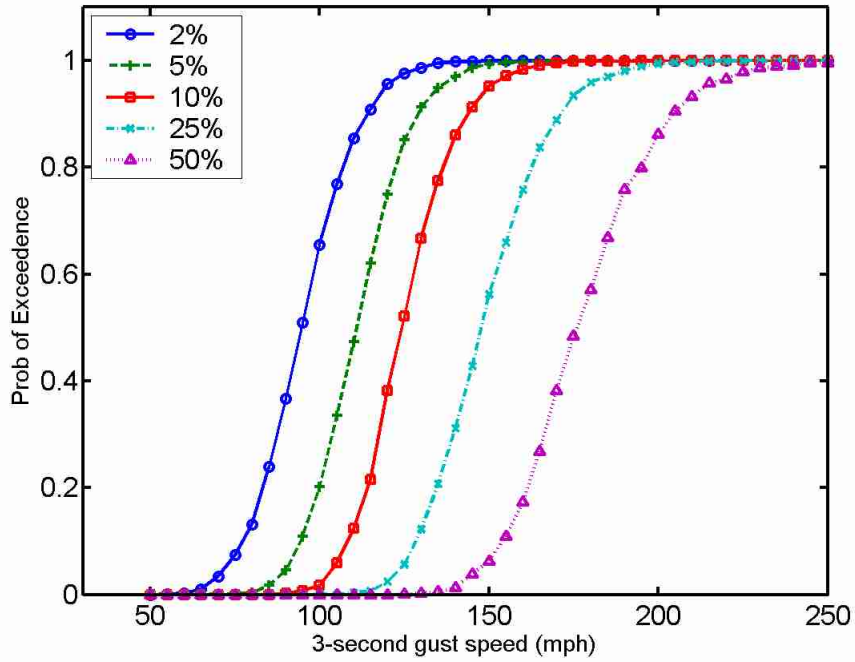


Figure A-3. Fragility curves for 2%, 5%, 10%, 25%, and 50% damage to roof cover for South/Keys CBG homes.

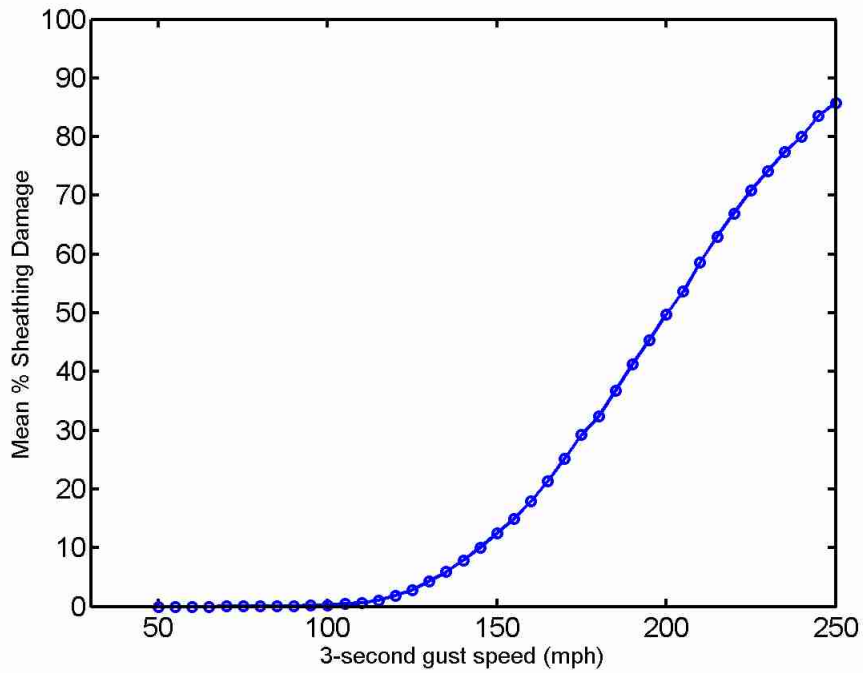


Figure A-4. Vulnerability to roof sheathing damage for South/Keys CBG homes.

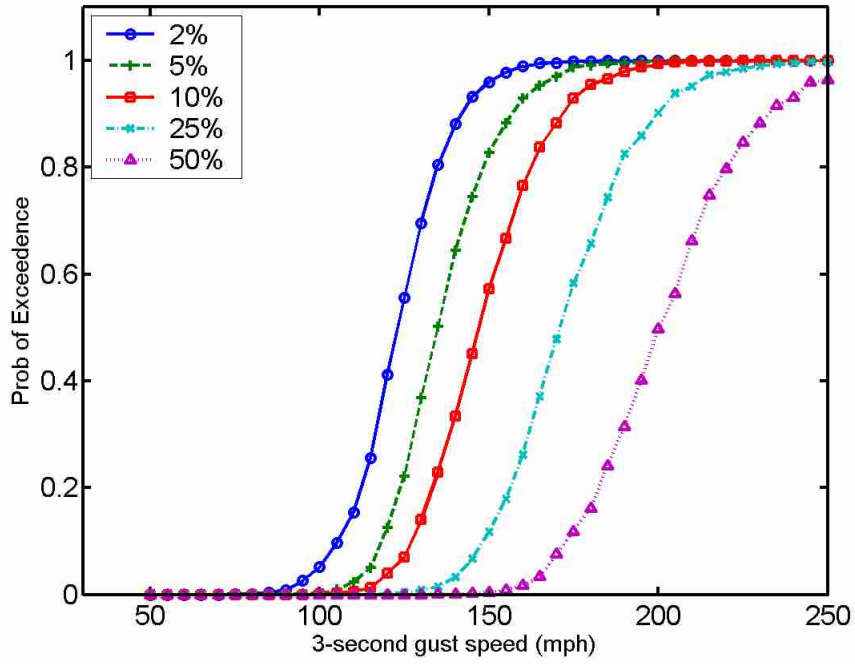


Figure A-5. Fragility curves for 2%, 5%, 10%, 25%, and 50% damage to roof sheathing for South/Keys CBG homes.

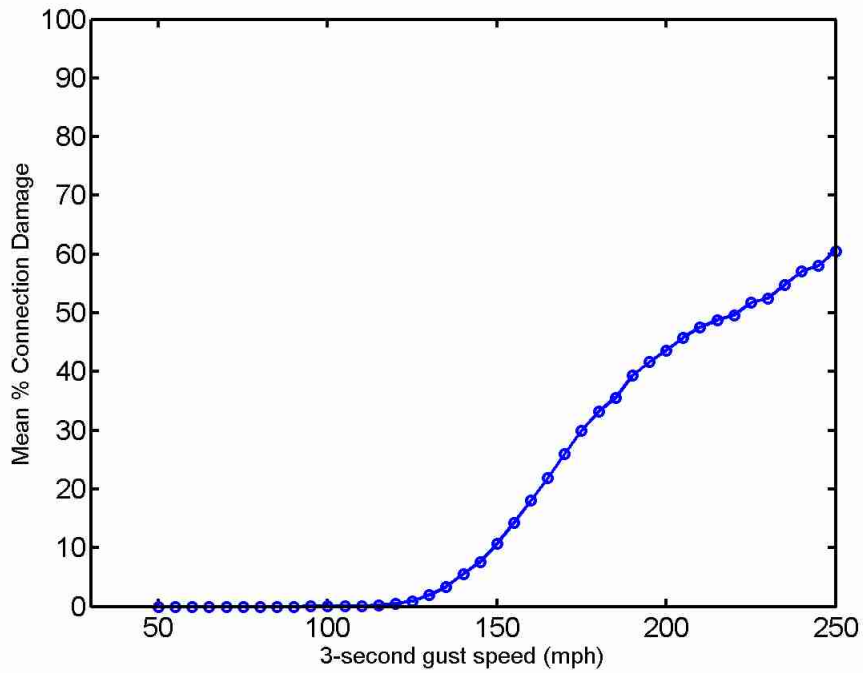


Figure A-6. Vulnerability to roof-to-wall connection damage for South/Keys CBG homes.

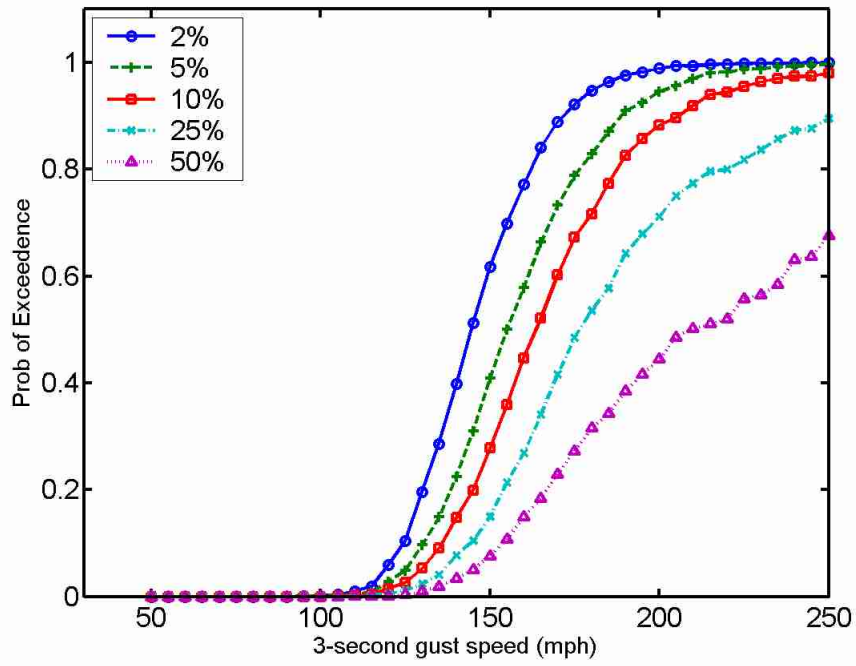


Figure A-7. Fragility curves for 2%, 5%, 10%, 25%, and 50% damage to roof-to-wall connections for South/Keys Region CBG homes.

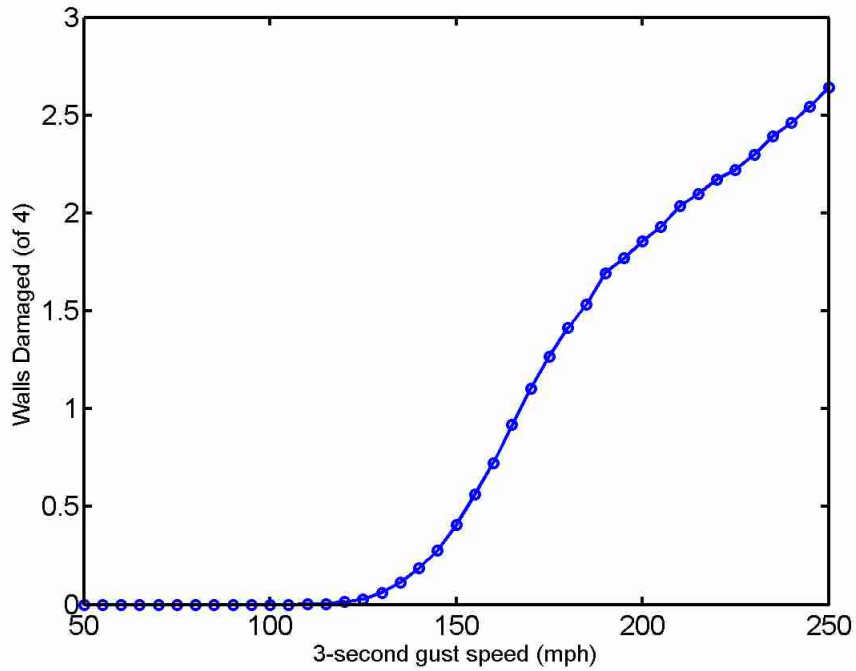


Figure A-8. Vulnerability to wall damage for South/Keys Region CBG homes.

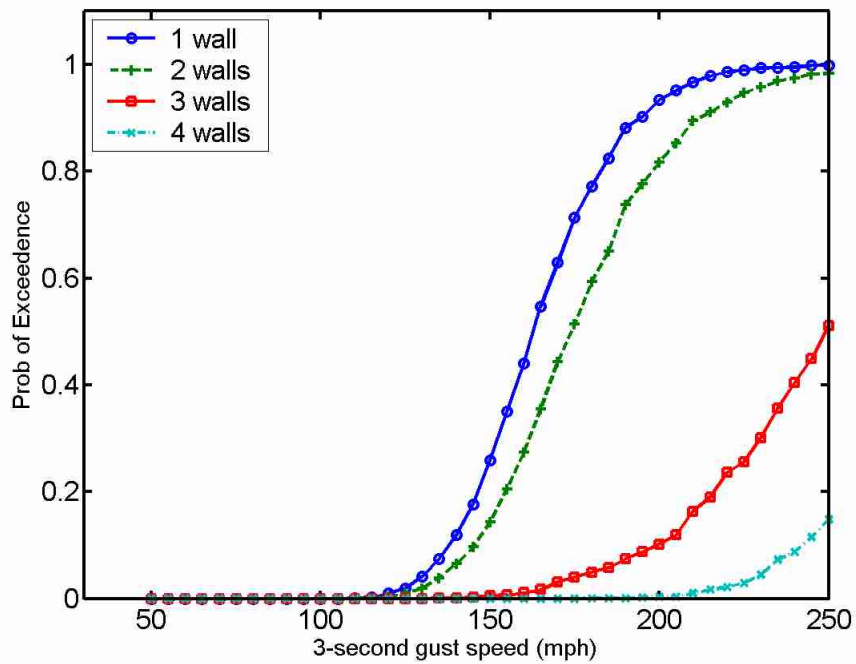


Figure A-9. Fragility curves for 1, 2, 3 and 4 damaged walls for South/Keys Region CBG homes.

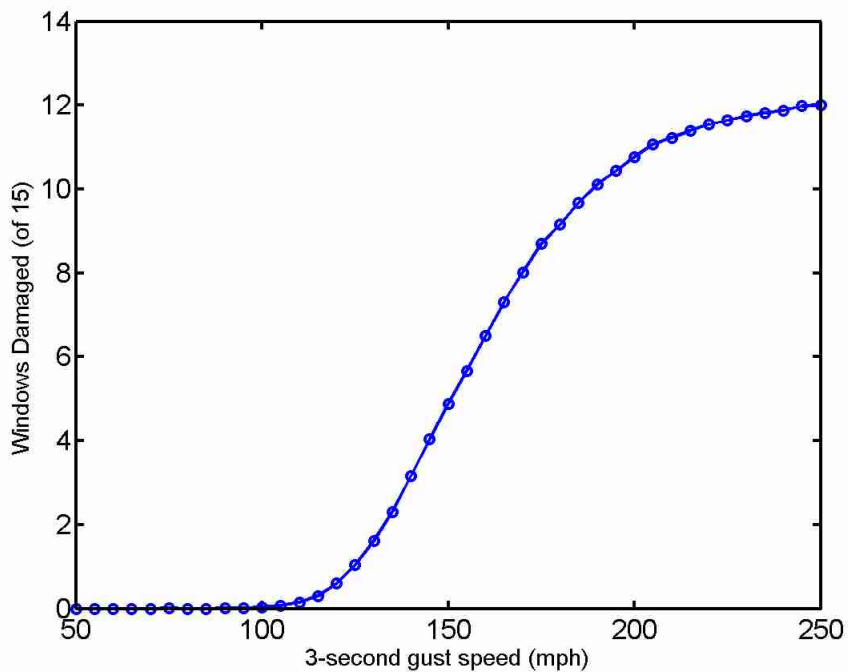


Figure A-10. Vulnerability to window damage for South/Keys Region CBG homes.

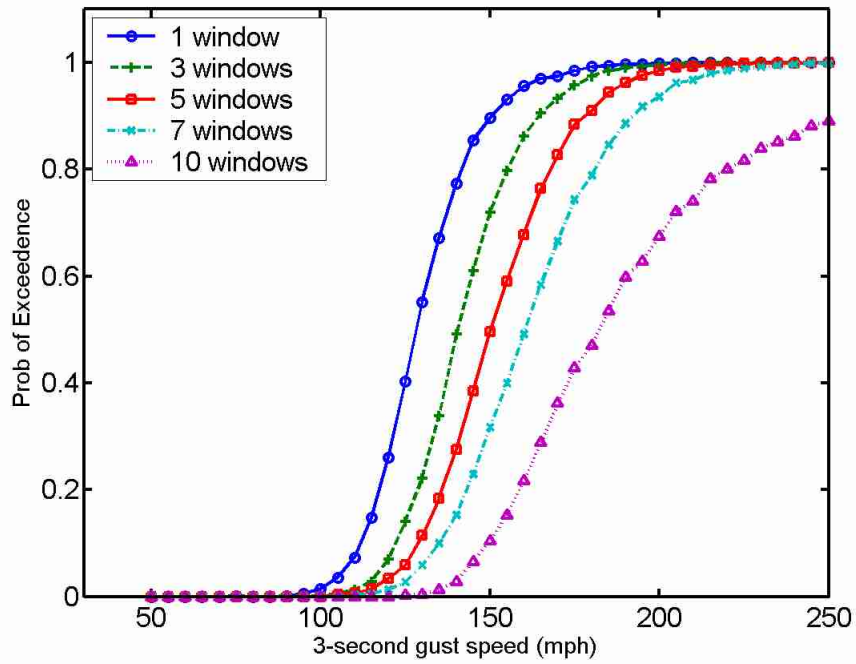


Figure A-11. Fragility curves for 1, 3, 5, 7, and 10 damaged windows for South/Keys Region CBG homes.

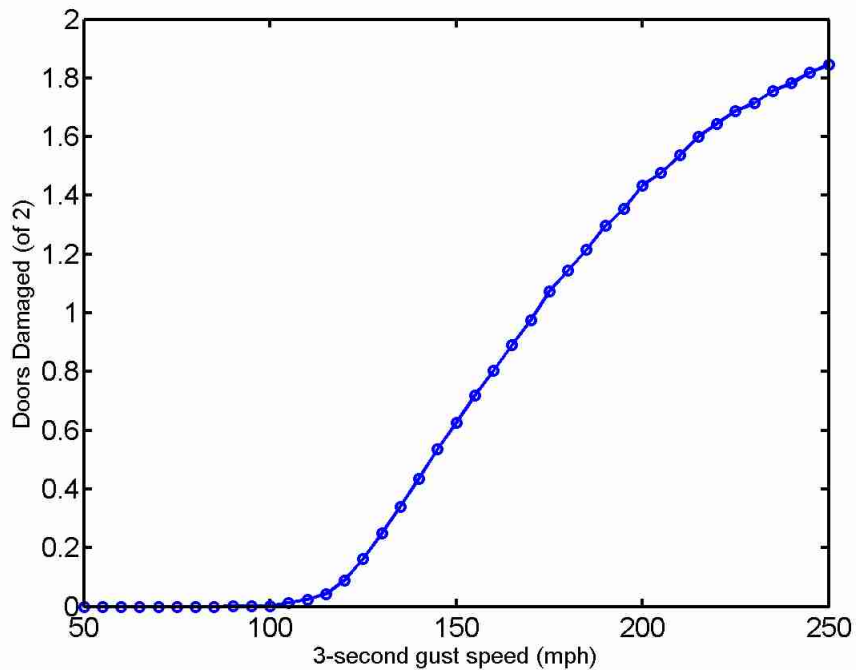


Figure A-12. Vulnerability to exterior door damage for South/Keys Region CBG homes.

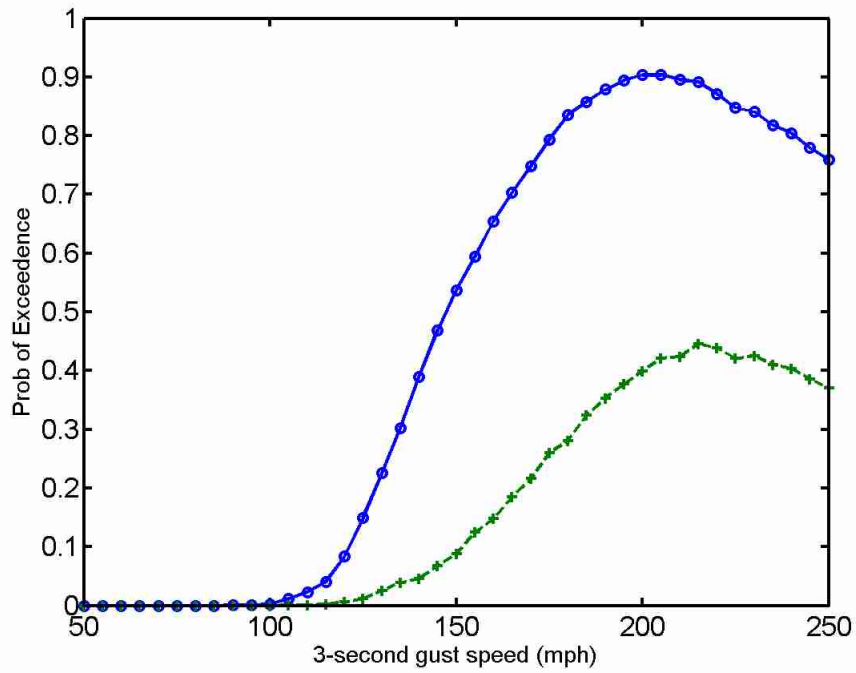


Figure A-13. Fragility curves for 1 and 2 damaged exterior doors for South/Keys Region CBG homes.

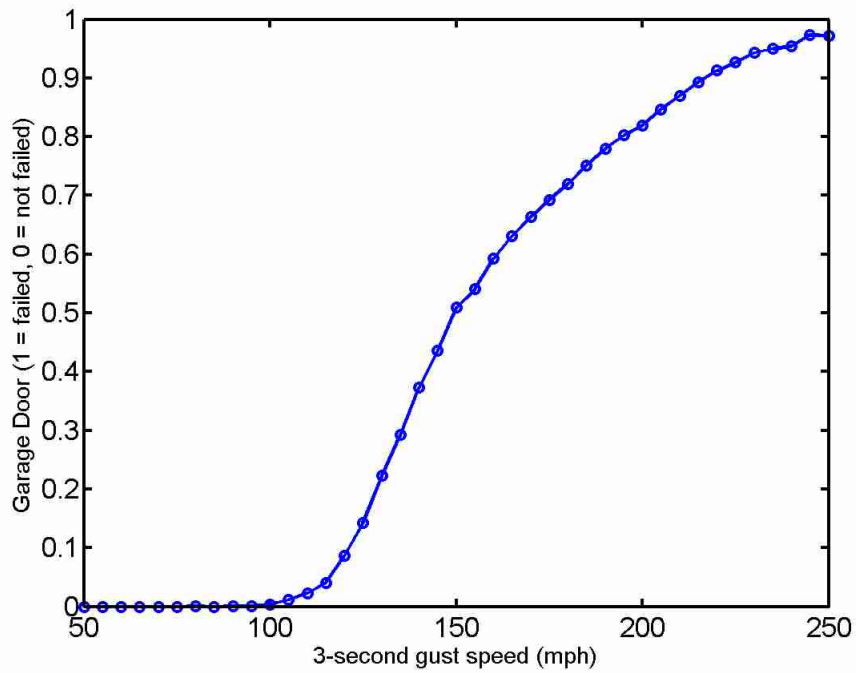


Figure A-14. Vulnerability to garage door damage for South/Keys Region CBG homes.

APPENDIX B
SOUTH / KEYS REGION CONCRETE BLOCK HIP ROOF (CBH) HOMES

This appendix contains figures showing simulated structural damage to typical concrete block homes in the South Florida and Florida Keys Region with hip roofs. Figure B-1 provides a measure of comparison between different building components. In this figure, the mean damages to roof cover, roof sheathing, and roof-to-wall connections are presented as a percentage of the total that is damaged. Wall damage is also presented as a percentage, with respect to the total of four walls. Additional figures provide the vulnerability (mean damage) or fragility (probability of exceeding defined damage states) for individual building components.

In a few cases, the fragility curves for simulated damages conflict with engineering judgment. One would expect damages to increase with wind speed, yet the damages to exterior doors (in Figure B-13) decrease after reaching 200 mph 3-second gust wind speeds. This anomaly is a function of the nature of the simulation routine. The damage-prediction engine simulates damages that would occur as a result of the entire storm from one snapshot of wind speed in time. It does not step through the entire duration of the storm, accumulating damages as the wind speed increases. For this reason, and due to internal pressure effects in the model, the damages to exterior doors decrease after 200 mph 3-second gusts. The monetary value of damage at the point at which the drop in damage to these two components occurs is already substantial; thus these unusual results will not adversely affect the end product of insurable loss.

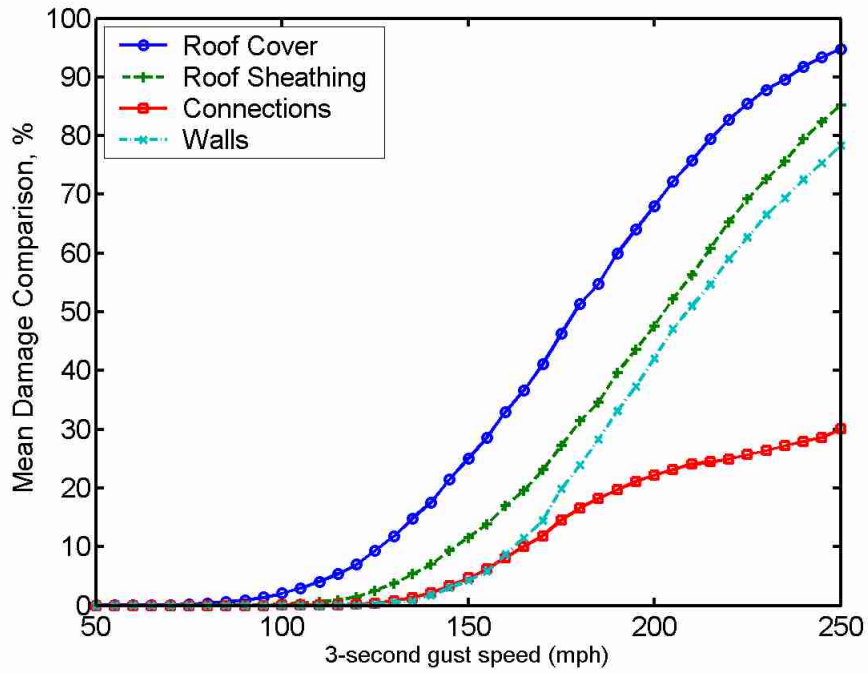


Figure B-1. Concrete block hip roof South/Keys Region home comparative levels of roof cover, roof sheathing, connections, wall, and gable end sheathing damage.

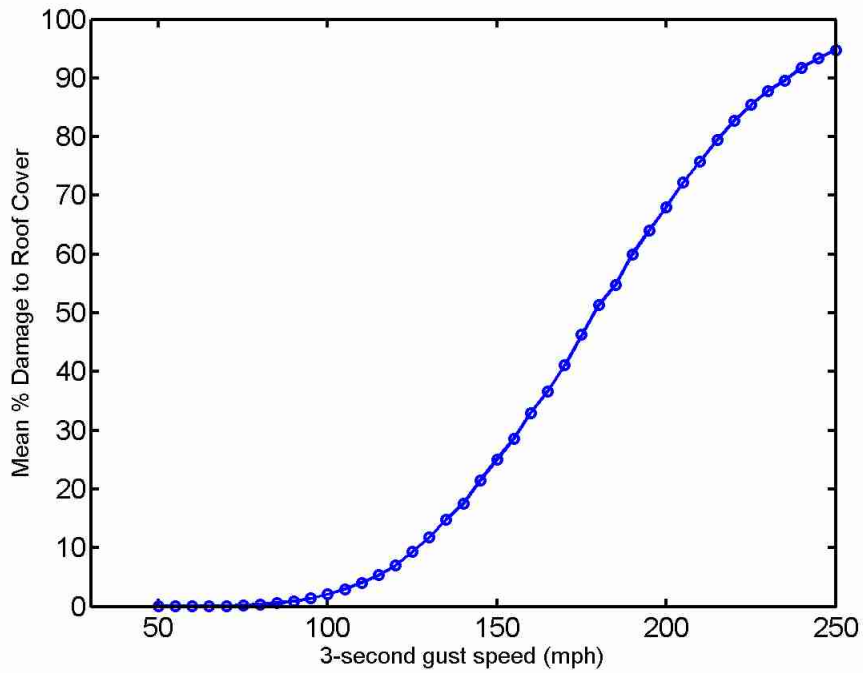


Figure B-2. Vulnerability to roof cover damage for South/Keys CBH homes.

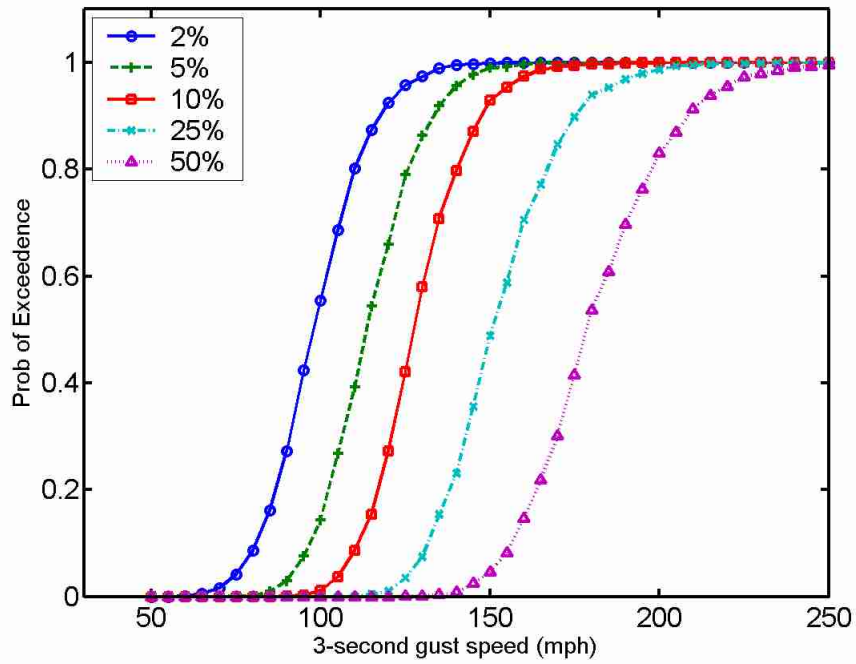


Figure B-3. Fragility curves for 2%, 5%, 10%, 25%, and 50% damage to roof cover for South/Keys CBH homes.

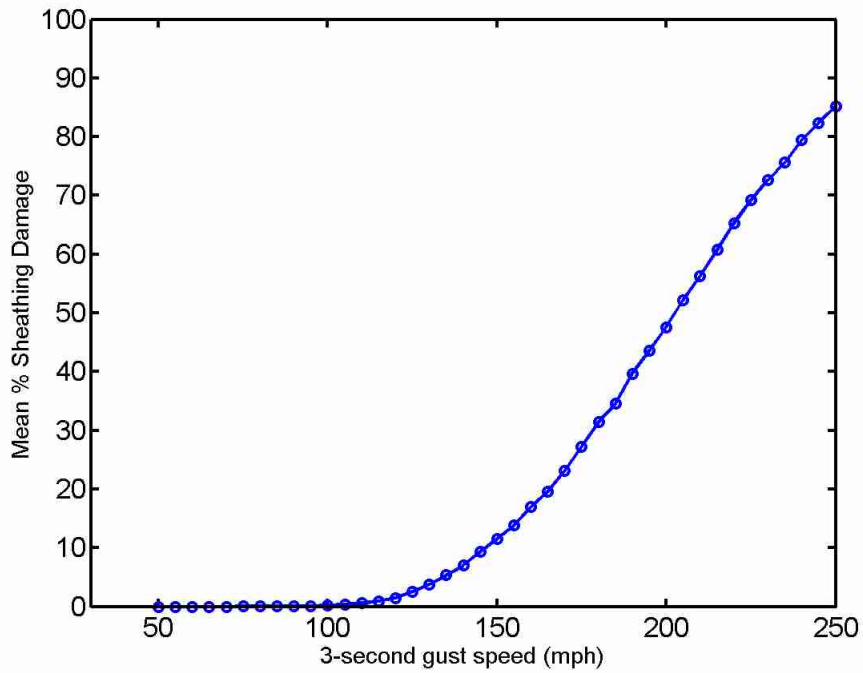


Figure B-4. Vulnerability to roof sheathing damage for South/Keys CBH homes.

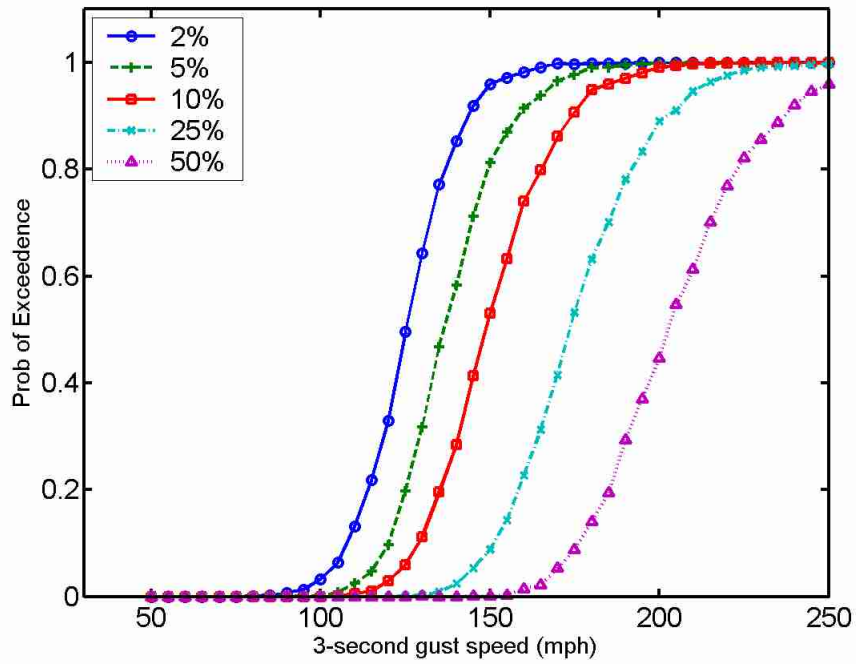


Figure B-5. Fragility curves for 2%, 5%, 10%, 25%, and 50% damage to roof sheathing for South/Keys CBH homes.

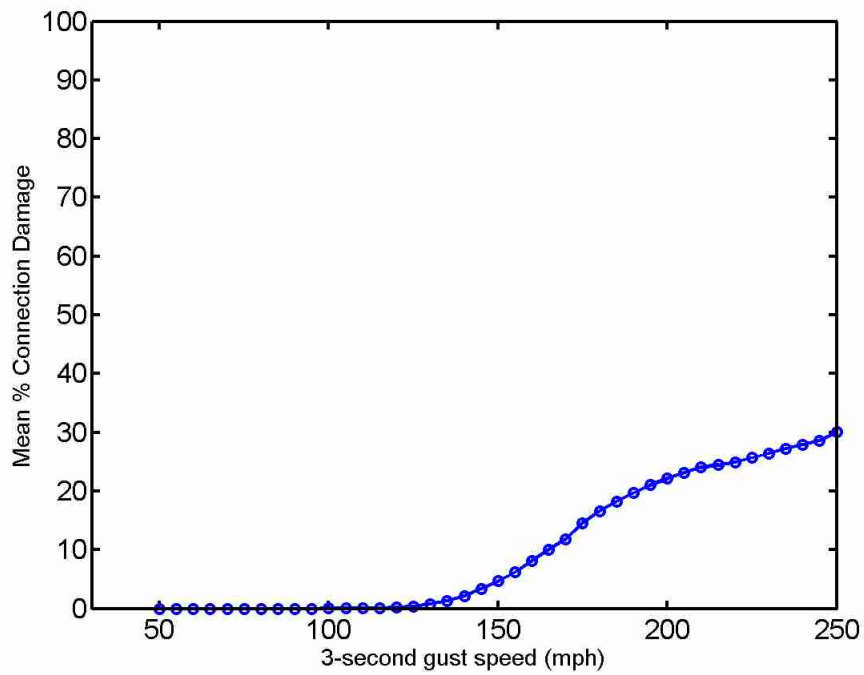


Figure B-6. Vulnerability to roof-to-wall connection damage for South/Keys CBH homes.

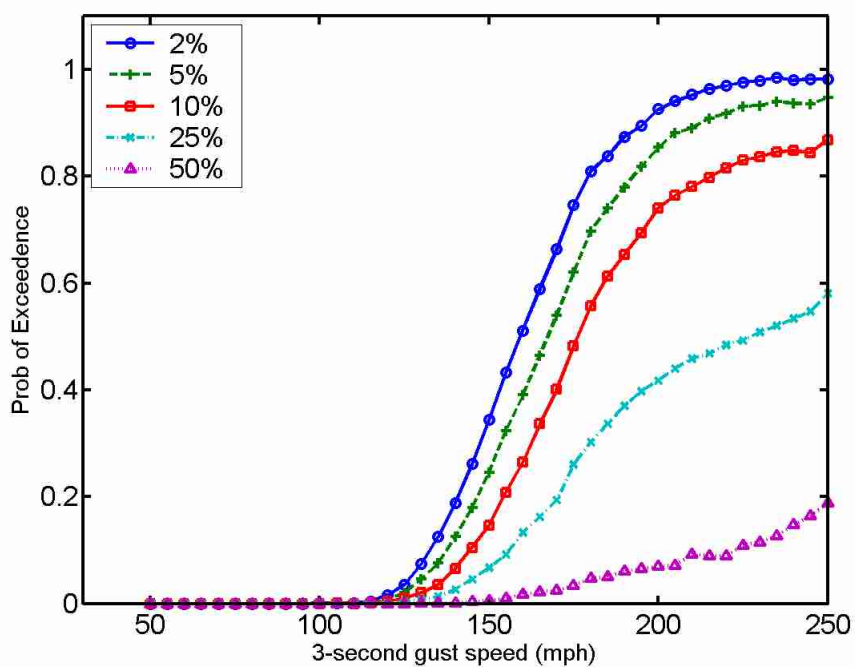


Figure B-7. Fragility curves for 2%, 5%, 10%, 25%, and 50% damage to roof-to-wall connections for South/Keys Region CBH homes.

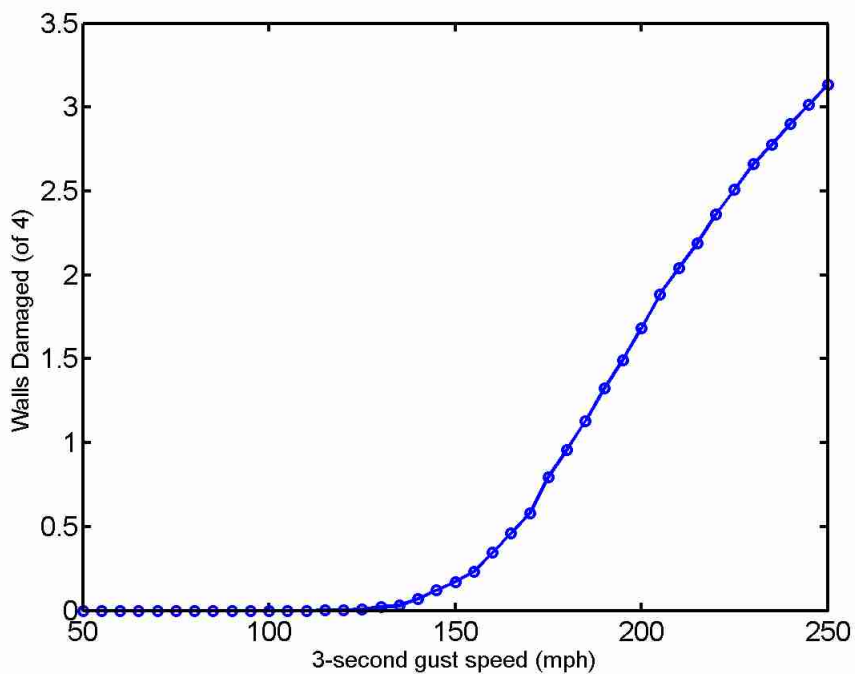


Figure B-8. Vulnerability to wall damage for South/Keys Region CBH homes.

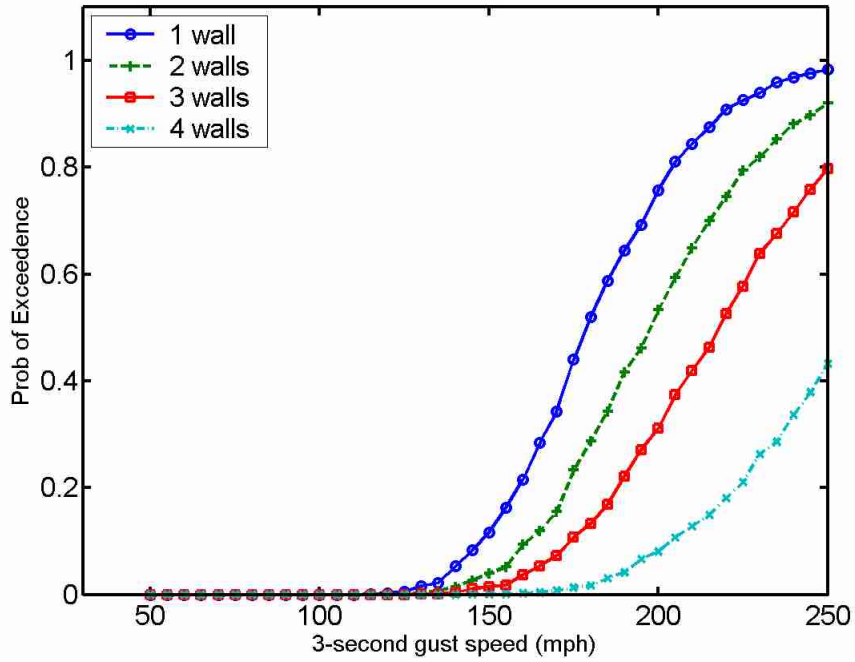


Figure B-9. Fragility curves for 1, 2, 3 and 4 damaged walls for South/Keys Region CBH homes.

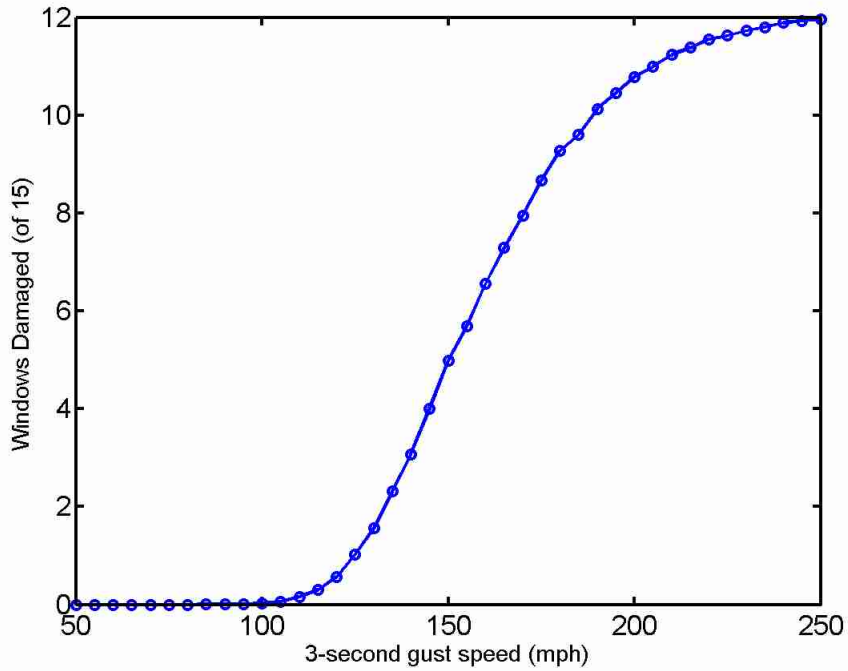


Figure B-10. Vulnerability to window damage for South/Keys Region CBH homes.

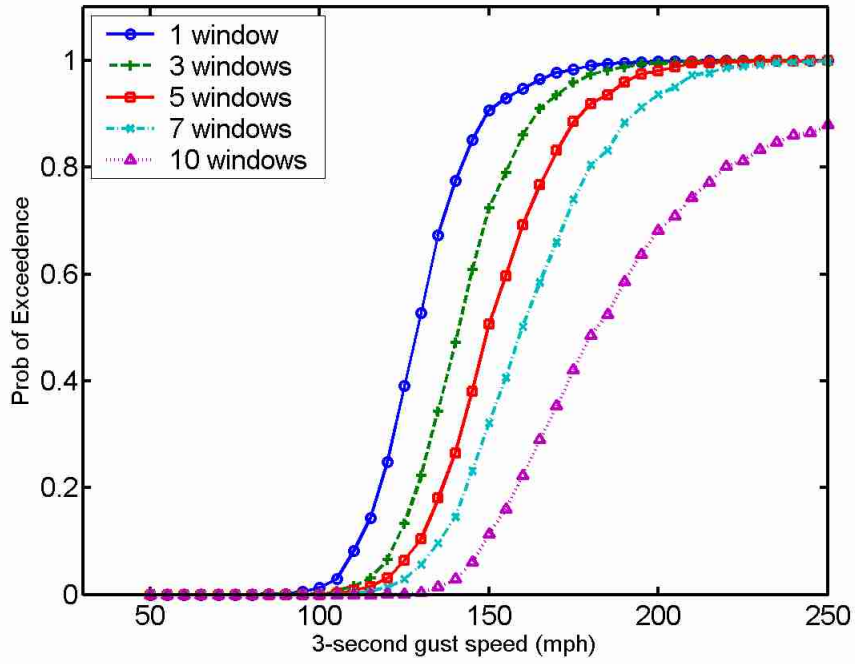


Figure B-11. Fragility curves for 1, 3, 5, 7, and 10 damaged windows for South/Keys Region CBH homes.

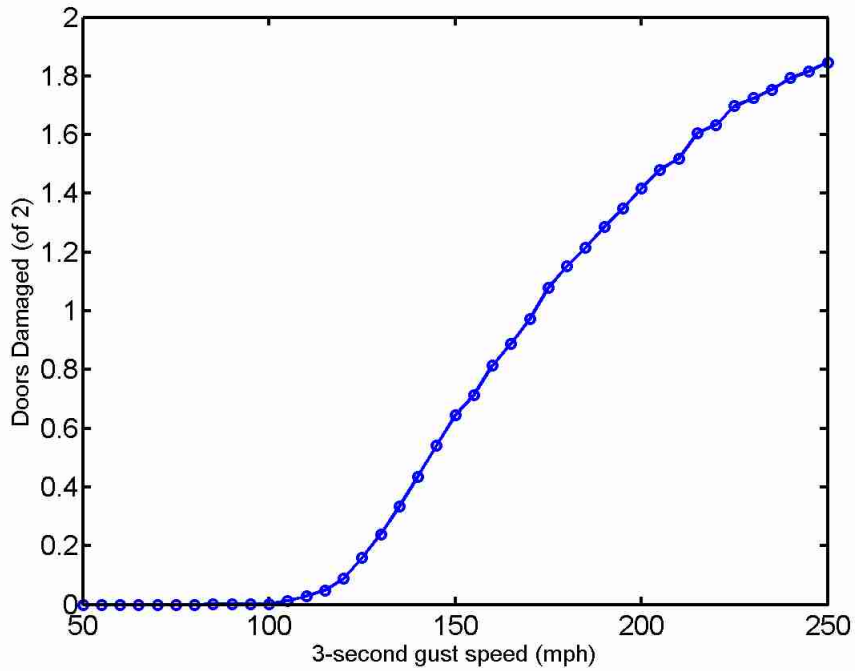


Figure B-12. Vulnerability to exterior door damage for South/Keys Region CBH homes.

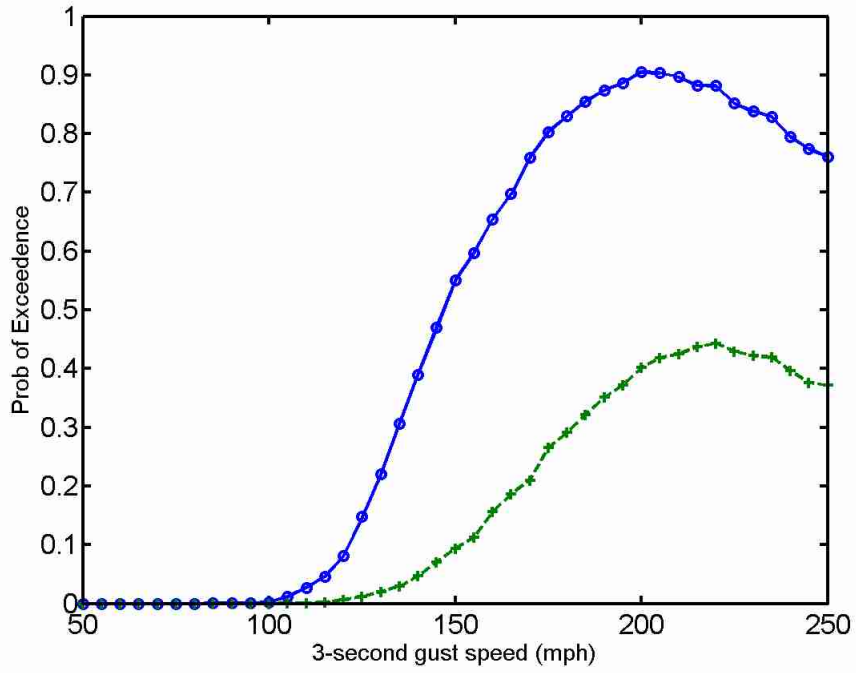


Figure B-13. Fragility curves for 1 and 2 damaged exterior doors for South/Keys Region CBH homes.

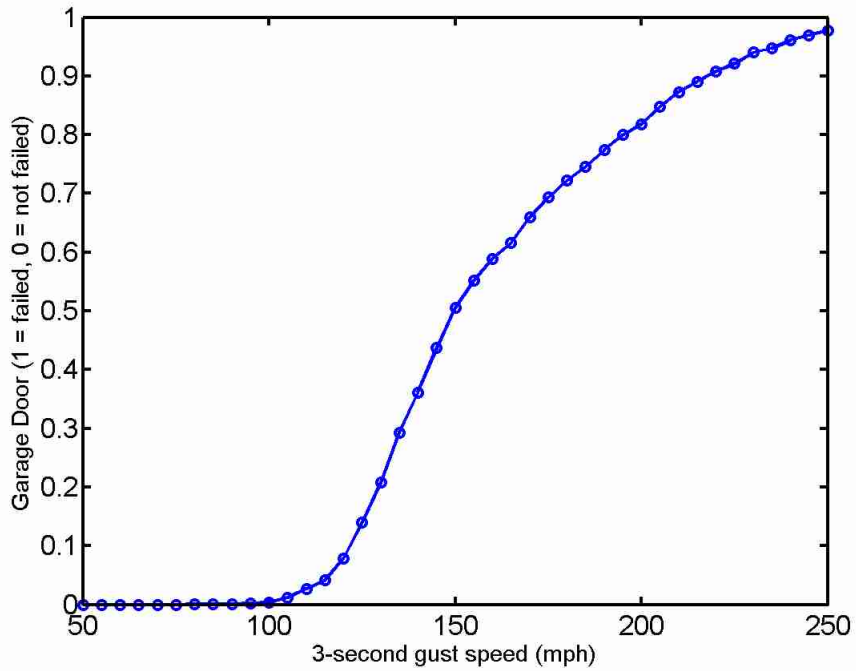


Figure B-14. Vulnerability to garage door damage for South/Keys Region CBH homes.

APPENDIX C
SOUTH / KEYS REGION WOOD FRAME GABLE ROOF (WG) HOMES

This appendix contains simulated structural damage to typical wood frame homes in the South Florida and Florida Keys Region with hip roofs. Figure C-1 provides a measure of comparison between different building components. In this figure, the mean damages to roof cover, roof sheathing, and roof-to-wall connections are presented as a percentage of the total that is damaged. Wall damage is also presented as a percentage, with respect to the total of four walls, and as a percentage of sheathing panels lost on gable ends. Additional figures provide the vulnerability (mean damage) or fragility (probability of exceeding defined damage states) for individual building components.

In a few cases, the fragility curves for simulated damages conflict with engineering judgment. One would expect damages to increase with wind speed, yet the damages to exterior doors (in Figure C-13) decrease after reaching 200 mph 3-second gust wind speeds. This anomaly is a function of the nature of the simulation routine. The damage-prediction engine simulates damages that would occur as a result of the entire storm from one snapshot of wind speed in time. It does not step through the entire duration of the storm, accumulating damages as the wind speed increases. For this reason, and due to internal pressure effects in the model, the damages to exterior doors decrease after 200 mph 3-second gusts. The monetary value of damage at the point at which the drop in damage to these two components occurs is already substantial; thus these unusual results will not adversely affect the end product of insurable loss.

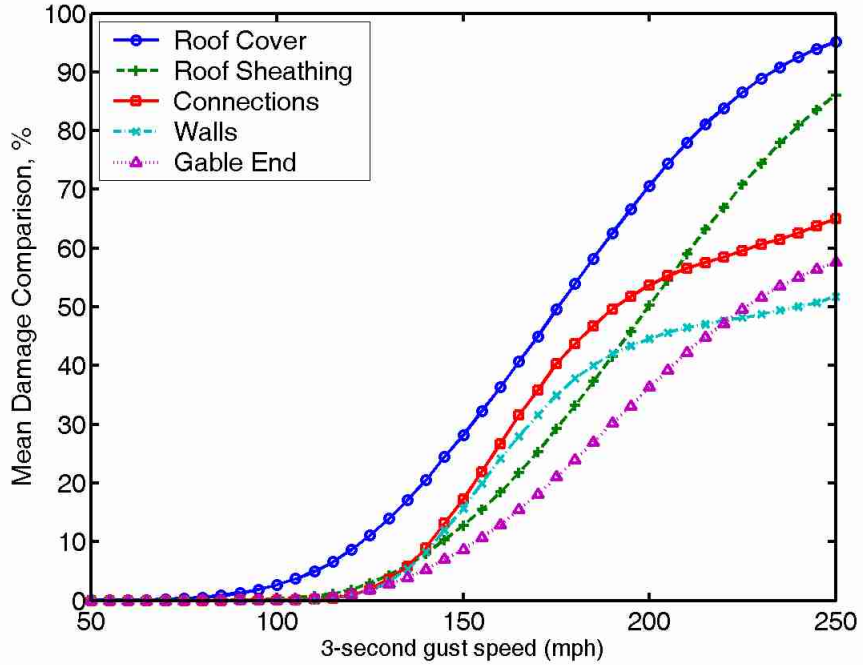


Figure C-1. Wood frame gable roof South/Keys Region home comparative levels of roof cover, roof sheathing, connections, wall, and gable end sheathing damage.

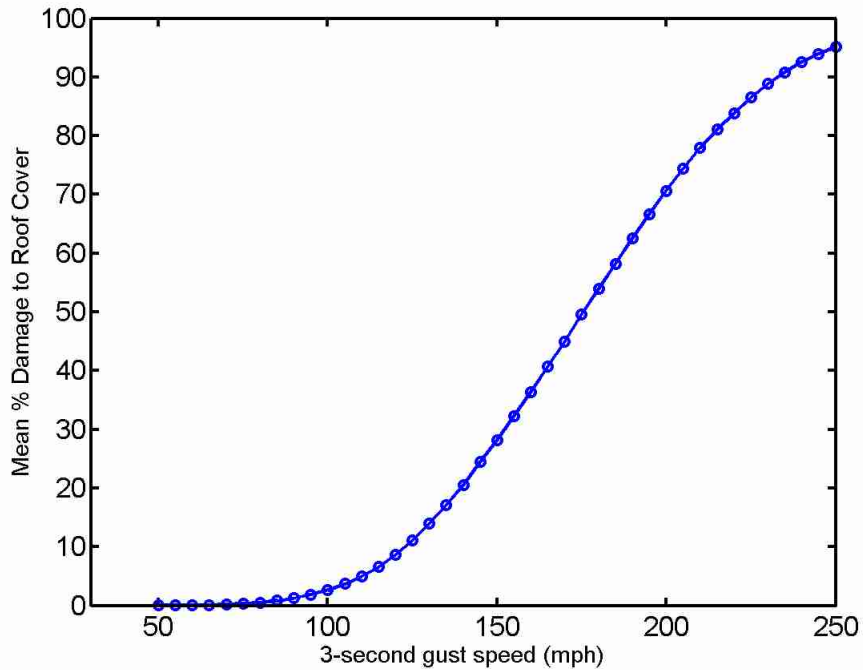


Figure C-2. Vulnerability to roof cover damage for South/Keys WG homes.

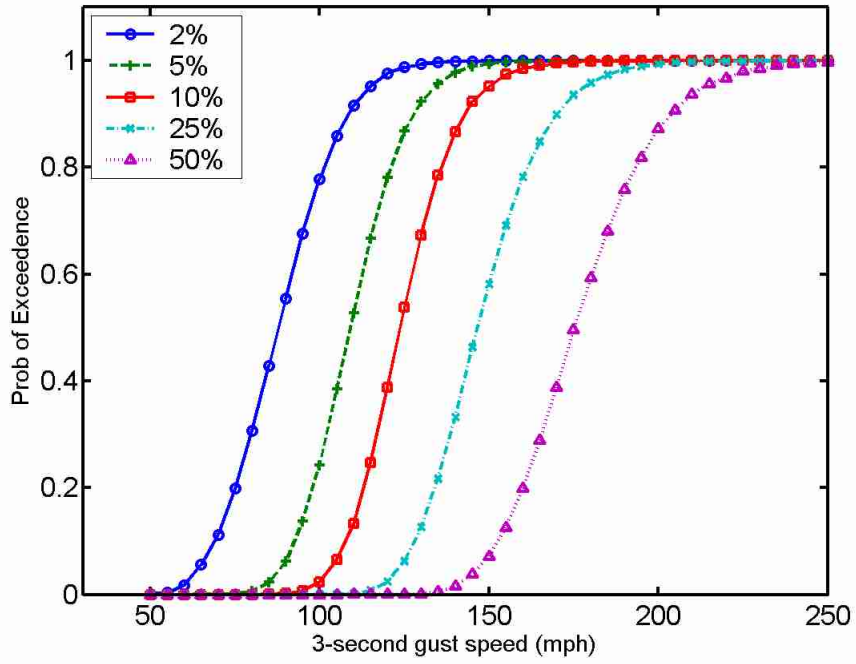


Figure C-3. Fragility curves for 2%, 5%, 10%, 25%, and 50% damage to roof cover for South/Keys WG homes.

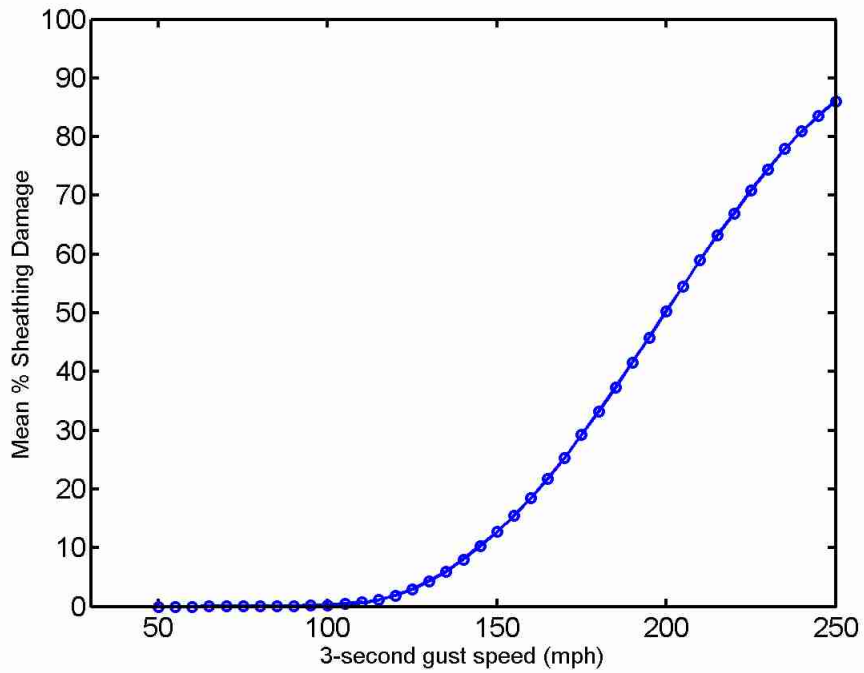


Figure C-4. Vulnerability to roof sheathing damage for South/Keys WG homes.

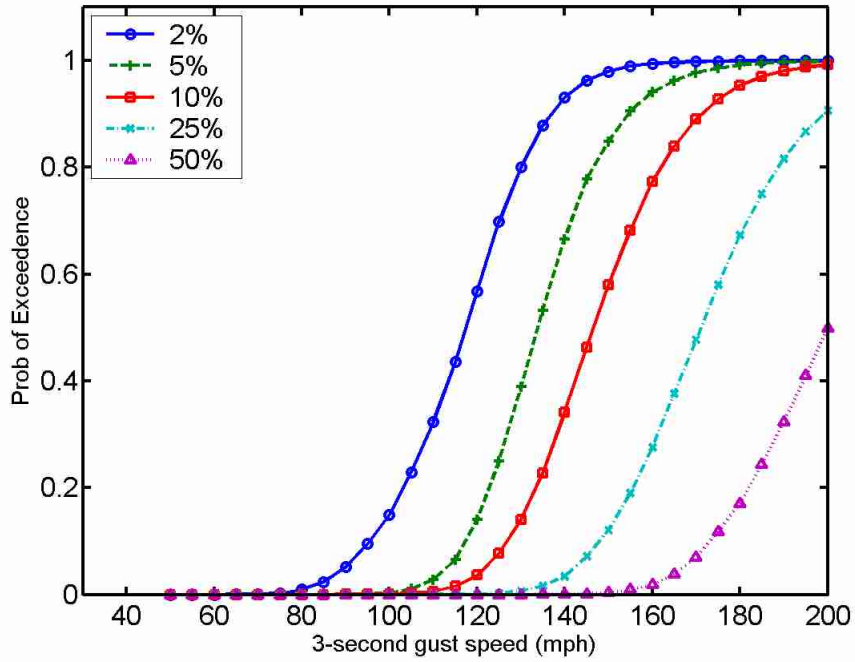


Figure C-5. Fragility curves for 2%, 5%, 10%, 25%, and 50% damage to roof sheathing for South/Keys WG homes.

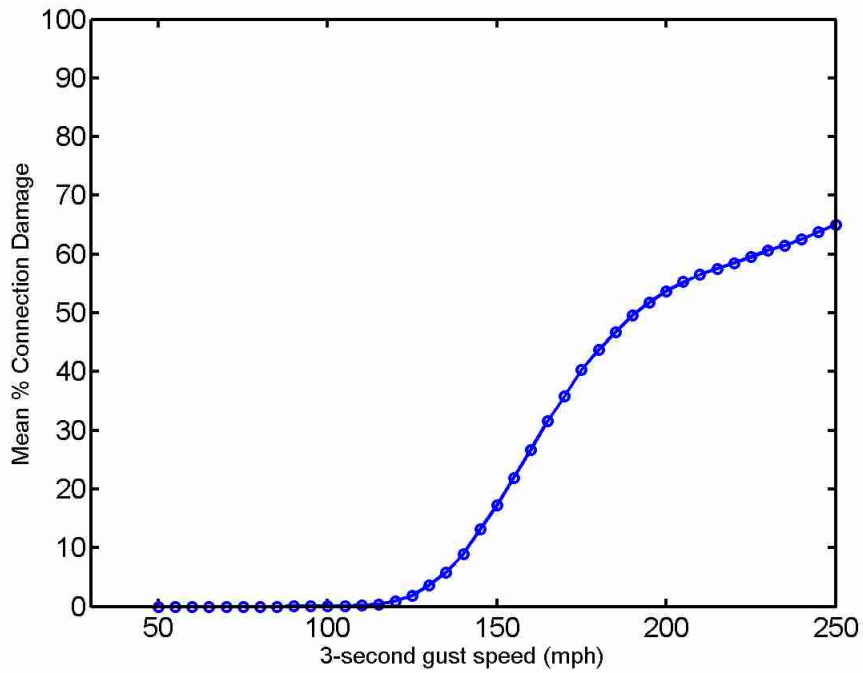


Figure C-6. Vulnerability to roof-to-wall connection damage for South/Keys WG homes.

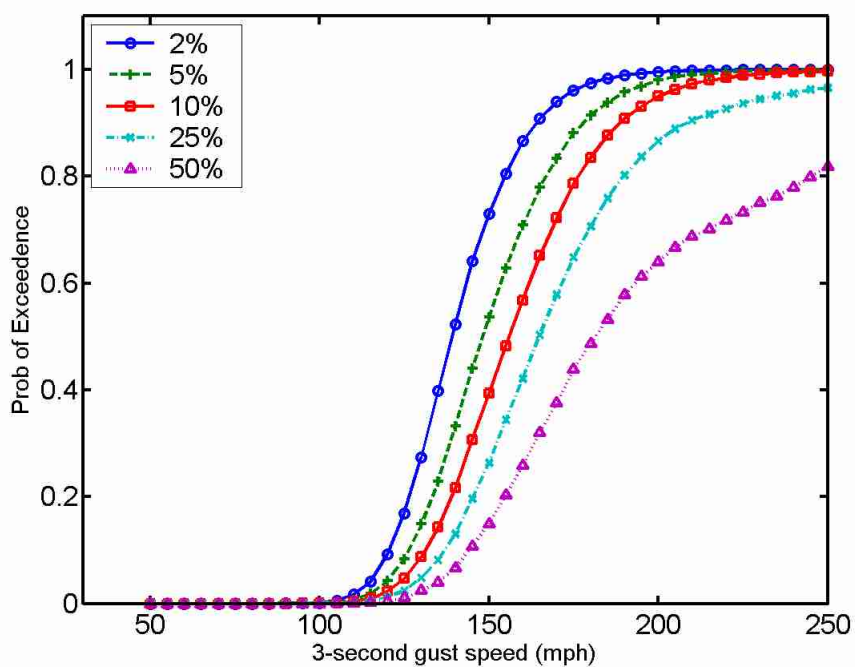


Figure C-7. Fragility curves for 2%, 5%, 10%, 25%, and 50% damage to roof-to-wall connections for South/Keys Region WG homes.

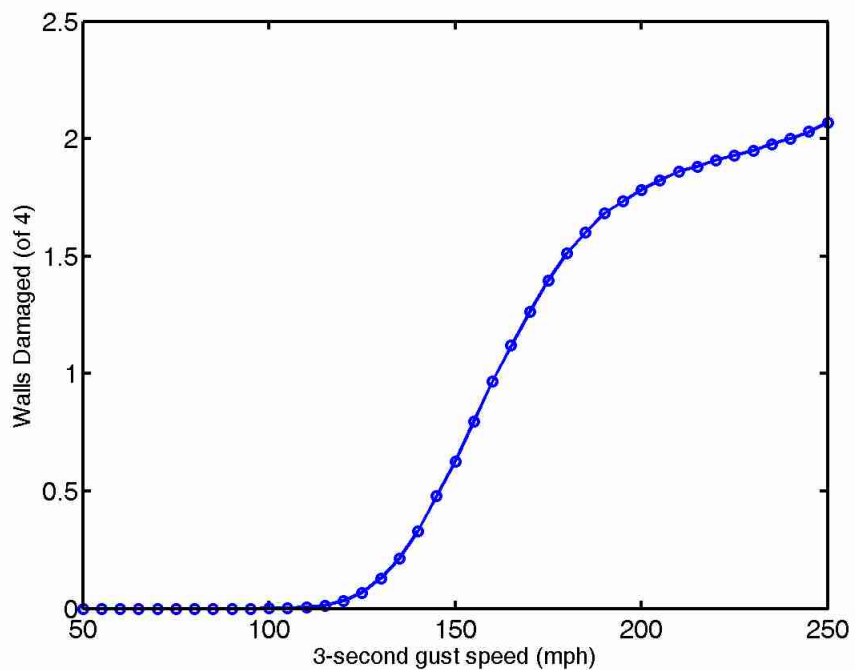


Figure C-8. Vulnerability to wall damage for South/Keys Region WG homes.

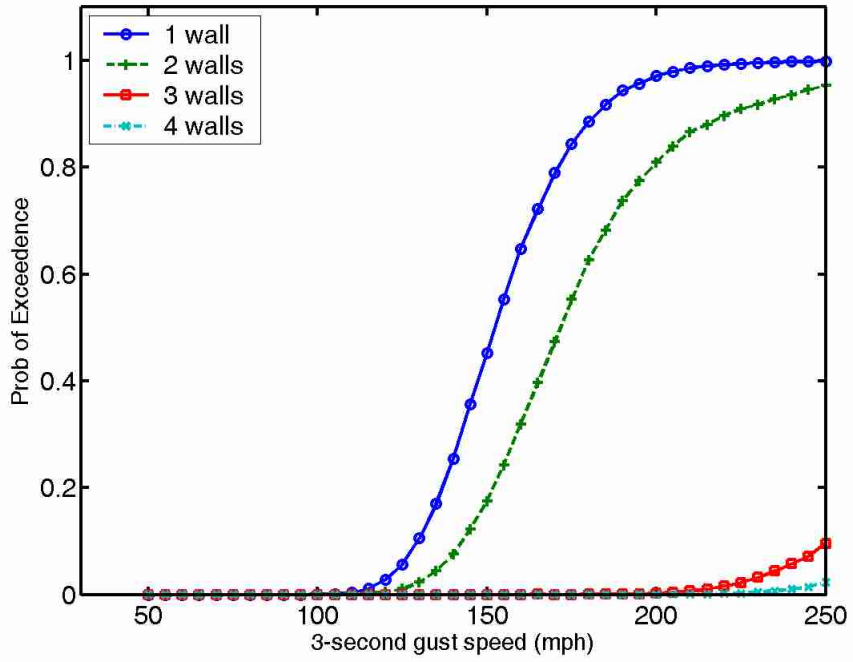


Figure C-9. Fragility curves for 1, 2, 3 and 4 damaged walls for South/Keys Region WG homes.

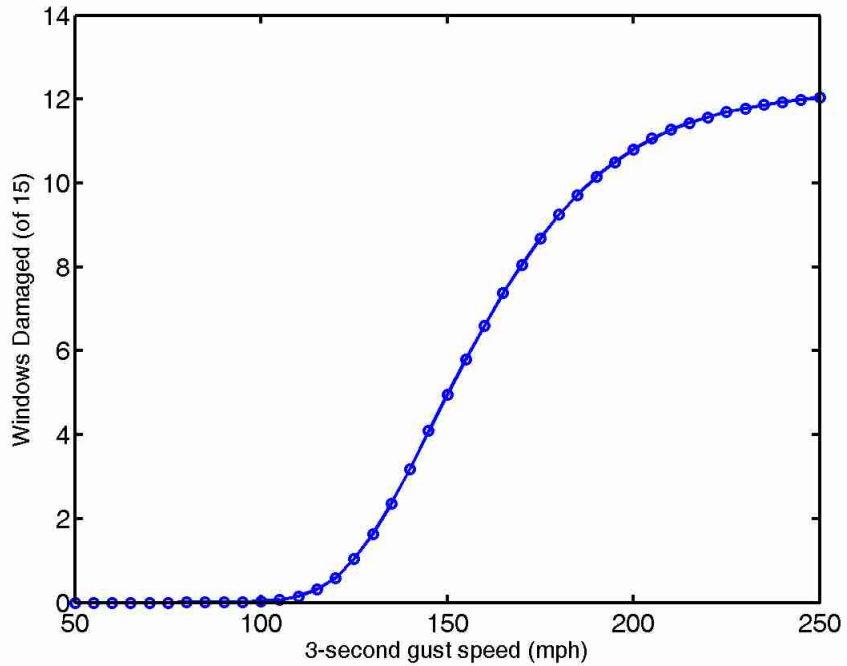


Figure C-10. Vulnerability to window damage for South/Keys Region WG homes.

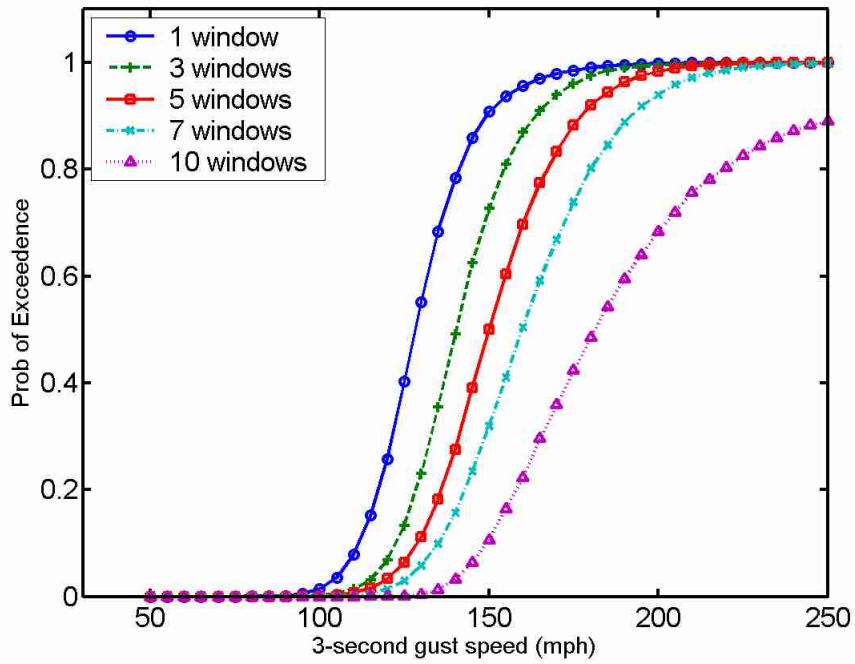


Figure C-11. Fragility curves for 1, 3, 5, 7, and 10 damaged windows for South/Keys Region WG homes.

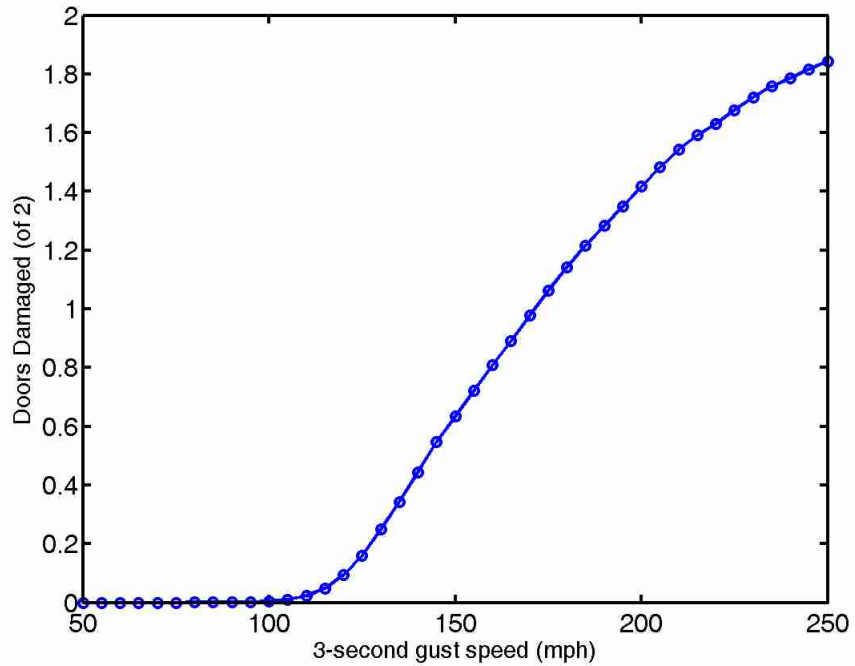


Figure C-12. Vulnerability to exterior door damage for South/Keys Region WG homes.

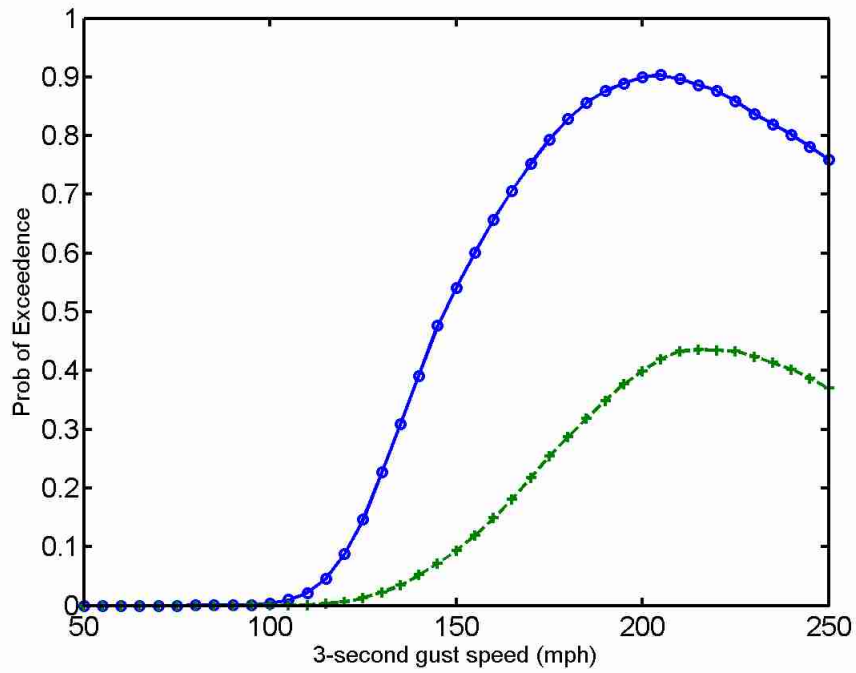


Figure C-13. Vulnerability to exterior door damage for South/Keys Region WG homes.

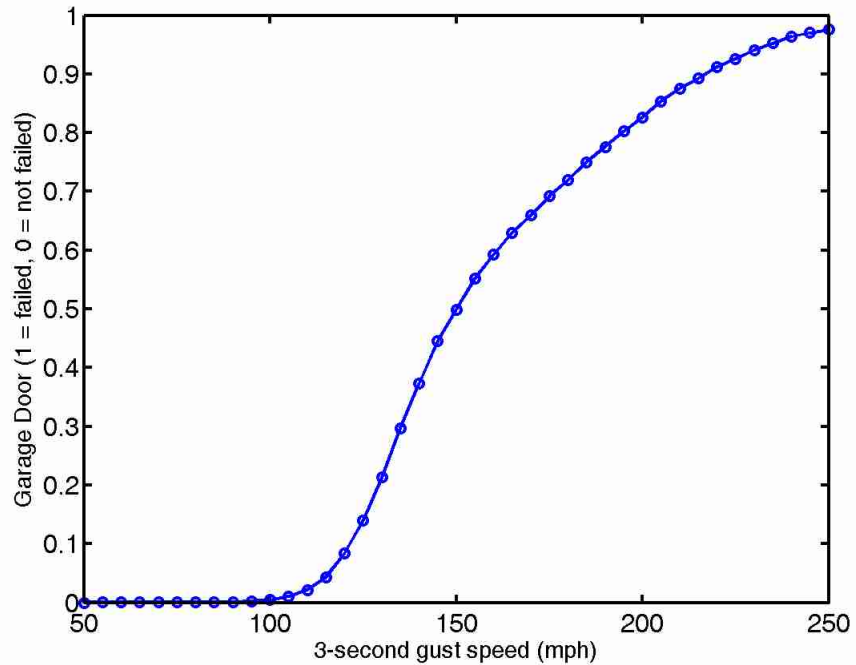


Figure C-14. Vulnerability to garage door damage for South/Keys Region WG homes.

APPENDIX D
SOUTH / KEYS REGION WOOD FRAME HIP ROOF (WH) HOMES

This appendix contains figures showing simulated structural damage to typical wood frame homes in the South Florida and Florida Keys Region with hip roofs. Figure D-1 provides a measure of comparison between different building components. In this figure, the mean damages to roof cover, roof sheathing, and roof-to-wall connections are presented as a percentage of the total that is damaged. Wall damage is also presented as a percentage, with respect to the total of four walls. Additional figures provide the vulnerability (mean damage) or fragility (probability of exceeding defined damage states) for individual building components.

In a few cases, the fragility curves for simulated damages conflict with engineering judgment. One would expect damages to increase with wind speed, yet the damages to exterior doors (in Figure C-13) decrease after reaching 200 mph 3-second gust wind speeds. This anomaly is a function of the nature of the simulation routine. The damage-prediction engine simulates damages that would occur as a result of the entire storm from one snapshot of wind speed in time. It does not step through the entire duration of the storm, accumulating damages as the wind speed increases. For this reason, and due to internal pressure effects in the model, the damages to exterior doors decrease after 200 mph 3-second gusts. The monetary value of damage at the point at which the drop in damage to these two components occurs is already substantial; thus these unusual results will not adversely affect the end product of insurable loss.

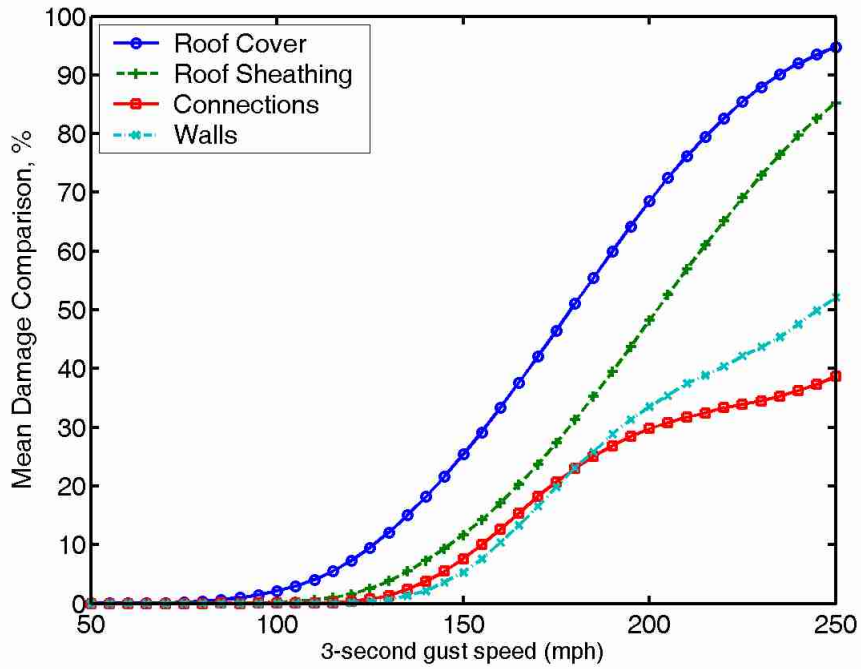


Figure D-1. Wood frame hip roof South/Keys Region home comparative levels of roof cover, roof sheathing, connections, wall, and gable end sheathing damage.

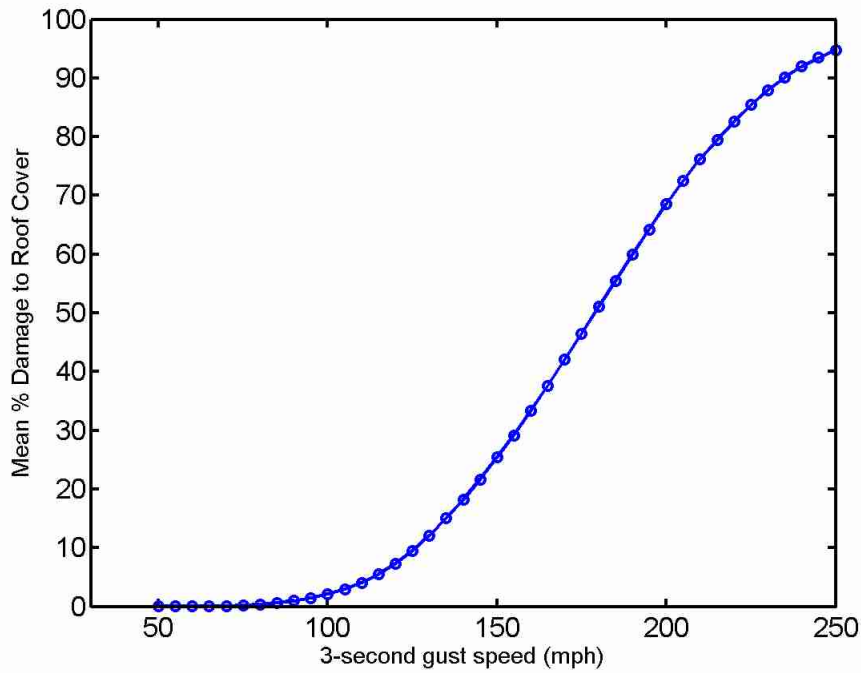


Figure D-2. Vulnerability to roof cover damage for South/Keys WH homes.

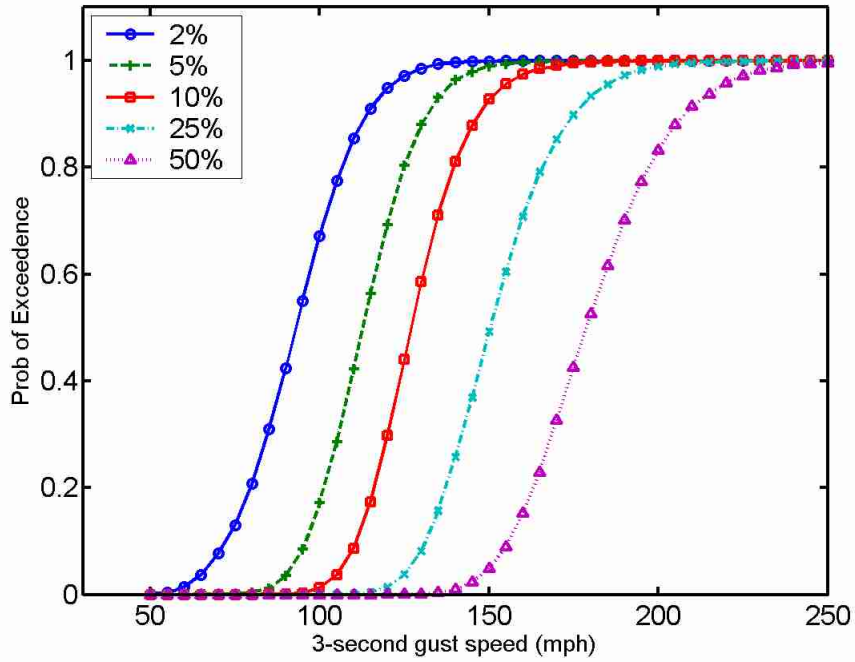


Figure D-3. Fragility curves for 2%, 5%, 10%, 25%, and 50% damage to roof cover for South/Keys WH homes.

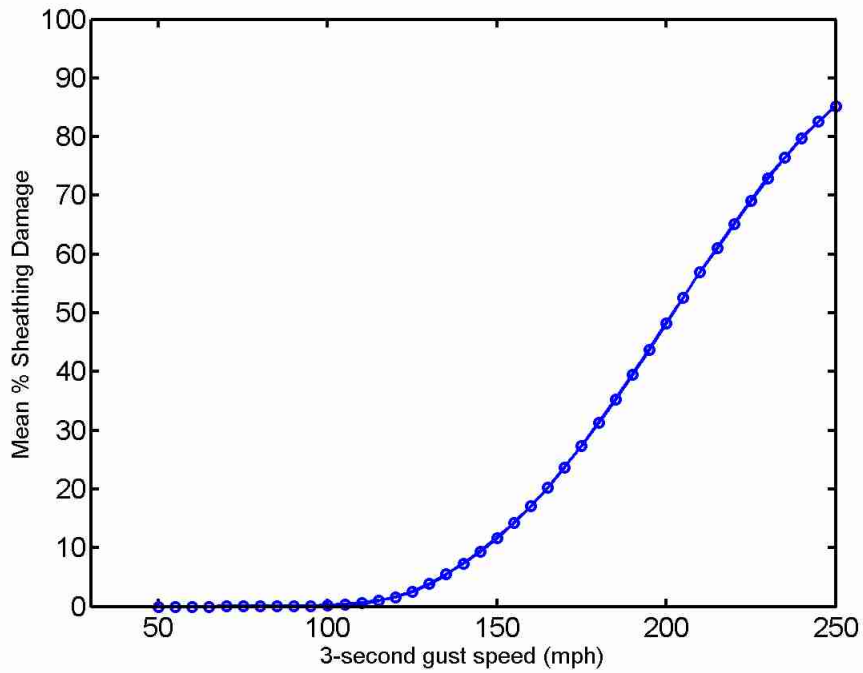


Figure D-4. Vulnerability to roof sheathing damage for South/Keys WH homes.

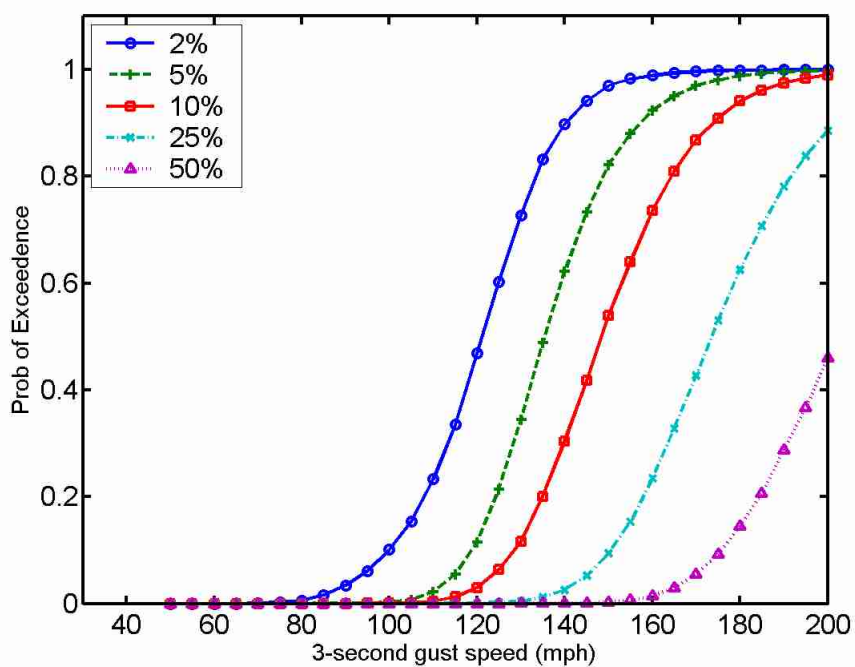


Figure D-5. Fragility curves for 2%, 5%, 10%, 25%, and 50% damage to roof sheathing for South/Keys WH homes.

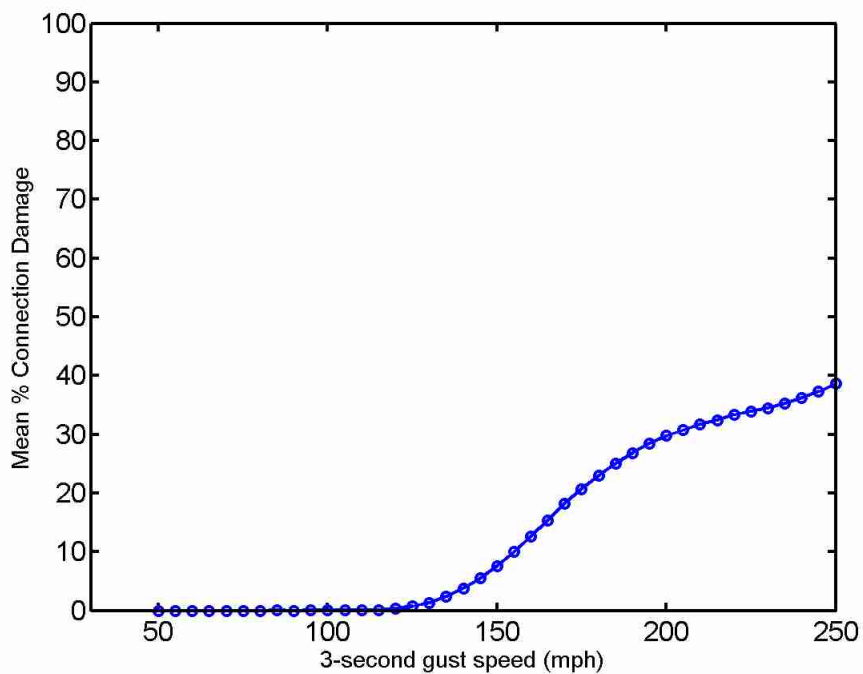


Figure D-6. Vulnerability to roof-to-wall connection damage for South/Keys WH homes.

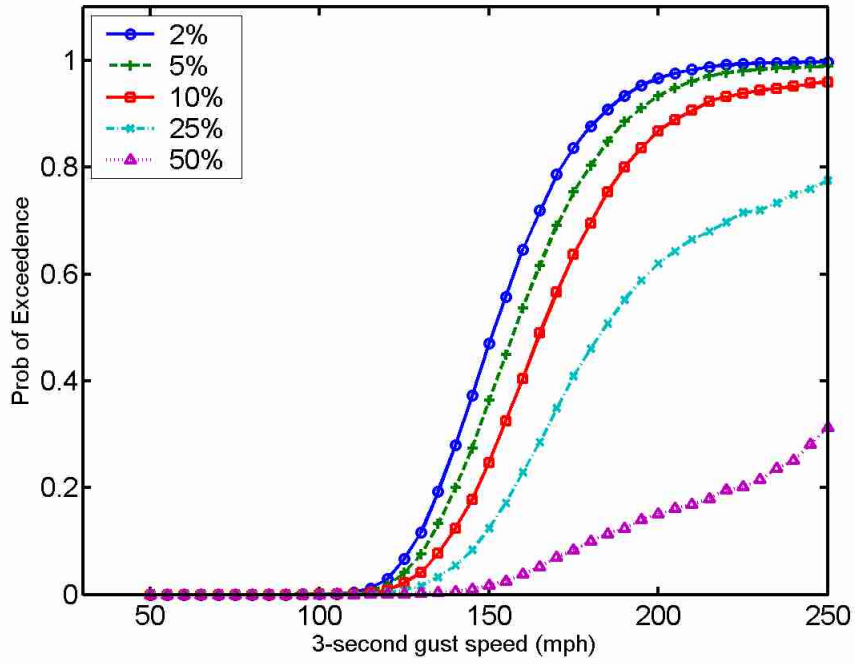


Figure D-7. Fragility curves for 2%, 5%, 10%, 25%, and 50% damage to roof-to-wall connections for South/Keys Region WH homes.

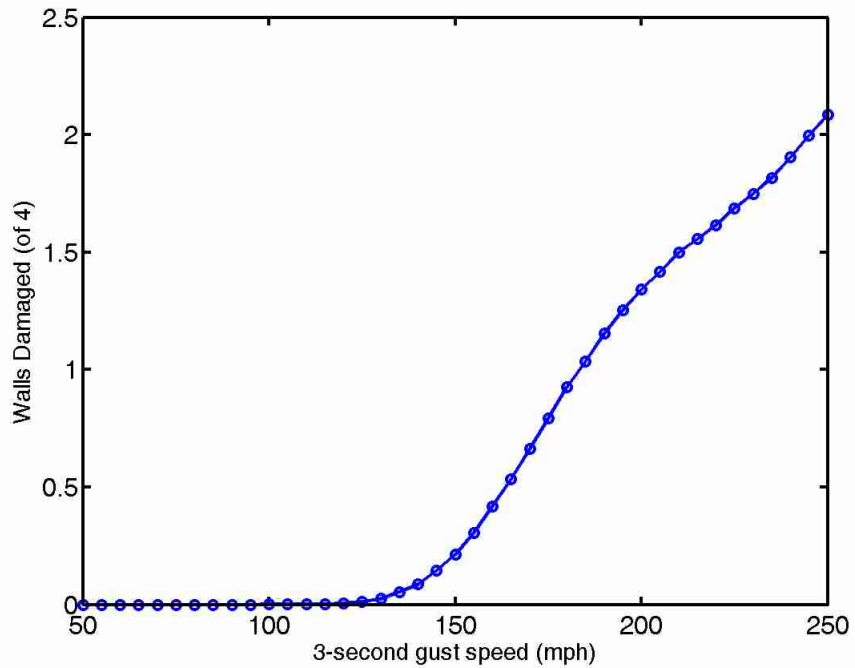


Figure D-8. Vulnerability to wall damage for South/Keys Region WH homes.

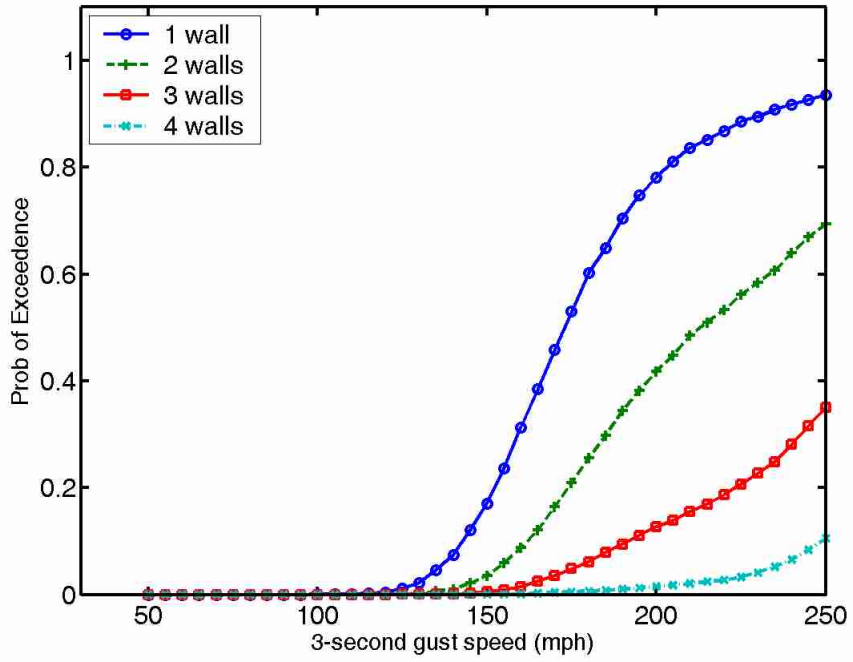


Figure D-9. Fragility curves for 1, 2, 3 and 4 damaged walls for South/Keys Region WH homes.

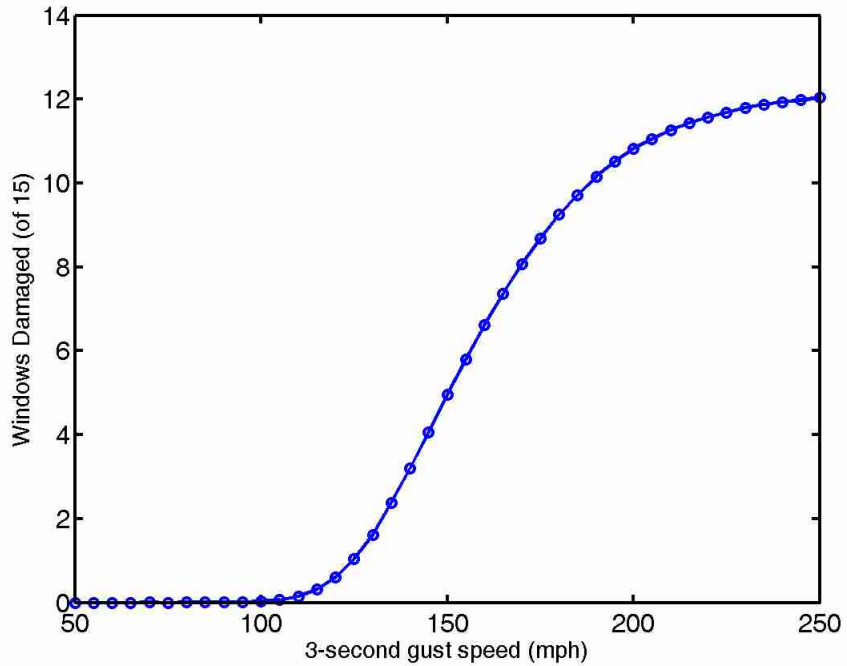


Figure D-10. Vulnerability to window damage for South/Keys Region WH homes.

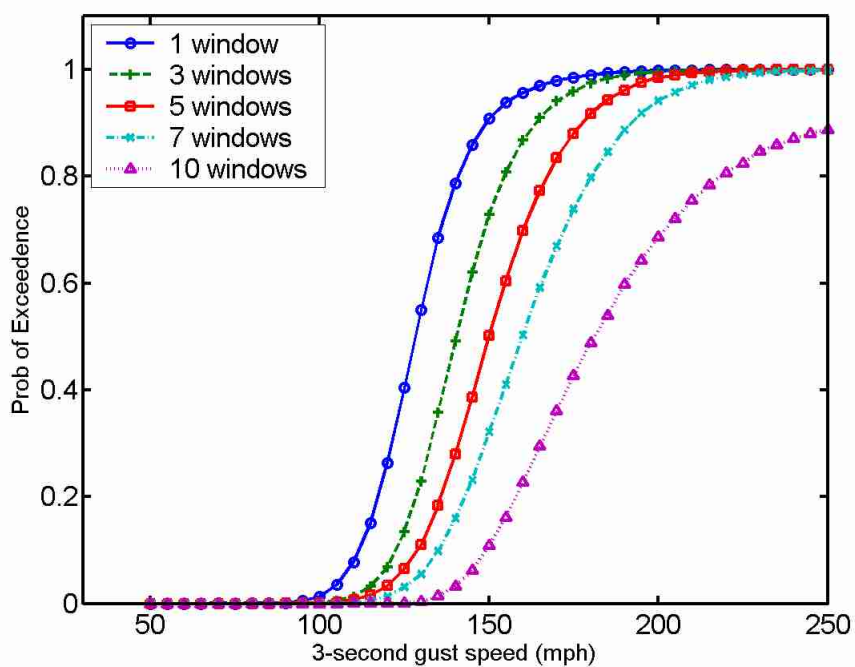


Figure D-11. Fragility curves for 1, 3, 5, 7, and 10 damaged windows for South/Keys Region WH homes.

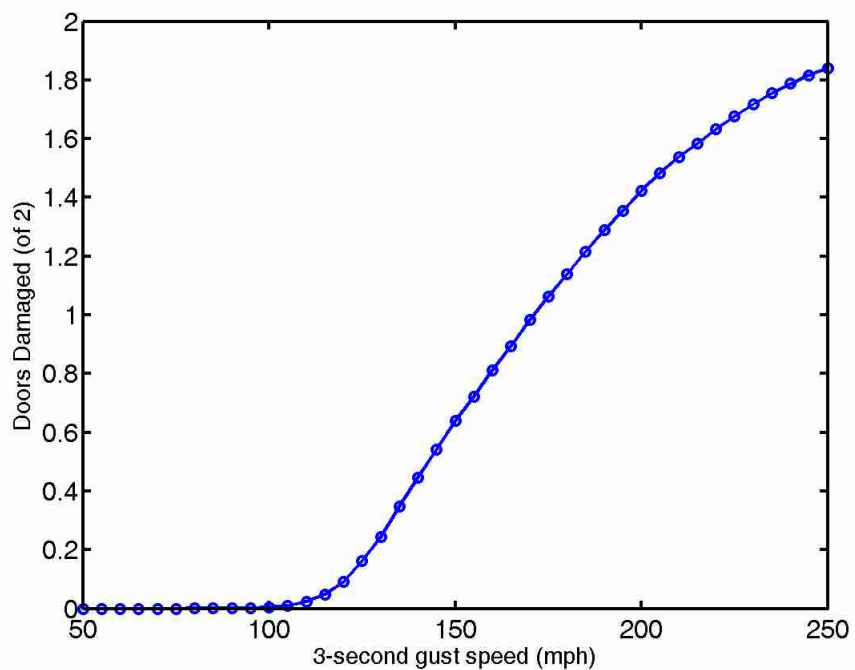


Figure D-12. Vulnerability to exterior door damage for South/Keys Region WH homes.

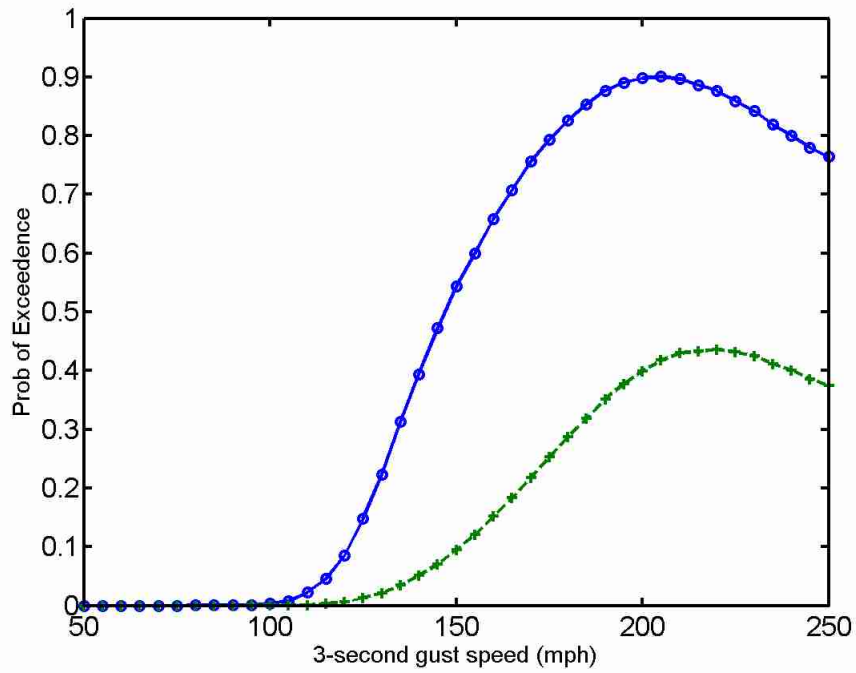


Figure D-13. Vulnerability to exterior door damage for South/Keys Region WH homes.

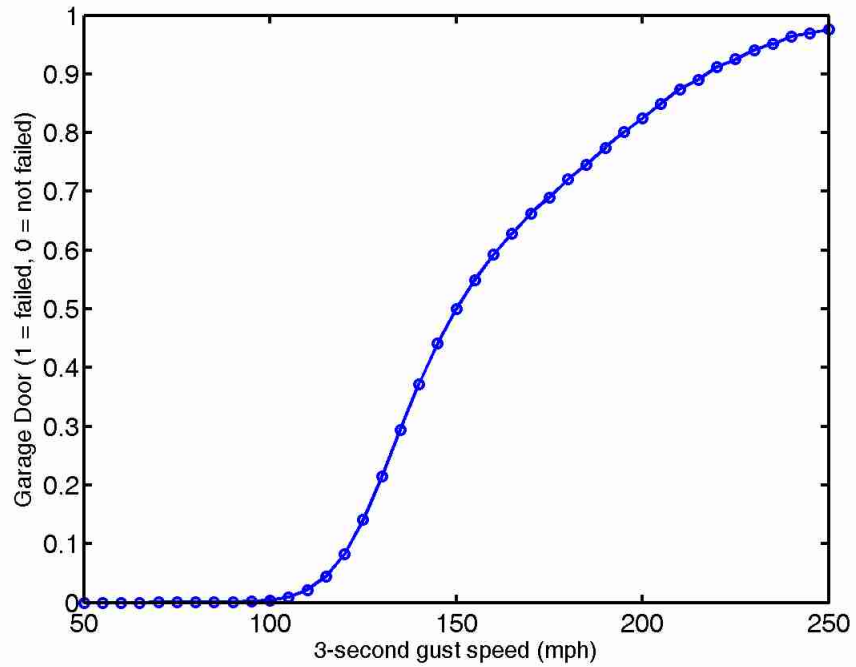


Figure D-14. Vulnerability to garage door damage for South/Keys Region WH homes.

APPENDIX E
FLORIDA MANUFACTURED SINGLEWIDE HOMES

This appendix contains figures representing simulated structural damage to typical singlewide manufactured homes in the State of Florida. Figure E-1 provides a measure of comparison between different building components. In this figure, the mean damages to roof cover, roof sheathing, roof-to-wall connections, and wall sheathing panels are presented as a percentage of the total that is damaged. For overturning, a percentage representing the likelihood of the home being overturned is provided. In the simulation model a value of one is recorded for overturned homes and a value of zero represents homes that do not overturn. At each wind speed, the mean overturning value is multiplied by 100 to obtain a comparative percent. A similar process is used for sliding, except that there are two possible sliding categories. In the simulated data, a value of one indicates minor sliding, while a value of two represents major sliding. Zero is used for no sliding damage. For each wind speed, the mean sliding value is multiplied by 100 and divided by 2 to obtain a comparative percent. Additional figures provide the vulnerability (mean damage) or fragility (probability of exceeding defined damage states) for individual building components.

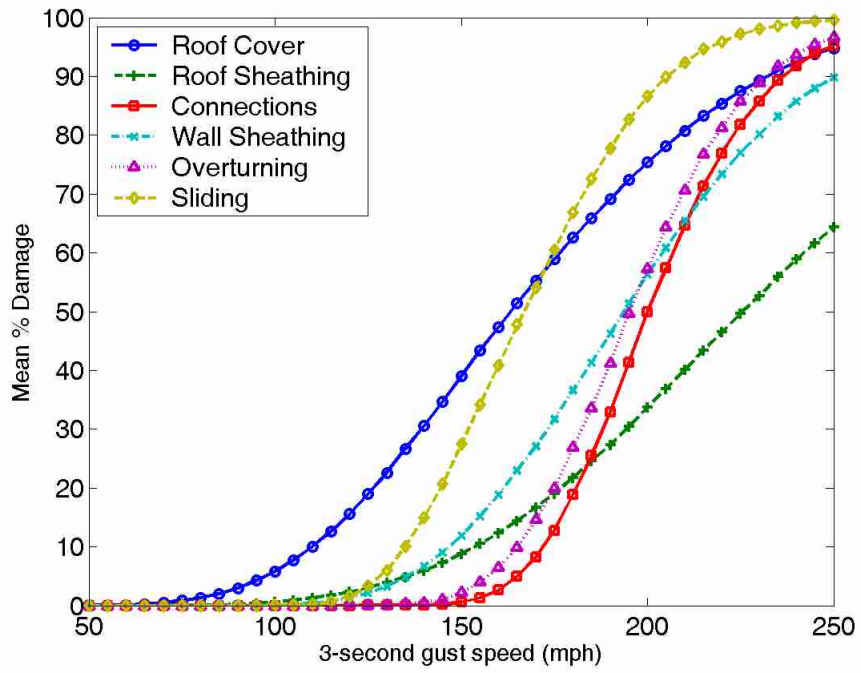


Figure E-1. Singlewide manufactured home comparative levels of roof cover, roof sheathing, connections, wall, and gable end sheathing damage.

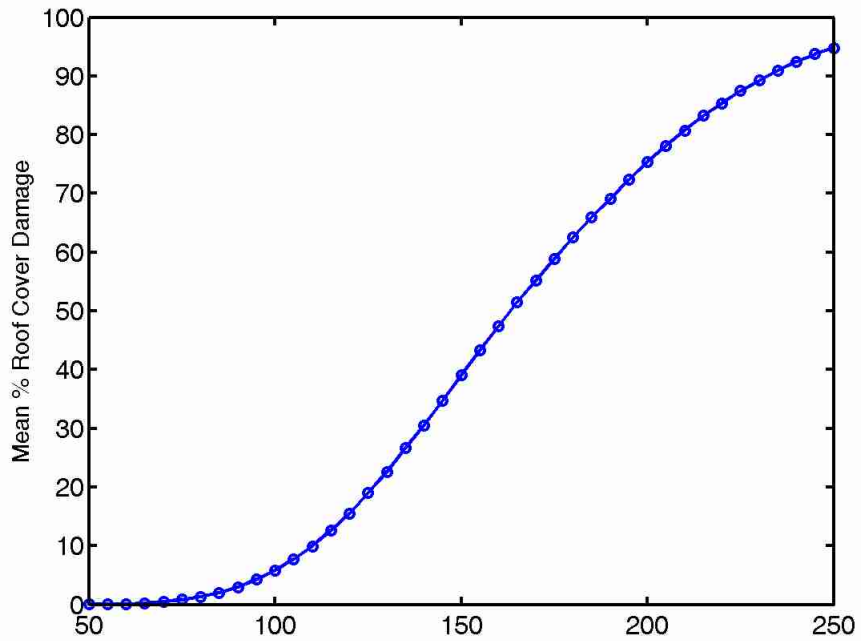


Figure E-2. Vulnerability to roof cover damage for singlewide manufactured homes.

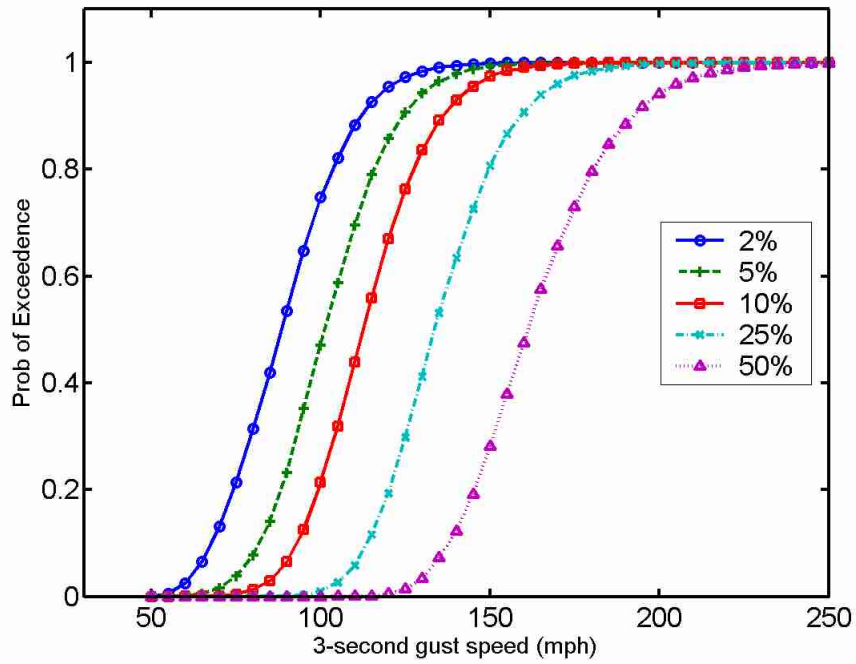


Figure E-3. Fragility curves for 2%, 5%, 10%, 25%, and 50% damage to roof cover for singlewide manufactured homes.

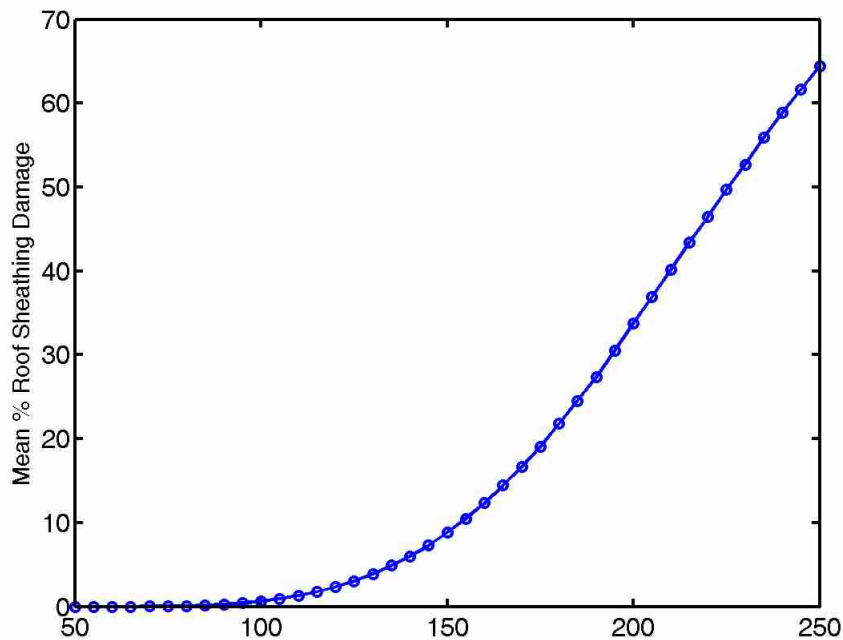


Figure E-4. Vulnerability to roof sheathing damage for singlewide manufactured homes.

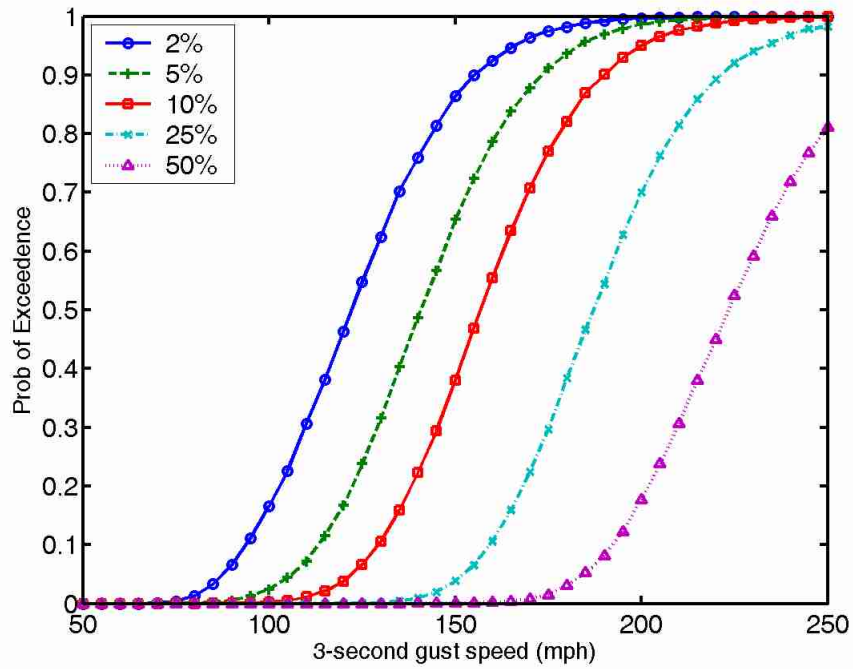


Figure E-5. Fragility curves for 2%, 5%, 10%, 25%, and 50% damage to roof sheathing for singlewide manufactured homes.

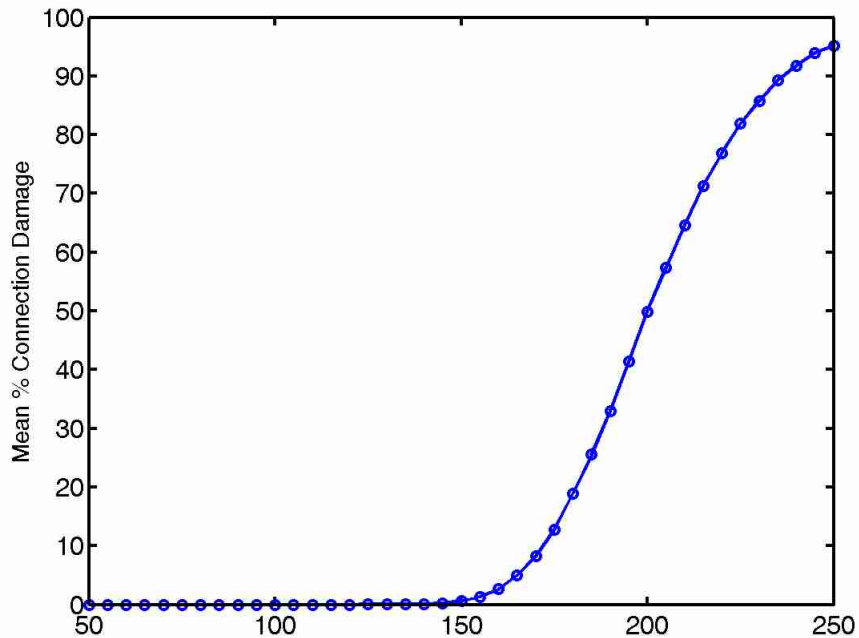


Figure E-6. Vulnerability to roof-to-wall connection damage for singlewide manufactured homes.

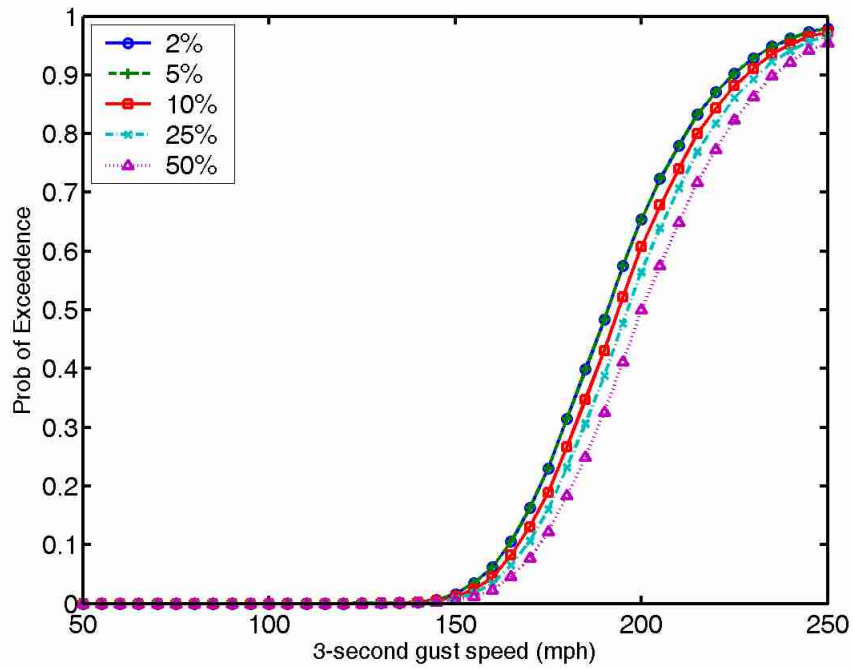


Figure E-7. Fragility curves for 2%, 5%, 10%, 25%, and 50% damage to roof-to-wall connections for singlewide manufactured homes.

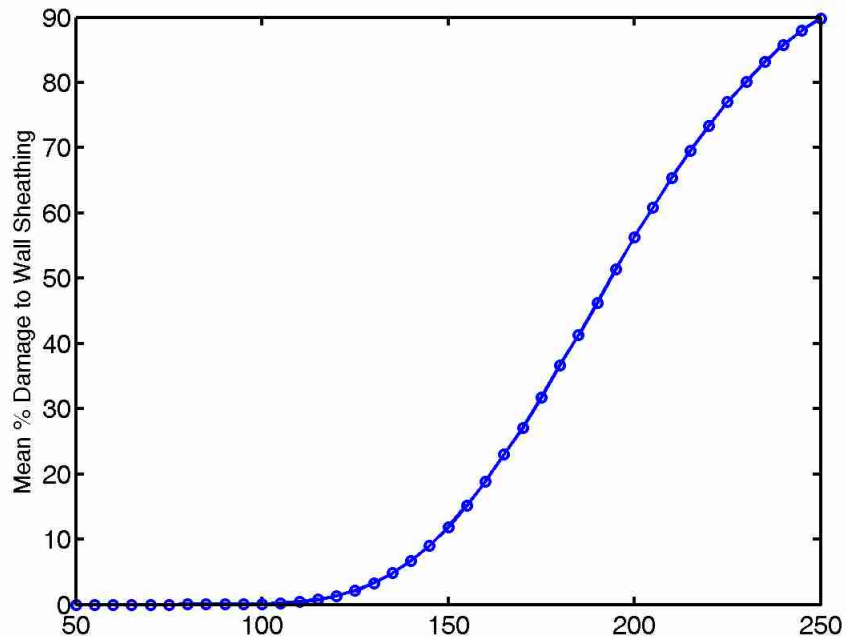


Figure E-8. Vulnerability to wall sheathing damage for singlewide manufactured homes.

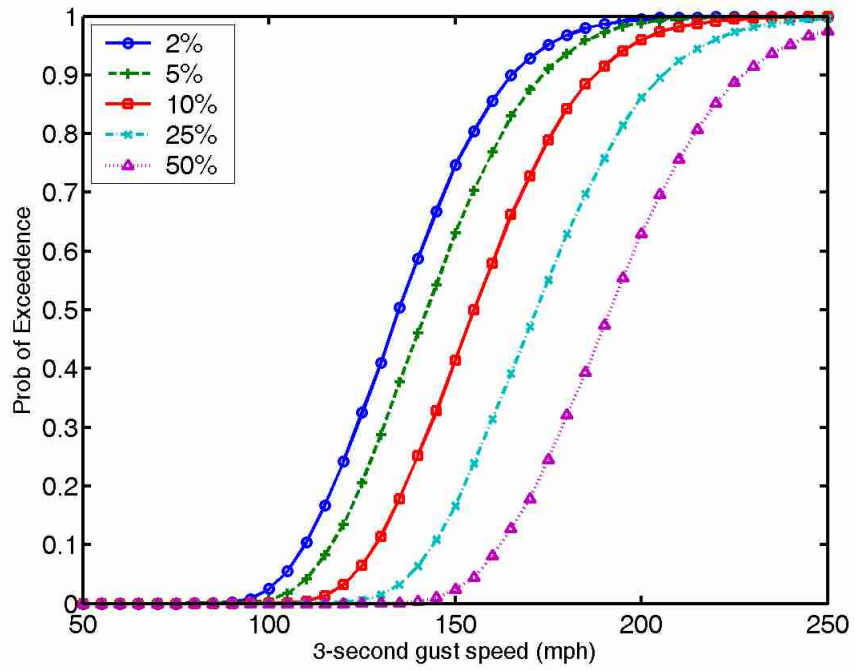


Figure E-9. Fragility curves for 2%, 5%, 10%, 25%, and 50% damage to wall sheathing for singlewide manufactured homes.

APPENDIX F
FLORIDA MANUFACTURED DOUBLEWIDE HOMES

This appendix contains figures representing simulated structural damage to typical doublewide manufactured homes in the State of Florida. Figure F-1 provides a measure of comparison between different building components. In this figure, the mean damages to roof cover, roof sheathing, roof-to-wall connections, and wall sheathing panels are presented as a percentage of the total that is damaged. For overturning, a percentage representing the likelihood of the home being overturned is provided. In the simulation model a value of one is recorded for overturned homes and a value of zero represents homes that do not overturn. At each wind speed, the mean overturning value is multiplied by 100 to obtain a comparative percent. A similar process is used for sliding, except that there are two possible sliding categories. In the simulated data, a value of one indicates minor sliding, while a value of two represents major sliding. Zero is used for no sliding damage. For each wind speed, the mean sliding value is multiplied by 100 and divided by 2 to obtain a comparative percent. Additional figures provide the vulnerability (mean damage) or fragility (probability of exceeding defined damage states) for individual building components.

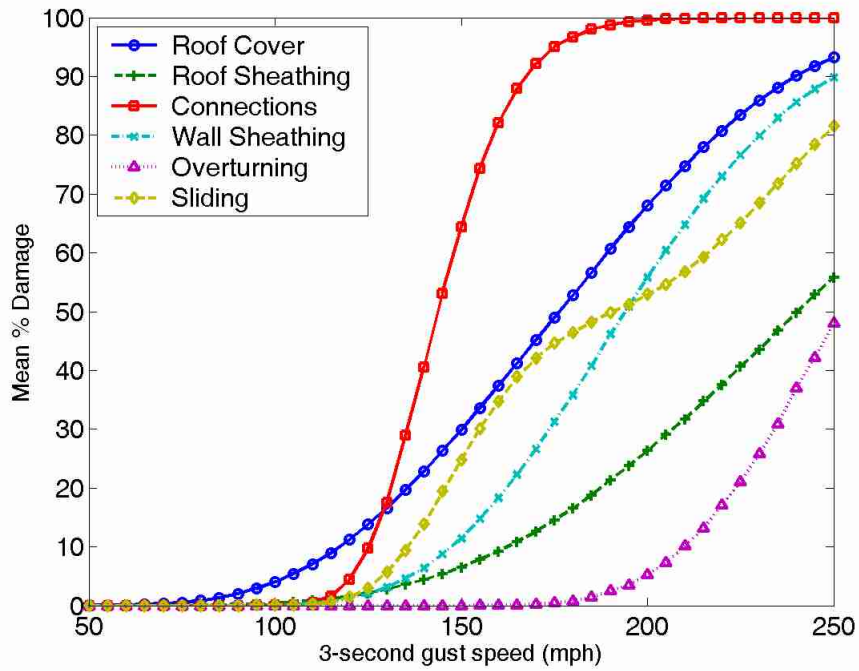


Figure F-1. Doublewide manufactured home comparative levels of roof cover, roof sheathing, connections, wall, and gable end sheathing damage.

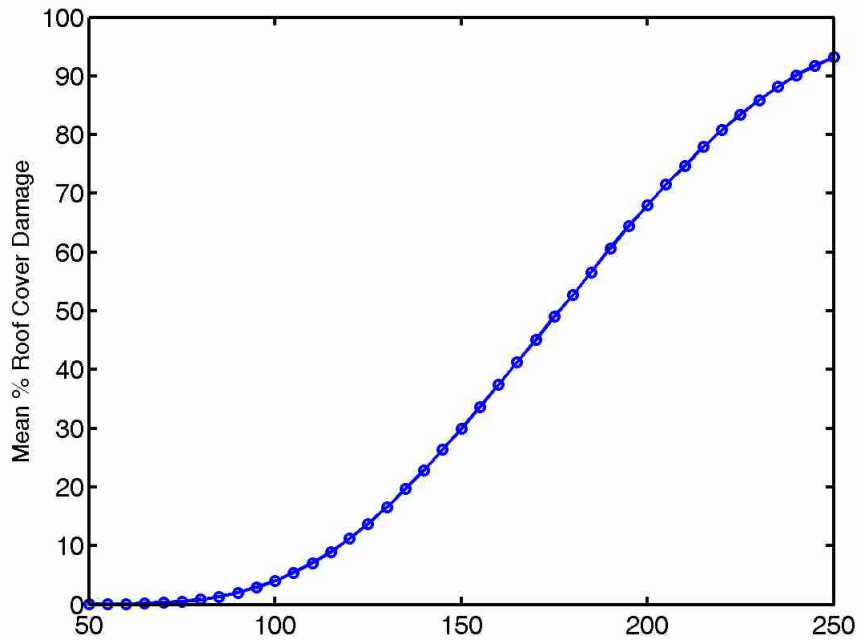


Figure F-2. Vulnerability to roof cover damage for doublewide manufactured homes.

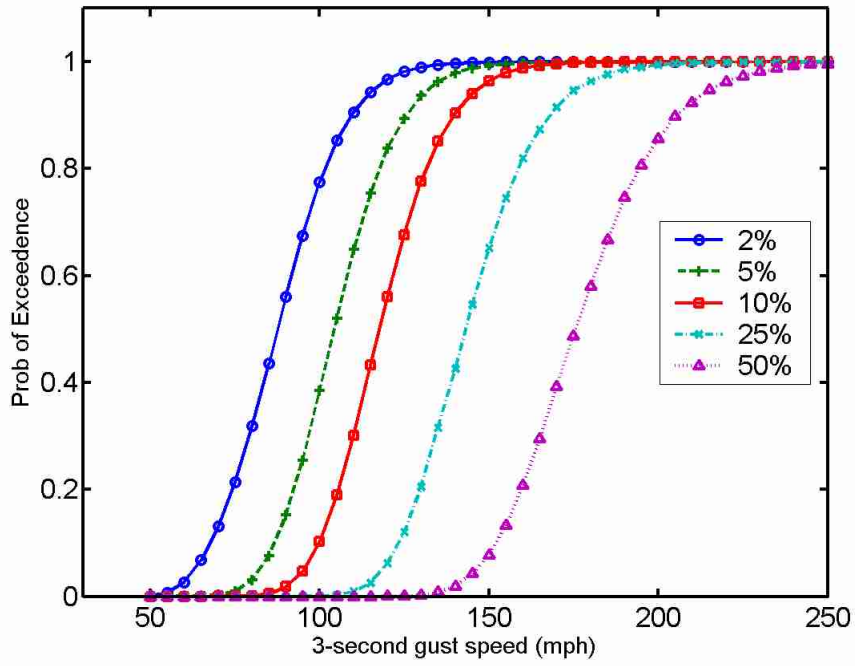


Figure F-3. Fragility curves for 2%, 5%, 10%, 25%, and 50% damage to roof cover for doublewide manufactured homes.

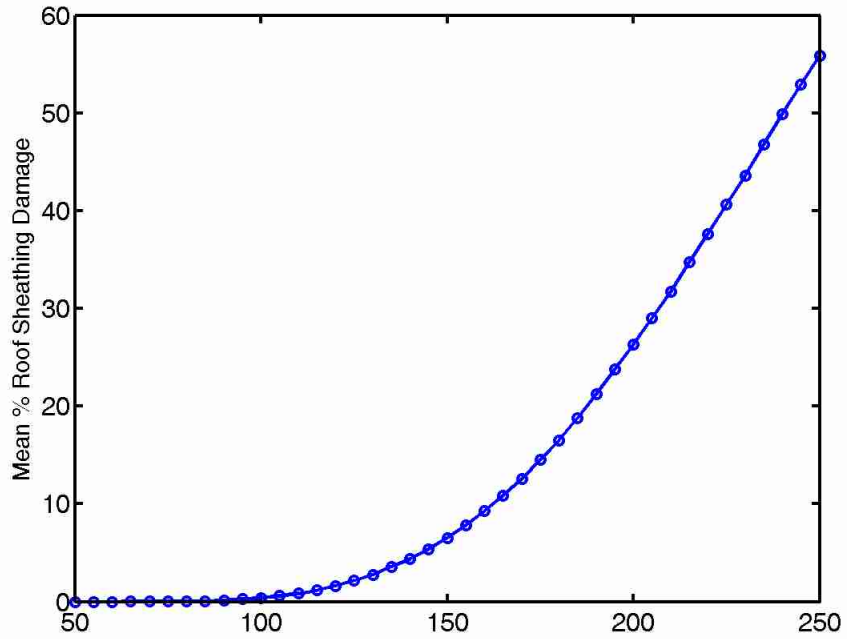


Figure F-4. Vulnerability to roof sheathing damage for doublewide manufactured homes.

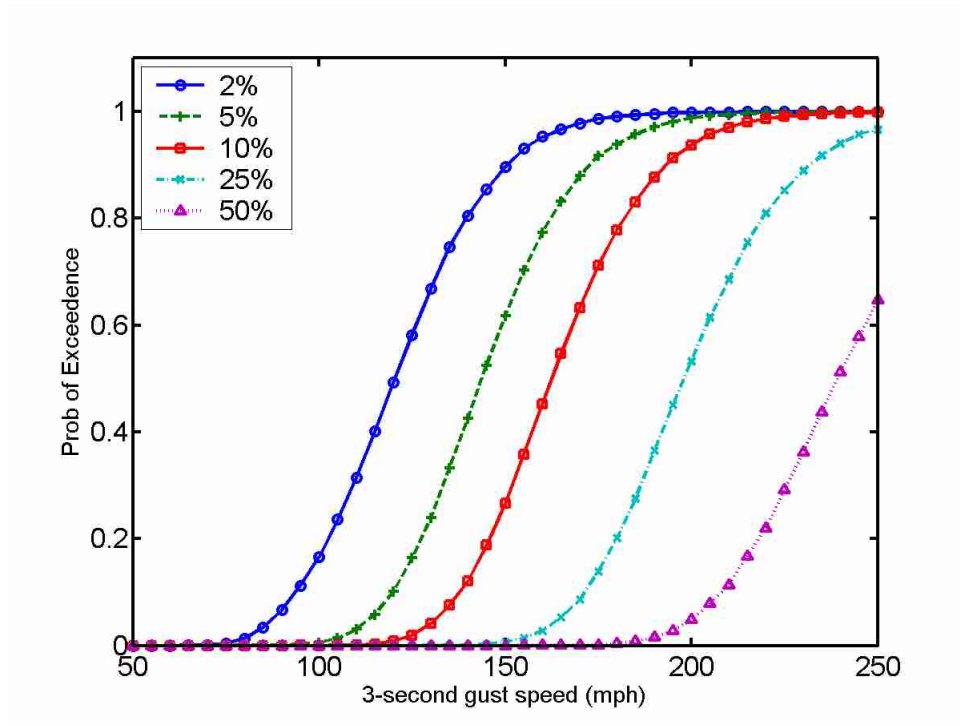


Figure F-5. Fragility curves for 2%, 5%, 10%, 25%, and 50% damage to roof sheathing for doublewide manufactured homes.

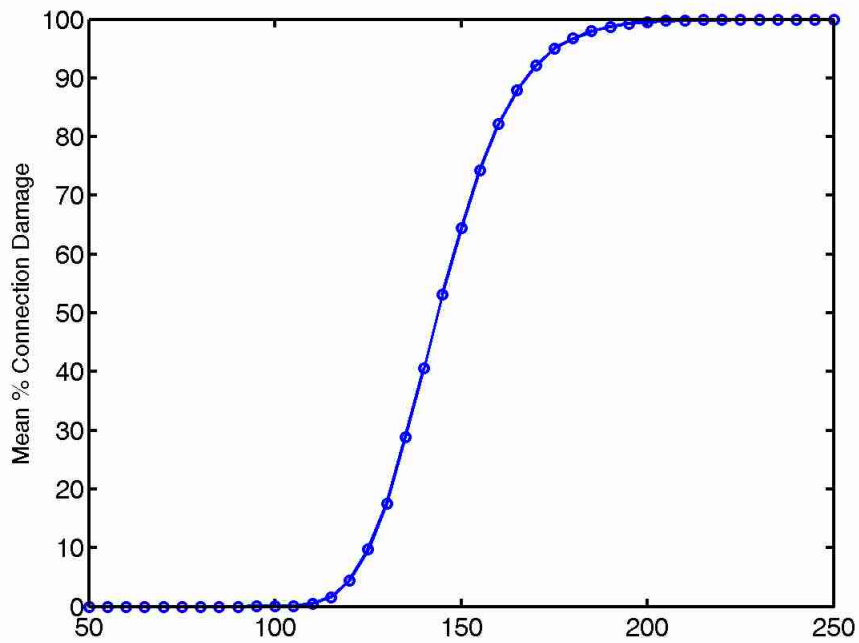


Figure F-6. Vulnerability to roof-to-wall connection damage for doublewide manufactured homes.

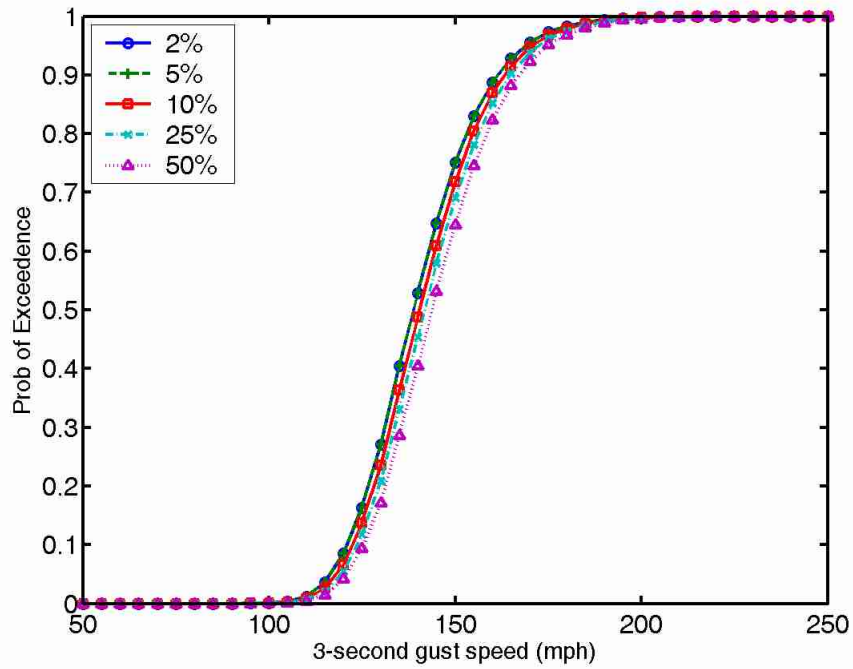


Figure F-7. Fragility curves for 2%, 5%, 10%, 25%, and 50% damage to roof-to-wall connections for doublewide manufactured homes.

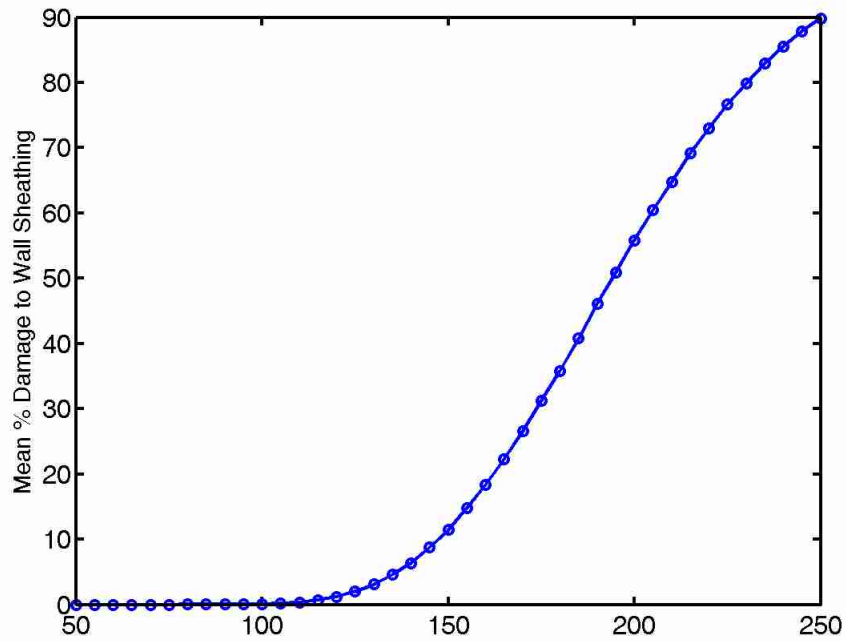


Figure F-8. Vulnerability to wall sheathing damage for doublewide manufactured homes.

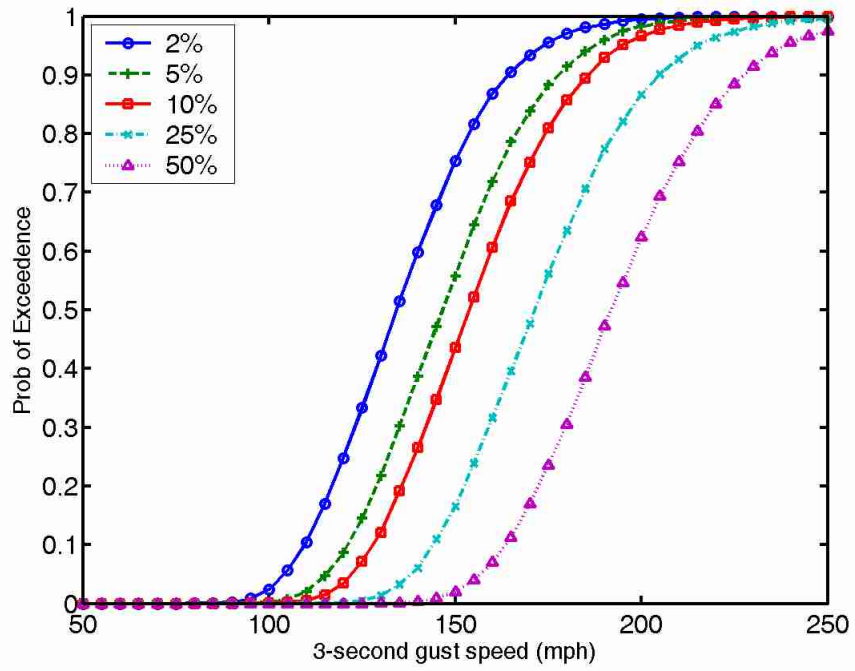


Figure F-9. Fragility curves for 2%, 5%, 10%, 25%, and 50% damage to wall sheathing for doublewide manufactured homes.

APPENDIX G
FLORIDA PRE-HUD CODE MANUFACTURED HOMES

This appendix contains figures representing simulated structural damage to typical manufactured homes in the State of Florida that pre-date the 1975 changes to the manufactured home building code. Figure G-1 provides a measure of comparison between different building components. In this figure, the mean damages to roof cover, roof sheathing, roof-to-wall connections, and wall sheathing panels are presented as a percentage of the total that is damaged. For overturning, a percentage representing the likelihood of the home being overturned is provided. In the simulation model a value of one is recorded for overturned homes and a value of zero represents homes that do not overturn. At each wind speed, the mean overturning value is multiplied by 100 to obtain a comparative percent. A similar process is used for sliding, except that there are two possible sliding categories. In the simulated data, a value of one indicates minor sliding, while a value of two represents major sliding. Zero is used for no sliding damage. For each wind speed, the mean sliding value is multiplied by 100 and divided by 2 to obtain a comparative percent. Additional figures provide the vulnerability (mean damage) or fragility (probability of exceeding defined damage states) for individual building components.

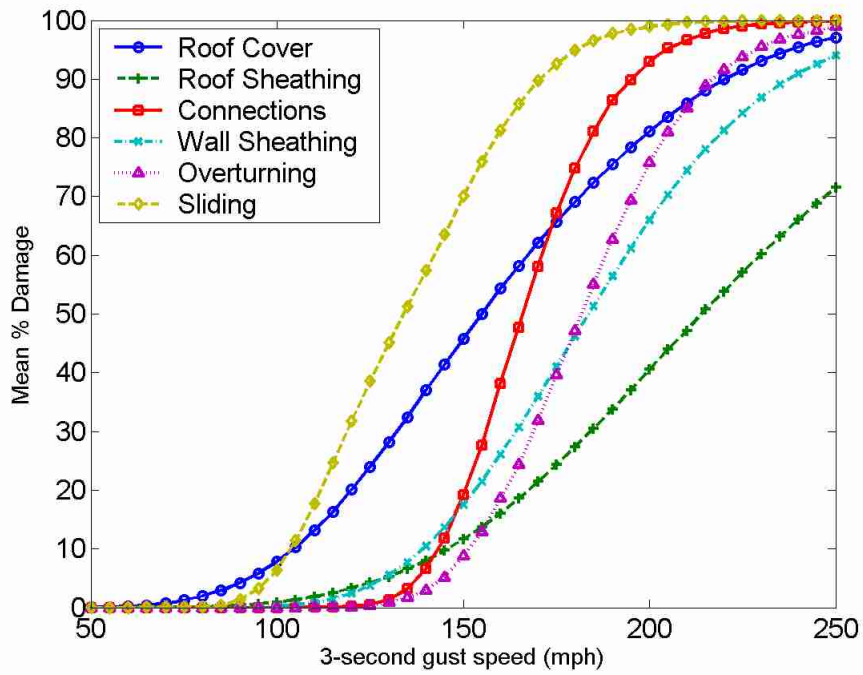


Figure G-1. Pre-HUD Code manufactured home comparative levels of roof cover, roof sheathing, connections, wall, and gable end sheathing damage.

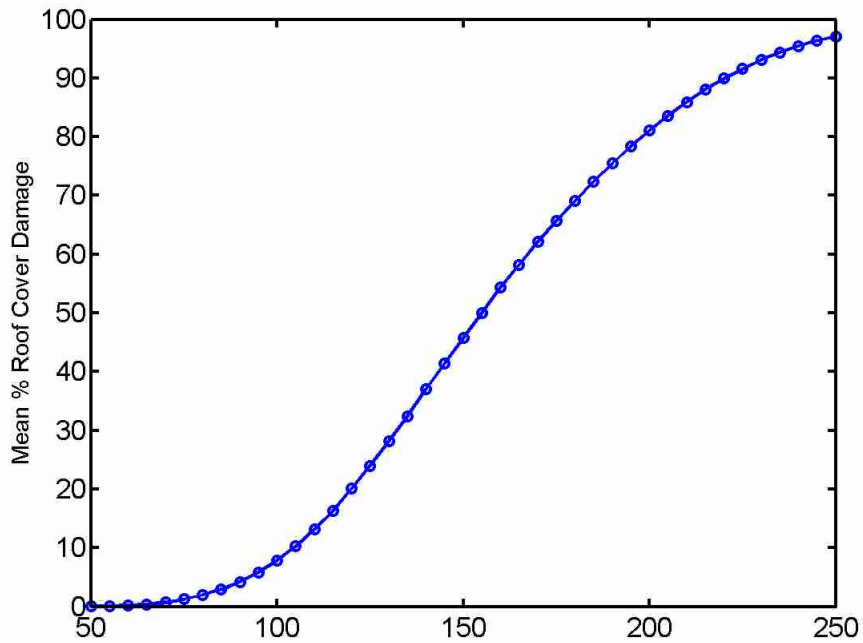


Figure G-2. Vulnerability to roof cover damage for pre-HUD Code manufactured homes.

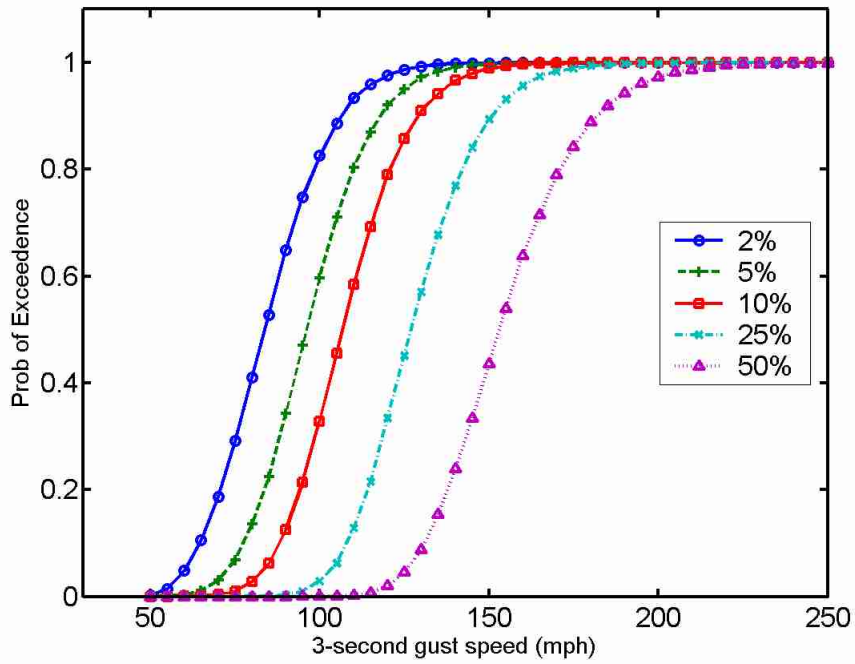


Figure G-3. Fragility curves for 2%, 5%, 10%, 25%, and 50% damage to roof cover for pre-HUD Code manufactured homes.

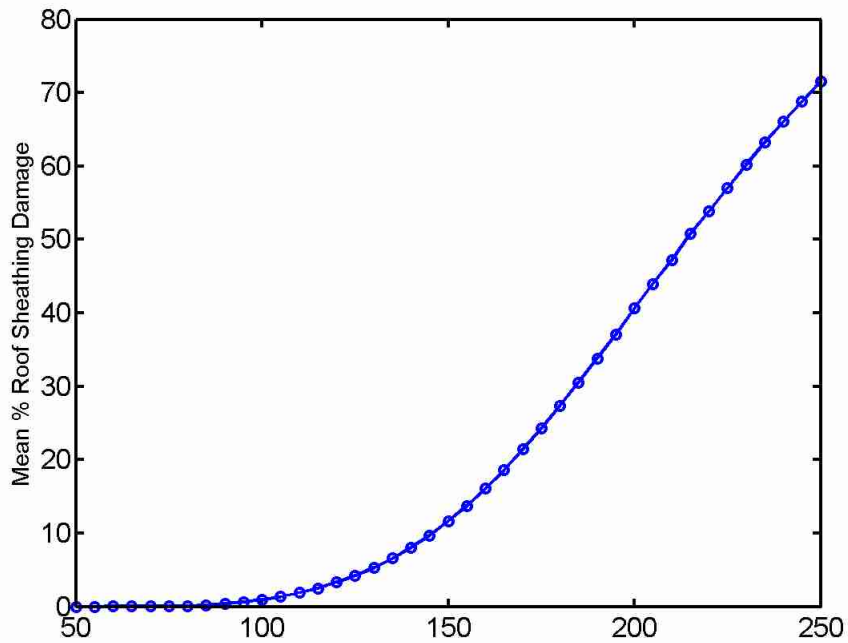


Figure G-4. Vulnerability to roof sheathing damage for pre-HUD Code manufactured homes.

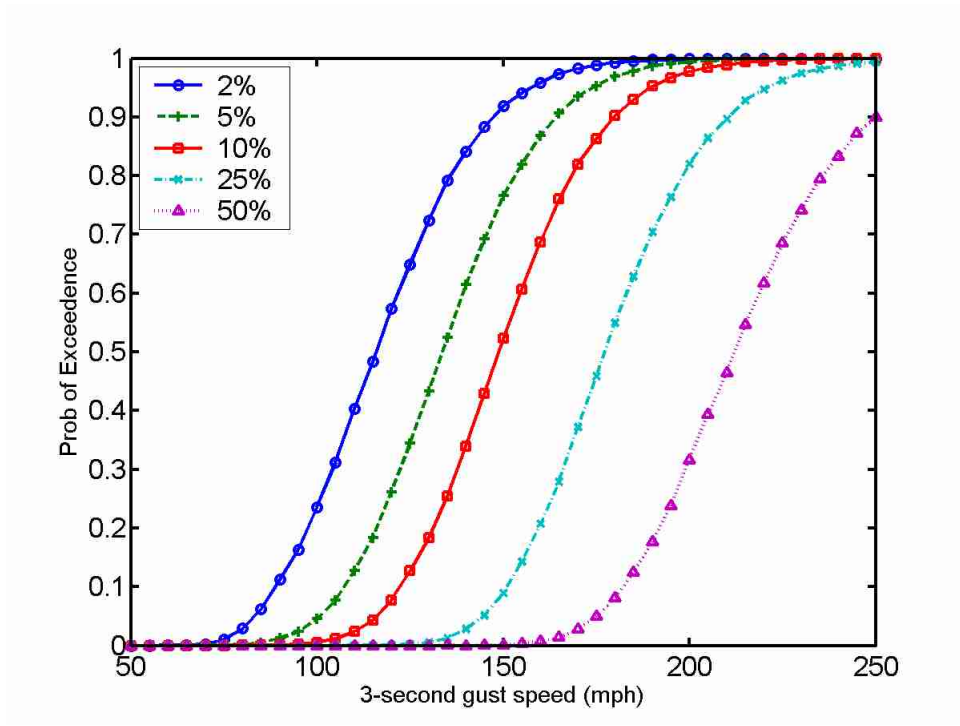


Figure G-5. Fragility curves for 2%, 5%, 10%, 25%, and 50% damage to roof sheathing for pre-HUD Code manufactured homes.

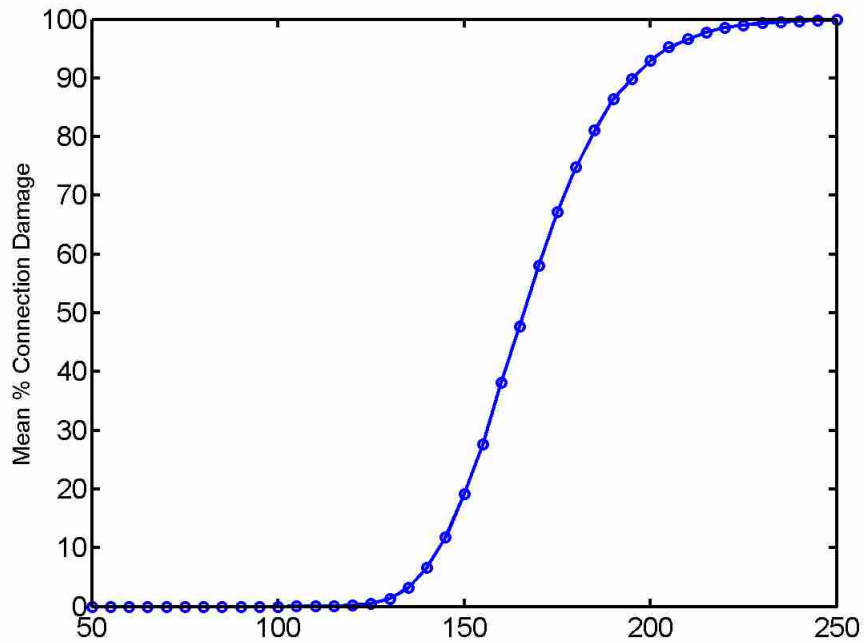


Figure G-6. Vulnerability to roof-to-wall connection damage for pre-HUD Code manufactured homes.

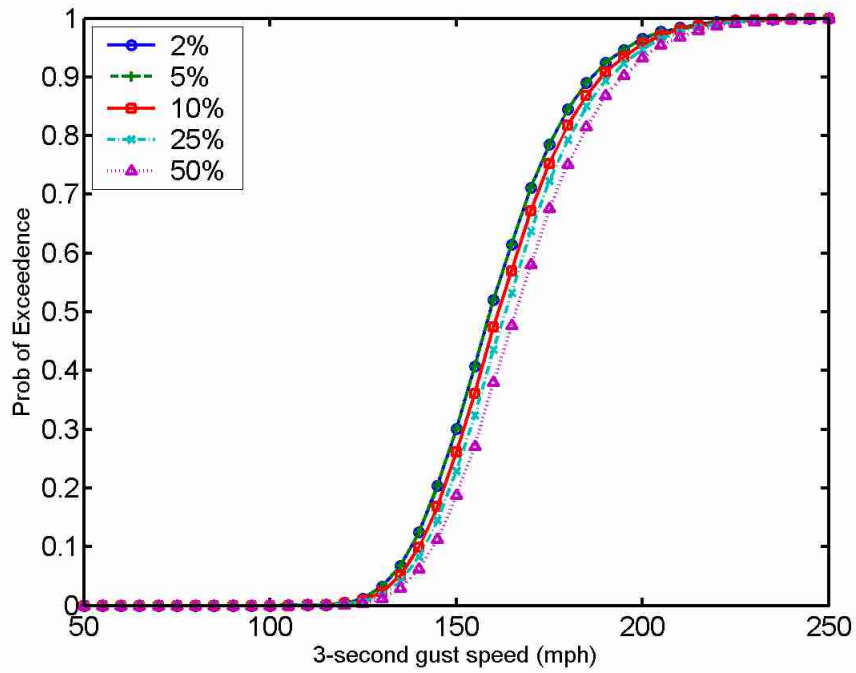


Figure G-7. Fragility curves for 2%, 5%, 10%, 25%, and 50% damage to roof-to-wall connections for pre-HUD Code manufactured homes.

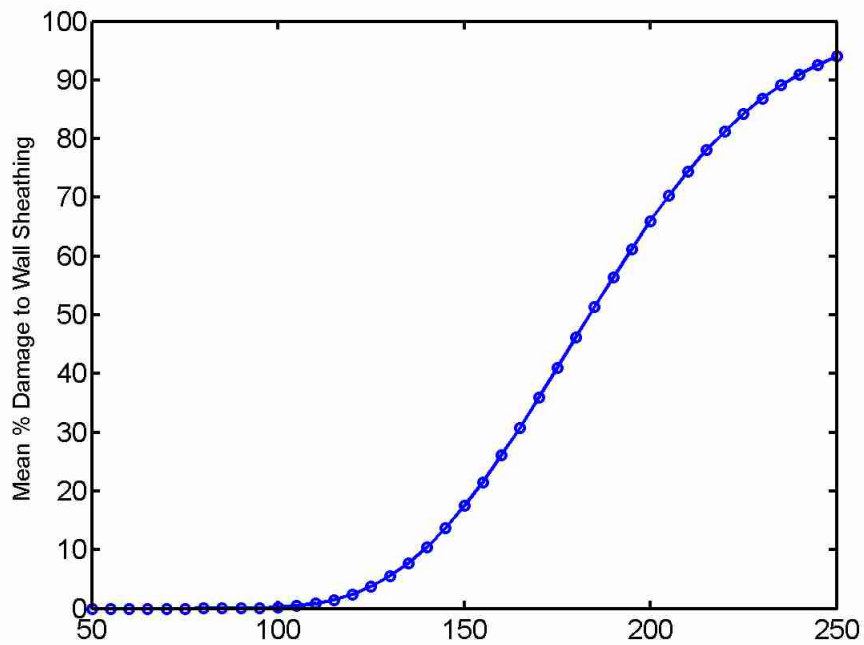


Figure G-8. Vulnerability to wall sheathing damage for pre-HUD Code manufactured homes.

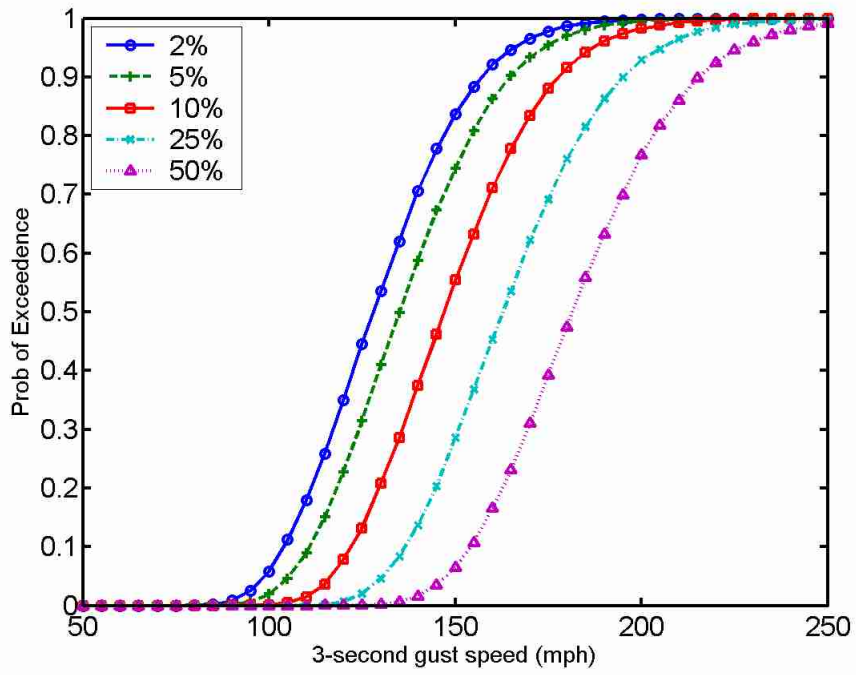


Figure G-9. Fragility curves for 2%, 5%, 10%, 25%, and 50% damage to wall sheathing for pre-HUD Code manufactured homes.

LIST OF REFERENCES

1. S. L. McCabe, Testimony of Dr. Steven L. McCabe on behalf of the American Society of Civil Engineers before the subcommittee on environment, technology and standards of the committee on science, U.S. House of Representatives, October 11, 2001.
2. J. E. Minor, P. J. Schneider, Hurricane loss estimation – the HAZUS preview model, Proceedings of the America’s Conference on Wind Engineering, Clemson, SC, 2001, 572–578.
3. Multi-hazard Loss Estimation Methodology Hurricane Model HAZUS®MH Technical Manual, Federal Emergency Management Agency, 2003.
4. F. Lavelle, P. Vickery, B. Schauer, L. Twisdale, E. Latch, The HAZUS hurricane model, Proceedings of the 11th International Conference on Wind Engineering, Lubbock, TX, 2003, 1015–1022.
5. C. Dyrbye, S. Hansen, Wind Loads on Structures, John Wiley & Sons, New York, NY, 1997.
6. E. Simiu, R. Scanlan, Wind Effects on Structures, Fundamentals and Applications to Design, Third Edition, John Wiley & Sons, New York, NY, 1996.
7. ASCE 7-98 Standard, Minimum Design Loads for Buildings and Other Structures, American Society of Civil Engineers, New York, NY.
8. B. Munson, D. Young, T. Okiishi, Fundamentals of Fluid Mechanics, John Wiley & Sons, New York, NY, 1990.
9. A. Rigato, P. Chang, E. Simiu, Database-assisted design, standardization, and wind direction effects, J. Struct. Eng., ASCE 127 (8) (2001) 855–860.
10. F. Sadek, E. Simiu, Peak non-Gaussian wind effects for database-assisted low rise building design, J. Eng. Mech., ASCE 128 (5) (2002) 530–539.
11. A. Kareem, Wind effects on structures: a probabilistic viewpoint, Probab. Eng. Mech., 2 (4) (1987) 166–200.
12. A. Cope, K. Gurley, Spatial characteristics of pressure coefficients on low rise gable roof structures, Proceedings of the America’s Conference on Wind Engineering, Clemson, SC, 2001, 719–728.

13. M. Gioffre, K. Gurley, A. Cope, Stochastic simulation of correlated wind pressure fields on low-rise gable roof structures, 15th ASCE Engineering Mechanics Conference, New York, NY, 2002.
14. T. Cunningham, Roof Sheathing Fastening Schedules for Wind Uplift, APA Report T92-28, American Plywood Association, Tacoma, WA, March 1993.
15. R. Cook, M. Soltani, editors, Hurricanes of 1992: Lessons Learned and Implications for the Future, ASCE, New York, NY, 1994.
16. Building Performance: Hurricane Andrew in Florida Observations, Recommendations, and Technical Guidance, FEMA, Federal Insurance Administration.
17. A. Kareem, Structural performance and wind speed-damage correlation in Hurricane Alicia, *J. Struct. Eng.*, ASCE 111 (12) 2596–2610.
18. A. Kareem, Performance of cladding in Hurricane Alicia, *J. Struct. Eng.*, ASCE 112 (12) 2679–2693.
19. NAHB Research Center, Assessment of Damage to Single-Family Homes Caused by Hurricanes Andrew and Iniki, Prepared for U.S. Department of Housing and Urban Development, Office of Policy Development and Research, 1993.
20. NAHB Research Center, Assessment of Damage to Homes caused by Hurricane Opal, Prepared for Florida State Home Builders Association, 1996.
21. NAHB Research Center, Reliability of Conventional Residential Construction: An assessment of Roof Component Performance in Hurricane Andrew and Typical Wind Regions of the United States, Prepared for U.S. Department of Housing and Urban Development and National Association of Home Builders, 1999.
22. M. Phang, Wind damage investigation of low rise buildings, Proceedings of the 1999 Structures Congress, ASCE, New Orleans, LA, 1999, 1015–1021.
23. B. Sill, P. Sparks, editors, Hurricane Hugo One Year Later, Proceedings of the Symposium and Public Forum, ASCE, September 1990.
24. M. Mahendran, Wind resistant low-rise buildings in the tropics, *J. Perform. Constr. Fac.*, ASCE 9 (11) (1995) 330–346.
25. Y. Mitsuta, T. Fujii, I. Nagashima, A predicting method of typhoon wind damages, Probabilistic Mechanics and Structural Reliability: Proceedings of the 7th Specialty Conference, Worcester, MA, 1996, 970–973.
26. S. Bhinderwala, Insurance Loss Analysis of Single Family Dwellings Damaged in Hurricane Andrew, Master's Thesis, Clemson University, Clemson, SC, Department of Civil Engineering, 1995.

27. J. Holmes, Vulnerability curves for buildings in tropical cyclone regions, Probabilistic Mechanics and Structural Reliability: Proceedings of the 7th Specialty Conference, Worcester, MA, 1996, 78–81.
28. B. Sill, R. Kozlowski, Analysis of storm damage factors for low-rise structures, J. Perform. Constr. Fac., ASCE 11 (4) (1997) 168–176.
29. Z. Huang, D. Rosowsky, P. Sparks, Event-based hurricane simulation for the evaluation of wind speeds and expected insurance loss, Wind Engineering into the 21st Century, 1999, 1417–1424.
30. J. Sciaudone, D. Freuerborn, G. Rao, S. Daneshvaran, Development of objective wind damage functions to predict wind damage to low-rise structures, Eighth U.S. National Conference on Wind Engineering, Johns Hopkins University, Baltimore, MD, 1997.
31. J-P. Pinelli, L. Zhang, C. Subramanian, A. Cope, K. Gurley, S. Gulati, S. Hamid, Classification of structural models for wind damage predictions in Florida, Proceedings of the 11th International Conference on Wind Engineering, Lubbock, TX, June, 2003, 999–1006.
32. L. Zhang, Public Hurricane Loss Projection Model: Exposure and Vulnerability Components, Master's Thesis, Florida Institute of Technology, Melbourne, FL, Department of Civil Engineering, 2003.
33. NAHB Research Center, Factory and Site Built Housing, A Comparison for the 21st Century, Prepared for U.S. Department of Housing and Urban Development, October 1998.
34. J. Wills, B. Lee, T. Wyatt, A model of wind-borne debris damage, J. Wind Eng. Ind. Aerod., 90 (4/5) (2002) 555–565.
35. J. Peterka, J. Cermak, L. Cochran, B. Cochran, N. Hosoya, R. Derickson, C. Harper, J. Jones, B. Metz, Wind uplift model for asphalt shingles, J. Archit. Eng., ASCE 3 (4) (1997) 147–155.
36. FM Global Technologies, 2002, Approval Standard for Class 1 Roof Covers, FM Global Technologies, http://www.fmglobal.com/approvals/resources/approval_standards/4470.pdf (retrieved February 2004).
37. Industry Perspective: Impact Resistance Standards, Natural Hazard Mitigation Insights, Institute for Business and Home Safety, (12), February 2000.
38. A. Ang, W. Tang, Probability Concepts in Engineering Planning and Design, John Wiley & Sons, New York, NY, 1975.
39. D. Mizzell, Wind Resistance of Sheathing for Residential Roofs, Master's Thesis, Clemson University, Clemson, SC, Department of Civil Engineering, 1994.

40. T. Cunningham, Roof Sheathing Fastening Schedules for Wind Uplift, APA Report T92-28, American Plywood Association, Tacoma, WA, March 1993.
41. D. Rosowsky, S. Schiff, T. Reinhold, P. Sparks, B. Sill, Performance of Light-Frame Wood Structures Under High Wind Loads: Experimental and Analytical Program, Wind Performance and Safety of Wood Buildings, FPS Specialty Publication, 1998.
42. T. Reinhold, 13 homes destroyed, Disaster Review, Fall 2002, 9–14.
43. L. Canfield, S. Niu, H. Liu, Uplift resistance of various rafter-wall connections, Forest Prod. J., 41 (7/8) (1991) 27–34.
44. T. Reed, D. Rosowsky, S. Schiff, Structural Analysis of Light-Framed Wood Roof Construction, a Wind Load Test Facility Report for Blue Sky, PBS-9606-02, 1996.
45. National Design Specification for Wood Construction: Allowable Stress Design (ASD) Manual for Engineered Wood Construction, American Wood Council, Washington D.C., 1997.
46. J-P. Pinelli, S. O'Neill, Effect of tornadoes on residential masonry structures, Wind Struct. J., 3 (1) (2000) 23–40.
47. J. Dawe, G. Aridru, Prestressed concrete masonry walls subjected to uniform out-of-plane loading, Can. J. Civil Eng., 20 (1993) 969–979.
48. Florida Building Code, Tallahassee, FL, 2001.
49. ACI 530-99/ASCE 5-99/TMS 402-99: Building Code Requirements for Masonry Structures, American Concrete Institute, Farmington Hills, MI, 1999.
50. DASMA, 2002, DASMA Garage Door and Commercial Door Wind Load Guide, Technical Data Sheet #155b, Door & Access Systems Manufacturer's Association International, <http://www.dasma.com/PDF/Publications/TechDataSheets/CommercialResidential/TDS155b.pdf> (retrieved March 2003).
51. Simpson Strongtie, 2002, Connectors for Factory Built Homes, Technical Bulletin T-FBS02, Simpson Strongtie, <http://www.strongtie.com/ftp/bulletins/T-FBS02.pdf> (retrieved August 2003).
52. Owens Corning, 2001, Certificate of Conformance, Owens Corning Select Vinyl Siding, Owens Corning, http://www.owenscorning.com/around/exteriors_new/pdfs/COCOwensSelect.pdf (retrieved August 2003).
53. Certainteed, 2000, Pro Edition™ 44 Vinyl Siding, Certainteed: <http://certainteed.com/NR/rdonlyres/E72BFEB7-459C-488D-86F2-BFC0955E8EBF/0/410.pdf> (retrieved August 2003).

54. Certainteed, 2001, Weather Happens: Test Results, Certainteed, <http://www.certainteed.com/cside/csct01208rig.html> (retrieved August 2003).
55. R. Marshall, Manufactured Homes – Probability of Failure and the Need for Better Windstorm Protection Through Improved Anchoring Systems, NISTIR 5370, Building and Fire Research Laboratory, Gaithersburg, MD, for Department of Housing and Urban Development, Washington, D.C., November 1994.
56. F. Yokel, R. Chung, F. Rankin, C. Yancey, Load-Displacement Characteristics of Shallow Soil Anchors, NBS Building Science Series 142, National Bureau of Standards, Washington D.C., 1982.
57. K. Hayes, Hurricane Data Collection Hardware: Design, Construction, and Testing, Master's Thesis, University of Florida, Gainesville, FL, Department of Civil and Coastal Engineering, 2000.
58. Carbide Depot, (undated), Coefficient for Static Friction of Steel Chart, Carbide Depot, <http://www.carbidedepot.com/formulas-frictioncoefficient.htm> (retrieved September 2003).
59. M. Powell, S. Houston, T. Reinhold, Hurricane Andrew's landfall in South Florida Part I: standardizing measurements for documentation of surface wind fields, *Weather Forecast.*, 11 (1996) 304–328.
60. J-P. Pinelli, J. Murphree, K. Gurley, A. Cope, S. Hamid, S. Gulati, Hurricane loss estimation, International Conference on Probabilistic Safety Assessment and Management, Berlin, Germany, June, 2004.
61. A. Cope, K. Gurley, J-P. Pinelli, J. Murphree, S. Gulati, S. Hamid, A probabilistic model of damage to residential structures from hurricane winds, Joint Specialty Conference on Probabilistic Mechanics and Structural Reliability, Albuquerque, NM, July, 2004.

BIOGRAPHICAL SKETCH

Anne grew up in Winter Haven, Florida, where she graduated second in her class from Winter Haven High School. As a National Merit Finalist, she was awarded the William A. Kenyon Scholarship from Clemson University. During her educational career at Clemson, Anne was a two-time recipient of the E. L. Clarke Award (the Civil Engineering departmental award for academic excellence). As an undergraduate, she completed a 9-month Eisenhower Fellow experience with the Department of Transportation, and participated in the National Science Foundation's Research Experience for Undergraduates Program. Anne graduated summa cum laude with senior departmental honors, earning a Bachelor of Science in civil engineering May 12, 1995. She then worked as a research fellow under the direction of Dr. Tim Reinhold, at Clemson, where she conducted wind-tunnel research on low-rise structures. She earned a Master of Science in civil engineering on August 9, 1997, with a thesis titled *Load Duration Effects on Peak Minimum Pressure Coefficients*. After completing degree requirements, Anne was commissioned as a second lieutenant in the United States Army. She spent 3 years on active duty as an officer and paratrooper at Fort Bragg, NC, before pursuing a Ph.D. at the University of Florida. She was awarded the University of Florida's Alumni Scholarship, and studied under the direction of Dr. Kurt Gurley. Her primary research interests lie in the area of wind-damage mitigation.